Phosphorylated Nanoaggregates as Multifunctional Agents in Oral Health

Harper, Robert Anthony

Awarding institution:
King's College London

Phosphorylated Nanoaggregates as Multifunctional Agents in Oral Health

Robert Anthony Harper

In fulfilment of the requirement

for the degree of Doctor of Philosophy (PhD)

in Pharmaceutical Sciences

Department of Pharmacy

King's College London

March 2017

Acknowledgments

Firstly, I give my upmost gratitude and thanks to my supervisors for allowing me to get the most out of this opportunity and for their continuous advice and guidance throughout the project. To Dr Stuart Jone's, whose endless help, encouragement and support inspired and motivated me to achieve the projects full potential. To Prof Robert Hider for his expert chemistry advise and wisdom throughout the project. My appreciation also goes to Dr Guy Carpenter and Prof Gordon Proctor for helping me bridge the gaps between pharmaceutical chemistry, oral microbiology and oral immunology. I would also like to thank Dr Arcadia Woods for her assistance in keeping the projects momentum going during Dr Jones year away. I also like to give my thanks to Dr Vincenzo Abbate and Dr Richard Harvey for their help and advice. My thanks also go to Johnson & Johnson London and Skillman for funding the project, organising quarterly global connect meetings and adding industrial scientific knowledge to the project. My thanks especially go to Dr Robert Gambogi, Dr Anthony Geonnotti, Dr Latrisha Petersen and Erin Zaleski for making my three month work placement in New Jersey so enjoyable. I am also thankful to my fellow students and technical staff at the Strand, Guys and Waterloo campuses for their help and friendship especially those on the 17th floor of Tower Wing and 5th floor of the Franklin-Wilkins buildings. I would also like to show my gratitude to the ESPRC for funding the project. Finally, I would like to thank my family for their encouragement and support. I give special thanks to my fiancée Katie Williams for her copious amounts of patience, understanding and love.

List of publications

Journal articles

Harper, R. A., Saleh, M., Abbate, V., Carpenter, G., Proctor, G., Harvey, R. D., Gambogi, R. J., Geonnotti, A., Hider, R., and Jones, S. A. (2017). Understanding how the physical and chemical characteristics of alpha tocopherol nanostructures influence their antimicrobial activity in the oral cavity. Intended journal submission: Colloids and surfaces b: biointerfaces.

Harper, R. A., Carpenter, G., Proctor, G., Harvey, R. D., Gambogi, R. J., Geonnotti, A., Hider, R., and Jones, S. A. (2017). Understanding how electrolytes modify the membrane interactions of nanomaterials to inhibit oral biofilm growth. Intended journal submission: Langmuir.

Harper, R. A., Petersen, P., Saleh, M., Carpenter, G., Proctor, G., Gambogi, R. J., Geonnotti, A., Hider, R., and Jones, S. A. (2017). Targeting macrophages and their recruitment in the oral cavity using swellable (+) alpha tocopheryl phosphate nanostructures. Intended journal submission: Journal of controlled release.

Abstract

Harper, R.A., Kong, X., Carpenter, G., Harvey, R. D., Proctor, G., Gambogi, R., Geonnotti, A., Hider, R., and Jones, S. A. (2016). Using a common buffering agent, Tris, to improve the antimicrobial effect of zinc in oral health products. Bioinorganic Chemistry, Gordon Research Conference, Ventura, CA, USA.

Abstract

Oral microbial disease is highly prevalent globally and is being associated with a multitude of systemic illnesses. There is a vast range of oral health products containing tooth hardening and antimicrobial agents yet the problem persists. The aim of this thesis was to chemically modify the anti-inflammatory vitamin E in order to introduce novel substantive antimicrobial activity giving it multifunctional activity to combat oral disease. (+) Alpha tocopherol (α-T) was chemically modified by phosphorylation to generate (+) alpha tocopheryl phosphate (α-TP). (+) α-TP was observed to form nano sized aggregates with a μM critical aggregation constant when dispersed in Tris buffer. The addition of the phosphate group was found to introduce substantive antimicrobial activity as (+) α-TP retarded *Streptococci* biofilm growth, adhered to hydroxyapatite and inhibited salivary biofilm growth whilst (+) α-T did not. This activity was related to nanostructure architectures as (+) α-T formed spherical, non-surface adherent liposomes (563 ± 1 nm, -10.5 ± 0.2 mV) whilst (+) α-TP formed surface adherent, planar bilayer islands (175 ± 21 nm, -14.9 ± 3.5 mV). Tris facilitated (+) α-TP antimicrobial activity as when it was dispersed in phosphate buffer it did not penetrate, kill or retard biofilm bacterial growth. This was shown to be due to the presence of the ions affecting bacterial membrane packing, aggregate packing and aggregate charge. The small monolayer pressure increase of the (+) α-TP bilayer planar island interactions suggested the antibacterial mechanism was not likely to be simple lyses, but perhaps internalisation and enzymatic inhibition. The (+) α-TP bilayer planar islands swelled into micron sized aggregates when dispersed in cell culture media, selectivity killed macrophages and selectively inhibited monocyte chemoattractant 1 production from human gingival fibroblast cells. The strategy of utilising phosphorylated vitamin E nanoaggregates as multifunctional agents in oral health described herein represents a potential technology platform worthy of clinical evaluation.

Table of Contents

List of Figures

List of Schemes

List of Equations

List of Tables

List of Abbreviations

ABS_{620}	Absorbance at 620 nm
ABSt	Absorbance at time
(+) α-T	(+) alpha tocopherol
(+) α-TP	(+) alpha tocopheryl phosphate
ABS_{max}	Asymptotic maximum absorbance
ABS_{min}	Asymptotic minimum absorbance
AFM	Atomic force microscopy
BA	Blood agar
BHI	Brain heart infusion broth
BM	Basic media
CPC	Cetylpyridinium chloride
CHX	Chlorhexidine digluconate
CD	Circular dichroism
A_{nc}	Corrected absorbance of negative control
A_{pc}	Corrected absorbance of positive control
A_s	Corrected absorbance of sample
CAC	Critical aggregation concentration
$CDCl_3$	Deuterated chloroform
DMSO	Dimethyl sulfoxide
MTS	3-(4,5-dimethylthiazol-2-yl)-5-(3-carboxymethoxyphenyl)-2-(4-sulfophenyl)-2H-tetrazolium with phenazine methosulfate for cell viability

DMEM	Dulbecco's modified Eagle's medium
ELISA	Enzyme-linked immunosorbent assays
EDTA	Ethylenediaminetetraacetic acid
FBS	Fetal bovine serum
FTIR	Fourier transform infrared spectroscopy
HPLC	High performance liquid chromatography
HGF-1	Human Gingival Fibroblast
HA	Hydroxyapatite
THP-1	Immortalised human peripheral blood monocyte/ macrophage
IL-6	Interluekin-6
IL-8	Interluekin-8
LD_{50}	Lethal dose 50%
LOD	Limit of detection
LOQ	Limit of quantification
F_{max}	Maximum sample fluorescence emission
μABS	Maximum specific growth rate
l_o	Maximum tail length
mRNA	Messenger ribose nucleic acid
MBC	Minimum bactericidal concentration
MIC	Minimum inhibitory concentration
F_{min}	Minimum sample fluorescence emission
MCP-1	Monocyte chemoattractant-1
F_n	Normalised fluorescence emission
η_c	Number of carbons in the surfactant tail

NMR	Nuclear magnetic resonance
ANOVA	One-way analysis of variance
POPC	1-palmitoyl-2-oleoyl-sn-3-glycerophosphocholine
POPG	1-palmitoyl-2-oleoyl-sn-3-glycerophospho-1-glycerol
PMA	Phorbol 12-myristate 13-acetate
PBS	Phosphate buffered saline
RPMI	Roswell park memorial institute-1640 medium
F_s	Sample fluorescence emission
S. mutans	*Streptococcus mutans*
S. oralis	*Streptococcus oralis*
Si_3N_4	Silicon nitride
SD	Standard deviation
t	Time
TFA	Triflouroacetic acid
ti	Time to inflection point
Tris	Trizma hydrochloride
UV-Vis	Ultra violet visible
UWMS	Unsterilised whole mouth saliva
v_o	Surfactant tail volume

CHAPTER ONE

Introduction

1.1 General introduction

Poor oral health can lead to halitosis, tooth cavities, tooth pain, tooth loss and periodontal tissue destruction. These oral health issues are highly prevalent which suggests a usable solution to the issues in not commercially available. According to the World Health Organisation (WHO) worldwide, 60–90% of school children and nearly 100% of adults have dental cavities which often leads to pain and discomfort whilst gum disease (periodontitis), which may result in tooth loss and more serious systemic illness, is found in 15–20% of middle-aged (35-44 years) adults; Globally, about 30% of people aged 65–74 have no natural teeth proving that more research needs to be carried out in the field of oral healthcare to improve these figures (World Health Organisation., 2012). Some of the serious health problems that have been linked to periodontitis include dementia (Kamera et al., 2008; Abbayya et al., 2015) and heart disease (Meurman, et al., 2004; Ionel et al., 2016) and this has added an another aspect to the importance of maintaining good oral health.

One consequence of this is that the oral healthcare market is growing. It was estimated that the oral healthcare consumer market was worth £833m in 2010, a 1% rise on 2009; toothpaste accounted for £353m, followed by toothbrush sales, which were worth £237m, however, mouthwash sales grew the most between 2005 and 2010, by 44% (Marketing magazine., 2011). One advantage of using a mouthwash compared to toothpaste is that the therapeutic liquid covers the entire mouth evenly and so removes some of the risk of the consumer not being thorough in their tooth cleaning. In June 2013 the market was worth almost £1 billion, growing 4% in 2012 and is expected to have continued growth (Mintel., 2013). This vast market is driving research and development into new products to help maintain oral health and one key area is the prevention of plaque build-up in the mouth.

Plaque generation correlates with oral disease as its formation means saliva can no longer penetrate to the tooth surface and maintain bacterial composition homeostasis which is needed to protect enamel and prevent gum disease (Marsh., 1994). Therefore preventing plaque formation or reducing its formation by mechanical and chemical removal has been the maintenance of good oral health to date (Loe., 2000). A good oral health regime is thought to include brushing teeth twice a day followed by flossing and rinsing with mouthwash. However, despite such a regime being shown to be effective to prevent plaque development, oral health remains to be a problem.

One of the major issues that render it difficult to maintain good oral health in modern life is diet, in which there is a high sugar content. Bacteria can metabolise carbohydrates from sugar to produce acid deposits, which demineralise enamel and encourages the growth of select species of oral bacteria (Touger-Decker & van Loveren., 2003). It is unlikely that social attitudes to diet will change significantly to reduce the issue of sugar in the oral cavity and therefore oral health products need to be capable of tackling this issue. This leads to the second major issue in the fight against poor user compliance with oral health products. It has been found that oral care regimens that provide complete oral health care are among strategies that attract new customers and keep existing ones (GCI magazine., 2012). Current oral health products include active ingredients such as arginine which when metabolised in the mouth can increase pH, xylitol which is a non-fermentable sugar or include fluoride to strengthen tooth resistance to acid attack (Featherstone., 1999). These agents prevent/ protect against acid build-up and therefore protects against enamel demineralisation (Marsh & Bradshaw., 1997).

The introduction of antimicrobial agents has greatly enhanced the ability to control plaque growth (Wilson., 1996) with chlorhexidine digluconate (CHX) and cetylpyridinium chloride (CPC) being capable of interacting with cell surfaces leading to cell death and also having tooth surface binding to give an enhanced retention time in the mouth leading to higher therapeutic effects (Elworthy et al., 1996). However, these products were also found to stain teeth and reduce taste sensitivity leading to poor user compliance (Sheen & Addy., 2003). Other ways of controlling plaque growth have included Lauroyl Arginate Ethyl (LAE) which prevents bacterial attachment to the acquired pellicle (Gallob et al., 2015).

The search for new generation of antimicrobial agents to have comparable effects to CHX whilst not having the undesirable side effects has to date been unsuccessful. However, if a natural, multifunctional compound could be found to have similar antimicrobial properties it is likely that the side effects would be reduced and user compliance increased as natural products are perceived as being more beneficial. In addition, within the mouthwash market their appears to be a focus on antimicrobial agents with any reduction in inflammation incidents resulting from reduced bacterial loads but not influencing inflammatory processes directly, and so as gum disease is so prevalent it would seem beneficial to have a natural multimodal antimicrobial agent that also has inherent anti-inflammatory properties. In order to achieve this, a natural anti-inflammatory molecule could be chemically modified to incorporate antimicrobial activity and if needed improve hydrophilicity. However, there is a need to appreciate the oral microbiological environment, biofilm development, oral disease and the current range of topically applied oral hygiene products *i.e.* antimicrobials, stronger teeth *etc.* which will now be discussed.

1.2 Oral microbiota

The oral microbiota includes a vast range of bacteria with most of the organisms that colonize the mouth benefiting human health by adding to the defence against exogenous harmful species, however some of the microbiota are pathogenic and can, if not controlled, lead to oral health problems (Avila et al., 2009).

Bacteria are present in saliva, but due to desquamation, accumulation on the soft tissue in the mouth is limited. This is exemplified by the fact that a robust biofilm is not formed in the oral cavity of infants until tooth eruption (Marsh., 2000). Bacteria can accumulate on tooth surfaces because they are hard non-shedding surfaces; some areas of the tooth are more prone to greater plaque depth due to physical protection *e.g.* fissures on occlusal surfaces, and the gingival margin (Marsh & Bradshaw., 1995).

Teeth and the gingival margin create a subgingival environment that contains gingival curricular fluid (GCF), which is rich in nutrients and allows migrating bacteria from supragingival biofilms to form subgingival biofilms. However, it has been hypothesised that it is a shift in the subgingival microbiological composition from predominantly gram-positive bacteria to gram-negative bacteria that is the cause of gum disease (Berezow & Darveau., 2011). This is a different process than observed with the formation of dental caries, which often occurs when there is a shift in microbiological composition within the gram-positive species to more cariogenic species, *i.e.* an increased in the population of *Streptococcus mutans* species (Marsh., 2000).

The difference between gram-positive and gram-negative bacteria is the number of cell walls an organism has which is determined through staining techniques; gram-positive species have one cell wall and gram-negative have 2 cell walls. Therefore antimicrobial agents will have varying efficacy on these categories depending on the mechanism of action (Neu & Gootz., 1996; Silhavy et al., 2010). The compositions of these two categories and indeed species within these categories of bacteria vary in the mouth depending on a person's health, diet and oral hygiene, but if they are not controlled they aggregate and form oral plaque.

1.3 Oral plaque

Some of the oral microbiota organisms are capable of adhering to tooth surfaces through long range interactions, which become covalent and hydrogen bonds. Other species of the microbiota adhere to bacteria already bound to a non-shedding surface through cell-cell interactions or through other organic and inorganic material in the extracellular matrix; this organized structure of microorganisms and their products is referred to as dental plaque due to its yellowish colour and represents a true biofilm (Chandki et al., 2011). Early stage colonisers are often gram-positive streptococci species whilst later colonisers in a mature biofilm are often gram-negative. However, the initial tooth surface bacterial attachment requires a pellicle layer on the enamel surface which consists of proteins and displays receptors for the early colonising bacteria to bind. This complex multi stage process of oral biofilm development will now be discussed in the subsequent sub sections.

1.3.1 Pellicle formation

The tooth surface contains both calcium and phosphate groups and so is amphoteric and can bind both acidic and basic proteins despite its surface having a net negative charge (due to more phosphate group exposure at the surface) (Beachey., 1980). As a consequence the tooth surface eventually becomes coated with salivary proteins and other macromolecules including albumin, glycoproteins, acidic proline–rich proteins, mucins, sialic acids which provide receptors for pioneering bacterial colonisation (Kreth et al., 2009) (Figure 1.1). This layer can be at least partially removed by brushing with toothpaste but the pellicle layer is restored by proteins in saliva within minutes (Waaler., 2014). This protein layer is known as the acquired pellicle and is a major part of biofilm development as micro-organisms depend on this layer to adhere to the tooth surfaces. Despite the fact that the acquired pellicle allows biofilm formation, hence it can be viewed as a precursor to oral disease, it is thought to be beneficial to teeth due to the fact it forms a barrier protecting the enamel from abrasion and acid attack. However, as the yellowing of teeth is due to the staining of the acquired pellicle, from a cosmetic point of view, it is beneficial to completely remove it occasionally (Viscio et al., 2000).

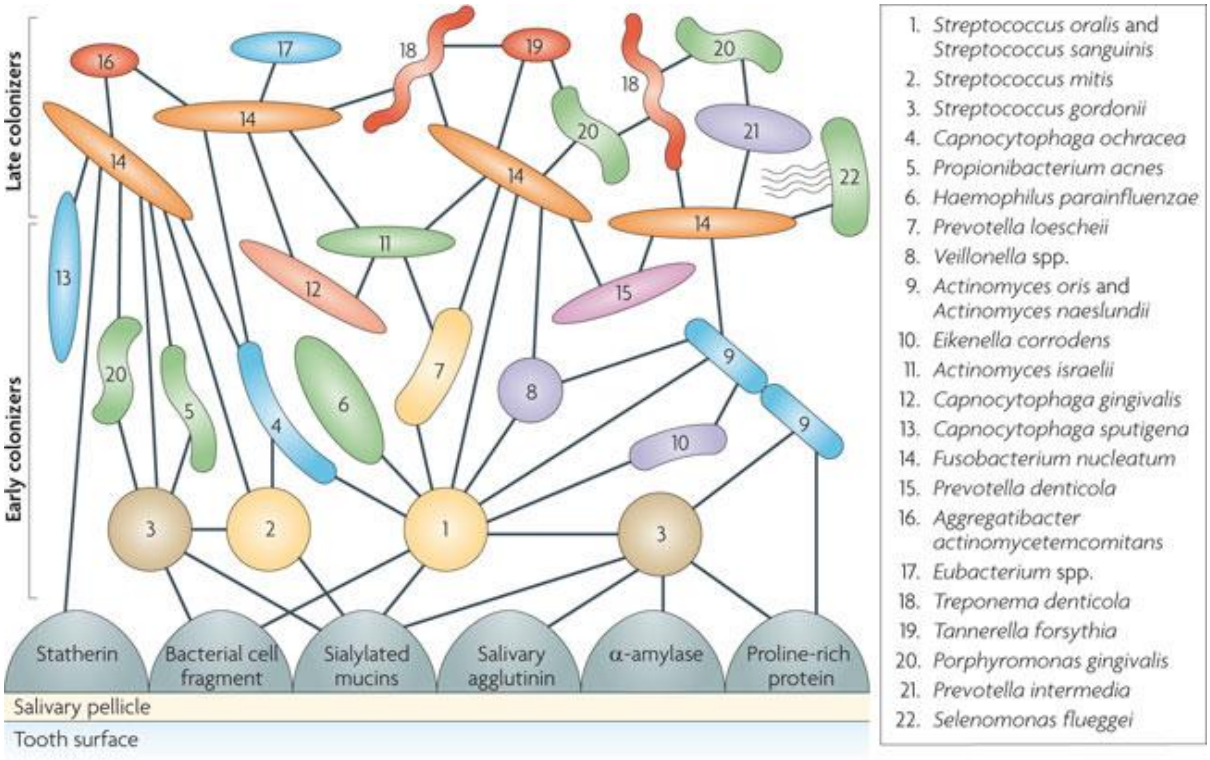

Figure 1.1. Selective interactions within an oral biofilm. (Kolenbrander et al., 2010).

1.3.2 Pioneering/ primary colonisers

Pioneering tooth colonising bacteria include streptococci species such as *S. mitis*, *S. oralis*, *S. sanguinis* and *S. gordonii* adhere irreversibly to different receptors on the acquired pellicle within 2-4 hours and then grow rapidly (Marcotte & Lavoie., 1998) (Figure 1.1). The reason why some species of streptococci bacteria successfully colonise the acquired pellicle is due to the expression of proteins on their surfaces which can interact with receptors in pellicle; this is an essential step in tooth surface colonisation and plaque development (Nobbs et al., 2009). It is thought that it is the fimbriae and fibrils proteins in the membranes of pioneering bacteria that have a strong affinity for pellicle receptors which gives them preferential binding after which the bacteria produce extracellular polymeric substance (EPS, predominantly alginic acid) which aids attachment (Huang et al., 2011). The pioneering bacterial colonizers then

allow the attachment of early colonisers through cell-cell surface interactions which in turn allows the colonisation of secondary colonisers.

1.3.3 Secondary colonisers

The secondary colonizers consist of gram-negative bacteria including *Fusobacterium nucleatum*, *Aggregatibacter actinomycetemcomitans* and *Porphyromonas gingivalis* (Kolenbrander et al., 2010) many of which are associated with gum disease. Like that of the pioneering bacterial colonisers (which require a bacterial surface protein to have a high affinity for a pellicle receptor), the secondary colonisers have varied surface proteins and lipopolysaccharide (LPS) that are recognised and have high affinity for certain early coloniser surface receptors or LPS. This selectivity for co-aggregation binding of secondary colonisers species to primary coloniser species can be seen in Figure 1.1.

1.3.4 Plaque maturation

Plaque structures are extremely complex and have multiple receptor binding sites on multiple co- adhered species of bacteria. The secondary colonizing bacterial species that adhere to the oral biofilm also produce EPS, it is estimated that once plaque has reached a mature state only 5-25% of plaque consists of bacterial cells whist 75-95% consists of the glycocalyx (tangled polysaccharide fibres), which often encases the bacterial cells; the oral biofilm does however contain many porous layers and water channels to provide the bacteria with essential nutrients (Huang et al., 2011). As biofilms mature there is a proportionality change from streptococci species to more gram-negative species, which has been attributed as a risk factor for gum disease. The risk factor is increased in mature plaque due to bacteria detaching from oral

biofilms as single cells or clusters; this dispersion has been explained by two hypotheses. Firstly as the biofilm matures, there is less nutrition available to bacteria or there is another undesirable change in the biofilm conditions (pH, oxygen tension and temperature) which result in some bacteria actively detaching in an attempt to find more favourable conditions. The second is that saliva flow which attempts to control plaque growth has an effect on passively dispersing surfaces of mature plaque through shear rate (Kaplan et al., 2010). The active dispersal of bacteria from oral biofilm to a planktonic state has been hypothesised as being a therapeutic target to reduce the proliferation of biofilm development (Filoche et al., 2010).

1.4 Oral plaque initiating disease

If oral plaque is left to proliferate and mature it is known to trigger oral health problems such as dental caries and gum disease. This is a consequence of a change in microbiological composition creating a disease risk biofilm hosting a high number of pathogenic bacterial species. The mechanistic causes and responses involved in both dental caries and gum disease will be discussed in the subsequent sub sections.

1.4.1 Enamel demineralisation/ remineralisation and dental caries

Enamel is the hardest substance in the human body. It coats the surface of teeth and is made up of 96% hydroxyapatite, 3% water and 1% organic matter. Tooth enamel is in a constant state of mineralisation and demineralisation; the tooth becomes mineralised *via* a controlled release of calcium and phosphate ions at neutral pH, but it can become mechanically eroded by attrition or demineralised by acid over time (Li et al., 2014). Acidic conditions can lead to the generation of white spot legions which can lead to cavity formation (Ferreira Zandoná et al., 2012). Below

the layer of enamel there is a material called dentin which has a lower composition of hydroxyapatite (70%) (Goldberg et al., 2011) and is therefore less resistant to abrasion and acid demineralisation (Mellberg, J. R. (1992). Cementum is the mineralised tissue that covers the entire root of the tooth and again has a lower composition of hydroxyapatite (50%) compared to enamel (Gonçalves et al., 2004). Proteins, in particular collagen are responsible for controlling the flux of ions into extracellular matrix, register signals that indicate when the mineralisation process should start and end and control the size to which the crystals will grow; collagen provides the template for mineral deposition in dentin and bone, without collagen the mineralisation process does not occur on a measurable time scale (Boskey., 2007). If the correct balance of oral bacteria is not maintained the tooth surfaces may become acidic (due to some bacteria's acidogenic behaviour). On average once the pH on the surface of the tooth reaches below 5.5, enamel demineralization occurs at a faster rate than mineralisation, although this differs slightly between individuals due to other biological parameters (Bowen., 2013). Also dentin and cementum are more susceptible to caries than enamel as they contain a lower mineral content, hence dental caries are more likely to form in cases of gingival recession and periodontal disease. The chemical equation for the process of acid based enamel demineralisation can be seen in equation 1.1.

$$Ca_{10}(PO_4)_6(OH)_2(s) + 8H^+(aq) \rightarrow 10Ca^{2+}(aq) + 6HPO_4^{2-}(aq) + 2H_2O(l)$$

Equation 1.1. Acid based enamel demineralisation (Stoker., 2012).

Harmful acid producing bacteria include *Lactobacillus acidophilus* and *Streptococcus mutans*. These bacteria are capable of breaking down sugars, such as sucrose *via* glycolysis to produce pyruvic and/ or lactic acid. However, when the numbers of these bacteria are kept in a healthy

number, the pH of the tooth surface is likely not to reach the 'critical pH' value of 5.5. It is only when there is debris, in particular sugar debris on the tooth surface that these harmful bacteria can produce more energy *via* glycolysis, resulting in more acid being produced and creating a lower pH environment that some beneficial bacteria cannot survive in but these bacteria multiply in. Hence a higher composition of harmful bacteria are produced which in turn produce more acid which in turn increase the number of cariogenic bacteria until the pH of the tooth surface reaches the critical pH value and demineralisation of enamel occurs. If the pH is not increased, then dental caries will form, this is the point at which tooth restructuring cannot occur (Islam et al., 2007). It has been noted that *S. mutans* in particular is capable of producing acid from metabolising sugars at a faster rate than other cariogenic bacteria, can survive and continue to produce acid at pH values that kill other streptococci species. *S. mutans* also produces three glucosyltransferases (GTFs) which catalyse the conversion of sucrose to glucans, a substance that is known to promote the adhesion of *S. mutans* to tooth surfaces. Hence *S. mutans* adhesion is sucrose dependent (Tao & Tanzer., 2002) and therefore research into GTF inhibitors is valuable. This section has illustrated the process of how cariogenic bacteria cause dental caries, a highly prevalent oral disease. However, gum disease is another prevalent disease caused by oral bacteria and will be discussed in the next section.

1.4.2 Gingivitis and periodontal disease

Gingivitis is a mild, reversible form of gum disease caused by an excess of gram-negative bacteria accumulated at the root of teeth as a result of supragingival plaque maturation. In particular *S. oralis* has been found to interact with common periopathogens such as *P. gingivalis*, allowing accumulation of gram-negative bacteria at supragingival levels and subsequent subgingival migration (Dziedzic et al., 2015). These bacteria produce

lipopolysaccharides (LPS), cytotoxic metabolites and immunoreactive molecules which irritate gingival tissue and result in an inflammatory response (Addy & Morann., 2000; Marsh et al., 2009). Gingivitis can usually be reversed with daily brushing, flossing and mouthwash (Witt et al., 2006). However, if not treated, it can lead to periodontitis (inflammation around the tooth) which is a severe chronic condition (Pihlstrom et al., 2005).

Inflammation is a biological response of vascular tissues to harmful stimuli and is a localised protective response to eliminate infection and to initiate healing (Handfeild et al., 2008). Microbiological composition change of subgingival plaque has the ability to induce a hyperimmune response which over time destroys gingival connective tissue; certain species of bacteria can also manipulate the immune response to their advantage (Ai et al., 2017). Periodontitis begins when supporting tissues of the teeth are attacked which can result in a breakdown of bone and connective tissue that hold teeth in place, the teeth may eventually become loose and have to be removed.

Therefore gingivitis can initiate the periodontitis process if untreated (remove plaque). Periodontitis allows harmful bacteria to areas in the mouth that were previously inaccessible (Sagile et al., 1982). In periodontitis, the junction epithelium at the base of the gingival crevice migrates down the root of the tooth to form a deeper periodontal pocket (from 1-2 mm to ≤ 5 mm) and is an ideal environment for the proliferation of microbes (Phaechamud & Setthajindalert., 2017). This pocket is highly anaerobic and preferentially attracts bacteria that do not metabolise carbohydrates but are proteolylic. As a result of this the pocket increases in pH to between 7.4-7.8 compared to a healthy value of 6.9 (the opposite of dental caries causing bacteria) (Marsh & Martin., 1992). This slightly basic condition allows periodontal pathogens like *P. gingivalis* to have enhanced growth (again opposite to dental caries causing bacteria).

Gingivitis is thought to affect every member of the human population at some stage and is the non-specific proliferation of the normal gingival crevice (Marsh et al., 2009). This is a common disease in developed countries and it is estimated that 5-10% of UK adults are particularly susceptible to periodontal disease and with an ageing population chronic periodontitis represents a significant healthcare burden with 85% of adults over 65 having periodontal destruction (Renz et al., 2007). These findings show that although antimicrobials are important in oral healthcare to prevent inflammation, anti-inflammatory agents are required to control the inflammatory response.

Therefore periodontal bacteria cause destruction of gingival tissue in two ways. Firstly, in a direct action of bacterial enzymes and the cytotoxic products of bacterial metabolism. Secondly, in an indirect response by where tissue destruction is a side-effect of a subverted and exaggerated host inflammatory response to plaque antigens, this has been termed 'bystander damage' (Hasan & Palmer., 2014). This indirect response is made more severe by the proteases of *P. gingivalis* deregulating the host control of inflammatory response and evades the action of other components of the immune response (How et al., 2016). Some other periodontal bacteria can however inactivate the host antimicrobial pathways by degrading peptides and enzymes. The entire immune response is dependent on complex intercellular signalling networks mediated by cytokines which some periodontal bacteria can manipulate (Marsh et al., 2009). Therefore the entire immune response is due to cellular signalling and so there appears to be two major ways of inhibiting this action. Firstly to use antimicrobial treatment so the inflammatory signals are not triggered and secondly to use an anti-inflammatory that is capable of inhibiting the signalling cascade and/ or have a selective toxic effect on recruited white blood cells in order to control the inflammatory response.

The initial response to bacterial irritation to the gingival margin is a humoral response, which is a non-cell mediated immune response and includes antibodies, proteins and small molecules (Cekici et al., 2014). During an inflammatory response gingival vasodilation also takes place due to vasoactive amine and prostaglandin release from cyclooxygenase enzymes whilst gingival cells generate intercellular adhesion molecule (ICAM-1) on their surfaces which complement adhesion molecules on the surface of polymorphonuclear leukocytes (PMN's, white blood cells) on arrival (Page., 1991). Vasodilation is the widening of blood vessels that result in an increased blood flow to the infected area and increased vascular permeability which allows required diffusible components (PMN's and monocytes) to the infected area. This leads to increased redness and gums that are more prone to bleeding. This mechanical process leads to the gum tissue parting from teeth and the jaw bone. Periodontal pockets are formed and thus accumulate bacteria; these bacteria can then initiate the destruction of bone structure leading to periodontal disease by producing toxins (direct response) that provoke further immune response (indirect response) (Cekici et al., 2014). The vasodilation which also allows peripheral white blood cells to access the infected area and engulf invading bacteria can also allow bacteria to enter the blood stream and initiate a systemic illness.

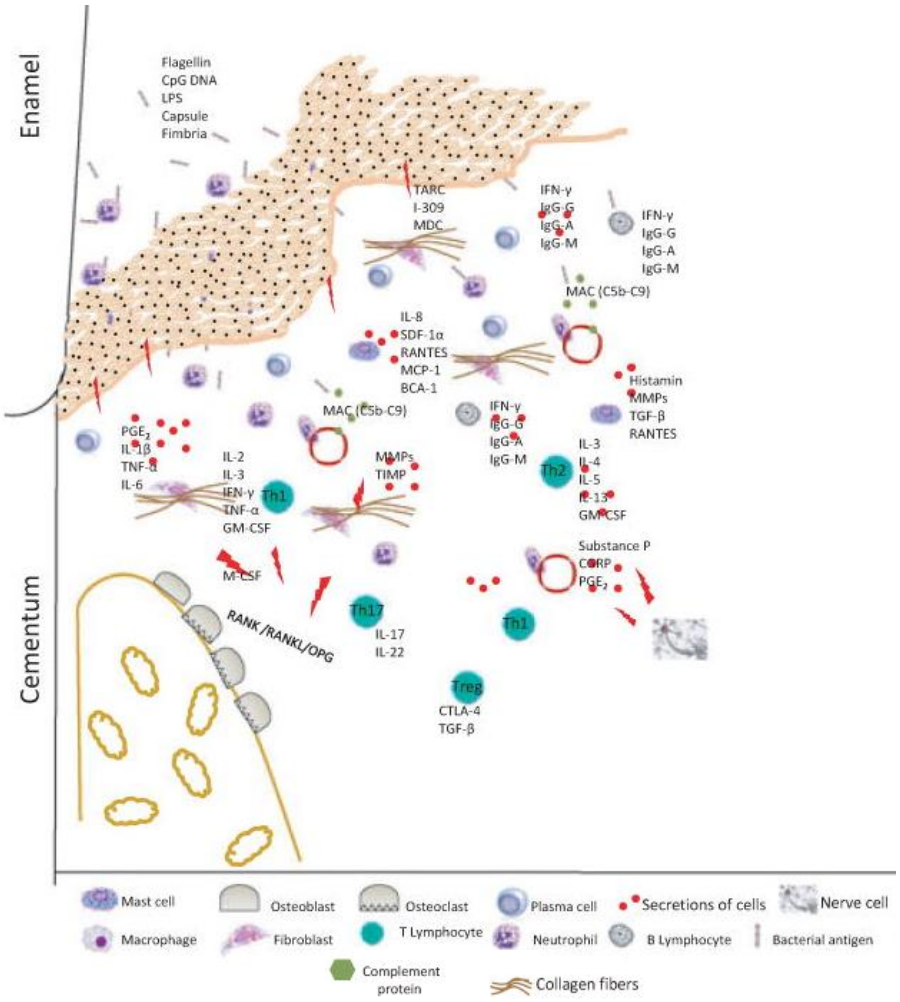

Figure 1.2. The complex immune inflammatory response in periodontal disease (Cekici et al., 2014).

Any subgingival bacteria can be associated with contributing to tissue destruction *via* indirect pathogenicity, if the bacterium is provoking a host inflammatory response. Bacteria (usually from gram negative bacteria) can release antigens *e.g.* LPS from the bacterial cell wall and can penetrate crevicular epithelium stimulating humoral or cell mediated immunity (Marsh et al., 2009) as cell receptors recognise these compounds are produced by bacteria and indicate bacterial invasions and so the cells respond through cytokine release to signal for an immune response to eradicate the invading bacteria.

Humoral immunity also leads to the release of cytokines which then initiates a cell immunity including activated T-lymphocytes which regulate macrophage activity (ingest dying cells) (Silva et al., 2015). Activated macrophages can then release more cytokines including TNF-α (Tumour Necrosis Factor – alpha), IFN-γ (InterFeroN – gamma), interleukin and monocyte chemoattractant proteins (Madianos et al., 2005). Pro-inflammatory cytokines *i.e.* TNF-α, IL-1 and IL-6 promote osteoclast activity causing bone resorption and can induce metalloprotease (MMP) activity which continue the degradation process (Heinz et al., 2015). Other proteolytic degradation enzymes include elastase and cathepsin-b which are both present in an inflamed gingival crevice and are likely to be derived from polymorphs, macrophages and fibroblasts (Eley & Cox., 1992). Mast cells can also gain access to periodontal pockets which release histamine and other vasodilator molecules as well as a range of chemokines and proteases (Sushma et al., 2013). Cells in the gingival crevice can contain protease inhibitors which are capable of inactivating proteases hence regulating the potential destructive forces of inflammation, however bacterial proteases are capable of degrading these regulators adding to 'bystander damage' (Laugisch et al., 2012).

Phagocytic cells form the main defence against periodontal pathogens but if not controlled can cause irreversible periodontal damage and some bacteria can evade the immune response all together. Strains of *A. actinomycetemcomitans* produce powerful leukotoxin capable of lysing human neutrophils, monocytes and lymphocytes whilst non-white blood cells *i.e.* epithelial and endothelial cells, fibroblast and erythrocytes are resistant, this allows periodontal pathogens to control (immunosuppressant) the host defences reducing tissue damage from the immune response but increasing it from the bacteria's toxins (Aberg et al., 2015). Bacteria including *A. actinomycetemcomitans, T. forsythia, P. gingivalis*, and other pathogens may also evade the host defences by invading epithelial cells intracellularly (Tribble & Lamont., 2010). In addition

P. gingivalis possesses a capsule, which protects cells against phagocytosis (Singh et al., 2011). Therefore antimicrobial agents are required to reduce the risk of the gram-negative composition increasing (through direct effect or inhibition the initial growth of plaque).

One cytokine often released is TNF-α which stimulates leukocyte (neutrophils, monocytes) adhesion through further causing monocytes/ PMN's to express adhesion molecules on their surface to interact with ICAM-1 on endothelial cells. It also increases the synthesis of prostaglandins (PG's), however, PG's in particular PGE2 limit the destructive nature of excessive TNF-α and in this respect reduce inflammation response (Gitlin & Loftin., 2009). In addition it recruits more monocytes and PMN's to the infected area. Other cytokines often generated from oral tissue upon bacterial irritation are interluekin 8 (IL-8) and monocyte chemoattractant-1 (MCP-1), these are key chemoattractants in neutrophil and monocyte recruitment respectively which if not controlled can lead to periodontal destruction (Fitzgerald & Kreutzer., 1995). IL-6 is another prominent cytokine in gingival inflammation and is responsible for the upregulation of antibodies, T (produce toxic granules) and B (produce antibodies) cell differentiation, increases vascular permeation and osteoclast (bone resorption) differentiation but can downregulate other pro-inflammatory cytokine expression (Nibali et al., 2013). Therefore an anti-inflammatory agent is required to allow a measured immune response.

1.5 Chemical prevention of oral disease

It has been observed that the mechanical removal of plaque through the means of saliva flow and brushing of teeth is not enough to prevent oral disease. Brushing of teeth in particular is not done often/ thoroughly enough to inhibit plaque formation whilst extensive brushing can lead to enamel erosion. Therefore there are a number of commercial products including

dentifrices and mouthwashes that contain chemical means of preventing tooth demineralisation and gum inflammation. The chemicals used in these products include bacterial adhesion controlling agents, bacterial composition controlling agents, tooth hardening agents and anti-inflammatories but to a large extent contain antimicrobial compounds.

1.5.1 Antimicrobials to control oral plaque growth

Antimicrobial agents have been used to treat disease for many years and can be classified as having bacteriostatic or bactericidal effects; a bacteriostatic effect refers to the agents ability to keep bacteria in a stationary phase of growth for an extended period of time whilst a bactericidal effect refers to an agents ability to kill bacteria, although in reality bacteriostatic agents commonly have some kill efficacy and bactericidal agents often do not kill the entire bacterial burden (Pankey & Sabath., 2004).

There are several different types of antimicrobial agents including biocides which are substances that specifically destroy microbes, antibiotics that treat disease through specific cellular targets which require entry into metabolically active cells (often suffer from bacterial resistance), antiseptics used externally on living tissues to supress bacterial growth to prevent disease and disinfectants which are used on non-living tissue to destroy microorganisms (McDonnell & Russell., 1999). In oral healthcare, antiseptics are used to control oral plaque growth but there are a wide range of these antimicrobial agents employed in different product that have different physicochemical properties and various mechanisms of action. These will be discussed in the subsequent sub sections.

1.5.1.1 Bisbiguanides

Chlorhexidine is considered the most effective antimicrobial agent since the 1950's and has been used in mouthwash since the 1970's. It is a substantive, potent oral antiseptic that reduces the population of many bacterial streptococci species through its ionic interference with cell membranes (Balagopal & Arjunkumar., 2013; Ferretti et al., 1990). Chlorhexidine inhibits oxygen utilisation by bacteria and this induces a subsequent fall in cellular ATP levels that results in a loss of periplasmic enzymes (degrade compounds to a utilizable form) in the cell membrane (Barrett-Bee et al., 1994). It is chlorhexidine's cationic charge that interacts with the negatively charged components in bacterial cell walls, which causes disruption. The agent is rapidly internalised bacteria and it interferes with osmosis. Once chlorhexidine hits the inner membrane, it ruptures it and this causes leakage of components leading to cell death. Chlorhexidine has been used in periodontitis in the form of a gelatine chip, which is placed in the gum pocket to destroy periodontal bacteria (Nair & Anoop., 2012). However, liquids containing chlorohexidine can have an unpleasant taste, deliver a burning sensation and it can stain teeth (Flotra et al., 1971). Therefore, it is typically recommended in many circumstances for only short-term use.

1.5.1.2 Quaternary ammonium compounds

Cetylpyridinium chloride is a less potent agent compared to chlorohexidine. It does not show a high degree of bio-retention and hence it is less effective against plaque and preventing gingivitis (Eley., 1999). Cetylpyridinium chloride still reduces bacterial adhesion, interferes with cell membranes and it has less side-effects compared to chlorohexidine (Sheen & Addy., 2003). Cetylpyridinium chloride also has a more significant impact on gram-positive bacteria

over gram negative bacteria (Pitten & Kramer., 2001; Mcdonnell & Russle., 1999). This compound is used in Colgate Total Pro Gum Health Mouthwash® as an bacteriostatic and inflammatory prevention agent. CPC is an amphiphilic molecule that aggregates in aqueous vehicles (Mukhim et al., 2010).

1.5.1.3 Triclosan

Triclosan is a biocide agent that has been used in oral, dermal and other household products over the last 50 years. It is thought to have multiple mechanisms of action ranging from cell wall disruption to enzyme inhibition and hence it is useful in overcoming antimicrobial resistance (Yazdankhah et al., 2006). It has been found to be active against yeast, gram positive and gram negative bacteria. It has therefore been formulated with polymers to improve its retention time and other antimicrobials, *i.e.* metal salts, that have been shown to have a synergistic effect (Brading & Marsh., 2003).

1.5.1.4 Metal salts

Using metal ions as anti-plaque agents is desirable as they do not induce tooth staining or other undesirable side-effects (Harrap et al., 1983). Perhaps one of the most commonly used antimicrobial metal salts is stannous fluoride (SnF_2). This antimicrobial agent has been of great interest since the 1980's and is still widely used today to improve oral health. The antimicrobial effectiveness of SnF_2 has been tested on bacterial plaques in chronic periodontal disease and has been found to alter morphological groups (composition of different shaped bacteria *i.e.* rods, spherical) of subgingival and supragingival plaque bacteria. It has been found that by using 1.64% SnF_2 causes a significant and sustained decrease in subgingival motile bacteria

and spirochetes, after six weeks bacteria was halved in concentration (Mazza et al., 1981). The antimicrobial active in SnF_2 is thought to be fluoride not tin. However, the tin component allows fluoride to be present at effective antimicrobial concentrations in the mouth whilst remaining non-toxic. Fluoride as well as strengthening enamel also has been shown to reduce the number of bacteria in cariogenic plaque, it is thought to effect bacterial metabolism and viability. Fluoride antimicrobial effectiveness depends on the organism, type of compound, concentration, pH and retention time of the species. It has been found that fluoride can be effective in reducing plaque and gingivitis severity (Mazza et al., 1981). However, the activity of SnF_2 in inflammatory conditions is debatable. One study found that 0.4% and 0.22% SnF_2 and sodium fluoride respectively resulted in no difference in gingivitis, bleeding or amount of bacteria when compared to a placebo group after 18 months of treatment (Wolff et al., 1989). However, a later study found that stabilising the SnF_2 with sodium gluconate did reduce gingivitis after 6 months (Beiswanger et al., 1995).

Another commercially tested antimicrobial metal is zinc. It has been found to adsorb to *S. mutans* and inhibit its ability to metabolise glucose to lactic acid, a process essential for the growth of bacteria. Zinc is also active against *S. sanguinis* and *A. naeslundii* through a similar mechanism. It is thought that zinc inhibits essential enzymes in the transport and metabolism of glucose including phosphotransferase transport system (PTS), sulphydryl enzymes and glyceraldehyde dehydrogenase. However, *S. mutans* can uptake glucose *via* two pathways, firstly, the PTS mechanism (which zinc inhibits) and secondly a metabolism driven by the energy of proton electro-chemical gradients (PMF, which zinc does not directly inhibit). PMF is important at low pH and although it is not inhibited by Zn^{2+} it is inhibited by Na^{+} (Cummins., 1991; Devulapalle & Mooser., 1994). Inhibiting glucose metabolism has the consequence of inhibiting acid production. The inhibition of acid makes zinc a good bacteriostatic agent. As

zinc inhibits both plaque formation and acid generation it is able to prevent both gingivitis and dental caries whilst keeping a healthy composition of bacteria in the mouth.

In addition to zinc inhibiting bacterial metabolism it is thought that it reduces bacterial colonisation by either modifying cell surfaces, altering cell proteins, inhibiting protease induced adhesion or attachment to cell membranes reducing negative charge (Cummins., 1991). These zinc antimicrobial properties have a modest but significant effect on reducing salivary bacterial counts (Addy et al., 1980). Plaque growth is also inhibited both *in vitro* and *in vivo* dose dependently but efficacy is reduced if bacterial growth time is increased before treatment (Harrap et al., 1983). This suggests that zinc salts are unable to effectively penetrate mature plaque and so cannot be a replacement for the mechanical removal of plaque. Zinc oxide (ZnO) increases *C. jejuni* membrane permeability, induces membrane leakage and when internalised causes a large amount of oxidative stress resulting in reducing cell growth and cell death (Xie et al., 2011). It may also undergo transmetallisation with vital metals hindering bacterial metabolism and growth. However, using zinc salts have previously given variable results; this is likely due to varying concentration or interference of the counter ion (Harrap et al., 1983).

1.5.1.5 Essential oils

Essential oils derived from plants have been used for their antioxidant, anti-cancer and antimicrobial effects for decades, but they have become more popular in recent times due to consumer perceptions that natural therapeutic agents are favourable to molecules due to safety concerns (Seow et al., 2014). Essential oils including menthol, thymol, methyl salicylate, and eucalyptol have been found to have bacteriostatic and bactericidal effect though cell wall

disruption and enzymatic inhibition. They can only be used at low concentrations due to poor water solubility but they are used in the Listerine® products. Essential oils display an optimal anti-biofilm effect when formulated with alcohol (Erriu et al., 2013).

1.5.2 Non-antimicrobial targets in oral health products

In addition to the various bacteriostatic and bactericidal antimicrobial agents used to maintain good oral health there are other agents employed which inhibit oral disease by other means *i.e.* inhibiting bacterial attachment, making teeth harder and controlling biofilm pH which will all be discussed in the subsequent sub sections.

1.5.2.1 Lauroyl arginate ethyl (LAE) inhibition of biofilm growth

LAE inhibits plaque build-up by forming a physical barrier that prevents the adherence of bacteria to tooth surfaces. Through this mechanism it elicits its anti-plaque and anti-gingivitis effects. Delmopinol is thought to work in a similar manner to LAE but unlike delmopinol, LAE is not considered to have a have a bacteriostatic or bactericidal antimicrobial response and so can be considered a medical device rather than a drug which makes regulatory approval easier for products containing this agent (Gallob et al., 2015).

1.5.2.2 Stronger teeth with fluoride

Fluoride inhibits enolase (an enzyme containing two magnesium atoms, which catalyses fermentation of sugars to lactic acid) by binding to the active site instead of PG

(phosphoglycerate). Enolase is responsible for the penultimate (9^{th}) step of glycolysis (Qin et al., 2006). Fluoride is perhaps more renowned for strengthening teeth against the acid dependent tooth demineralisation process. This is because fluoride can become a part of the enamel crystal structure, replacing the hydroxyl groups, generating fluorapatite ($Ca_{10}(PO_4)_6)F_2$ which is a less acid soluble mineral than hydroxyapatite (Featherstone., 1999).

1.5.2.3 Stronger teeth with zinc

Zinc is also thought to have a role in biomineralisation, where it stimulates both bone growth and mineralisation and influences osteoclast activity. Retardation of bone growth in animals is commonly associated with conditions linked to zinc deficiency; also reduced bone density has been linked to a zinc-deficient diet. Zinc is found naturally in saliva (0.0465 PPM to 0.244 PPM) and plaque (7.86 PPM to 31.6 PPM) (Fatima et al., 2016). As zinc is naturally abundant in the mouth it is thought that a relatively large amount of zinc is incorporated into enamel prior to tooth eruption, however, after eruption the concentration of zinc in the surface of enamel increases. Therefore zinc is likely to be incorporated during the constant demineralisation and remineralisation of enamel. This is likely to be beneficial because enamel with zinc content has reduced acid solubility and may be more resistant to acid attack. However, zinc can inhibit the enamel remineralisation process but zinc adsorbed to enamel can be displaced by calcium or an overgrowth of newly deposited minerals takes place to minimise the negative effect of inhibited remineralisation. Therefore using zinc as an antimicrobial agent is likely to also have an effect on increasing the resistance of enamel to dental caries (Lynch., 2011).

1.5.2.4 Arginine in controlling cariogenic bacteria

Oral bacterial biofilms consist of a variety of both acidogenic and arginolytic/ ureolytic bacterial strains which form part of the dynamic equilibrium between hydroxyapatite demineralisation influenced through acid generation, and remineralisation influenced through alkali generation which allows calcium and phosphate supersaturation. It is favourable to maintain conditions that promote arginolytic and to a lesser extent ureolytic bacteria in microflora because the acidogenic bacteria such as *Lactobacillus casei* and *S. mutans* ferment carbohydrates (which are in excess in modern diets) to generate acid and increase acidogenic bacterial composition (Wijeyeweera & Kleibergn., 1989; Sharma et al., 2014). Arginolytic bacteria including *Streptococcus gordonii* and *Streptococcus sanguinis* can catabolise arginine through the arginine deiminase system (ADS) producing ammonia, bacteria that express ADS maintain biofilm pH neutrality and are associated with dental health (Huang et al., 2016). Therefore, the use of arginine in oral health products has been reported to reduce the risk of dental caries by being a nutrient for non-cariogenic bacteria and raising plaque pH (Tada et al., 2016).

1.5.3 Anti-inflammatory agents to prevent and/ or treat gum disease

When considering the high incidents rate of gum disease in people worldwide it is perhaps surprising to find that there are a limited number of anti-inflammatory agents used in mouthwashes compared to antimicrobials. Non-steroidal anti-inflammatory drugs (NSIAD's) are frequently used as dentistry pain relief treatments but not to prevent periodontal disease. Therefore an approach to both prevent and treat gum disease simultaneously would be desirable to minimise the possibility of periodontal destruction but such a product does not yet seem to

exist with the potential exception of those that contain triclosan. Products that contain triclosan and diclofenac inhibit prostaglandins which are only one small part of the gum disease process. Subanitmicrobial dose doxycycline has been found to have a wider spectrum of oral anti-inflammatory properties but appears to be the only one and therefore other anti-inflammatory's should considered. The use of these oral anti-inflammatory agents will be discussed in the following sub sections.

1.5.3.1 Triclosan

It is thought that some phenols are not only antimicrobials but also may prevent gum disease through anti-inflammatory properties. For example, triclosan inhibits COX, lipoxygenase pathways, cell mediated immunity, mRNA expression, translocation of NF-Kb (a protein that controls the transcription of DNA) and inhibition of IL-1β and IFN-γ. (Sreenivasan & Gaffar., 2008) but this is only a small area of the overall gingival inflammatory process.

1.5.3.2 Diclofenac

Diclofenac an NSAID (Non-Steroid Anti-Inflammatory Drug) is found in mouthwashes such as Disoral®. It is known to inhibit the formation of prostaglandins and thromboxane which are pro-inflammatory molecules as well as having a stabilizing effect on cell membranes, allowing membranes to have a higher tolerance to pro-inflammation molecules (Segre & Hammarström., 1985). Diclofenac is commonly used to treat gum inflammation and relieve pain in mouthwash but is not used to prevent it (Serafini et al., 2012).

1.5.3.3 Subantimicrobial doxycycline

Doxycycline is a member of the tetracycline family. At subantimicrobial dosages doxycycline has been found to have anti-inflammatory properties on some biomarkers including IL-6, IL-8 and TNF-α (Di Caprio et al., 2015). These non-antimicrobial anti-inflammatory properties also overcome the problem of encouraging antimicrobial resistance. In addition subantimicrobial doxycycline has been found to inhibit MMP and osteoclast activity, reducing gingival connective tissue destruction and periodontal bone resorption (Golub et al., 2009) but this is the only product to do so and by definition does not have antimicrobial properties.

1.5.3.4 Vitamin E

Naturally occurring vitamin E is a biologically active agent and a well-known anti-inflammatory agent but is not currently used in oral health. It is found in vegetable oils such as corn, rapeseed, soybean and sunflower oil and was discovered in 1922 by Evans and Bishop as an essential nutrient for reproduction in rats (Gliszczyńska-Świgło et al., 2007; Zingg et al., 2010). Since its discovery the importance of tocopherols (vitamin E) have increased in the pharmaceutical and food industries, this is due to their antioxidant properties inhibiting lipid oxidation and quenching reactive singlet oxygen species. Epidemiological tests indicate beneficial effects against atherosclerosis, cardiovascular disease, some cancers, Alzheimer's and Parkinson's disease as well aging process in general (Lienau et al., 2002). Vitamin E functions as a chain-breaking antioxidant that prevents the propagation of free radical reactions (Nishio et al., 2011). There has been increasing interest in the structural variations of tocopherols and this has led to additional applications of these agents in health including their use as anti-inflammatory agents.

1.5.4 Natural isomers of vitamin E and their anti-inflammatory properties

The tocopherol isomers (Figure 1.3) only differ with respect to their aromatic methyl group structure.

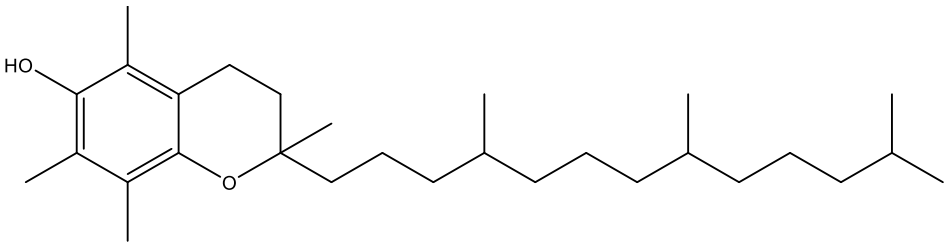

α-tocopherol

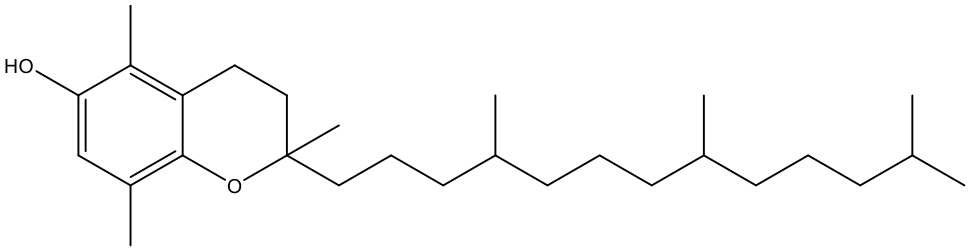

β-tocopherol

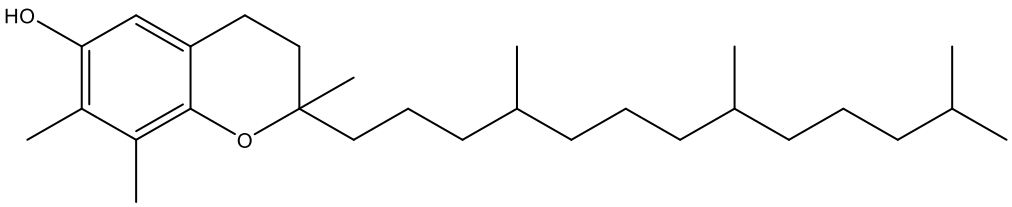

γ-tocopherol

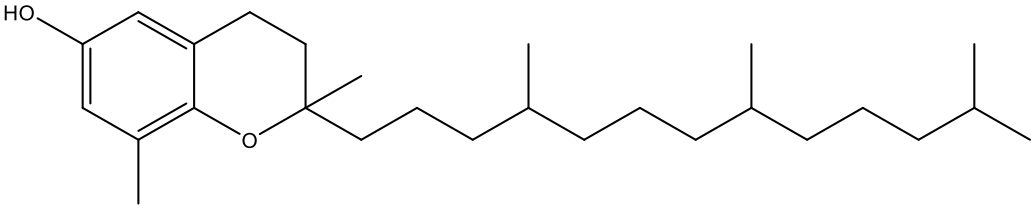

δ-tocopherol

Figure 1.3. Geometric isomers of vitamin E; tocopherols.

They also have the structure of non-ionic surfactants and have been found to self-assemble in aqueous environments (Wa & Gebicki., 1983). The small changes in the molecule architecture can make a profound difference to the aggregate architectures, bioactivity and biological function of each species. The tocotrienol isomers (Figure 1.4) have an identical Greek alphabet labelling system. However, in these cases three alkene groups can be found on the carbon 'tail' of the molecules, which makes these molecules non-chiral.

It is widely recognised that tocopherols/ tocotrienols are antioxidant agents by acting as hydroxyl radical scavengers. They maintain cellular integrity *via* protecting polyunsaturated fatty acid moiety's of phospholipids. Vitamin E has also recently been found to elicit anti-inflammatory properties by inhibiting cytokine production leading to a reduction in IL-1β, IL-6 and TNF-α production (Tahan et al., 2011). The anti-inflammatory activity of vitamin E is achieved by blocking the activity of NF-κB (proinflammatory gene regulator, controls glycoprotein mediating leukocyte-endothelial and marker of active inflammation, this is up regulated in inflammation) which leads to a decreased production of pro-inflammatory cytokines (Mirbagheri et al., 2008). In addition, it is thought that vitamin E reduces F2-isoprostanes produced by COX.

α-Tocopherol (α-T) is the most abundant form of vitamin E in nature, it generally has the highest biological activity and has signalling functions in vascular smooth muscle cells it decreases protein kinase C activity, increases phosphoprotein phosphatase 2A activation and controls expression of the α-tropomyosin gene that other forms of tocopherol with similar antioxidant properties cannot (Brielius-Flohe & Traber., 1999). α-T is thought to do this by affecting binding affinity between neutrophil and endothelial cells by decreasing the expression of adhesion molecules on endothelial cells (Mirbagheri et al., 2008).

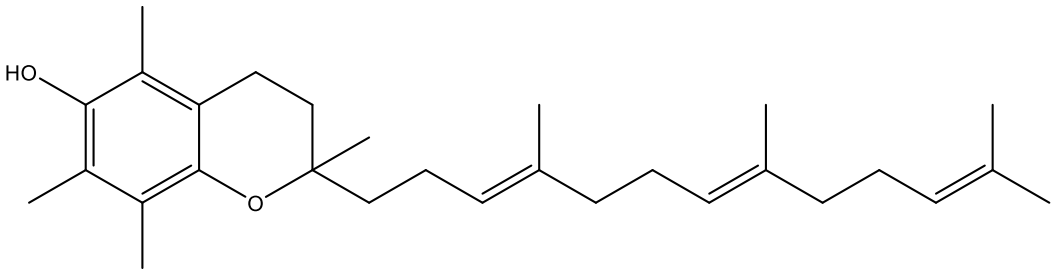

α-tocotrienol

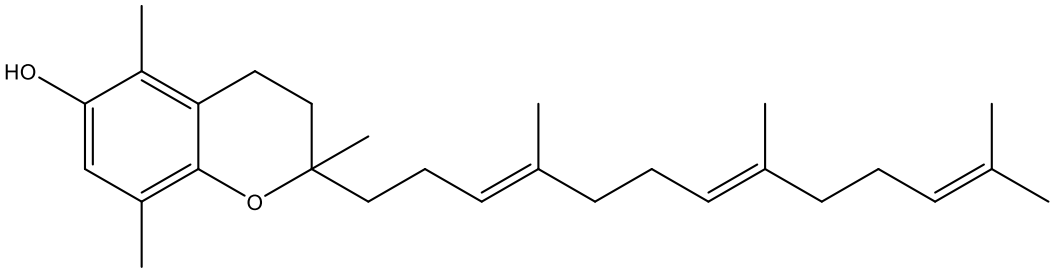

β-tocotrienol

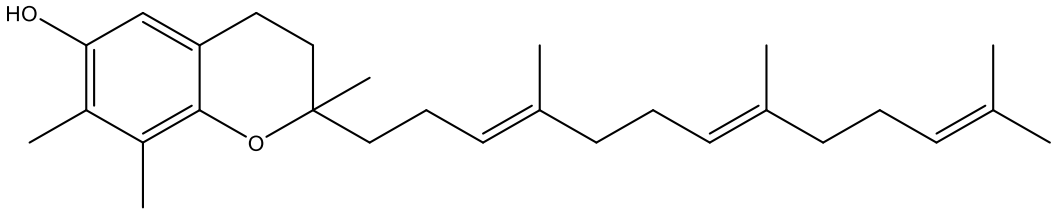

γ-tocotrienol

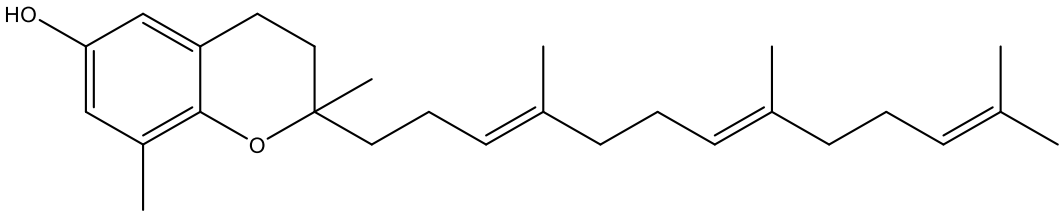

δ-tocotrienol

Figure 1.4. Geometric isomers of vitamin E; tocotrienols.

γ-T is found in nuts, seeds and vegetable oils and has been found to promote health and protect against disease predominantly defending against reactive nitrogen species (NOS). Furthermore it has been found to reduce inflammation, prevent certain types of cancer and activate genes that protect against Alzheimer's disease. γ-T has anti-inflammatory properties as it inhibits COX-2, this is a property not shared with α-T. γ-T also acts as a powerful nucleophile that traps electrophilic mutagens. Thus γ-T may protect lipids, DNA and proteins from peroxynitrte-dependent damage (Brielius-Flohe & Traber., 1999). This point demonstrates the sensitivity that the geometric structures of vitamin E have on their respective therapeutic properties. In this case one methyl group changes anti-inflammatory properties from decreasing binding affinity between neutrophil and endothelial (α-T) to the inhibition of COX-2 (γ-T) with the first acting as a signalling molecule and the second as an enzyme binding inhibitor.

Recent studies have shown that the reason the α-T has the highest bioactivity is due to it preferentially appearing in plasma after passage through the liver. The reason for this is thought to be α-T is binding to the α-tocopherol transport protein (Brielius-Flohe & Traber., 1999). Although this is not directly relevant to oral healthcare it does show that the human body is preferentially increasing α-T in plasma for some reason, possibly because it is the tocopherol with the most beneficial properties.

1.5.5 Stereo isomers of vitamin E

In addition to the 8 geometric isomers of vitamin E listed in section 2 there are a further 8 stereoisomers associated with each tocopherol isomer which can be seen in Figures 1.5 and 1.6 (R symbols represent either H or Me depending on geometric isomer).

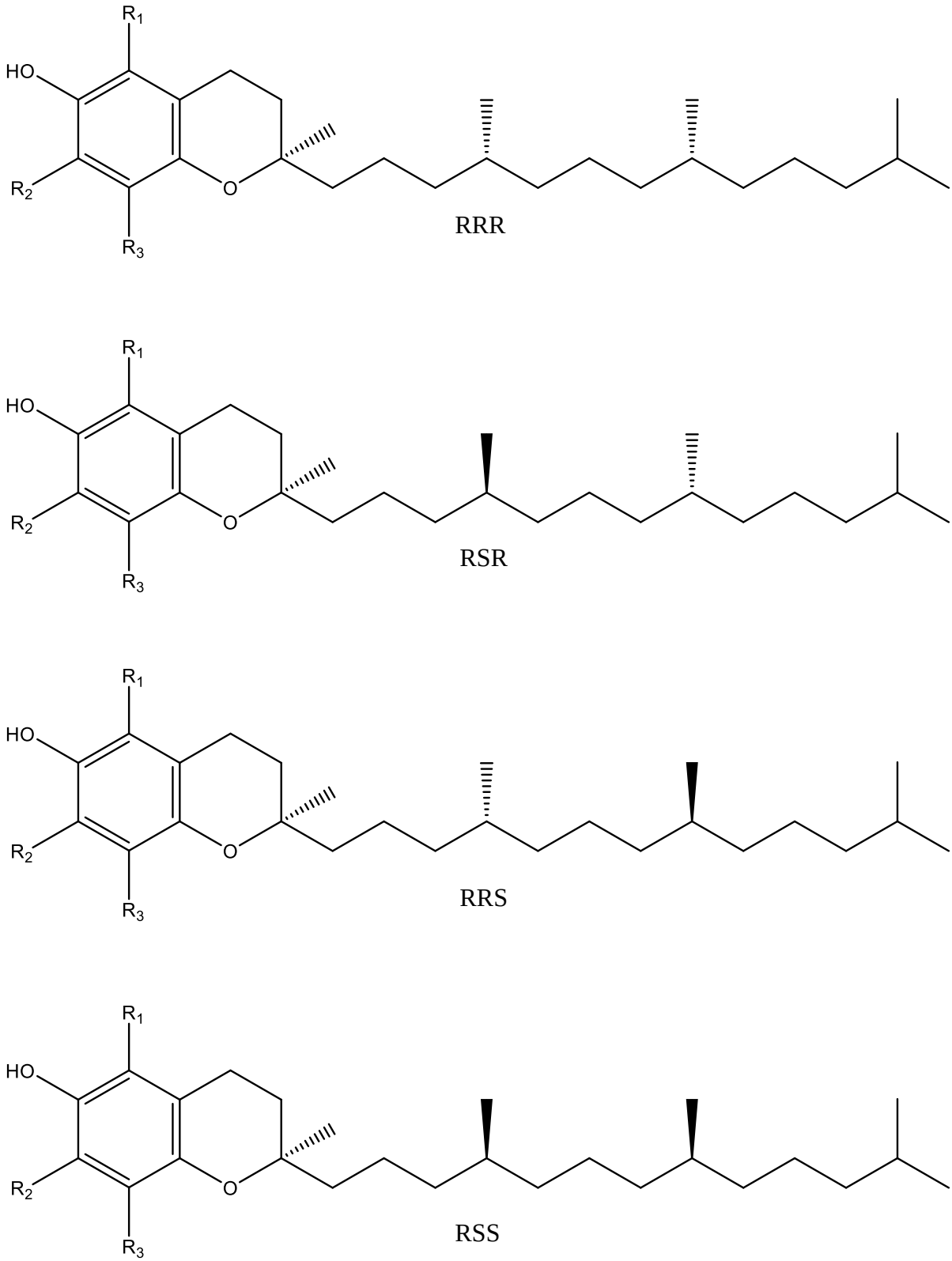

Figure 1.5. Stereoisomers of vitamin E.

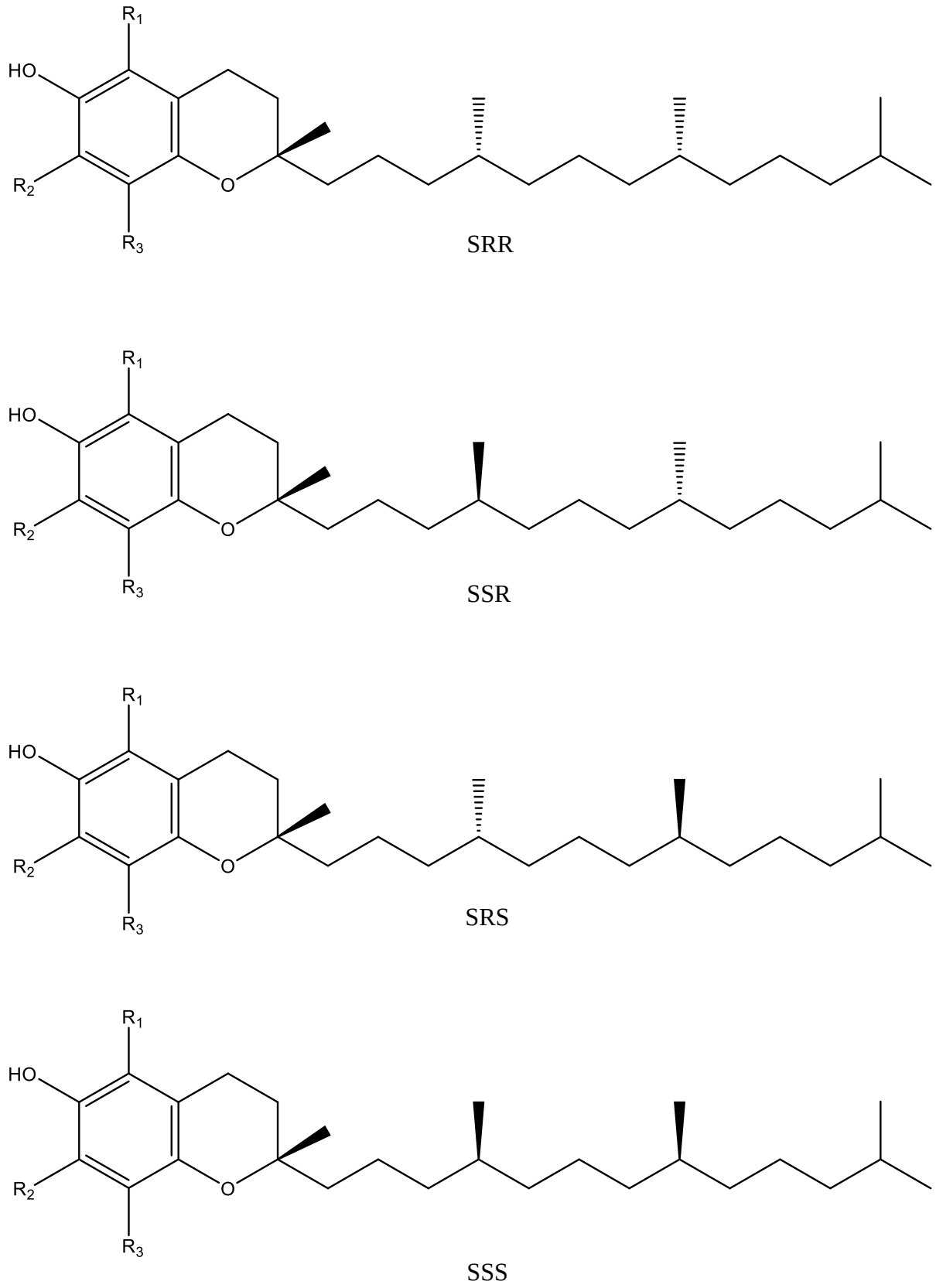

Figure 1.6. Stereoisomers of tocopherol.

The stereochemistry of α-T has a direct effect on the bioactivity of the molecule and most likely affects aggregate architecture. It has been found that the RRR, d, (+) stereoisomer is the most bioactive. This is because the α-tocopherol transport protein as well as specifically binding α-T also specifically binds the RRR α-T isomer and incorporates it into plasma lipoproteins. This is thought to be because this stereoisomer is most resistant to degradation (Brielius-Flohe & Traber., 1999). This is a significant factor for using tocopherols in oral healthcare products as if a higher retention time of the actives are required then the active chosen should have the most resistance to degradation, in this case RRR α-T.

1.5.6 Ester derivatives of (+) α-T

In addition to the 8 geometric isomers and the 8 stereoisomers of the tocopherols there can be more vitamin E generated by esterification of the alcohol functional group on the aromatic ring of the molecule. Figure 1.7 shows some examples of esterified tocopherols (using (+) α-T in all examples).

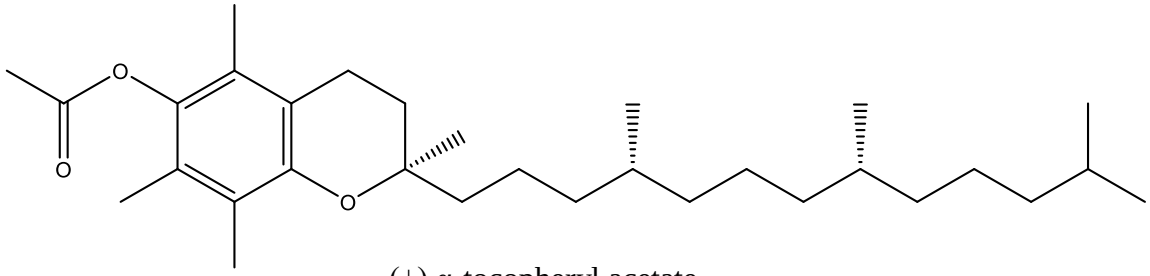

(+) α-tocopheryl acetate

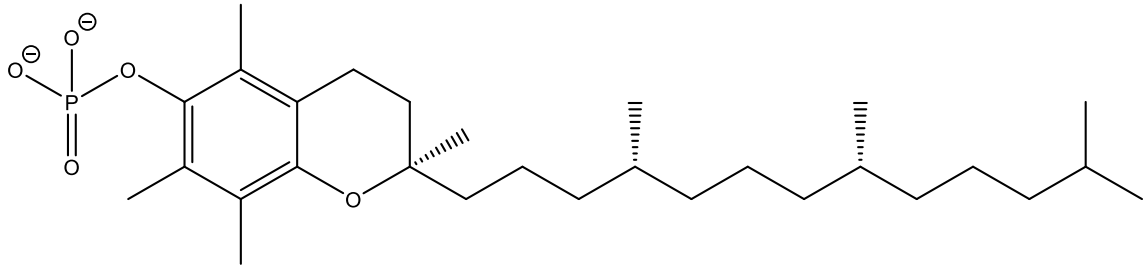

(+) α-tocopheryl phosphate

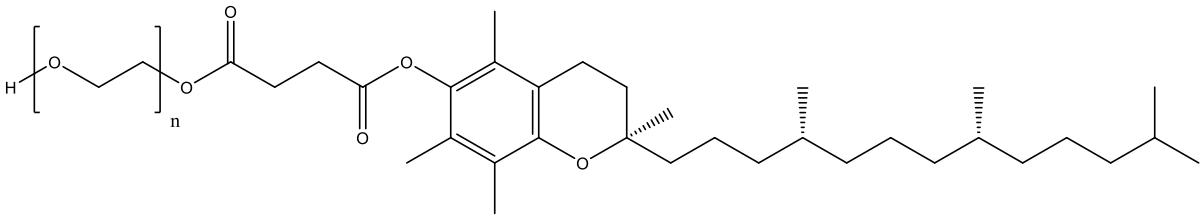

(+) α-tocopheryl polyethylene glycol succinate

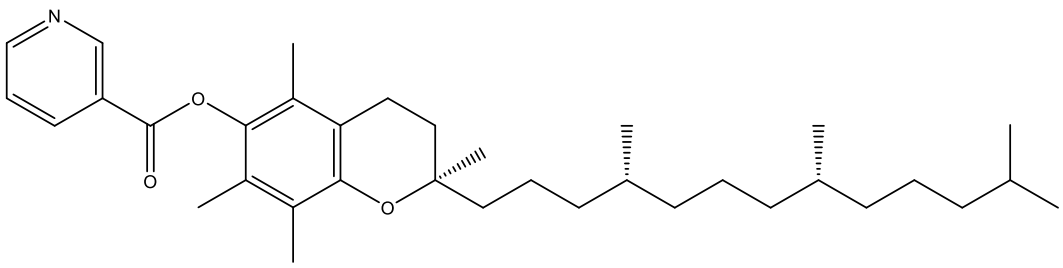

(+) α-tocopheryl nicotinate

Figure 1.7. Esterified derivatives of (+) α-tocopherol.

In theory any functional group can be added to any species of vitamin E providing that the functional group being added can undergo an esterification reaction with an alcohol. This is significant as in theory each variation of functional group will change the molecules physical and chemical properties which will provide different aggregation properties for drug delivery and a variation of therapeutic effects. For example it is known that the esterified derivatives are more stable than there alcohol equivalents as they no longer behave as antioxidants because the hydroxyl group no longer exists and so can no longer act as a radical scavenger (Moddaresi., 2010). This chemical modification would also likely effect aggregate architecture.

In the case of some esterified derivatives the compounds become more water soluble compared to their alcohol precursors which are lipid soluble. This is of high importance in an oral healthcare product as the mouth retains water and so in order for a product to be successful the product must be water soluble. An example of this is α-TA (alpha tocopheryl acetate), in this case a study has been carried out to assess α-TA's ability to accumulate in the gingival margin. The study verified that enriched vitamin E can be found in gingival tissue if treated with toothpastes containing α-TA. This is significant is showing that tocopherols can prevent or even cure gingivitis which is thought to affect 95% of all people (Lienau et al., 2002). However, it is known that α-T is the most biologically active form of vitamin E and α-TA is significantly less active than α-T. In comparison alpha tocopheryl phosphate (α-TP) shows relatively high levels of biological activity whilst still being water soluble (Thiele et al., 2005).

1.5.7 Vitamin E phosphate biological activity

Recently (2003) it has been found that there are significant amounts of endogenous α-tocopheryl phosphate (α-TP) in animal and plant tissue as well as in some foods (chocolate and

cheese) and exhibits anti-inflammatory capabilities (Ogru et al., 2003). The reason why this has been a recent discovery is because during the purification of α-T there is a hydrolysis procedure to break any ester bonds. However, the phosphate group in α-TP is not hydrolysed by the conditions in this purification and instead forms a salt. Therefore, α-TP always remained in the aqueous layer during extraction and was never detected. It has since been discovered that ESMS (ElectroSpray Mass Spectrometry) is convenient for α-TP analysis (Ogru et al., 2003).

Only small amounts of α-TP are found in endogenous tissue hence it is not likely to be a storage isomer (α-T reserves) but rather an active molecule in its own right. In fact α-TP is more potent than α-T as an anti-inflammatory in the signalling cascade. Therefore it is likely that this low level of α-TP is regulated by alkaline phosphatases and kinases to maintain a healthy level of α-TP, alkaline phosphatase removes the phosphate group and so converts α-TP to α-T with kinases completing the reverse reaction (Zingg et al., 2010). This is demonstrated in scheme 1.1.

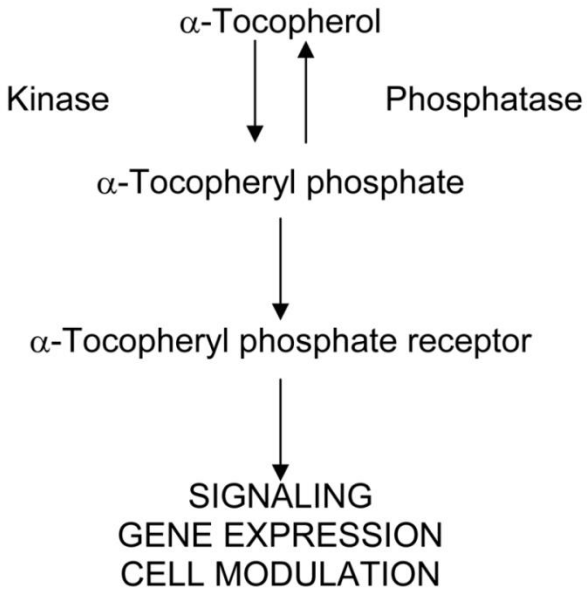

Scheme 1.1. Hypothetical function and regulation of α-TP (Negis et al., 2005).

Glibenclamide, an oral anti-diabetic drug and probenecid inhibit cellular internalisation of α-TP. It is also known that Glibenamide and Probencid are Organic Anion Transporter (OAT) inhibitors. Therefore it is hypothesised that α-TP enters cells *via* OAT's and not membrane diffusion (Negis et al., 2007). Interestingly α-tocopheryl succinate (α-TS) has also shown signs of having anti-inflammatory properties similar and as potent as α-TP suggesting that α-TS can substitute α-TP at cellular receptors (Gianello et al., 2005).

α-TP has been shown to be a potent anti-inflammatory as it is capable of interacting in both the humoral or cell mediated immunity inflammatory immune response. This is due to α-TP's ability to act as a mediator for modulating signal transduction (interaction with cell mediated inflammation) and gene expression (interaction with humoral mediated inflammation).
Firstly, the way in which α-TP acts as a mediator for signal transduction is that α-TP inhibits the generation of pro-inflammatory cytokins and markers including IL-1β, IL-6, plasminogen activator inhibitor-1, TNF-α and C-reactive protein (Nishio et al 2011). α-TP is also effective in inhibiting smooth muscle cell, monocyte and smooth muscle proliferation, inhibition of oxLDL (oxidised low density lipoprotein) uptake and the scavenger receptor CD36 (signals macrophages) (Munteanu et al., 2004). Secondly, the way in which α-TP acts as a mediator for gene expression is by increasing in stimulator-induced cyclooxygenase 2 mRNA expression and suppressing p38 MAPK phosphorylation reducing PGE2 synthesis (Kato et al., 2011). This shows that α-TP has a wide range of anti-inflammatory properties, inhibiting both damaging cytokines which in turn reduces immune destruction and also inhibits prostaglandins which reduce likelihood of bone resorption occurring (bone loss, release of minerals in advanced forms of periodontal disease).

Other uses for α-TP include reducing the risk of atherosclerotic (hardening of artery walls *via* a build-up of plaque resulting in an inflammatory response) cardiovascular disease (Libinaki et al., 2010) and a use in human skin care products as it can protect against skin damage caused by UVB radiation (prevents damaged cell formation and PGE2 synthesis). In fact α-TP has shown enhanced protection against inflammation markers in skin tissue compared to α-TA and glycyrrhizin acid which are known anti-inflammatory agents (Kato et al., 2011). Also the regulatory influence of α-T and α-TP on P13K/Akt activity could represent an import signal for neurons and so would have an essential role in preventing predominant neurological symptoms of severe vitamin E deficiency and other neurodegenerative diseases (Zingg et al., 2010). This shows that α-TP is likely to have many therapeutic and essential roles *in vivo* in addition to the hypothesis of being an anti-inflammatory agent in the prevention of gingivitis.

Interestingly it has been found that HGF's (Human Gingival Fibroblast's) are critical in sustaining inflammation in periodontal disease. This is because HGF's are intolerable to LPS and generates prolonged, excessive responses of macrophages and monocytes (other cells are likely to be involved) (Ara et al., 2009). It has also been found that α-T is able to accelerate proliferation which increases the synthesis of bFGF (basic fibroblast growth factor) which results in more LPS intolerance and so pro inflammatory compounds are maintained (Nizam et al., 2014). This is an interesting contrast to α-TP which inhibits proliferation showing that perhaps *in vivo* α-T and α-TP regulate HGF proliferation. However, one hypothesis could be that periodontal bacteria hinder the production of α-TP resulting in no inhibition of proliferation of HGF's and a down regulation in anti-inflammatory capabilities. Therefore in this case external α-TP would be required to maintain a homogeneous environment.

Therefore in the context of oral healthcare it can be seen that α-TP is an attractive anti-inflammatory molecule and could be used to prevent gingivitis and periodontal disease. It has been seen that synthetic α-TP is soluble in water at high pH (9.5), inorganic solvents, aqueous THF (1:9 respectively, with 1% NH_3) (Gianello et al., 2005) and ethanol and is likely to be soluble in any neutral – basic pH polar solvent due to the charged nature of the phosphate group. It is also soluble in organic solvents at low pH as the phosphate group is protonated (pKa of α-TP phosphate protons is predicted at 1.80 and 6.74, hence phosphate group should be mostly completely deprotonated at neutral pH) but its supramolecular chemistry effect on biological activity is yet to be investigated. α-TP has also been found as an endogenous form within animal/ plant tissue and some foods making it a suitable and relatively safe candidate for oral use. In addition to this vitamin E toxicity is very rare and supplements are widely considered to be safe. The Cosmetic Ingredients Review Expert Panel (CIREP, 2002) concluded that α-TP is safe as used in cosmetic formulations, with the understanding that the vitamin E used in cosmetic products is of similar grade to that used in food (Libinaki et al., 2005).

The major problem to date is the predicted poor tissue retention time of α-TP due to its physiochemical properties: this is because α-TP is negatively charged and does not interact readily with the negatively charged membrane surfaces. However, studies need to be carried out to prove this and if necessary improve tissue resonance (Nishio et al., 2011). Hypothetically, these physiochemical properties could be altered by formulating α-TP with different electrolytes so that the α-TP aggregate architecture is transitioned. This should result in good uptake of α-TP and so would gain improved/ controlled retention time and perhaps accumulation of this active could be achieved resulting in an improved oral hygiene.

1.6 Nanomaterials in oral health

Nanomaterials largely consist of rigid nanoparticles and amphiphilic self-assembling molecules (*i.e.* synthetic surfactants and natural phospholipids) that can form micelles (spherical, ellipsoids, cylindrical), liposomes (small univalent liposomes, large univalent liposomes, multilamella liposomes) planar bilayers, disorganised globular structures and hexagonal conformation packing structures. It is often thought that it is 'free' soluble active molecules that are released nanomaterials lead to the greatest therapeutic effect but more recently it has been found that supramolecular structures with hydrophobic cores and hydrophilic surfaces are capable of penetrating hydrophilic tissue, releasing the active molecules at a desirable location, enhancing activity (Sutariya & Pathak., 2015). Nanoparticles can be engineered such that the hydrophilic actives adhere to their surfaces improving drug delivery whilst the self-assembling structures can be used to encapsulate hydrophobic actives to improve their delivery.

Functionalising nanomaterial surfaces controls the surface chemistry and therefore controls the interactions between the nanomaterial and the biosystem in which it is applied to improve drug delivery and disease therapy providing a versatile platform in biomedical applications (Mout et al., 2012; Wang et al., 2009). In the case of nanoparticles the surface has been functionalised with small molecules, surfactants, dendrimers, polymers, and biomolecules (including anti-bodies/ receptors) by covalent and non-covalent attachment. However, in the case of amphiphilic bioactives, they themselves aggregate though drug-drug interactions. These nano-assemblies are commonly characterised by their critical micelle concentrations (CMC)/ critical aggregation concentrations (CAC) by where there is an abrupt change in the samples physical

properties *i.e.* surface tension, electrical conductivity, viscosity and light scattering with increasing molecule concentration.

There are some examples of nanotechnologies being employed in the oral heath market. Zinc oxide (ZnO), copper oxide (CuO), titanium dioxide (TiO_2) and silver (Ag) nanoparticles have been found to improve the consilient agents antimicrobial properties when administered as colloidal dispersions in aqueous vehicles. The nanomaterial form has been found to be have lower minimum inhibitory concentration (MIC) and minimum bactericidal concentration (MBC) values than chlorohexidine against *S. mutans* and *S. sanguis (*Ahrari et al., 2015). In addition the antimicrobial CHX has been found to have enhanced solubility and stability when formulated with nano carriers leading to an enhanced antimicrobial effect against *C. albicans* and *S. mutans* (Pupe et al., 2011). However, this is a new and rapidly growing area of research and therefore much investigation needs to be performed to fully exploit it. Interestingly supramolecular structures such as liposomes have been found to have enhanced biofilm penetration, tooth surface binding, deliver an encapsulated active or themselves being therapeutic (Nguyen & Hiorth., 2015). Vitamin E phosphate being a phospholipid is likely to aggregate and hence may have enhanced drug delivery.

1.7 Aim and scope of the PhD

Nanomedicines are increasingly being used for the improvement of oral health (Narang & Narang., 2015; Ozak & Ozkan., 2013). (+) α-T has been found to self-assemble in aqueous solutions and it is likely that the amphiphilic (+) α-TP will also form aggregates when *in vivo*. However, the introduction of the phosphate, that will be charged at physiological pHs will affect aggregate architecture, which may modify the agents biological response compared to

the parent compound (+) α-T. The tocopherols may function as both antimicrobial and anti-inflammatory agents in the oral cavity according to the literature that describes these and similar compounds, but as yet these actions have not yet been systematically investigated. The aim of this project was to assess if (+) α-TP could be employed as a multi-functional antimicrobial and anti-inflammatory nanomedicine that could be used as part of an oral healthcare routine. In order to address this aim the following objectives were set:

1. To develop a robust esterification method for synthesising high purity naturally derived (+) α-TP, spectroscopically characterise the product and assess its aggregation behaviour.

2. To observe if (+) α-TP had enhanced anti-biofilm activity over (+) α-T against single bacterial species and multispecies salivary biofilms. Assess its hydroxyapatite binding and compare (+) α-TP's antimicrobial potency with commercially available antimicrobial agents found in mouthwash.

3. To investigate how the (+) α-TP nanostructure physical properties (conformation, size and charge) influence its ability to interact with bacterial membranes, penetrate, kill and inhibit the growth of oral biofilms..

4. To compare (+) α-T, (±) α-TP and (+) α-TP nanostructure swellability upon delivery to the mouth, assess their toxicity on gingival cells and develop an inflammatory cell culture assay that closely resembles the *in vivo* conditions in order to assess their oral anti-inflammatory properties.

CHAPTER TWO

Synthesis, Characterisation, Aggregation and Chemical Stability of (+) Alpha Tocopheryl Phosphate

2.1 Introduction

The name Vitamin E includes a range of different molecular isomers (tocopherols/ tocotrienols) (Figures 1.3, 1.4, 1.5 and 1.6). Their phosphorylated derivatives could be useful compounds for use in maintaining good oral health as they have been found to have anti-inflammatory efficacy (Ogru et al., 2003; Libinaki et al., 2010). However, only one phosphorylated vitamin E derivative is commercially available and that is the synthetic (±) α-TP racemic mixture (8 isomers, Figure 1.5 and 1.6). The natural and most bioactive stereoisomer configuration of the vitamin E phosphate derivatives is the +, d, RRR tocopherols and so a phosphorylation method was required. The four natural (+) tocopherol geometric isomers (Figure 1.2) derived from plant extracts are commercially available and this in principle could provide a starting material for the synthetic production of the desired (+) isomers. However, the naturally sourced (+) tocopherol activity is also influenced by the geometric isomer in which it is used.

Naturally occurring vitamin E is found in vegetable oils such as corn, rapeseed, soybean and sunflower oil and was discovered in 1922 by Evans and Bishop (Gliszczyńska-Świgło et al., 2007; Zingg et al., 2010). Vitamin E functions as a chain-breaking antioxidant that prevents the propagation of free radical reactions (Nishio et al., 2011). The structures of vitamin E have recently had their therapeutic relevance expanded (Zhao et al., 2011; Mirbagheri et al., 2008), but not all of the structures have been synthesised in pure form. Variations of vitamin E include geometric changes on the aromatic ring, geometric changes on the hydrocarbon chain and stereochemistry changes on the hydrocarbon chain (Brigelus-Floshe & Traber., 1999). Alpha Tocopherol (α-T) is the most abundant geometric form of vitamin E in nature; it has the highest biological activity with the (+), d, RRR species being the most bioactive stereoisomer (Brigelus-Floshe & Traber., 1999) (Figure 1.5). In addition, only the (+) isomer has been found

in nature due to specific enantiomeric synthesis by photosynthetic organisms (Caretto et al., 2010; Schulze-Siebert et al., 2000).

(+) α-T has two major drawbacks for use in an oral health product. The first being it is highly lipophilic (Thiele et al., 2005) and hence would limit the concentrations that could be used in aqueous mouthwash products. Secondly, (+) α-T is known to be chemically unstable due to its sensitivity to light which could reduce its shelf life. The esterification of α-T is a method that has been used to overcome these issues (Moddresi., 2010). These esterification reactions have included formation of acetate, polyethylene glycol succinate, nicotinate and phosphate esters (Figure 1.7). In this project the focus will be on the potential use of (+) alpha tocopheryl phosphate (α-TP) to improve oral health.

(+) α-TP has been found to be endogenous in animal and plant tissue (Ogru et al., 2003). Phosphorylation reactions are common in nature, and so the presence of small amounts of α-TP in plants and animals, which have α-T in their diet, is unsurprising. However, it was surprising that α-TP has only recently been discovered in animal and plant cells. This was due to the pH dependent solubility of the compound in aqueous/ organic extractions (Gianello at al., 2005). The detection of α-TP in animal and plant tissue was missed for so long due to the fact that vitamin E extraction processes ended with a basic pH extraction into an organic layer. The basic conditions generated the water soluble α-TP salt which did not partition into the organic phase. The aqueous phase was not tested as the researchers at the time did not anticipate a water soluble form of the vitamin.

Two reactions that can be used to phosphorylate α-T have been published. One reaction used phosphorus oxychloride ($POCl_3$) as the phosphorus source (Reaction 1) (Nishio et al., 2011)

whilst the other used phosphorus pentoxide (P_4O_{10}) (Reaction 2) (Gianello et al., 2005). Reaction 1 did not state product purity, but the researchers claimed to achieve a 47% yield of α-TP after purification by trituration with boiling ethanol. Reaction 2 claimed a pure product was produced but did not state a yield. This literature provided a starting point for the development of a synthetic route, but a more systematic approach to the synthesis and characterisation was required. In addition, as (+) α-TP is an amphiphilic molecule it can be reasonably assumed it will form aggregates when dispersed in polar solutions with a –ve charge due to the phosphate group. However, its critical aggregate concentration (CAC) and physical stability over time has not been reported, but would likely influence any potential biological activity in the mouth and so also needs to be studied.

The aim of this Chapter was to synthesise, characterise the molecular aggregation and assess the chemical stability of (+) α-TP when in a vehicle suitable for topical use in an oral health product. This was because the most biologically active and only naturally occurring stereoisomer of α-TP (RRR, + or d) was not easy to extract from natural sources, a synthetic esterification method, which generated (+) α-TP from plant extracted (+) α-T, was developed. (+) α-TP from this synthesis was still classified as natural due to the natural origin of the starting material (Moddresi., 2010). Following the synthesis, it was considered necessary to analyse the physical characteristics of (+) α-TP in an aqueous vehicle suitable for application to the oral cavity as very little was known about the aggregation behaviour of this amphiphilic agent in an aqueous system and how this could influence antimicrobial activity. A 20% ethanol, 80% water mixture at pH 7.4 (Tris buffer) was selected as the vehicle for (+) α-TP as it was able to solubilise a good amount of the active and it could be used in an oral healthcare product as there are commercial products available with a similar alcohol content such as Listerine Original antiseptic mouthwash.

2.2 Materials

(+) α-T (Type VI, ~40% purity), phosphorus oxychloride ($POCl_3$) (≥ 99%), tetrahydrofuran (THF) (anhydrous) (≥ 99.9%), triethylamine, trizma hydrochloride (Tris) (≥ 99%), trifluoroacetic acid (TFA) (≥ 99%), deuterated chloroform ($CDCl_3$), C18 silica and (±) alpha tocopheryl phosphate (≥ 97%) were purchased from Sigma Aldrich, UK. Hexane fractions (60-80), propan-2-ol, methanol, formic acid (FA), absolute ethanol, disodium hydrogen phosphate, monosodium dihydrogen phosphate, hydrochloric acid, sodium hydroxide and HPLC mobile phase membrane filters (nylon 0.2µm pore size 47mm diameter) were purchased from Fisher Scientific Ltd, UK. All chemicals without a purity displayed were reagent grade. De-ionised water was used from laboratory supply. Disposable clear dynamic light scattering cuvettes (macro, PMMA) and disposable folded capillary cells (DTS1070) where purchased from VWR, Germany.

2.3 Methods

2.3.1 Nuclear Magnetic Resonance (NMR) spectroscopy

^{1}H, ^{13}C and ^{31}P NMR spectra were recorded using a DRX 400 instrument (Bruker, UK) using TOPSPIN software for data acquisition and analysis. Spectra were obtained in $CDCl_3$ at 296 K using a 5 mm switchable broadband probe. Proton NMR parameters included a sweep width of 8250.825 Hz, an acquisition time of 4.0 sec, an interpulse delay time of 1 sec and 16 scans within a zg30 pulse program. Carbon NMR used a sweep width of 24038.461 Hz, an acquisition time of 1.4 sec, an interpulse delay time of 2 sec and 1000 scans all within a zgpg30

pulse program. Phosphorus NMR used a sweep width of 64724.918 Hz, an acquisition time of 0.5 sec, an interpulse delay time of 2 sec and 16 scans all within a zgpg30 pulse program.

2.3.2 Fourier Transfer Infer-Red (FTIR) analysis

Deuterated chloroform ($CDCl_3$) was employed in the infrared analysis of the (+) α-TP solutions. The samples were loaded into a demountable universal transmission cell system (Omni-Cell, Specac Ltd, UK) fitted with calcium fluoride (CaF2) windows and a 25 μm Mylar spacer (Specac Ltd., UK). All spectra were produced using 32 scans collected at a spectral resolution of 4 cm-1. The data was recorded using a Spectrum One spectrometer (Perkin-Elmer Ltd., UK) and analysed with Spectrum software (version 10, Perkin-Elmer Ltd., UK).

2.3.3 Mass spectrometry

Mass spectra were recorded using a micromass ZQ 2000 instrument (Waters, UK), operating in negative electrospray ionisation (ESI) mode. The sample was directly infused into the ESI source at a 20 μl/ min flow rate. The nebulization gas was N_2, the capillary potential was 2.80 kV, the drying gas was 500 l/ h and the RF lens was set to – 0.5 V. The sample cone voltage was set to -40 V and the source temperature was 100 °C whilst the desolvation temperature was set to 250 °C. The sample concentration was 100 μg/ mL, prepared in 50% methanol, 50% water and 0.1% FA.

2.3.4 High Performance Liquid Chromatography (HPLC)

The HPLC system used Millenium 32 software, which employed a p200 pump (Spectraseries, UK), autosampler (Waters 717 plus) and a photodiode array detector (Waters 996, UK). The column (Phenomenex, Luna C8(2), UK) had a pore size of 100 Å, a particle size of 5 µm and column dimensions of 4.6 mm x 250 mm. The mobile phase consisted of 70% propan-2-ol, 30% water and 0.1% TFA and was filtered and sonicated (PS40A - 10 Litre Bath with Heater, Monmouth Scientific, UK) prior to use. The injection volume was 50 µL, the flow rate was 1 mL/ min and a UV detection wavelength range of 214 - 350 nm was employed with run times of 14 minutes.

2.3.5 Elemental analysis

(+) α-TP samples were submitted to Medac Ltd, UK, for further proof of identity and purity confirmation by elemental analysis. Carbon and hydrogen compositions were assessed by microanalysis. The technique used was based on the quantitative "dynamic flash combustion" method. The samples were held in a tin capsule, placed inside the autosampler drum (FlashEA®1112 Elemental Analyzer, UK) where they were purged by a continuous flow of helium and dropped at pre-set intervals into a vertical quartz tube maintained at 900ºC. When the samples were dropped inside the furnace, the helium stream was temporarily enriched with pure oxygen and the sample and its container melted with the tin promoting a violent reaction (flash combustion). Under these favourable conditions, even thermally resistant substances are completely oxidised. Quantitative combustion was then achieved by passing the mixture of gases over a catalyst layer. The mixture of combustion gases was then passed over copper to remove excess oxygen and to reduce the nitrogen oxides to elemental nitrogen. The resulting

mixture was then directed to a chromatographic column where the individual components were separated and eluted as carbon dioxide and water by the TCD signal, which fed the automatic workstation (EAGER300™, USA). The instrument was calibrated with the analysis of standard compounds using K factor calculations or the linear regression method incorporated in the EAGER300™ software.

2.3.6 Circular dichroism (CD)

QS cuvettes (0.5 mm, Starna Scientific Ltd, UK or 10 mm, Hellma, UK) were used for UV-Vis and circular dichroism (CD) experiments. They were washed with water then ethanol and dried with nitrogen before use. Samples of either the (+) or (±) alpha tocopheryl phosphate (100 µM in 20% ethanol, 80% water, 25 mM Tris, pH 7.4) were then added to cuvettes and were inserted into a spectrophotometer (Applied photophysics, Leatherhead, UK) for measurements using Chirascan plus software (version 4.2.15). The photodiode detector (Avalon, UK) CDDC channel used 1000 volts. Wavelengths were measured from 180 – 400 nm taking a reading every 1 nm with a bandwidth of 2 nm. Measurements were completed at 25 °C set by a temperature jack (Quantum northwest (TC-125), USA). Vehicle spectra were used as a blank for background subtraction.

2.3.7 (+) α-TP aggregation analysis

Molecular aggregation was analysed by photon correlation spectroscopy (Malvern Nanoseries Zetasizer, Malvern Instruments Ltd, UK). Detection of the light scattering signal was performed at 173 ° at 25 °C. Samples were placed in low volume disposable cuvettes. The

material refractive index was set at 1.59, the material absorbance at 0.01, the dispersant refractive index at 1.3469 and the sample viscosity (cP) at 2.143. The duration of experiments ranged from 60 - 100 second during which the measurement position and attenuation was automatically optimised by the machine. All the (+) α-TP samples were dissolved in 20% ethanol 80% water solvent systems buffered at pH 7.4 +/- 0.2 with Tris. Blank solutions (containing just solvent) and (+) α-TP (100 μM) solutions were assessed for aggregation over a 7 day period by monitoring the non-attenuated derived count rate (Kcp) and size (nm) in triplicate.

Critical aggregation constant (CAC) data was calculated by monitoring the non-attenuated light scattering of 0.00512, 0.0062, 0.008, 0.01, 0.02, 0.1, 1, 10, 75, 300, 600, 900, 1200 and 1500 μM solutions of (+) α-TP at 18 h and 164 h time points in triplicate. The CAC was calculated by finding the intersection of two $\log_{10}$ models applied to the (+) α-TP concentration verses non-attenuated light scattering plots. This was calculated by solving the two $\log_{10}$ equations of the models. The second $\log_{10}$ model was considered to start at the first (+) α-TP concentration that showed a significant difference in the non-attenuated light scattering signal when compared to the blank. The two data sets (18 h and 164 h) were also used to compare aggregate size and polydispersity index of the (+) α-TP concentrations to assess aggregate stability. Previous aggregate stability has been monitored over a 3 day refrigerated period and so a longer time course was selected (Correia et al., 2012). Sedimentation occurred at higher concentrations over time and hence all samples were re-suspended by vortexing (Whirlimixer, Fisherbrand, UK) prior to measurement.

(+) α-TP aggregate zeta potentials were analysed by electrophoresis spectroscopy (Malvern Nanoseries Zetasizer, Malvern Instruments Ltd, UK). Detection of voltage signals were

performed at 25 °C. The disposable folded capillary cells material refractive index, material absorbance, dispersant refractive index and viscosity were set as per the light scattering experiments and the dielectric constant was set at 78.5. The Henry's function (F(Ka)) to interpret the data was the Smoluchowski (1.5) option. The duration of the equilibration time was set at 120 seconds with the experiment measurement positions and attenuations automatically optimised by the machine. The number of runs was set at a minimum of 10 and a maximum of 100. The measurements were carried out in triplicate. (+) α-T aggregates in Tris buffer (25mM) were used as a control to observe the effect of phosphorylation on the aggregate zeta potential values.

2.3.8 HPLC chemical stability comparison of (+) α-T and (+) α-TP

The chemical degradation rates of (+) α-TP and (+) α-T (20 µg/ mL, 39 µM) when dispersed in a 20% ethanol, 80% water at pH 7.4 (Tris buffer, 25 mM) vehicle was calculated over a 12 week period. Samples were stored at 37°C in clear HPLC snap neck vials (1 mL) and the concentration was assessed every 4 weeks. The HPLC system was equilibrated (0.1 mL/ min flow rate) overnight prior to calibration/ sample testing and calibrated ((+) α-TP - 2, 5, 10, 20, 50 and 100 µg/ mL) one day prior to sample testing to ensure the system was operating consistently allowing time points to be compared. The HPLC method used to generate each chromatogram was as described in section 2.3.5. Peak area was used to calculate sample concentration with the linear gradient of the data time points being used to calculate the degradation rate. The limit of detection (LOD) and limit of quantification (LOQ) were calculated using the LINEST function on the calibration curve data and were found to be 1.13 and 3.78 µg/ mL respectively for (+) α-TP and 2.34 and 7.81 µg/ mL respectively for (+) α-T. The precision (CV/ relative standard deviation) and linearity (R^2 value) for both the HPLC

calibration curves were found to be 2% and ≥ 0.99 respectively. These values showed the assay was 'fit for purpose'. This assay allowed an assessment of the two molecules commercially viable in this formulation as the industrial chemical degradation tolerance is below 10% degradation of a 0.05% w/v (500 µg/ mL) solution over 12 weeks at 40°C. This assay also enabled an assessment as to how long (+) α-T and (+) α-TP laboratory formulations could be stored without affecting any potential biological activity.

2.3.9 Data analysis

All error values were expressed as their mean ± standard deviation (SD). Statistical analysis of data was performed using Levine's homogeneity test and ensured all sample group data was of acceptable distribution ($P > 0.05$) before statistical significance between the sample groups was assessed by one way analysis of variance (ANOVA) tests with post-hoc Tukey analysis in Origin 2016. Statistically significant differences were assumed when $p \leq 0.05$.

2.4 Results

2.4.1 Synthesis and chemical characterisation of (+) α-TP

The synthesis of (+) α-TP was performed according to Scheme 2.1 which was a modified version of the synthesis used by Nishio et al, 2011.

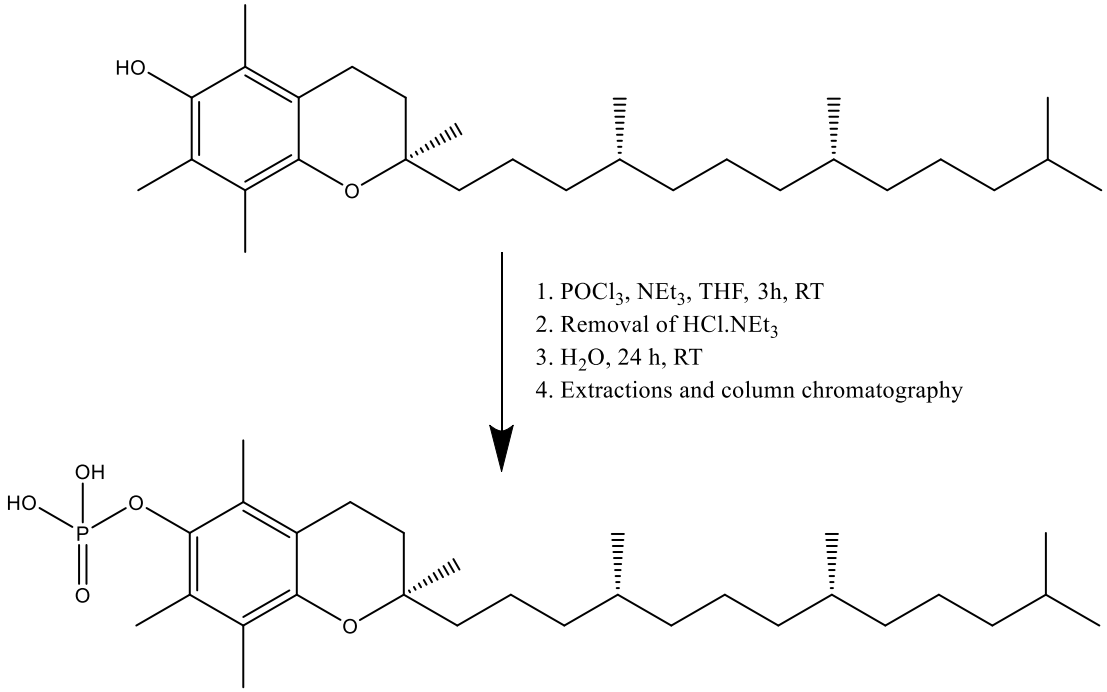

Scheme 2.1. Chemical synthesis of (+) alpha tocopheryl phosphate from (+) alpha tocopherol.

Over a period of 30 minutes (+) α-T (3.0395 g, 7.057 mmol) in anhydrous THF (25 mL) with triethylamine (2.854 mL, 20.47 mmol, 2.9 equivalence) was added to a solution of phosphorus oxychloride (1.973 mL, 21.17 mmol, 3 equivalence) in anhydrous THF (15 mL) under nitrogen, stirring, at room temperature (3 hours). Only a small trace of (+) α-T (Rf = 0.32) was detected using thin layer chromatography (TLC) analysis (9:1, hexane: ethyl acetate), compared to the (+) α-TP product (Rf = 0). The white triethylamine hydrochloride (side

product) was removed (suction filtration). Distilled water (75 mL) was added to the mixture and allowed to stir for 24 hours. Hexane (75 mL) was added to generate a two phase system. The product preferentially partitioned into the hexane layer and was extracted from the hexane by shaking with disodium hydrogen phosphate (10 mM, 50 mL, pH 10.8). An aliquot of absolute ethanol (25 mL) was added to the product in order to eliminate foaming. The disodium hydrogen phosphate solution containing the product was then acidified with hydrochloric acid (2M, 20 mL) and the product was extracted for a third time using hexane (40 mL). This third hexane extraction was repeated and the combined hexane layers placed under vacuum to generate an off white flaky solid which was considered to be the crude (+) α-TP product (0.7221 g, 50.1%). The crude product was purified using C18 silica packed glass column (30 cm x 3 cm) with a 70% propan-2-ol, 30% water and 0.1% TFA mobile phase.

(+) α-TP was obtained with a 27% yield. There was no (+) α-TP analytical standard to enable the calculation of the absolute purity of the product; hence an assessment of relative purity was performed using HPLC. A value of 99% was obtained by calculating the relative area of the (+) α-TP peak as a percentage of all other peaks in the liquid chromatographic run. Preliminary phosphorus NMR experiments found that sodium phosphate generated a peak at -0.05 ppm and phosphorus oxychloride generated a peak at 4.53 ppm. The phosphorus NMR analysis of the (+) α-TP product showed one signal at -1.27 ppm which matched the theoretical structure of the product (Figure 2.1). With carbon NMR, 29 signals were observed, which matched the 29 theoretical signals for the (+) α-TP product (Figure 2.2, see Table 2.1 for peak assignment). The proton NMR spectra contained numerous overlapping signals because the magnetic environments of protons on the hydrocarbon ‘tail’ are similar. However, the three aromatic methyl groups of (+) α-T and (+) α-TP were assigned (highlighted in Figures 2.3A and B) and they indicated that the conversion from (+) α-T to (+) α-TP was successful. This was because

the aromatic methyl group protons changed in the chemical environment when the hydroxyl group was converted to a phosphate ester. This resulted in a change in their H^1 NMR chemical shift signals from two singlet peaks at 2.11 and 2.16 ppm (two peaks overlapping) for (+) α-T to three singlet peaks at 2.05, 2.07 and 2.11 ppm for (+) α-TP. This was also useful in ensuring there was no starting material was in the product because if both compounds were present 4 aromatic methyl proton singlet peaks were observed.

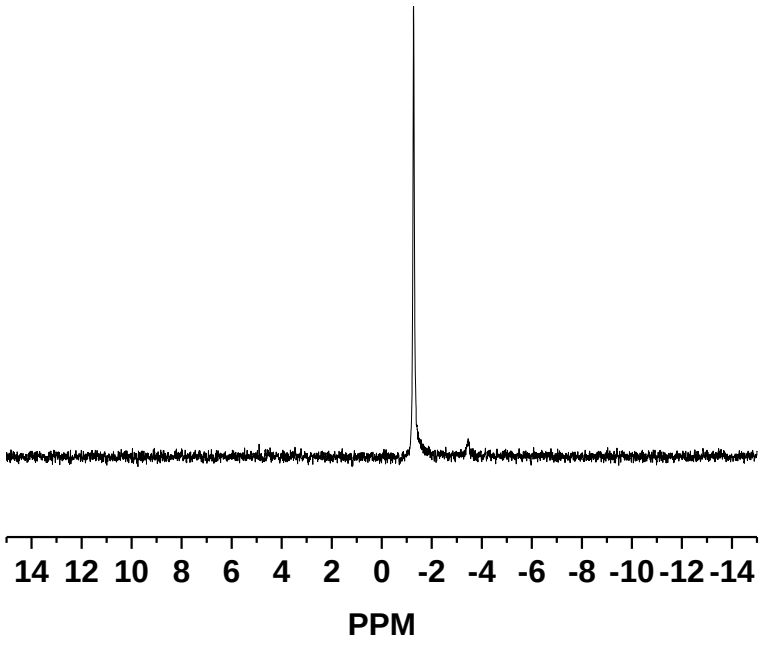

Figure 2.1. Phosphorus nuclear magnetic resonance spectra of the (+) alpha tocopheryl phosphate naturally derived product in deuterated chloroform.

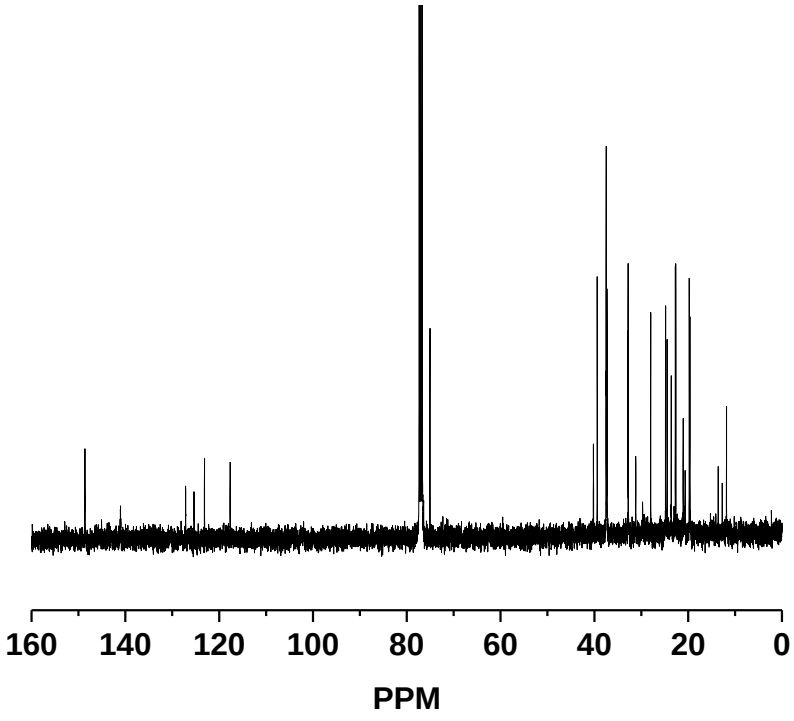

Figure 2.2. Carbon nuclear magnetic resonance spectra of the (+) alpha tocopheryl phosphate naturally derived product in deuterated chloroform.

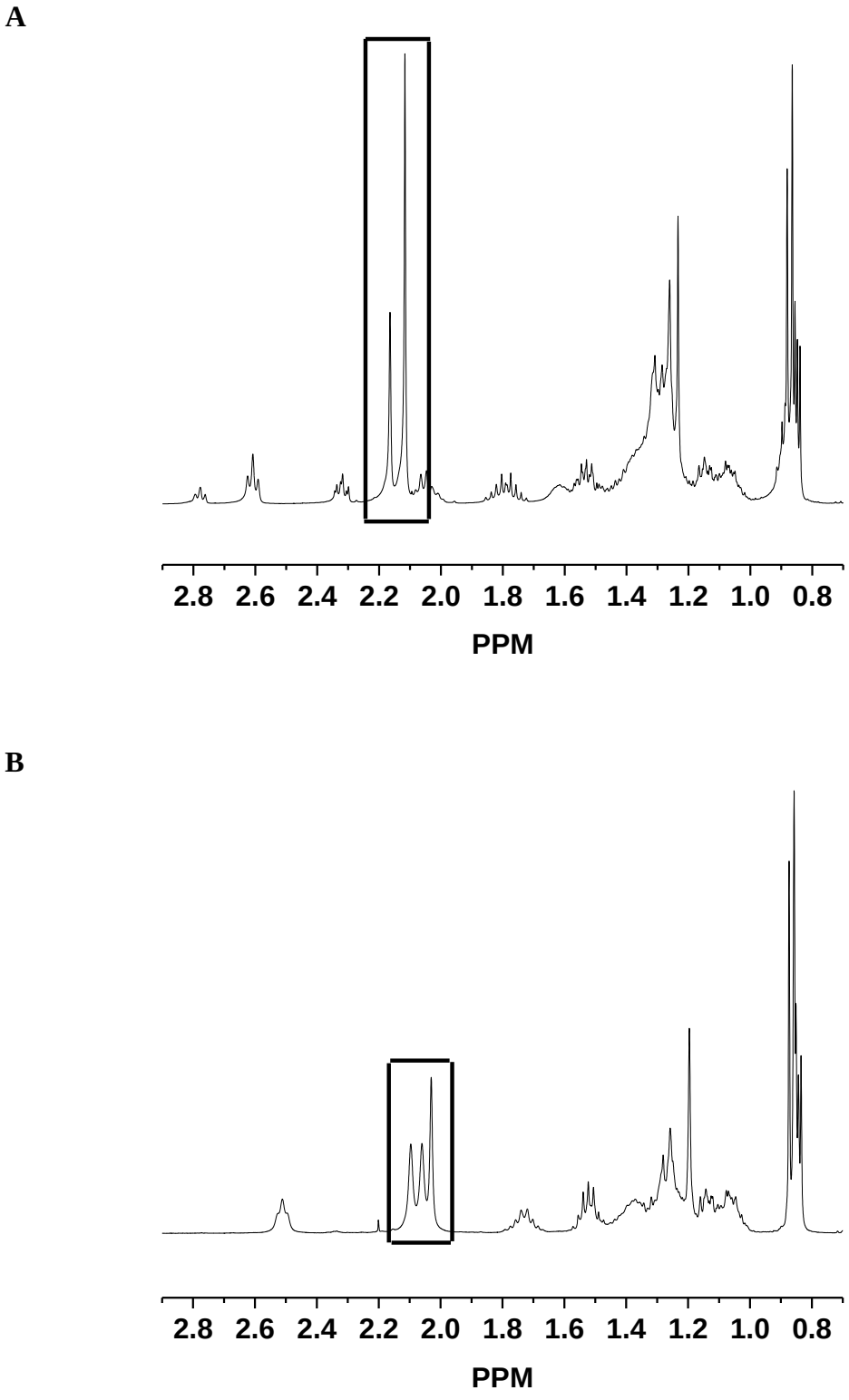

Figure 2.3. Proton nuclear magnetic resonance spectra of the (+) alpha tocopheryl phosphate naturally derived product (A) and the (+) alpha tocopherol starting material (B) in deuterated chloroform. The changes in aromatic methyl group proton environments caused by phosphorylation are highlighted.

Assignment	PPM
C5 - CH_3	12.2
C8 - CH_3	13.4
C7 - CH_3	14.3
C4' - CH_3	20.3
C8' - CH_3	20.4
C4	21.7
C2'	22.0
C13'	23.1
C12' - CH_3	23.2
C2 - CH_3	24.2
C6'	25.4
C10'	25.9
C12'	29.2
C3	32.7
C4'	33.8
C8'	33.9
C7'	38.35
C5'	38.37
C9'	38.48
C3'	38.53
C11'	40.6
C1'	40.7
C2	76.1
C10	118.9
C8	123.9
C5	126.8
C7	128.5
C6	142.9
C9	149.6

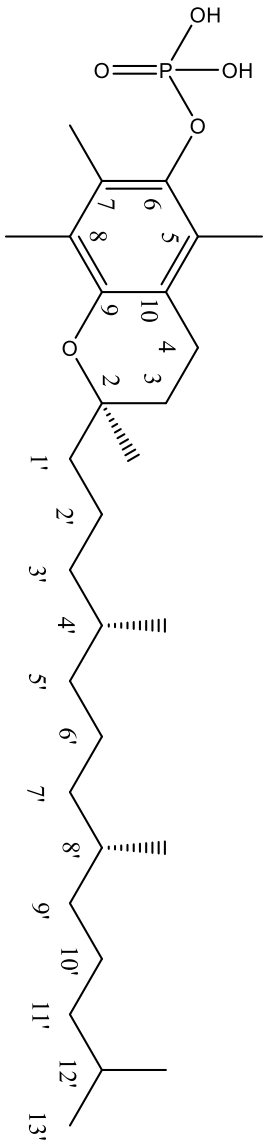

Table 2.1. Assignment of naturally derived (+) alpha tocopheryl phosphate carbon nuclear magnetic resonance spectrum (Baker & Myers., 1991).

The carbon NMR of the commercially available (±) α-TP isomers demonstrated that the three chiral carbon atoms had different chemical shift values which were dependant on the isomer stereochemistry configuration (Figure 2.4A). There are 8 variations of the chiral carbon arrangements (RRR, RRS, RSR, SRR, RSS, SSR, SSS and SRS) and so theoretically each chiral carbon would have had a different chemical shift for each isomer but as the chemical environment remained similar not all 8 peaks were resolved but did show multiplet like peaks (Figure 2.4A inset). However, the synthesised naturally derived (+) just had the predicted 29 peaks for the 29 different carbon environments with the chiral carbons peaks being fully resolved singlets (Figure 2.4B inset) showing stereochemistry was retained throughout the synthesis.

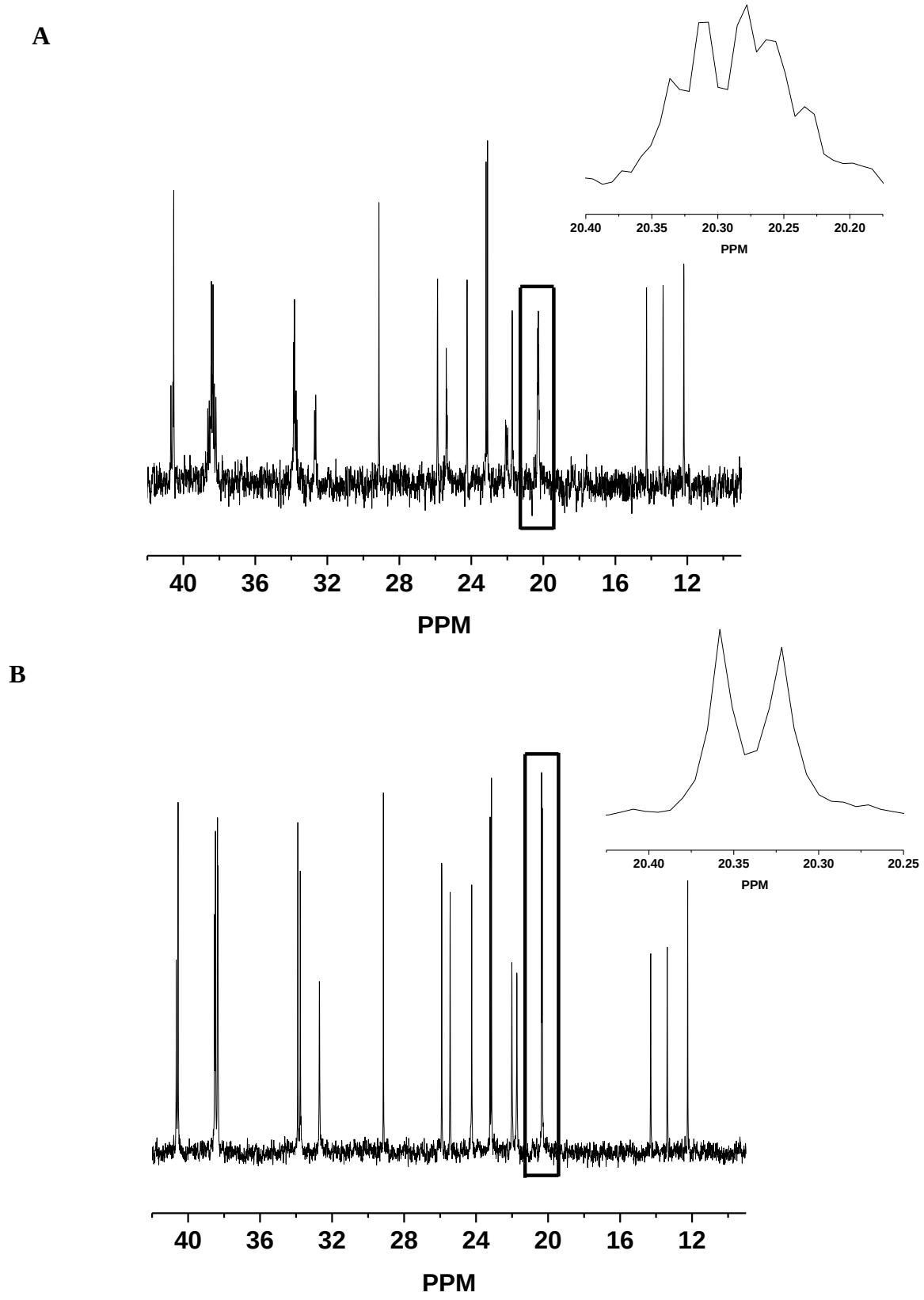

Figure 2.4. Carbon nuclear magnetic resonance spectrums of commercial (±) alpha tocopheryl phosphate (A) and naturally derived (+) alpha tocopheryl phosphate (B) aliphatic regions with highlighted and enlarged C4' and C8' CH_3 peaks inset.

The FTIR confirmed the functional groups within the (+) α-TP structure (Figure 2.5). The absorption bands between 2959 - 2843 cm^{-1} are associated with the asymmetric and symmetric stretching vibrations of the CH_2 and CH_3 groups, the bands between 1462 - 1375 cm^{-1} relates to the aromatic (C=C) stretching, CH_3 asymmetric bending and CH_3 symmetrical bending, the band at 1221 cm^{-1} results from the CH_2 torsion mode and the band at 1090 cm^{-1} is associated with the plane bending of phenyl (Silva et al., 2009). The band at 985 cm^{-1} results from the phosphate ester as this band is commonly seen in phospholipid esters *i.e.* phosphatidylcholine (Nzai & Proctor., 1998).

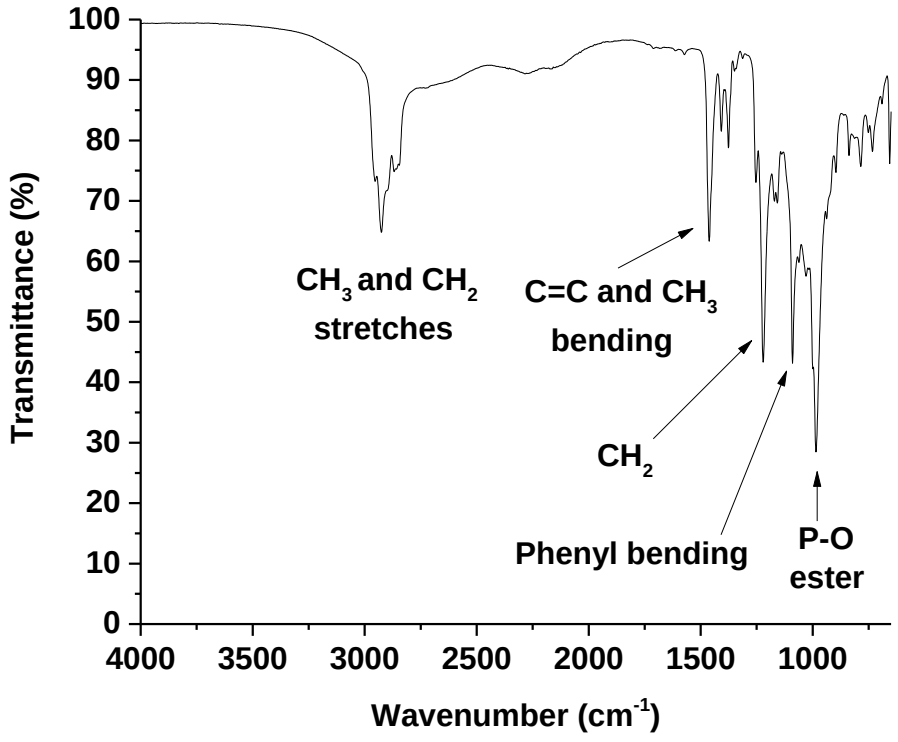

Figure 2.5. Fourier transform infra-red spectra of the (+) alpha tocopheryl phosphate naturally derived product in deuterated chloroform.

The calculated M/Z of the (+) α-TP free acid is 510.4 g/ mol. The synthetic (+) α-TP showed a mass of 509.3 when assessed by negative mode ESI (Figure 2.6). The mass of the parent ion $[M-H]^-$ was therefore as expected for the phosphorylated product.

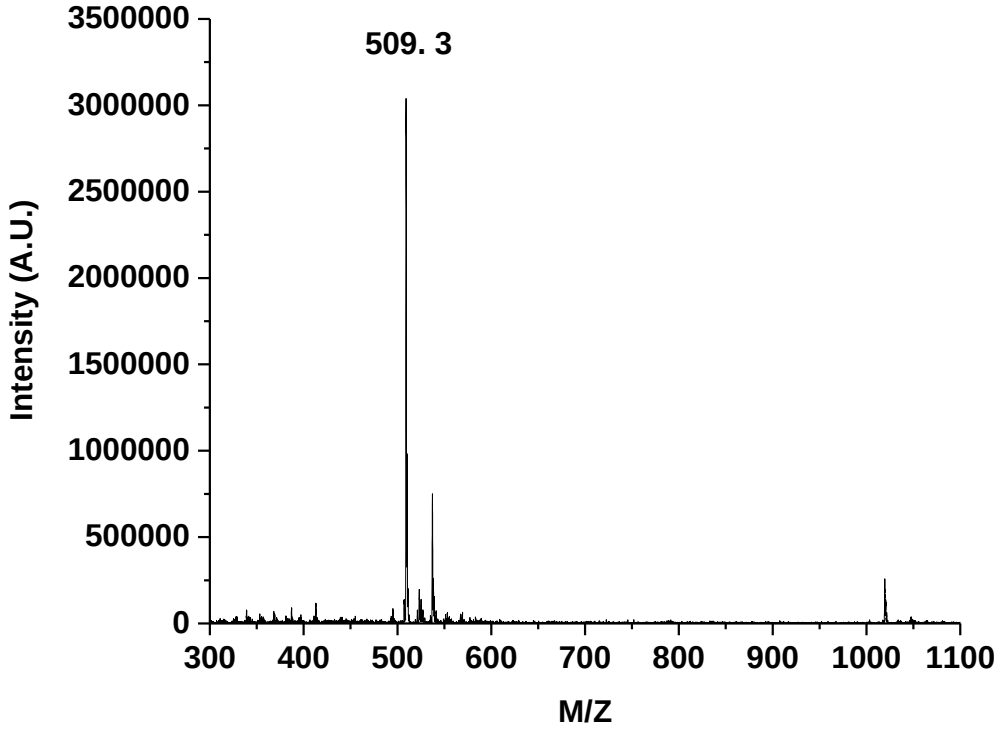

Figure 2.6. Mass spectrum of naturally derived (+) alpha tocopheryl phosphate (100 µg/ mL) in a 50% methanol, 50% water and 0.1% formic acid solvent system.

The HPLC analysis of the (+) α-TP showed that the phosphorylation of (+) α-T (retention time 10.8 min) resulted in the production of a new peak with a retention time of 7.9 min (Figure 2.7). This reduction in retention time of the (+) α-TP compared to the (+) α-T was expected as (+) α-TP is more hydrophilic when compared to the reaction starting material. This data and the fact that no peak was observed at 10.8 min in (+) α-TP chromatograms provided further evidence that there was no starting material in the purified product. In addition, the peak observed at 2.9 min was found to be the solvent front as this was observed in the vehicle control injections.

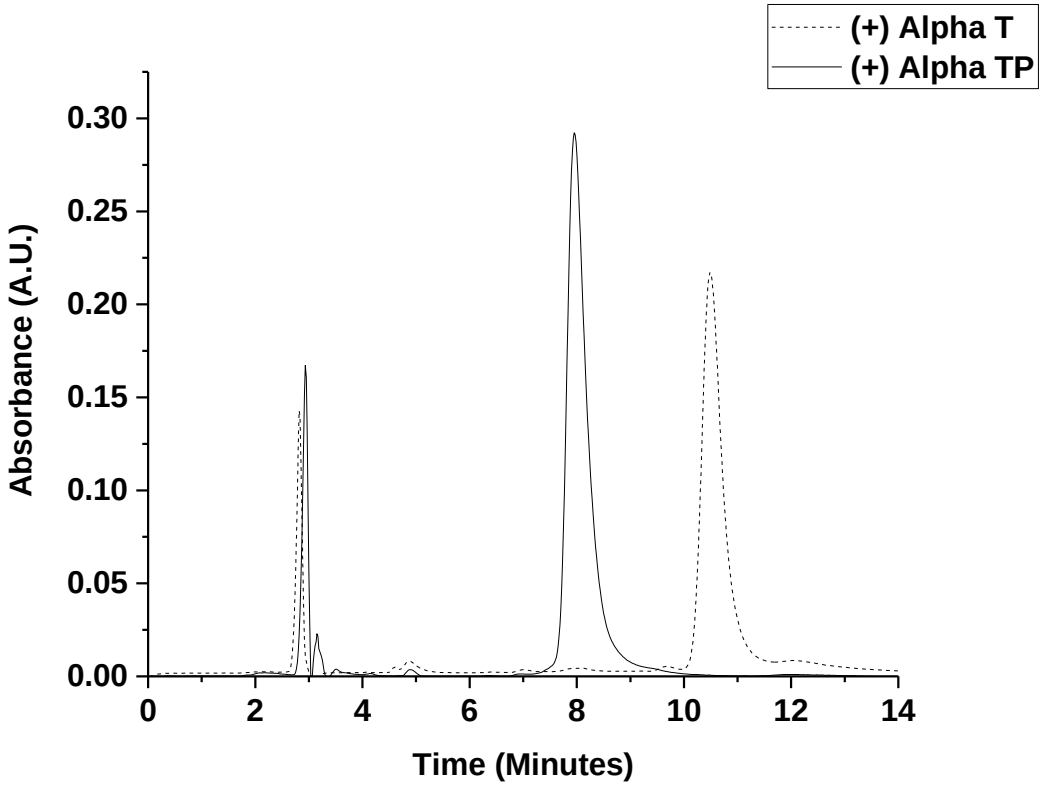

Figure 2.7. High performance liquid chromatography chromatograms of (+) alpha tocopherol starting material and (+) alpha tocopheryl phosphate naturally derived product (100 µg/ mL, dispersed in 20% ethanol, 80% water, 25 mM Tris, pH 7.4). C8 column, 50 µL injection volume, flow rate 1 mL/ min and 214 - 350 nm UV detection wavelengths, mobile phase; 70% propan-2-ol, 30% water and 0.1% Trifluoroacetic acid (v/v).

The theoretical composition of carbon and hydrogen in (+) α-TP is 68.21 and 10.07% respectively. In the elemental analysis the compositions were found to be 68.25 and 10.30%, this showed a carbon match of 99.94% and a hydrogen match of 97.77%. This provided additional evidence that the phosphorylated product had been synthesised in high purity.

The (+) and (±) α-TP were found to have UV absorption bands at 288 nm ($n \rightarrow \pi^*$), 219 and 207 nm ($n \rightarrow \pi^*$ and $\pi \rightarrow \pi^*$) (Figure 2.8). However, in the CD the (±) isomer gave a flat line in both the 10 mm and 0.5 mm path length samples indicating that the different isomers were cancelling out each other's rotation of light as expected (Figure 2.9A and B). The (+) isomer was found to have positive bands at 298, 240 and 207 nm and negative bands at 291, 231 and

217 nm in the 10 mm path length (Figure 2.9A). In addition when monitored in the 0.5 mm path length it was observed that there was a major peak at 207 nm (Figure 2.9B). For the (+) isomer the rotation bands appeared as differential signals but always first increased as wavelength decreases, this is denoted as positive (+) cotton effect (Person et al., 1995) and suggested aggregation could have been occurring (Cassim & Yang., 1967). Although there are three chiral centres in the α-TP molecule it is likely that the chiral centre within the pyran ring had the strongest influence on the aromatic electronic excitation bands of α-TP as the other two chiral centres were further away from the conjugated system. However, the pyran ring chiral centre was the most reactive chiral carbon for the stereochemistry to be altered as it had an oxygen atom bound making this chiral carbon more susceptible to nucleophilic attack. The other two chiral centres were hydrocarbons and hence not reactive.

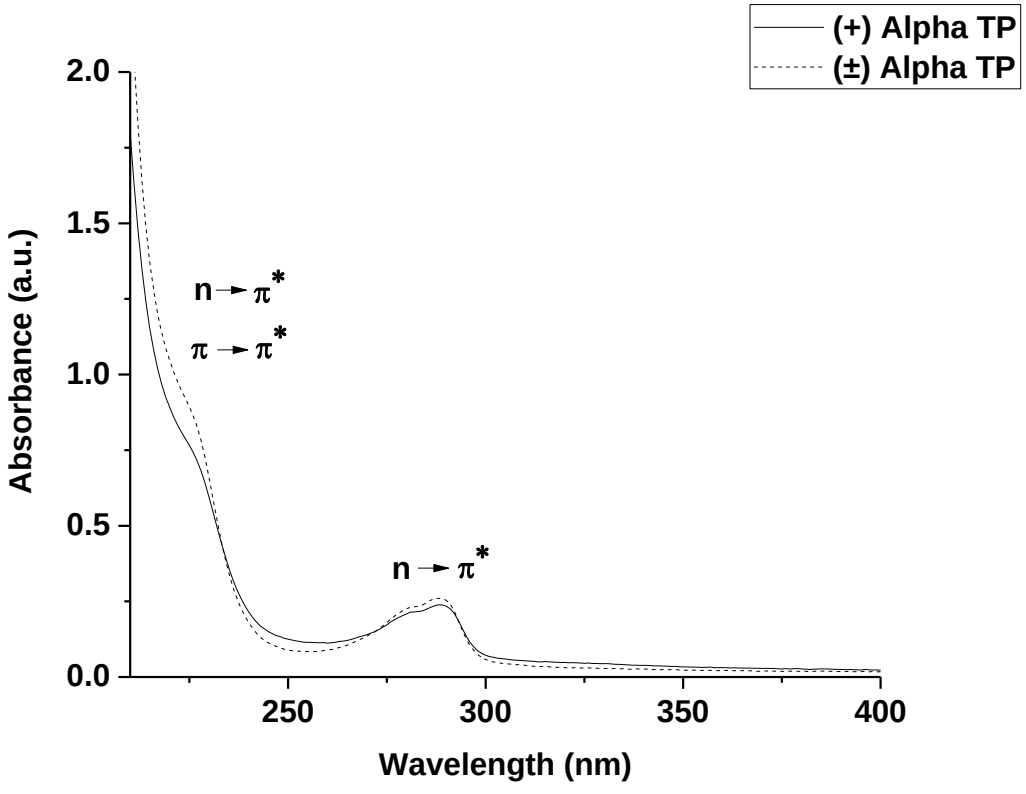

Figure 2.8. UV absorption spectra with 10 mm path length (with annotated electronic transition bands) comparing the in house synthesised (+) alpha tocopheryl phosphate ((+) alpha TP) (1 isomer) and the commercially available racemic (±) alpha tocopheryl phosphate ((±) alpha TP) (8 isomers). Alpha TP concentrations were 100 µM dispersed in a 20% ethanol, 80% water, 25 mM Tris vehicle at pH 7.4.

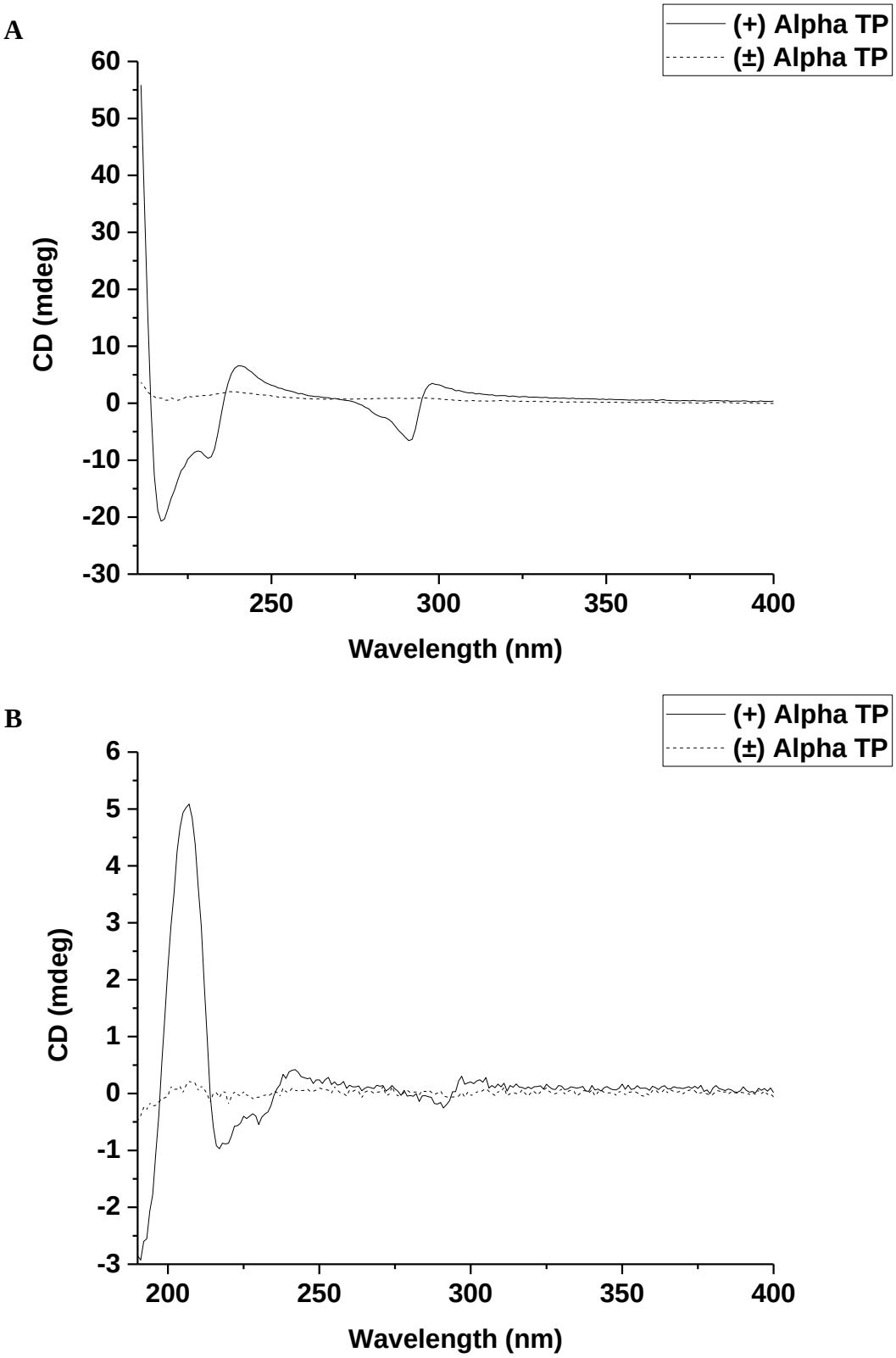

Figure 2.9. Circular dichroism spectra with 10 mm path length (A) and with 0.5 mm path length (B) comparing the in house synthesised (+) alpha tocopheryl phosphate ((+) alpha TP) (1 isomer) and the commercially available racemic (±) alpha tocopheryl phosphate ((±) alpha TP) (8 isomers). Alpha TP concentrations were 100 µM dispersed in a 20% ethanol, 80% water, 25 mM Tris vehicle at pH 7.4.

2.4.2 (+) α-TP Aggregation and Physical Stability Analysis

Light scattering data demonstrated that (+) α-TP, when dispersed in 20% ethanol 80% water at pH 7.4 ± 0.2 (Tris buffer) generated aggregates (Figure 2.10 and 2.11). The attenuated derived count rate of the vehicle (blank) was 149 ± 59.4 kcps, but the (+) α-TP between 0.01 and 1.5 mM resulted in an attenuated derived count rate increase which ranged from 1563 ± 36 to 6421 ± 87 kcps after 18 h. The CAC of (+) α-TP was found to be 5.5 ± 0.2 µM 18 h after preparation (Figure 2.10). The z-average diameter of the (+) α-TP (0.1 mM/ 0.005% w/v) aggregates was found to be 175 ± 21 nm; they had a slight negative charge of -14.9 ± 3.5 mV, a PDI value of 0.359 ± 0.06 and a unimodal distribution (Figure 2.11). The z-average diameter of the (+) α-T (0.1 mM, 56044 ± 175 kcps) aggregates was found to be 563 ± 1 nm; they also had a slight negative charge of -10.5 ± 0.2 mV, a PDI value of 0.179 ± 0.03 and a unimodal distribution (Figure 2.12).

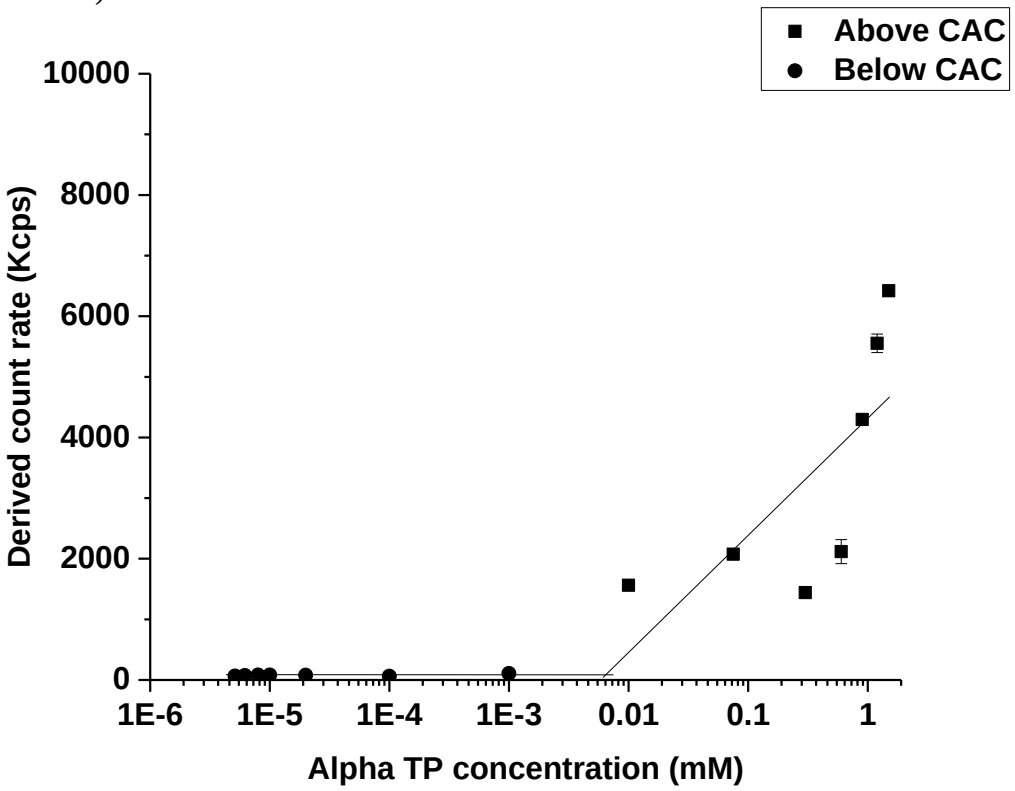

Figure 2.10. Dynamic light scattering critical aggregate concentration calculation (CAC) of (+) alpha tocopheryl phosphate at 18 hours in 20% ethanol, 80% water at pH 7.4 ± 0.2 (25 mM Tris).

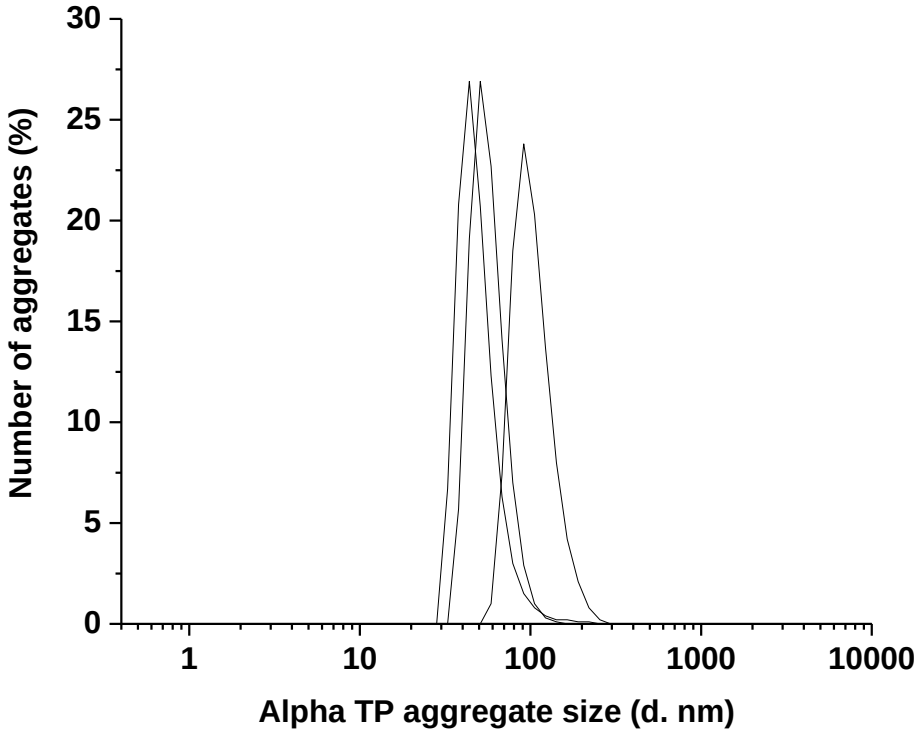

Figure 2.11. Aggregate size distribution (0.1 mM) (B) of (+) alpha tocopheryl phosphate at 18 hours in 20% ethanol, 80% water at pH 7.4 ± 0.2 (25 mM Tris).

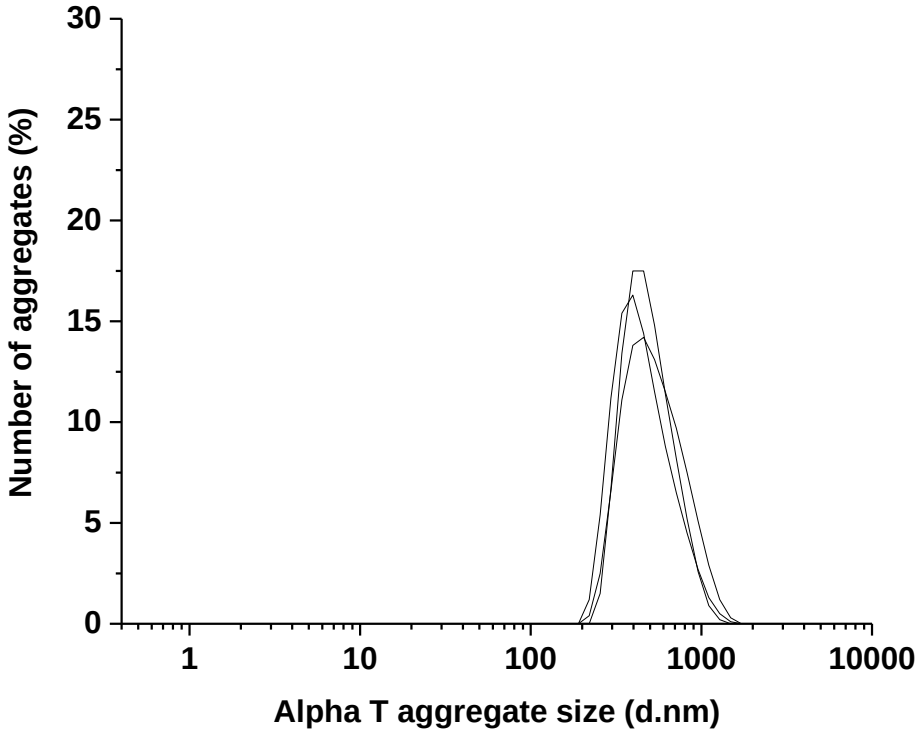

Figure 2.12. Aggregate size distribution (0.1 mM) (B) of (+) alpha tocopherol at 18 hours in 20% ethanol, 80% water at pH 7.4 ± 0.2 (25 mM Tris).

Reducing the concentration of (+) α-TP in the Tris vehicle increased aggregate sizes below 300 µM (Figure 2.13) but this was likely an artefact due to the low derived count rate produced at low (+) α-TP concentrations. The (+) α-TP aggregates were found to be stable over an 8 day timescale as the size and polydispersity index of the aggregates remained the same ($P > 0.05$) (Figure 2.13 and 2.14). The CAC measured after 8 days was 8.4 ± 1.2 µM, just 2.9 µM higher than that of the 18 hour CAC but was statistically significant ($p = 0.01$) (Figure 2.15).

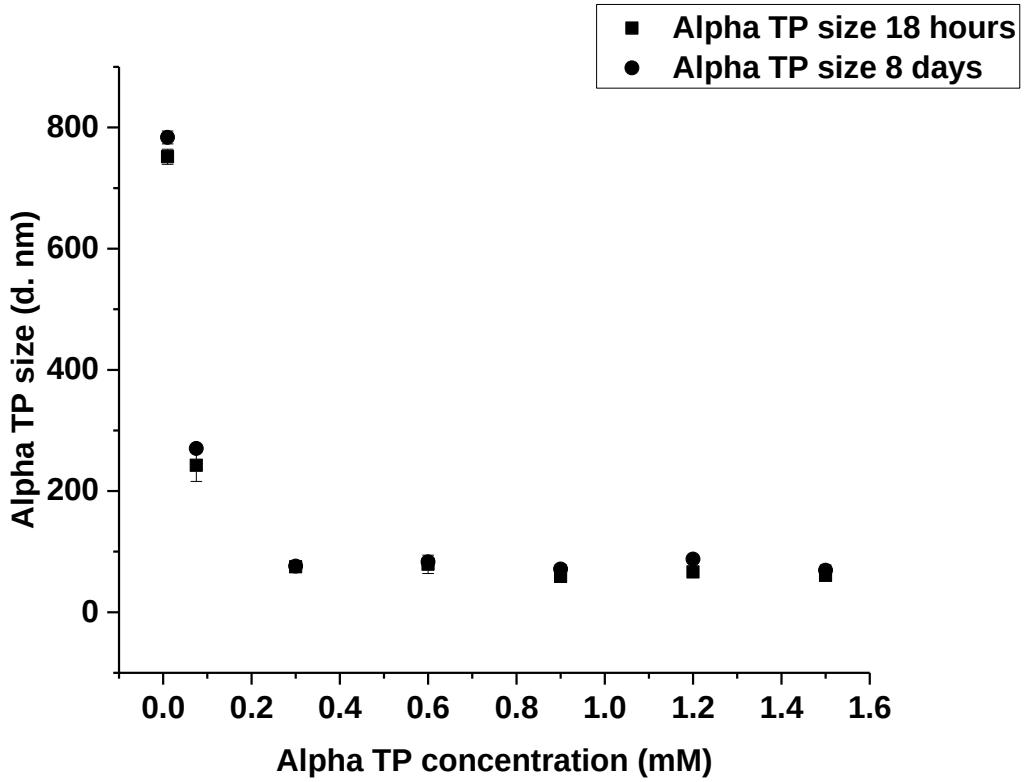

Figure 2.13. Dynamic light scattering size comparison at 18 Hours and 8 days of (+) alpha tocopheryl phosphate (0.1 mM) in 20% ethanol, 80% water at pH 7.4 ± 0.2 (25 mM Tris).

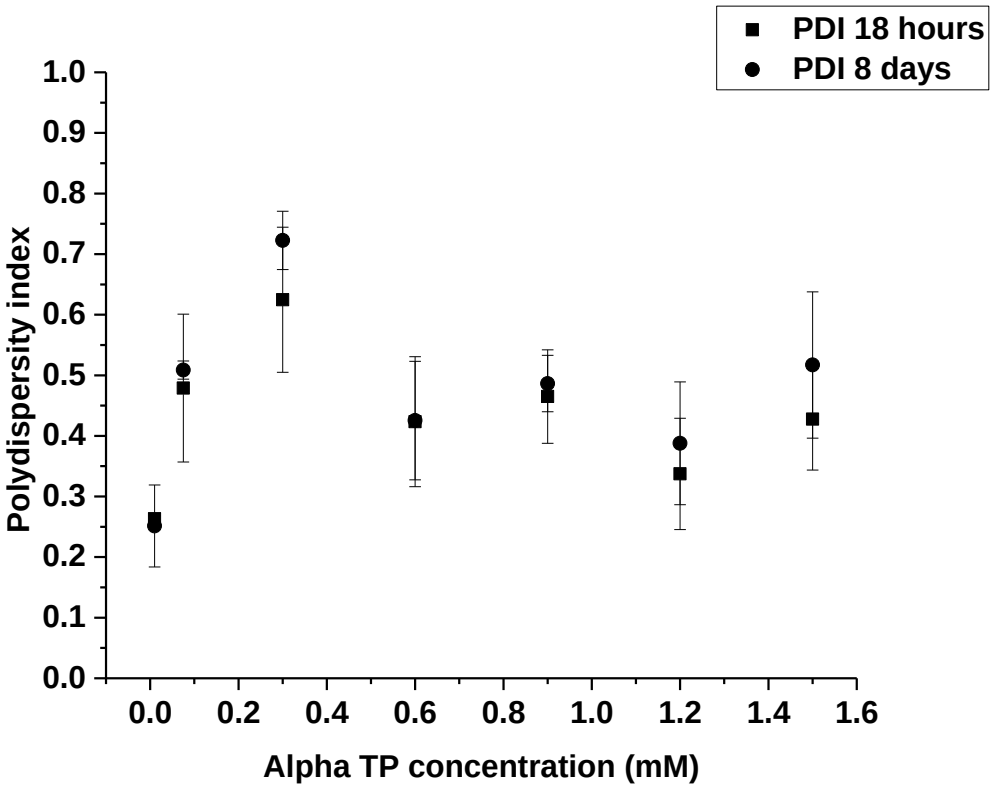

Figure 2.14. Polydispersity index comparison at 18 hours and 8 days of (+) alpha tocopheryl phosphate (0.1 mM) in 20% ethanol, 80% water at pH 7.4 ± 0.2 (25 mM Tris).

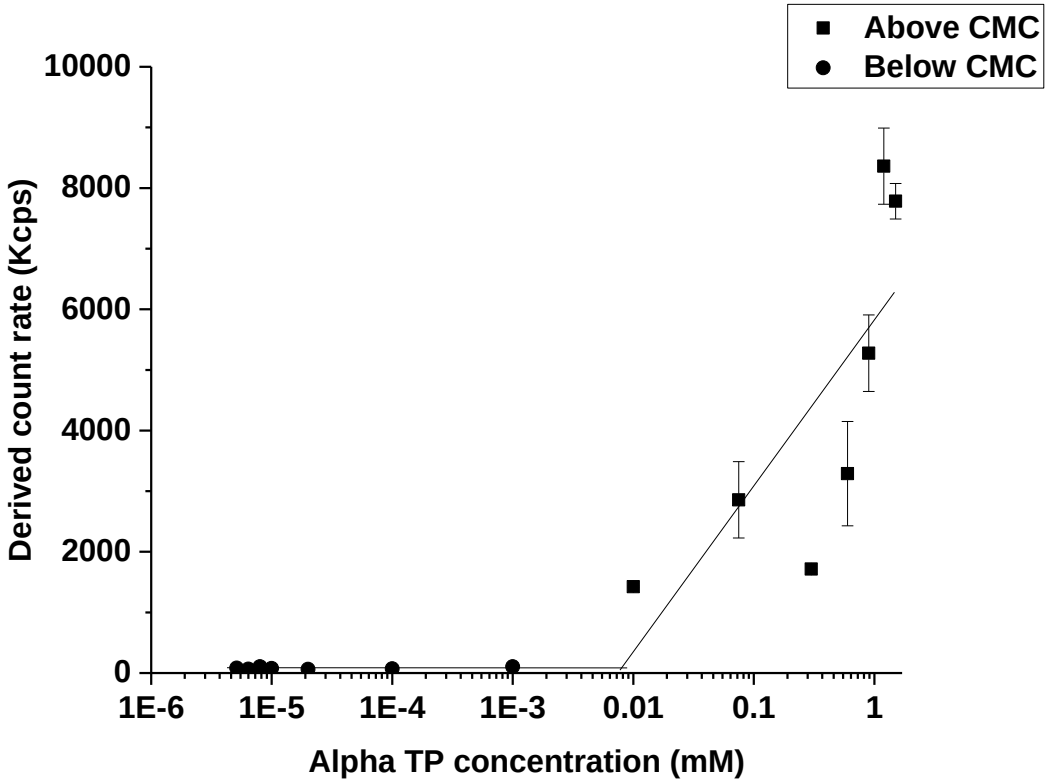

Figure 2.15. 8 day critical aggregation concentration (CAC) calculation of (+) alpha tocopheryl phosphate (0.1 mM) in 20% ethanol, 80% water at pH 7.4 ± 0.2 (25 mM Tris).

2.4.3 Chemical stability comparison of (+) α-T and (+) α-TP

The chemical stability studies demonstrated that (+) α-TP has a degradation rate of ~ 1.2 µg/ mL/ week indicating that chemical degradation did not influence the study's results (Figure 2.16). This data also demonstrated that the product was within the chemical degradation range to be commercially viable as the industrial chemical degradation tolerance is below 10% degradation of a 0.05% w/v (500 µg/ mL) solution over 12 weeks at 40°C. (+) α-TP was degraded by 14.4 µg/ mL over 12 weeks which corresponded to a 2.9% degradation of a 0.05% w/ v solution. Interestingly (+) α-TP was more chemically stable than (+) α-T, suggesting (+) α-TP may be less susceptible to oxidation. In addition (+) α-T failed the industry degradation tolerance test as it was calculated to be 11% but is likely higher than this due to the first time point being below the assays LOQ and so time points less than 4 week intervals would be needed to get this exact degradation rate of (+) α-T in this vehicle. The laboratory samples of (+) α-TP could be stored for 8 days before use but (+) α-T samples had to be freshly prepared before each microbiology or biophysical analysis assay.

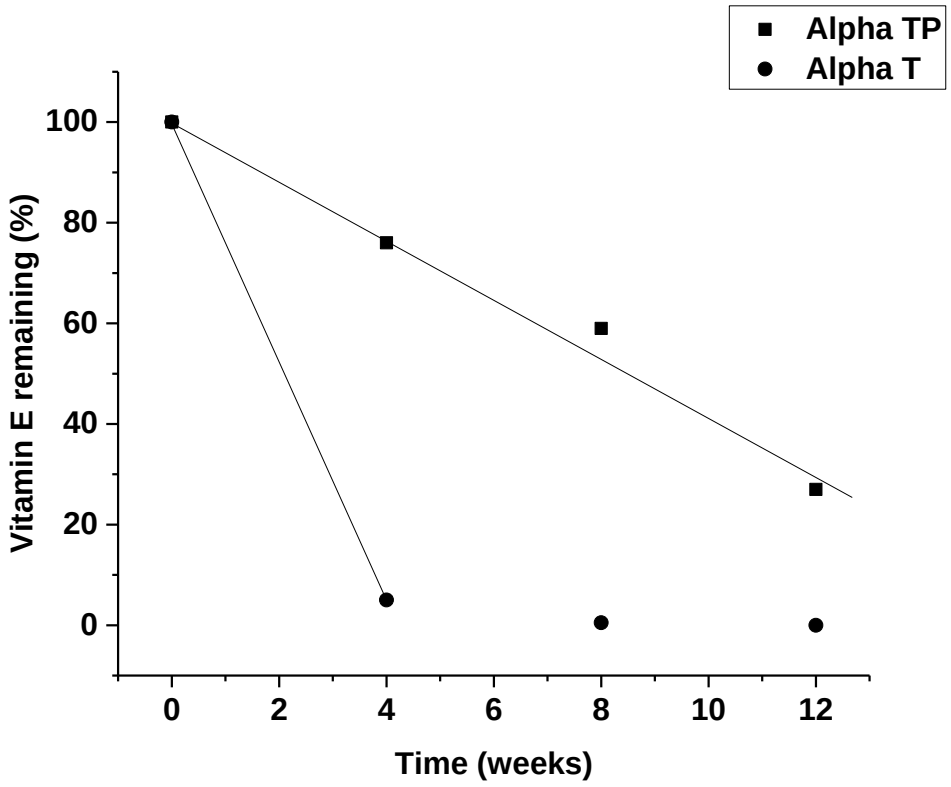

Figure 2.16. Chemical degradation rates of (+) alpha tocopheryl phosphate and (+) alpha tocopherol (20 µg/ mL, 1 mL) dispersed in 20% ethanol, 80% water at pH 7.4 (Tris buffer, 25 mL) stored at 37°C in clear snap neck HPLC vials.

2.5 Discussion

α-TP is a water soluble derivative of the highly lipophilic α-T (Thiele et al., 2005). The natural, most biologically active structural isomer of α-TP, the (+) isoform, is not commercially available and so it was synthesised specifically for this project. Two reaction schemes that conserve the natural structural configuration, which is known to be the most biologically active form of (+) α-T (Brigelus-Floshe & Traber., 1999), have previously been reported (Nishio et al., 2011; Gianelo et al., 2005). As a prelude to this work both of these schemes were attempted, but neither was found to provide a suitable material for an oral healthcare product and hence modifications to the synthesis used by Nishio et al, 2011 were adopted. The chemical structure

of (+) α-TP was confirmed by NMR (phosphorus, carbon and proton), infra-red, mass spectrometry and elemental analysis. The adopted synthetic procedure generated a product that was of high purity (≥99%) according to HPLC in 27% yield.

Each step of the synthetic process contributed to the loss of material. Firstly, not all the (+) α-T starting material reacted with the $POCl_3$, as indicated by TLC. A small trace of (+) α-T was still observed after the 3 hour reaction (Rf = 0.32). Secondly, when manipulating the pH dependent solubility of (+) α-TP for purification, there would have been losses of material at each of the three extractions as in immiscible solvent systems there is only a preferential partitioning of molecules, not an absolute partitioning. As an example, when the acidic water layer containing (+) α-TP was added to hexane, (+) α-TP being protonated and more hydrophobic, preferentially partitioned into the hexane layer but some (+) α-TP remained in the water layer. It would appear these two steps accounted for 50% of the material loss. The column chromatography purification of the crude (+) α-TP accounted for 23% loss of material. Apparently some of the (+) α-TP bound tightly to the C18 silica solid phase and could not be eluted. Attempts could be made to further optimise the reaction in order to achieve a higher yield. Perhaps the immiscible solvent (+) α-TP extractions could be removed and instead purify the 24 h water/ THF reaction mixture just using column chromatography.

ICH guidelines state that the purity of new compounds should be calculated using an analytical standard. However, there was no analytical standard for (+) α-TP, only the (±) isomer was available which contained 8 isomers, which could have had an effect on the extinction coefficient and hence concentration based UV absorbance. Therefore the purity was calculated based the (+) α-TP peak areas as a percentage of all other peak areas in the HPLC chromatograms. The weakness of this approach is that any non UV active impurities present in

the sample would not be observed. However, elemental analysis of the (+) α-TP compound reinforced the purity value generated using our HPLC method as the % compositions of carbon and hydrogen were close to those of the theoretical values for the (+) α-TP structure.

The chemical analysis of the product showed that the stereochemistry of (+) α-TP was retained as the carbon NMR generated 29 carbon peaks that closely resembled the 29 carbon peaks assigned by Baker & Myers, 1991 for (+) α-T (whereas the commercial available (±) α-TP carbon NMR control was shown to have more than 29 peaks due to the presence of the 8 stereoisomers).

The CD data generated from (+) α-TP gave confidence that the pyran chiral carbon remained at least predominantly in its R configuration throughout the reaction as (+) peaks were observed in the CD experiment and no peaks observed in the racemate mixture control. Again there was no (+) α-TP analytical standard to compare the (+) isomer CD peak intensities. The differential CD signals (Cotton effect) have been previously observed in dyes were the chromophoric groups acquired asymmetry through macromolecule interactions (Blout & Stryer L., 1959) and has been used for secondary, tertiary, quaternary structures and aggregation studies (Cassim & Yang., 1967). The ‘s’ shape signals in the CD suggested that (+) α-TP in this vehicle was interacting with other molecules and aggregating, which was having an influence on the aromatic electronic excitation bands by effecting molecular symmetry.

The introduction of the hydrophilic phosphate group into (+) α-T generated an amphiphilic character. The (+) α-T (which only has a small non-charged hydrophilic domain) and the (+) α-TP aggregates possess different self-assembly characteristics *i.e.* the (+) α-TP nanostructures were smaller, more negatively charged and had a lower derived count rate. The (+) α-TP self-

association generated nanostructures with a micro molar CAC, similar to the vitamin E derivative α- tocopheryl polyethylene glycol succinate 1000 (α-TS), which has previously been found to have a critical micelle concentration of 20 μM (Sadoqi et al., 2009; Muthu et al., 2012). These initial aggregation studies showed that at concentrations relevant to its use as an oral health care product the (+) α-TP would likely form aggregates. The low CAC also suggested that the (+) α-TP aggregates should display a good physical stability (Wanga et al., 2012). This was supported by the data derived in this study which showed the aggregates were found not to grow over time. The good physical stability was not surprising as high stability is common with phospholipid structures (Wu et al., 2010). Imaging techniques confirm the aggregate structures and are investigated in the next chapter.

Drug aggregation can have a negative impact on antimicrobials, which often need to interact with the microorganisms to elicit their action as it can reduce the quantity of bioavailable substance (Balagopal & Arjunkumar., 2013; Ferretti et al., 1990). However, in the case of oral antimicrobials, which are required to enter biofilms to have their full effect on bacteria, the formation of nano-sized objects can be seen to be an advantage. For example, it has been shown that antimicrobial agents encapsulated in charged aggregates in the hundreds of nano meters size range (*i.e.* phospholipid liposomes and nanoparticles) can interact readily with biofilm surfaces, upon doing so the nanostructure is destabilised allowing the encapsulated antimicrobial to seep out into the biofilm and have an improved, targeted *in vivo* efficacy compared to the free drug (Meers et al., 2008; Drulis-Kawa & Dorotkiewicz-Jach., 2010). In this work it is envisioned that the (+) α-TP nanostructures themselves will have both the biofilm targeting and antimicrobial activity.

The chemical stability studies, which demonstrated that (+) α-TP has a degradation rate of ~ 1.2 μg/ mL/ week indicated that chemical degradation would not influence future biological results and that it was a commercially viable molecule. Interestingly (+) α-TP was more chemically stable than (+) α-T, suggesting (+) α-TP may be less susceptible to oxidation (Sabliov et al., 2009). This is probably due to the mechanism of (+) α-T degradation starting with the formation of a free radical on the hydroxyl group. When phosphorylated this can no longer occur, and therefore the (+) α-TP must presumably be hydrolysed back to (+) α-T for the established vitamin E degradation pathways to be observed which would make degradation dependent on the rate of (+) α-TP hydrolysis.

2.6 Conclusion

(+) α-TP was successfully synthesised using $POCl_3$ as an intermediate. The product was shown to self-assemble into physically and chemically stable negatively charged nanostructures when dispersed in a polar vehicle at micro-molar CAC values. It was established that (+) α-TP is more chemically stable than (+) α-T. This material was used to investigate whether or not the addition of a phosphate group generates important biological properties, for example superior antimicrobial activity when compared to (+) α-T. In addition, it was considered to be important to understand if phosphorylation could provide substantive interactions with components of the mouth. These aspects of (+) α-TP formed the focus of the work described in Chapter 3.

CHAPTER THREE

The Effect of (+) Alpha Tocopherol Phosphorylation on Oral Biofilm Growth

3.1 Introduction

Currently available substantive antimicrobial agents that can be used chronically to control the growth of oral micro-organisms, show undesirable side-effects, which limit their use in oral health products (Elworhy et al., 1996; White et al., 1997; Haps et al., 2008). Molecules displaying similar physicochemical properties to (+) α-TP have been found to have antimicrobial activity *via* membrane interactions (Cohen et al., 2000; Obando et al., 2007). In addition, organic phosphates, similar to (+) α-TP, are known to adhere to enamel surfaces strongly (Ganesan., 2008). Binding to enamel is desirable property for oral health actives as the continual bathing of the mouth with saliva makes it difficult to sustain the activity of locally administered agents (McBain et al., 2003; Tanomaru et al., 2008; Rao et al., 2001; Pan et al., 1999). Therefore, (+) α-TP could be a promising substantive oral antimicrobial agent but its antimicrobial activity against relevant oral micro-organisms needs to be tested.

In Chapter 2 (+) α-TP was shown to produce nanostructures. Interestingly, nanostructures can be engineered to control their size, shape, surface chemistry and functionality and this can influence an agents oral anti-biofilm properties including: biofilm penetration, biofilm dismantlement and bacterial kill. In addition, nanostructure properties can potentially be manipulated to maximise tooth surface adherence (Paula & Koo, 2016). Therefore, when testing the antimicrobial activity of (+) α-TP in biofilms the physicochemical properties of the nanostructures that it forms in water should be considered.

The bacterial biofilms used for oral antimicrobial agent testing commonly include both single species biofilms and salivary biofilms to assess which bacteria are more susceptible to particular antimicrobial agents and how the agent affects salivary biofilm development to

prevent oral disease. When using the single species approach there must be some careful consideration of which species to employ. As streptococci species are early colonizers of the tooth surface and are thought to be fundamental to the formation of a biofilm, thus plaque, they are often used in single strain antimicrobial testing (Jakubovics & Palmer., 2013; Nobbs et al., 2009; Catuogno & Jones., 2003).

Streptococcus oralis is a highly proficient pioneering coloniser species, which is also known to produces glucan polymers, providing a surface that later bacterial colonisers can adhere to which is considered a major factor in the initialization of biofilm development (Dorkhan et al., 2013; (Fujiwara et al., 2000). Therefore, limiting *S. oralis* growth, delays plaque maturation and is thought to inhibit the attachment of the later pathogenic colonizing bacteria which cause gum disease. A second streptococci species, which is prominent in the development of dental caries, that can be selected for antimicrobial susceptibility is *Streptococcus mutans* (Nobbs et al., 2009). *S. mutans* in particular is thought to be a major contributor to the prevalence of the dental caries disease due to its ability to metabolise and generate acids faster than other streptococci species and it has the ability to survive and continue to metabolise sugars even at pH levels that inhibit or kill other streptococci (Matsui & Cvitkovitch., 2010).

The aim of this Chapter was to assess if (+) α-TP could bind to components in the mouth and provide a substantive effect on the growth of oral biofilms. To allow adequate (+) α-TP to be dissolved in solution for the antimicrobial testing a 20% ethanol, 80% water mixture at pH 7.4 (Tris buffer) was selected as the vehicle to deliver the test agent. *Streptococcus oralis* and *Streptococcus mutans* were selected for single species biofilm growth studies. For the biofilm experiments the bacteria were only exposed to the test agents for 2 minutes because the application time of such agents in the mouth is relatively short. Following exposure the ability

of the tested agents to retard the exponential growth phase of the bacteria and their capability to inhibit the maximum population of bacteria were monitored. A charge neutralising agent was used after the test substances were applied to bacteria in several experiments to observe cell surface binding potential of the test agents. For the planktonic *S. oralis* and *S. mutans* experiments, a minimum bactericidal concentration (MBC) method was selected as the antimicrobial output as (+) α-TP aggregation would most likely result in turbidity and so the visible growth of bacteria could not be monitored in order to determine the minimum inhibition concentration (MIC) using a traditional methodology (Andrews., 2001). Binding studies between hydroxyapatite (HA) (majority composition of enamel) and (+) α-TP/ (+) α-T simulated the binding to the tooth in order to investigate the agent's potential substantively in the mouth. However, it was also thought important to also test the test systems in biofilms produced from unsterilized whole mouth saliva (UWMS) grown on the treated hydroxyapatite as this more closely represented the situation *in vivo*. The application of (+) α-TP to HA was considered to be a close mimic to tooth surface conditions after brushing with toothpaste as the pellicle (salivary proteins) layer adsorbed to tooth surface is at least partially removed for a few minutes providing enamel exposure (Waaler., 2014).

3.2 Materials

(+) α-T (Type VI, ~40% purity), trizma hydrochloride (Tris) (≥ 99%), Tween 80, lecithin, triflouroacetic acid (TFA) (≥ 99%), chlorhexidine digluconate (CHX) 20 % (w/v) in water, brain heart infusion (BHI) broth and glycerol were purchased from Sigma Aldrich, UK. Propan-2-ol, absolute ethanol, blood agar (BA) plates containing blood agar base no. 2 with 5 % horse blood, hydrochloric acid, sodium hydroxide and sterile 0.2 μM nylon syringe filters

were purchased from Fisher Scientific Ltd, UK. All chemicals without a purity displayed were reagent grade. De-ionised water was used from laboratory supply. *S. oralis* NCTC 7864T and *S. mutans* NCTC 10449T were purchased from LGC standards, USA. Hydroxyapatite discs (5 mm diameter x 2 mm thick) were purchased from Himed Inc, USA. Mica was purchased from Agar scientific, Elekron technology, UK. AFM cantilevers uncoated Si_3N_4 cantilevers with integrated pyramidal tips (Model: NSC15/noAl) were purchased from MikroMasch, Germany. Clear sterile polyester adhesive films were purchased from Starlab, UK. Live/ dead BacLight bacterial viability kit was purchased from Life technologies, UK.

3.3 Methods

3.3.1 *S. oralis* and *S. mutans* biofilm antimicrobial growth retardation assay

The deionised water, Tris buffer$_{(aq)}$ (0.5M), NaOH$_{(aq)}$/ HCl$_{(aq)}$ (2M), and the 20% ethanol, 80% water, Tris (150 mM) (pH at 7.4) vehicles used for test sample preparations were filtered sterilised using sterile 0.2 μM nylon syringe filters. (+) α-T and (+) α-TP stock solutions were prepared by weighing out the appropriate amount of each and dissolving in absolute ethanol for sterilisation. The stock solutions were then diluted with deionised water and Tris (0.5 M) to generate a 20% (v/v) ethanol, 80% (v/v) water solutions with Tris (150 mM) to control pH at 7.4 (adjusted if required). Then a series of (+) α-T/ (+) α-TP dilutions were prepared in the Tris vehicle. CHX samples (positive controls) were prepared by serial dilutions of the CHX commercial solution (20% w/v in water) into deionised water with 20% ethanol. All samples were refrigerated when stored (maximum 8 days) and vortexed prior to use.

S. oralis NCTC 7864T and *S. mutans* NCTC 10449T aliquots were stored in brain heart infusion (BHI) broth with 10% glycerol at -70°C. When required for the experiments they were cultivated on blood agar (BA) plates containing blood agar base no. 2 and 5 % horse blood, at 37°C under aerobic conditions. Plates were subcultured every 48 h and passaged no more than 6 times.

Aliquots of BHI broth (20 mL) were inoculated with 3-4 colonies of bacteria from plates that had been growing the bacteria for 24 h. After 18 h of planktonic growth, 20 µl of bacteria suspension were then transferred into fresh BHI broth (20 mL, 37 °C). Cell growth in this fresh BHI was monitored on a UV-Vis plate reader (iEMS Incubator/Shaker, Thermo Scientific, UK) until an optical density reading between 0.2-0.3 was obtained at 620 nm (ABS_{620}). The bacterial cells were then washed twice by centrifugation (1614 g, 10 min, 25°C) with sterile saline (20 mL), and resuspended in saline to provide an ABS_{620} reading of 0.16 measured with the UV-Vis plate reader (200 µL aliquot). Aliquots (200 µL) of the cell suspension were transferred to the wells of a sterile 96-well microtitre plate, the plate was sealed and centrifuged for 60 min at 2046 g. The supernatant was removed by inverting the plate, and the wells were treated with 200 µL aliquots of the test solutions for 2 min. The test solutions were removed and the cells washed twice with 200 µL aliquots of saline making sure to cause minimal agitation to the cells. Aliquots (200 µL) of fresh BHI were added to the wells. The plates were sealed and both bacterial strains were incubated in aerobic conditions at 37°C in the UV-Vis plate reader for 24 hours, taking 620 nm absorbance readings every 15 minutes. The Richards model (Equation 3.1.) was used to describe the growth curves (Dalgaard & Koutsoumanis., 2001).

$$ABS_t = ABS_{min} + \frac{ABS_{max} - ABS_{min}}{[1 + exp\,(-\mu ABS^{*} m^{*} (t - t_i)]^{1/m}} \qquad \text{[Equation 3.1.]}$$

Where ABS_t was the absorbance at time, ABS_{min} and ABS_{max}, were the asymptotic minimum and maximum absorbance's, μABS was the maximum specific growth rate, t was the time (h), ti was the time to inflection, or time to the point at which the sign of the curve changes from a positive curvature to a negative curvature or vice versa, and m was the modifier for growth dampening. The growth curve data were entered into the Origin 9.1 software programme (OriginLab Corp., USA) and a nonlinear curve fit was performed on each growth curve to determine ti and ABS_{max} for each treatment run. The ti value was selected to measure lag phase whilst ABS_{max} was selected to measure post-growth maximum population density. Each experiment was performed in triplicate on three separate occasions.

To understand if (+) α-TP was binding to the cell surfaces of *S. oralis,* the antimicrobial growth retardation assay was performed and the cells exposed to test solutions were washed twice with a neutralising rinse (200 μL) instead of saline. The neutralising rinse consisted of Tween 80, 10% (v/v), lecithin, 0.5% (w/v), and phosphate buffer (281 μM pH 7.2 ± 0.2) in distilled water. The negatively charged phospholipids bind the positively charged CHX and the zwitterion phospholipids bind the negatively charged phosphate groups of (+) α-TP to inhibit antimicrobial substantive effects. Each experiment was performed in triplicate on three separate occasions.

3.3.2 MBC assay

In order to assess if (+) α-TP had antimicrobial properties its MBC against *S. oralis* and *S. mutans* was assessed and compared with other established antimicrobial agents. Aliquots of BHI broth (20 mL) were inoculated with 3-4 colonies of bacteria from plates that had been

growing the bacteria for 24 h. After 24 h of planktonic growth the inoculated broth culture was then diluted to 4 x 10^5 CFU/ mL and plated at 100 µL/ well in 96 well plates. A series of (+) α-TP concentrations (1024, 512, 256, 128, 64, 32, 16, 8, 4, 2, 1 and 0.5 µg/ mL) were prepared from the stock solution. The test solutions (100 µL) were then added to the wells providing final (+) α-TP concentrations of 512, 256, 128, 64, 32, 16, 8, 4, 2, 1, 0.5 and 0.25 µg / mL. Plates were sealed and incubated for 24 h at 37 °C, 100 µL aliquots from each well transferred to blood agar plates and the plates were incubation for 24 h at 37 °C. The blood agar plates were then assessed for colony formation with the first plate not to show any growth being considered to represent the minimum bactericidal concentration. A sterility (no bacterial inoculation) negative control and vehicle (no (+) α-TP) positive control were used. Each experiment was performed in triplicate on three separate occasions.

3.3.3 Unsterilised whole mouth saliva biofilm growth inhibition

HA discs pre-treated with (+) α-TP (0.15% w/v, 300 µL) or (+) α-T (0/15%w/v, 300 µL) statically for 10 minutes were washed with saline (600 µL, 2 min) and placed in UWMS from one donor (400 µL) (fasted for at least 8 h) in micro centrifuge tubes vertically and incubated at 37 °C for 18h (without supplements). The HA discs were then washed with saline (600 µL, 2 min) and exposed to the live/ dead stain (200 µL) for 30 minutes followed by imaging. Live/ dead bacterial viability kit was prepared as per the vendors' procedure. Biofilms were observed using 10x oil immersion objective and a Leica sp2 confocal microscope with 488 and 568 nm excitation and 500-530 nm (green fluorescence representing up take of Syto 9 by live cells) and > 620 nm (Red fluorescence representing up take of propidium iodide by dead cells) emission filters. Biofilm height was measured using the z-stacking tool taken each side of the HA discs. There was no cross over between emission spectra and excitation intensities were ≤

31%. Biofilms grown on HA discs pre-treated with the vehicle were used as controls. Experiments were performed by measuring biofilm height once, each side of each HA disc and were performed in triplicate. All images were taken from the middle of each disc.

3.3.4 Hydroxyapatite binding assay

HA discs were placed into micro centrifuge tubes containing (+) α-TP or (+) α-T test solutions (0.01% w/v, 300 μL in 20% ethanol, 80% water, pH 7.4 with 150 mM Tris vehicle) statically for 10 minutes. Discs were then removed and placed in saline (600 μL) for 2 minutes. Vehicle (300 μL) was added to the 10 minute samples (1/2 dilution). This procedure was replicated with (+) α-TP and (+) α-T samples without the presence of HA as controls. Test solutions with and without HA disc treatments and saline rinse were tested *via* HPLC for the concentration of (+) α-TP and (+) α-T in triplicate.

3.3.5 Characterisation of (+) α-T and (+) α-TP aggregates

The packing parameter was used to predict aggregate structure. It was calculated from v_o/ael_o, where v_o is the surfactant tail volume ($Å^3$), l_o is the maximum tail length (Å), and ae is the equilibrium area per molecule at the aggregate surface ($Å^2$). Values between ≤ 0 and $1/3 \geq$ are predicted to be spherical micelles, $\leq 1/3$ and $1/2 \geq$ are predicted to be globular micelles or cylindrical micelles, $\leq 1/2$ and $1 \geq$ are predicted to be spherical bilayers (liposomes) and ≤ 1 are predicted to form planar bilayers (Nagarajan., 2002). Equations 3.2 and 3.3 where used to calculate v_o and l_o (Tanford., 1972).

$$v_o = 27.4 + 26.9\eta_c \quad \text{[Equation 3.2.]}$$

$$l_o = 1.5 + 1.265\eta_c \quad \text{[Equation 3.3.]}$$

Where η_c is the number of carbon atoms in the surfactant tail. The value of ae used was 54 $Å^2$, this is a value that has been experimentally determined for n-$C_8H_{17}OPO_3NaH$ (Chevalier & Chachaty., 1984) and has been previously used to predict the shapes of branched monoalky phosphate aggregates (Ravoo & Engberts., 1994).

Height and phase images of the untreated mica, the Tris vehicle (20% ethanol, 80% water, 150 mM Tris at pH 7.4), the (+) α-T (0.15% w/v) and the (+) α-TP (0.15% w/v) (dispersed in 20% ethanol. 80% water at pH 7.4 with and without 150 mM Tris) were obtained to assess the size and shape of the aggregates using atomic force microscopy (AFM; Bruker icon dimension, UK). All images were obtained in tapping mode using high resonance frequency (HRF = 320 kHz) pyramidal cantilevers with uncoated Si_3N_4 tips having force constants of 46 N/m in air. Mica was chosen as a solid substrate on to which 2-3 drops of the test samples were placed, the samples were dried with nitrogen and then imaged. Scan speeds were set at 0.9 Hz. Measurements were recorded using the NanoScope 1.50 AFM image analysis software (Bruker, USA) and were analysed using Gwyddion 2.45, a free SPM data visualisation and analysis programme.

3.3.6 Data analysis

All error values/ bars were expressed as their mean ± standard deviation (SD). Statistical analysis of data was performed using Levine's homogeneity test before statistical significance

between the sample groups was assessed by one way analysis of variance (ANOVA) tests with post-hoc Tukey analysis in Origin 2016. Statistically significant differences were assumed when $p \leq 0.05$.

3.4 Results

3.4.1 Substantive antimicrobial growth retardation effect of (+) α-T (+) α-TP against streptococci species

Both single species bacterial biofilms used in this work were shown to have classical s-shaped growth profiles, with there being a bacterial growth lag phase at the early stage of the experiments followed by an exponential phase of bacterial growth and finally a plateauing of the curve at a maximum bacterial population. These growth profiles were fitted with a non-linear fit model and this allowed two antimicrobial outputs to be monitored; the growth time inflection points (midpoint of exponential growth) and maximum population density (ABS_{max}) outputs as they monitor the delaying of growth and population limitation. Figure 3.1 shows the growth profile of *S. oralis* after treatment with (+) α-TP (0.51% w/v), indicating the two indices used to assess antimicrobial activity, growth time to inflection point and post-growth turbidity equilibrium (ABS_{max}).

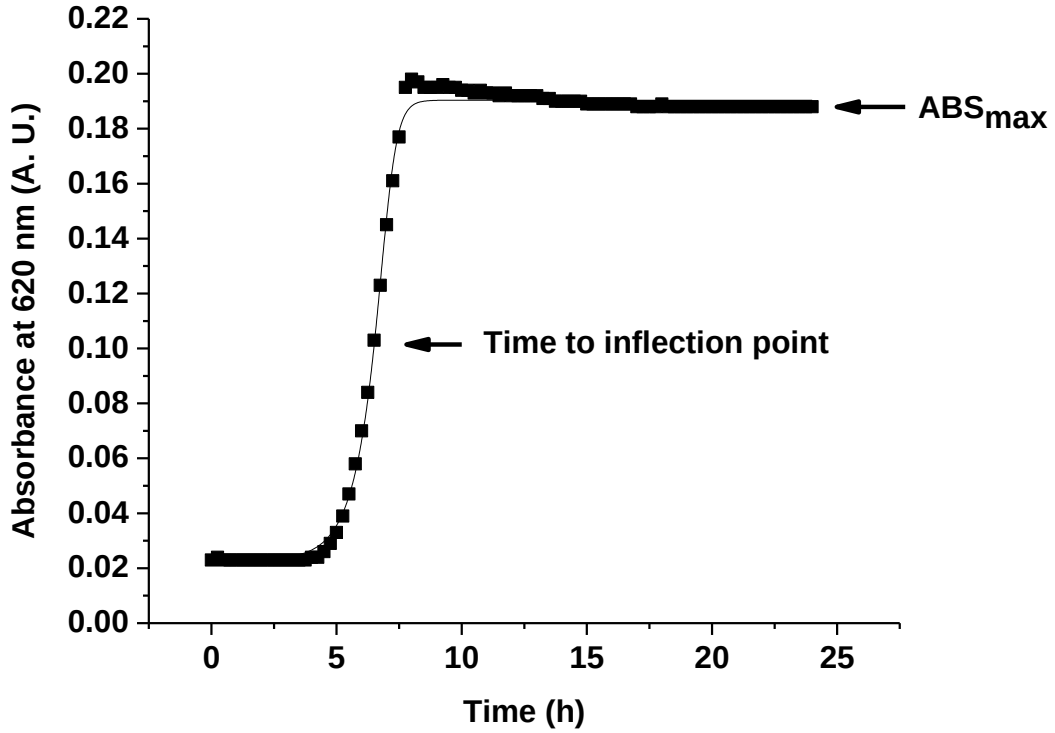

Figure 3.1. Nonlinear fit growth curves of Streptococcus oralis measured by absorbance at 620 nm every 15 minutes post 2 minute treatment with 0.51% w/v (+) alpha tocopheryl phosphate using the Richards equation (Equation 3.1.).

S. oralis was found to have a growth time inflection point at 2.2 ± 0.9 h when treated with water for two minutes (Figure 3.2 A). Treating *S. oralis* with Tris gave a growth time inflection point of 1.7 ± 0.2 h (Figure 3.2 A). These two results were not statistically different ($p > 0.05$). A dose dependent increase of the growth time inflection was observed when *S. oralis* was treated with the positive control, CHX, in the concentration range of 0.00125% w/v to 0.01% w/v (washed with saline). (+) α-TP was found to retard *S. oralis* bacterial growth to a maximum of 5.4 ± 1.3 h (Figure 3.2 A), but it did not generate a dose dependent effect (Figure 3.2 A). (+) α-T gave a statistically significant antimicrobial response ($P < 0.05$) against *S. oralis*, but this was much smaller in magnitude compared to (+) α-TP ($P=0.002$).

The maximum population of *S. oralis* post-growth after the treatment with (+) α-TP was reduced in a dose dependant manner. Each of the reductions was statistically different from each other, the vehicle and (+) α-T (Figure 3.2 B, $p < 0.05$). For CHX there was little effect on *S. oralis* post-growth population density for concentrations between 0.00125% and 0.005% w/v, however, there was a dramatic drop in post growth population density after using 0.01% w/v solution of CHX ($p = 0.000005$).

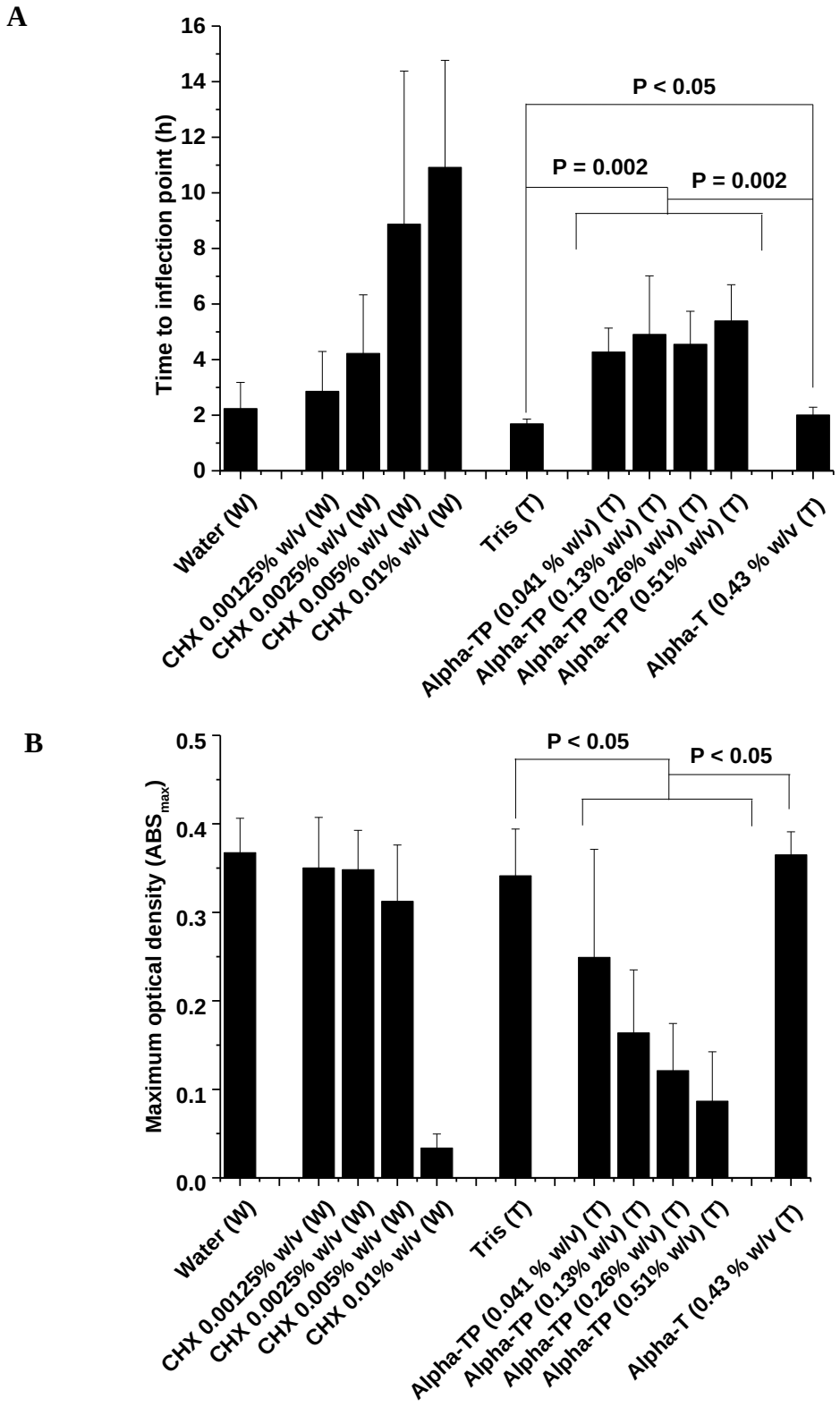

Figure 3.2. Time to inflection points of *Streptococcus oralis* biofilms treated then washed with saline (A) and (B) post-growth maximum population densities. Where CHX is chlorhexidine, Alpha TP is (+) alpha tocopheryl phosphate and Alpha T is (+) alpha tocopherol. Data represents mean ± standard deviation (n=3). (Tris (T) consists of 20% ethanol, 80% water (v/v) with 150 mM Tris made pH 7.4 ± 0.2) (Water (W) contains 20% ethanol). % concentrations were w/v.

When *S. oralis* was washed with a charge neutralising rinse instead of saline after the application of test solutions the time to inflection points and post-treatment maximum growth density profiles changed for both CHX and (+) α-TP. CHX no longer gave a dose dependent response and its activity appeared to be supressed. For example, the 0.01% w/v CHX solution displayed reduced time to inflection from 10.9 ± 3.9 h (Figure 3.2 A) to 3.5 ± 0.5 h (Figure 3.3 A) upon use of the neutralising rinse and the post-growth maximum population densities of bacteria increased from 0.03 ± 0.02 (Figure 3.2 B) to 0.33 ± 0.02 (Figure 3.3 B). Similarly, when the (+) α-TP treated bacteria were washed with the neutralising rinse the activity of the (+) α-TP 0.51% w/v solution reduced from 5.4 ± 1.3 h (Figure 3.2 A) to 2.7 ± 0.3 h (Figure 3.3 A) in terms of time to inflection and increased from 0.09 ± 0.06 (Figure 3.2 B) to 0.34 ± 0.05 (Figure 3.3 B) in terms of post-treatment population density.

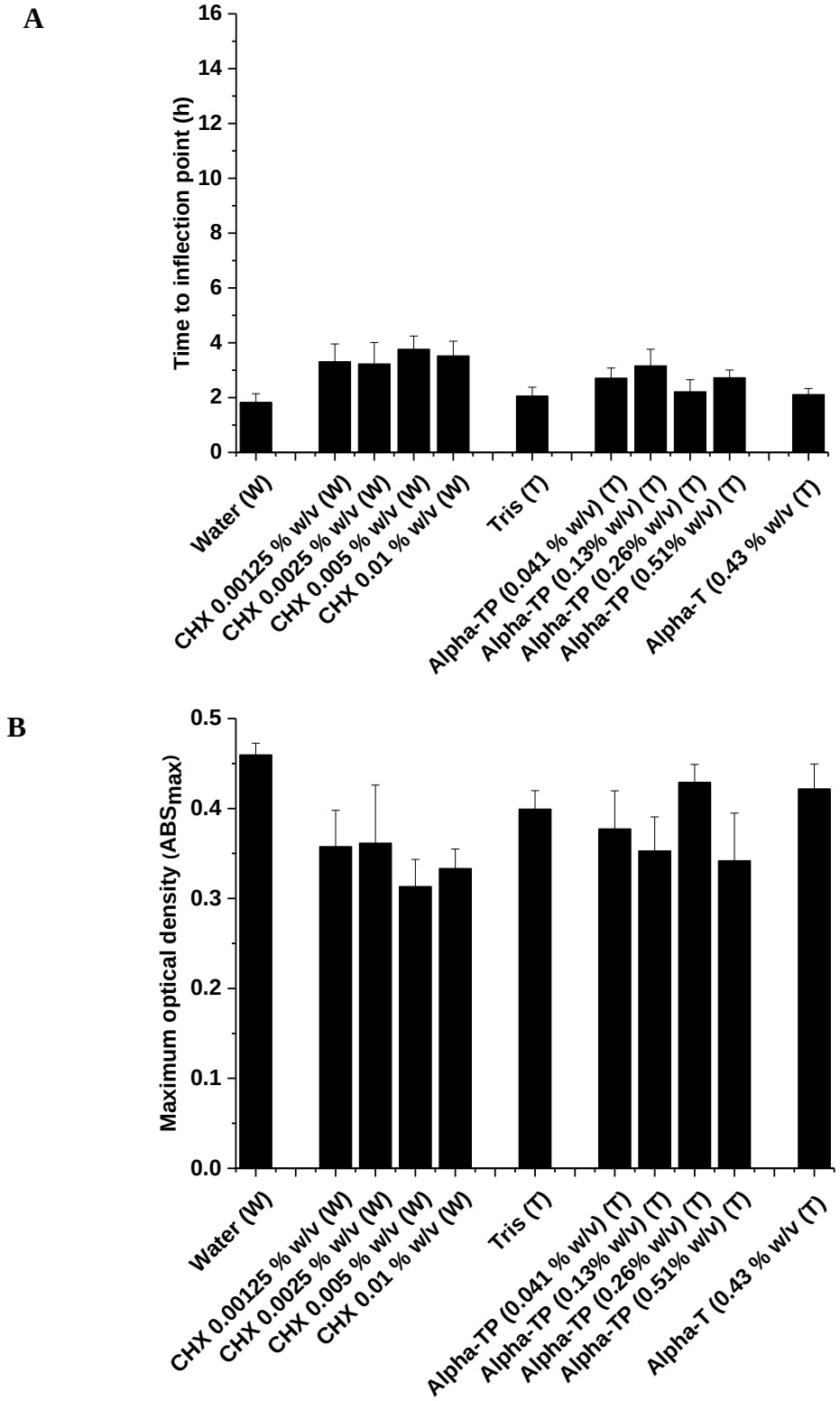

Figure 3.3. Time to inflection points of *Streptococcus oralis* biofilms treated then washed with neutralising rinse (A) and post-growth maximum population densities. Where CHX is chlorhexidine, Alpha TP is (+) alpha tocopheryl phosphate and Alpha T is (+) alpha tocopherol. Data represents mean ± standard deviation (n=3). (Tris (T) consists of 20% ethanol, 80% water (v/v) with 150 mM Tris made pH 7.4 ± 0.2) (Water (W) contains 20% ethanol). % concentrations were w/v.

As (+) α-TP and CHX were effective in inhibiting *S. oralis* growth these two samples were also tested against *S. mutans*. When *S. mutans* were treated with CHX and washed with saline using the same concentration range as *S. oralis* the bacteria did not recover. However, when *S. mutans* were treated with the same concentration range of (+) α-TP and washed with saline the comparative growth time to inflection points between *S. oralis* and the *S. mutans* was reduced from 5.4 ± 1.3 h (Figure 3.2 A) to 3.0 ± 0.5 h (Figure 3.4 A) (0.51% w/v), but the *S. mutans* data was still statistically different from the vehicle ($p = 0.01$). There was also a reduced effect on the post-growth maximum population density when comparing the (+) α-TP effects on *S. oralis* and the *S. mutans* which were 0.09 ± 0.06 (Figure 3.2 B), and 0.22 ± 0.04 (Figure 3.4 B) respectively, but the *S. mutans* data was still significantly different compared to the vehicle ($p = 0.0007$).

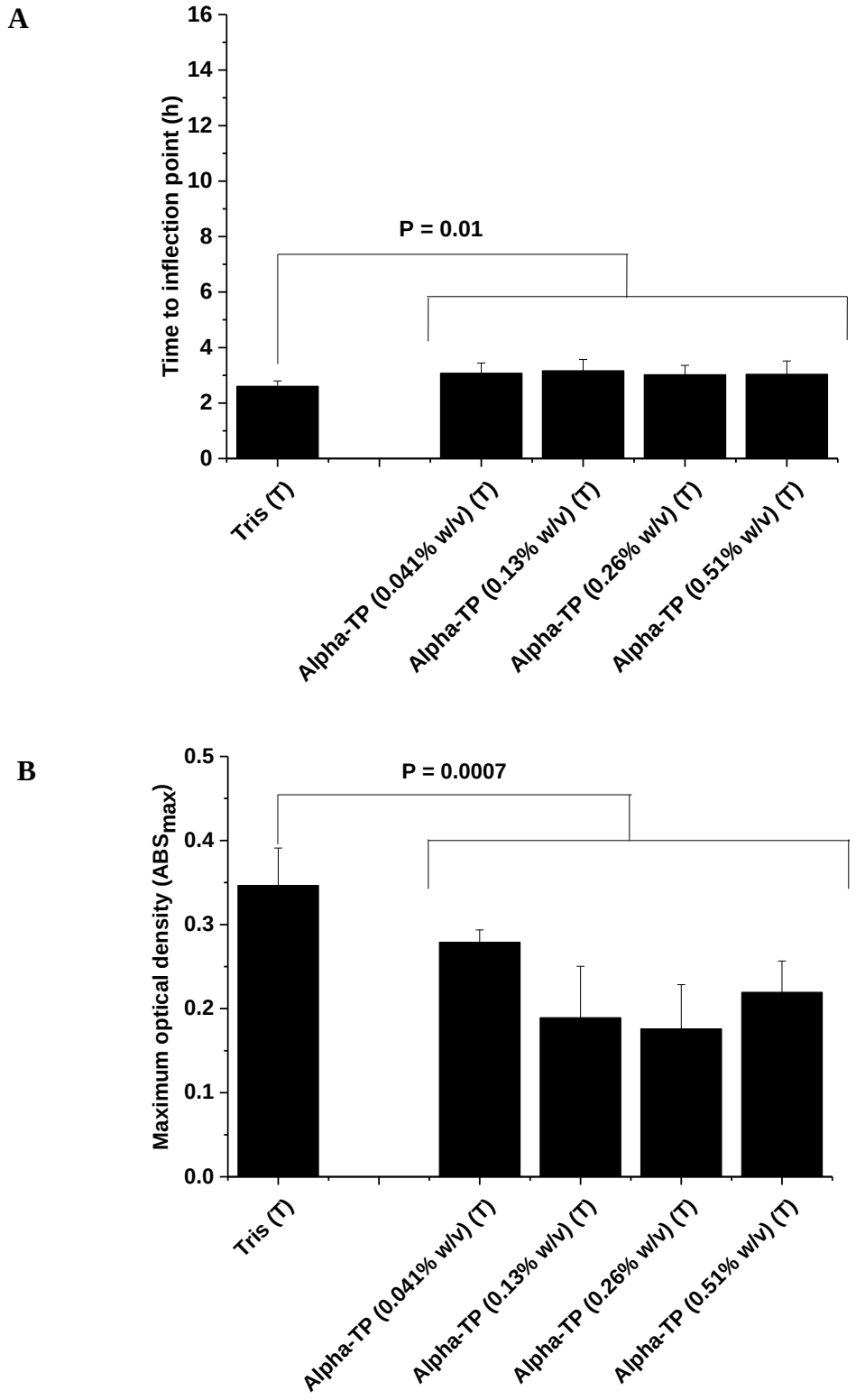

Figure 3.4. Time to inflection points of *Streptococcus mutans* biofilms treated then washed with saline (A) and (B) post-growth maximum population densities. Where Alpha TP is (+) alpha tocopheryl phosphate. Data represents mean ± standard deviation (n=3). (Tris (T) consists of 20% ethanol, 80% water (v/v) with 150 mM Tris made pH 7.4 ± 0.2). % concentrations were w/v.

3.4.2 Minimum bactericidal concentration of (+) α-TP against *S. oralis* and *S. mutans*

(+) α-TP (in the Tris vehicle) when diluted in the broth culture resulted in turbidity and so the visible growth of bacteria could not be monitored in order to determine the minimum inhibitory concentration using a traditional methodology. However, the MBC could still be assessed and was found to be 1 µg/ mL (Figure 3.5) whereas the MBC against *S. mutans* was > 512 µg/ mL as the bacteria grew on all the blood agar plates even when incubated with the highest concentration of (+) α-TP.

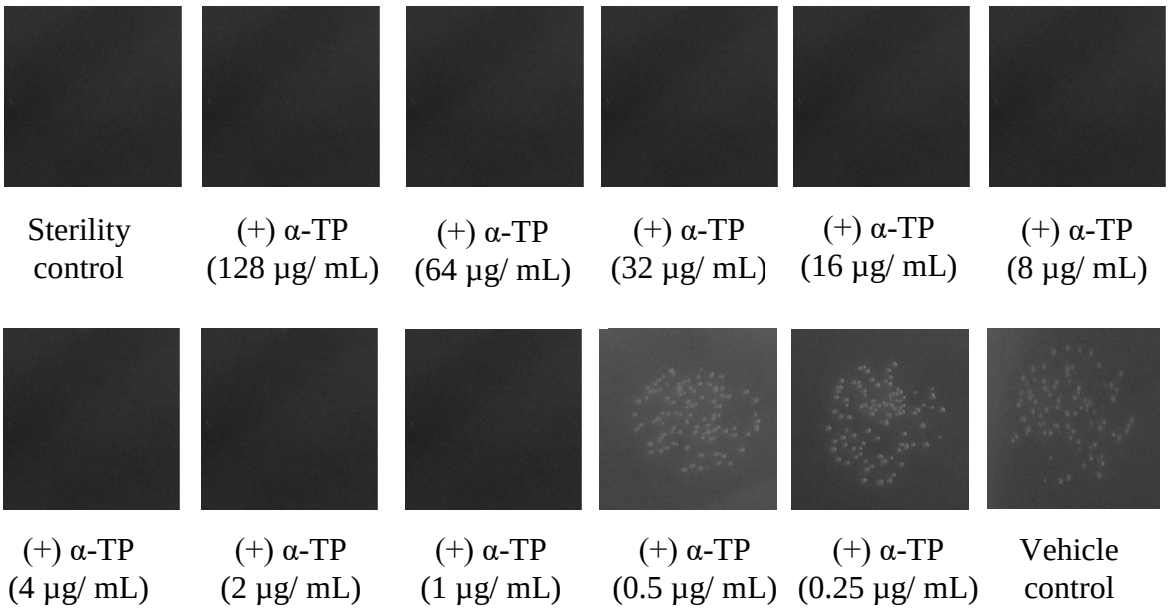

Figure 3.5. Photographs of grown *Streptococcus oralis* (100 µL aliquots) colonies when incubated on blood agar plates at 37˚C after 24 h in the minimum bactericidal concentration assay. The aliquots were from planktonic bacteria (4 x 10^5 CFU/ mL)) that had been dispersed in brain-heart infusion (BHI) broth and incubated at 37˚C with varying concentrations of (+) alpha tocopheryl phosphate (α-TP) for 24 h. The (+) α-TP was dispersed in 20% ethanol, 80% water with 150 mM Tris at pH 7.4 and diluted 1:1 with the bacterial inoculated BHI broth.

3.4.3 Unsterilized whole mouth saliva biofilm growth inhibition of (+) α-T and (+) α-TP

Confocal imaging showed that discs pre-treated with the vehicle for 10 minutes (80% water, 20% ethanol, 150 mM Tris at pH 7.4) followed by a 2 minute saline rinse produced a biofilm height of 76 ± 15 μm after 18 hour incubation with UWMS (400 μL) (Figure 3.6). Discs pre-treated with (+) α-T (3 mM) resulted in a biofilm height of 58 ± 18 μm, which was not statistically different to the vehicle control ($p > 0.05$). HA discs pre-treated with (+) α-TP (3 mM, 0.15 % w/v) resulted in a biofilm of 38 ± 7 μm in height, which was statistically smaller compared to the vehicle control ($p = 0.0006$) and (+) α-T ($p < 0.05$) pre-treated discs. These results suggested that the (+) α-TP bound to the HA and elicited an antimicrobial response even after attempts were made to wash the drug off the surface.

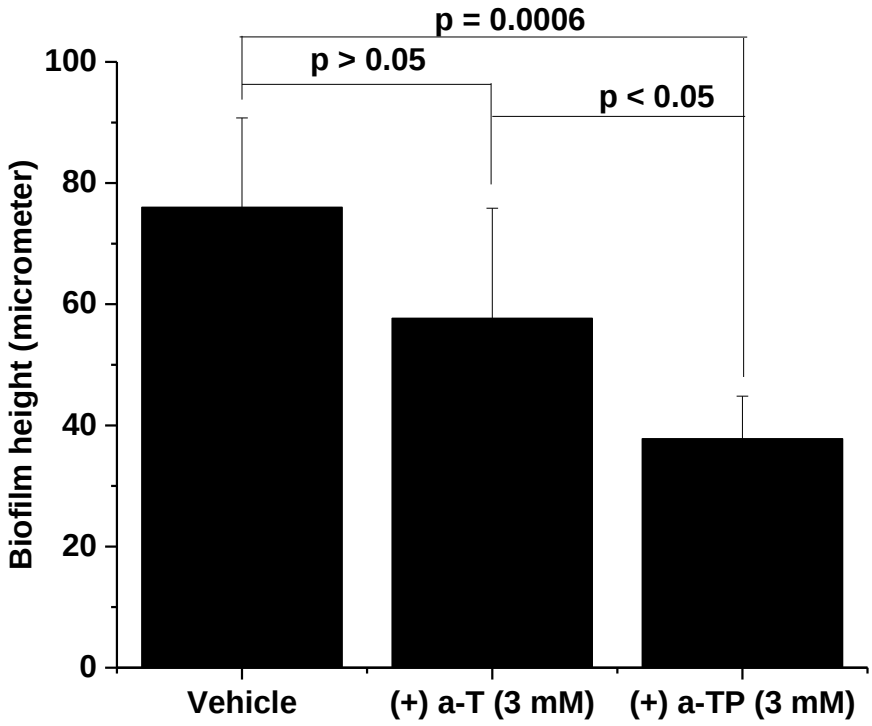

Figure 3.6. Height of oral biofilms formed on hydroxyapatite pre-treated discs after 18 hours incubation with unsterilized whole mouth saliva (10 x magnification, confocal microscopy, live/dead staining). Where (+) a-T was alpha tocopherol, (+) a-TP was (+) alpha tocopheryl phosphate and the vehicle is 20% ethanol, 80% water, 150 mM Tris, pH 7.4. Data represents mean ± standard deviation (n=3).

3.4.4 Binding of (+) α-T and (+) α-TP to hydroxyapatite

When (+) α-TP (200 µM, 0.01% w/v, 300 µL) was incubated with HA the concentration of (+) α-TP remaining in the incubation fluid was 25 ± 12 % of its initial concentration. This suggested that (+) α-TP were binding to the HA. Using the same concentration of (+) α-T, 99 ± 18% was found in the incubation solution, which suggested that it did not to bind to HA (Figure 3.7). The difference in (+) α-TP and (+) α-T HA binding was statistically different ($p = 0.00006$). Attempts to wash the (+) α-TP off the HA using saline were not successful, which suggested the binding was relatively strong.

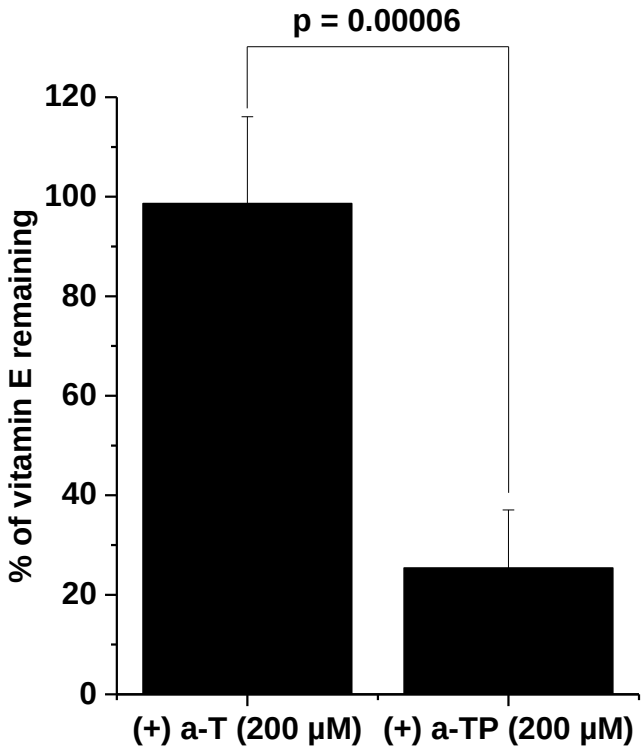

Figure 3.7. Comparison of (+) alpha tocopheryl and (+) alpha tocopheryl phosphate remaining in solution after 10 minute exposure to hydroxyapatite discs inset (high performance liquid chromatography). Where (+) a-T was alpha tocopherol, (+) a-TP was (+) alpha tocopheryl phosphate and the vehicle is 20% ethanol, 80% water, 150 mM Tris, pH 7.4. Data represents mean ± standard deviation (n=3).

3.4.5 (+) α-T and (+) α-TP biophysical analysis – Atomic Force Microscopy

It has been shown that in Chapter 2 (+) α-TP formed Nano sized aggregates. Supramolecular aggregates can form a variety of shapes and transition into different structures depending on molecular characteristics and formulation conditions (Scheme 3.1). The η_c values for substantive antimicrobial (+) α-TP was 17 for v_o and 13 for l_o resulting in a v_o value of 484.7 $Å^3$ and a l_o value of 17.945 Å; its packing parameter was calculated to be 0.50. These indices suggested that (+) α-TP would form cylindrical micelles or spherical liposomes in the polar vehicle used in this work. AFM imaging showed (+) α-T formed liposomes with diameters of 551 ± 43 nm and heights of ~ 86 nm (Figure 3.8) and confirmed that the (+) α-TP structures were cylindrical in shape (Figure 3.9) with heights of ~ 22 nm when formulated in an ethanol, water mix. When (+) α-TP was formulated in the Tris vehicle the shape transitioned from cylinders to planar bilayer islands with diameters < 500 nm and heights of ~ 4.6 nm (Figure 3.10), the theoretical length of two (+) α-TP molecules, end to end, was calculated to be 4.4 nm. The shape of the (+) α-T liposomes was not affected by the presence of Tris (Figure 3.11). Untreated mica and the Tris vehicle were imaged as controls and where found to have smooth surfaces (Figure 3.12 and 3.13).

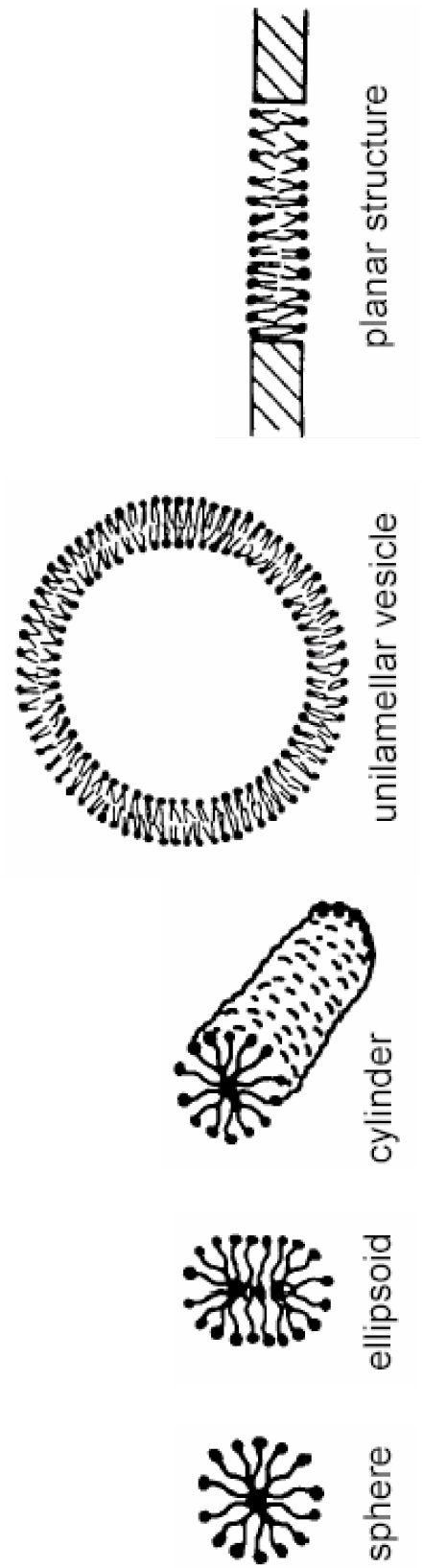

Scheme 3.1. Aggregate shape transitions.

i)

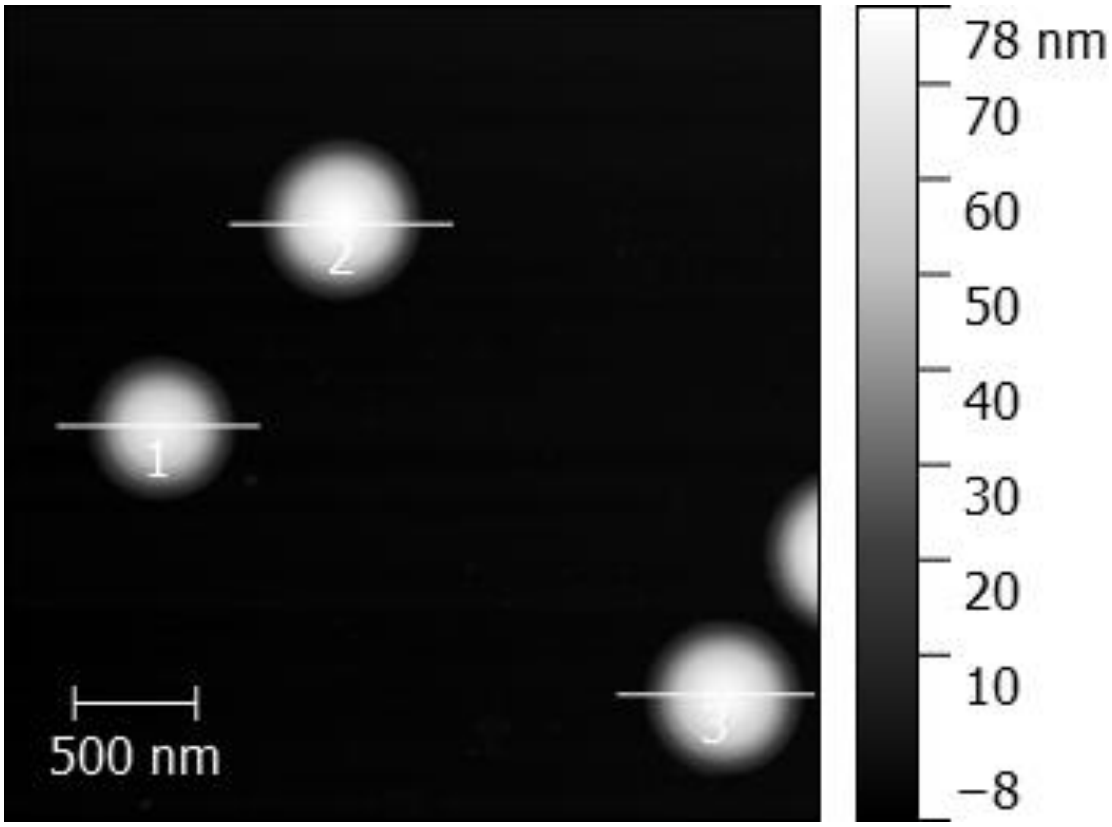

ii)

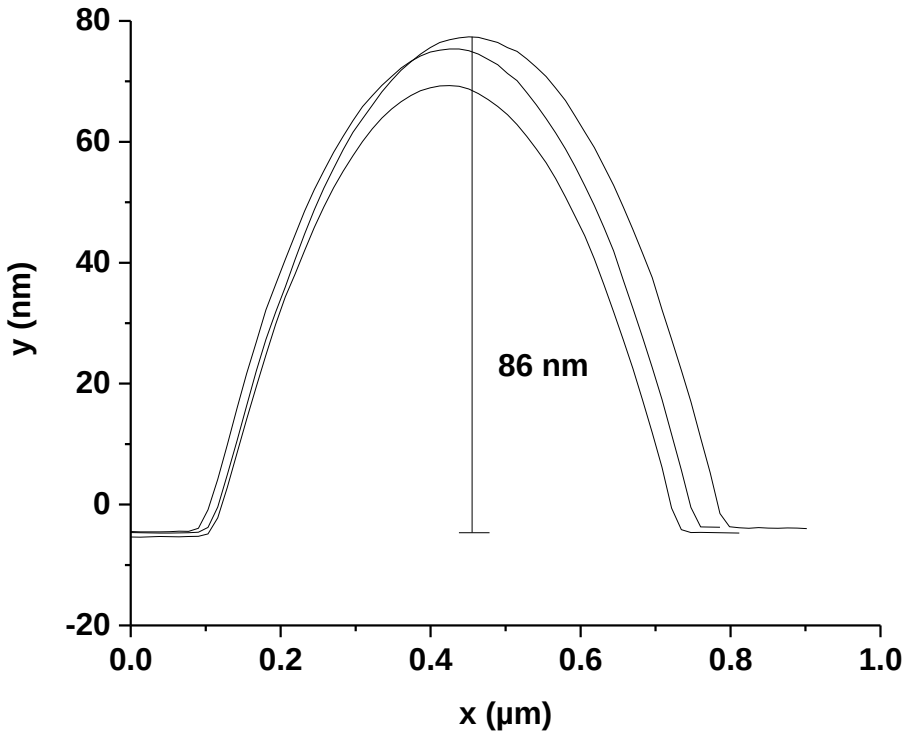

Figure 3.8a. Atomic force microscopy tapping height image (i), and cross-sectional profile (ii) of (+) alpha tocopherol. Samples were 3 mM dispersed in a 20% ethanol, 80% water, pH 7.4 vehicle.

i)

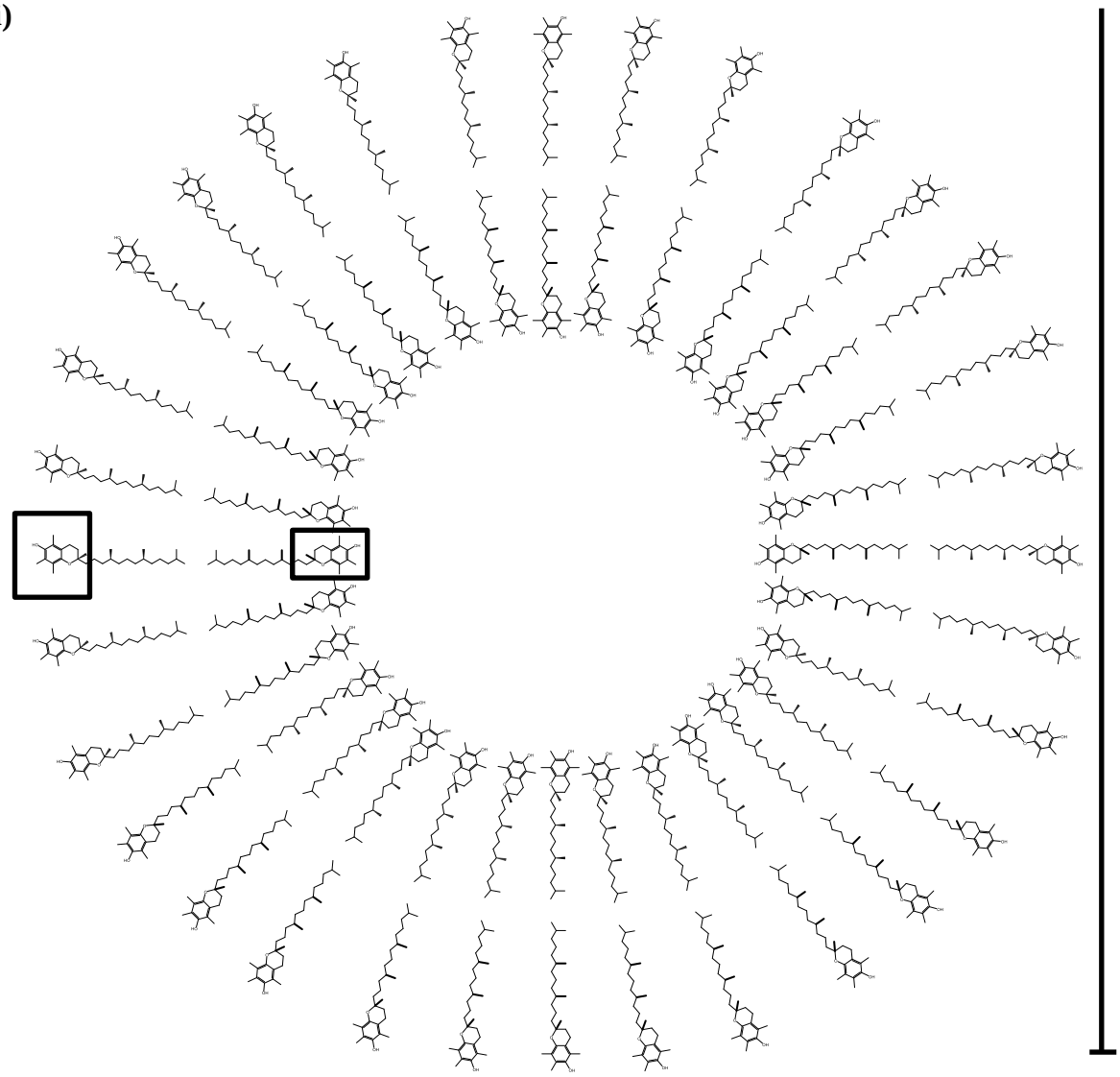

Spherical vesicle; 86 nm

ii)

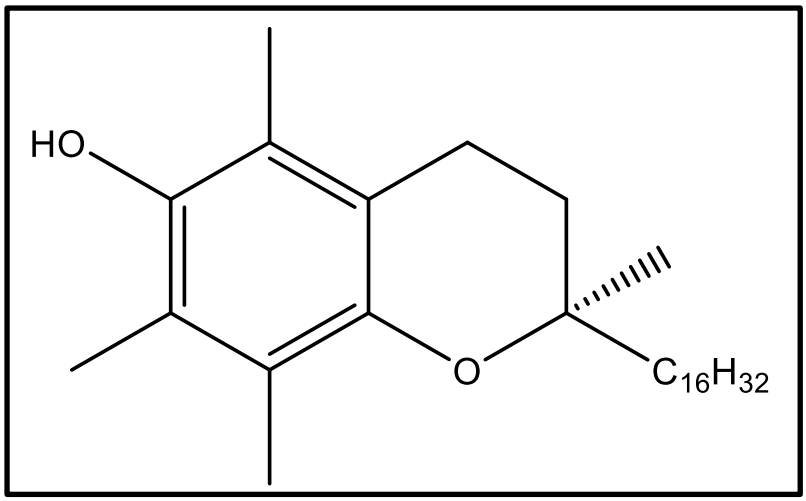

Figure 3.8b. Theoretical molecular packing of (+) alpha tocopherol aggregate structures (i), based on the AFM image in 3.8a, with enlarged head group (ii).

i)

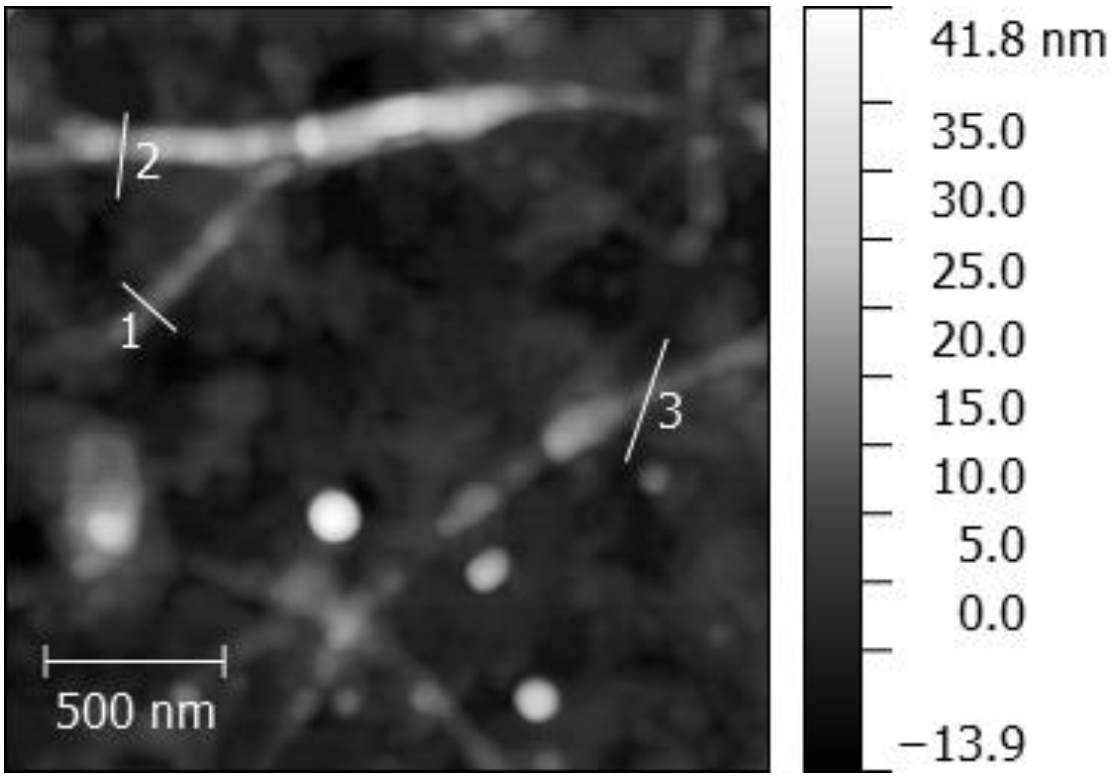

ii)

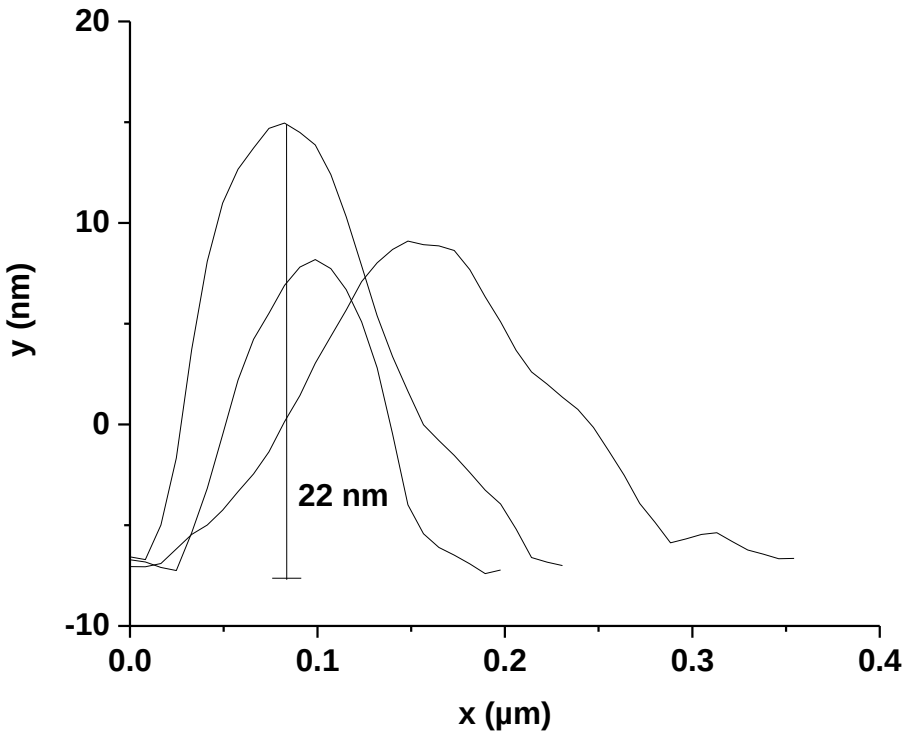

Figure 3.9a. Atomic force microscopy tapping height image (i), and cross-sectional profile (ii) of (+) alpha tocopheryl phosphate. Samples were 3 mM/ 0.15% w/v dispersed in a 20% ethanol, 80% water, pH 7.4 vehicle.

i)

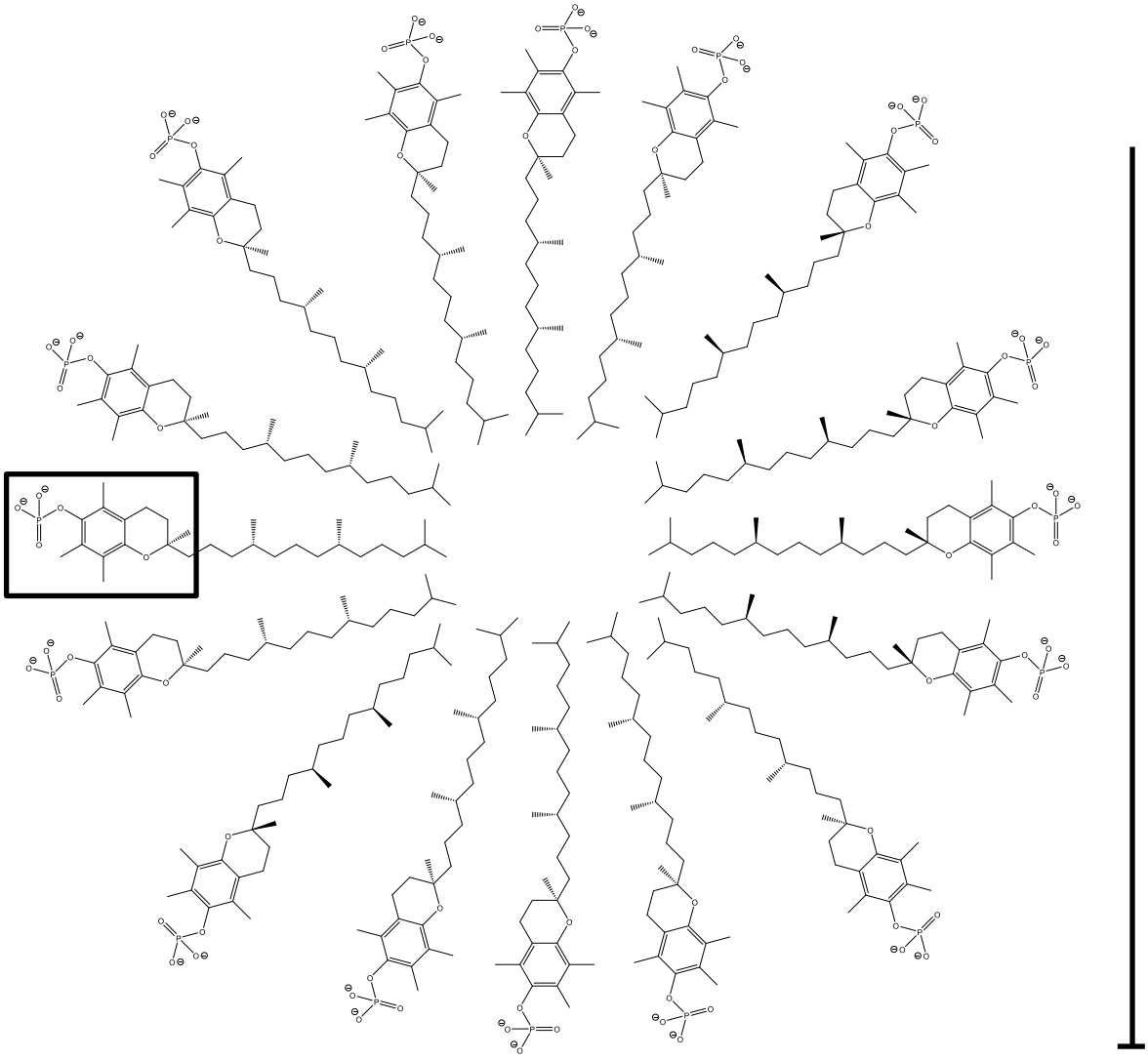

Cylinder; 22 nm

ii)

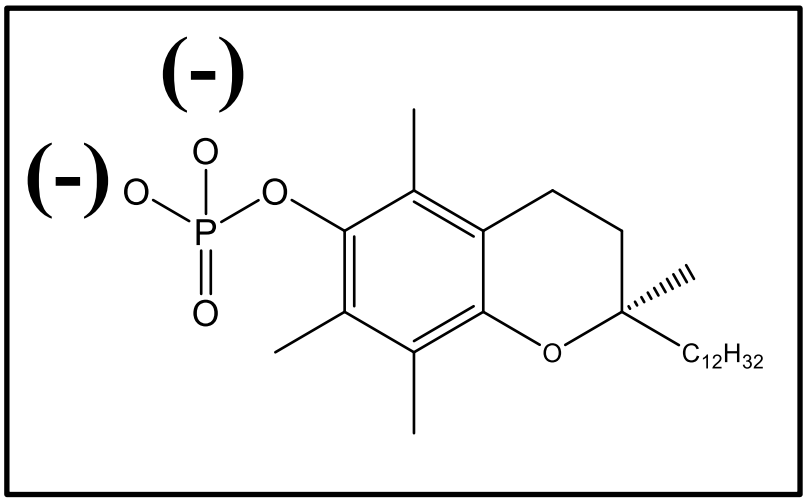

Figure 3.9b. Theoretical molecular packing of (+) alpha tocopheryl phosphate aggregate structures (i), based on the AFM image in 3.9a, with enlarged head group (ii).

i)

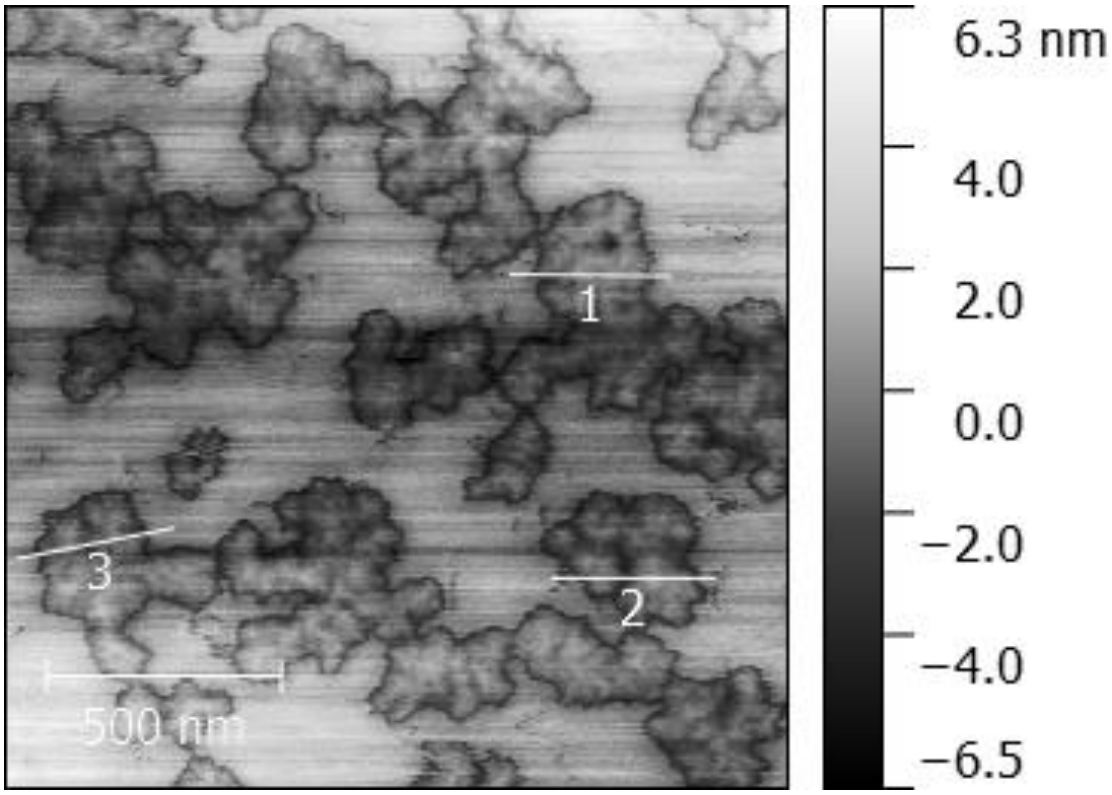

ii)

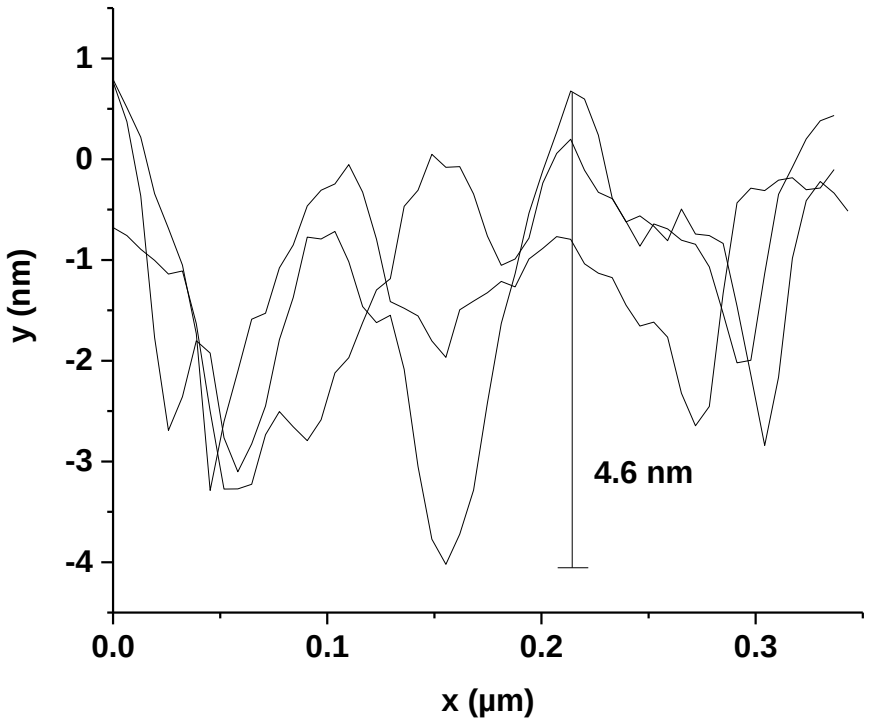

Figure 3.10a. Atomic force microscopy tapping height image (i), and cross-sectional profile (ii) of (+) alpha tocopheryl phosphate with Tris (150 mM). Samples were 3 mM/ 0.15% w/v dispersed in a 20% ethanol, 80% water, pH 7.4 vehicle.

i)

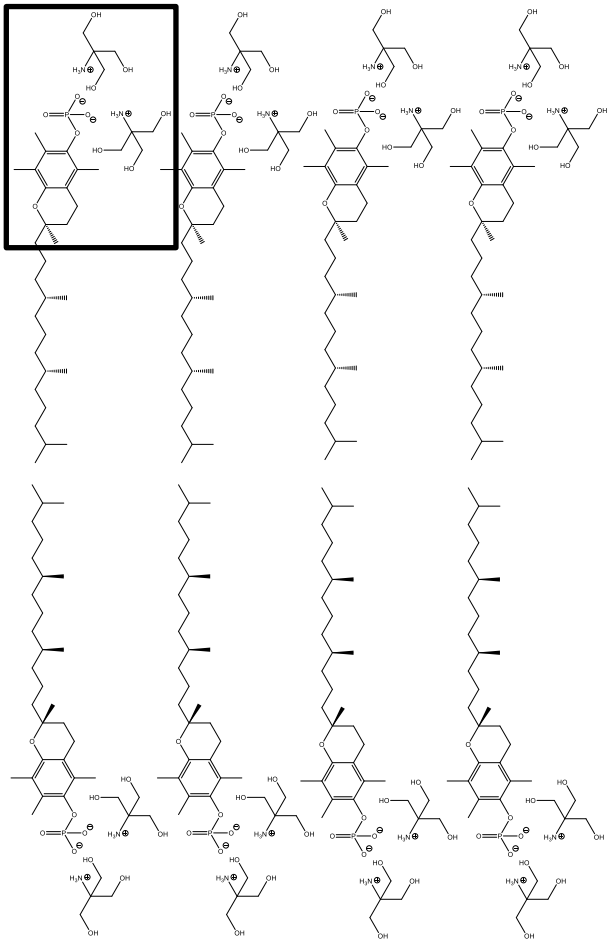

Planar structure: 4.6 nm

ii)

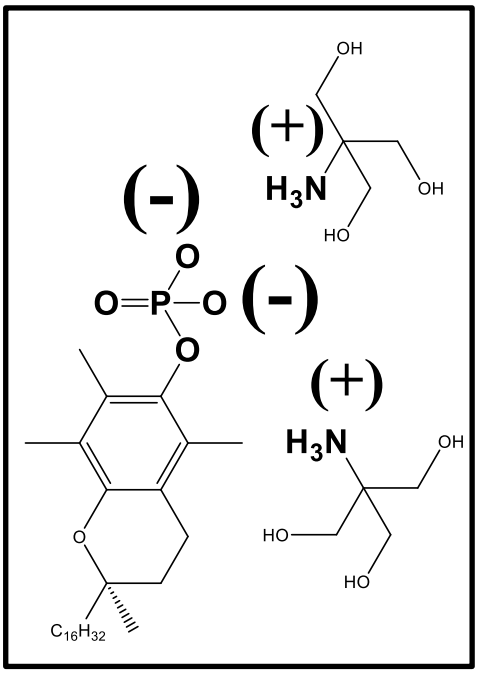

Figure 3.10b. Theoretical molecular packing of (+) alpha tocopheryl phosphate aggregate structures when formulated with Tris (i), based on the AFM image in 3.10a, with enlarged head group (ii).

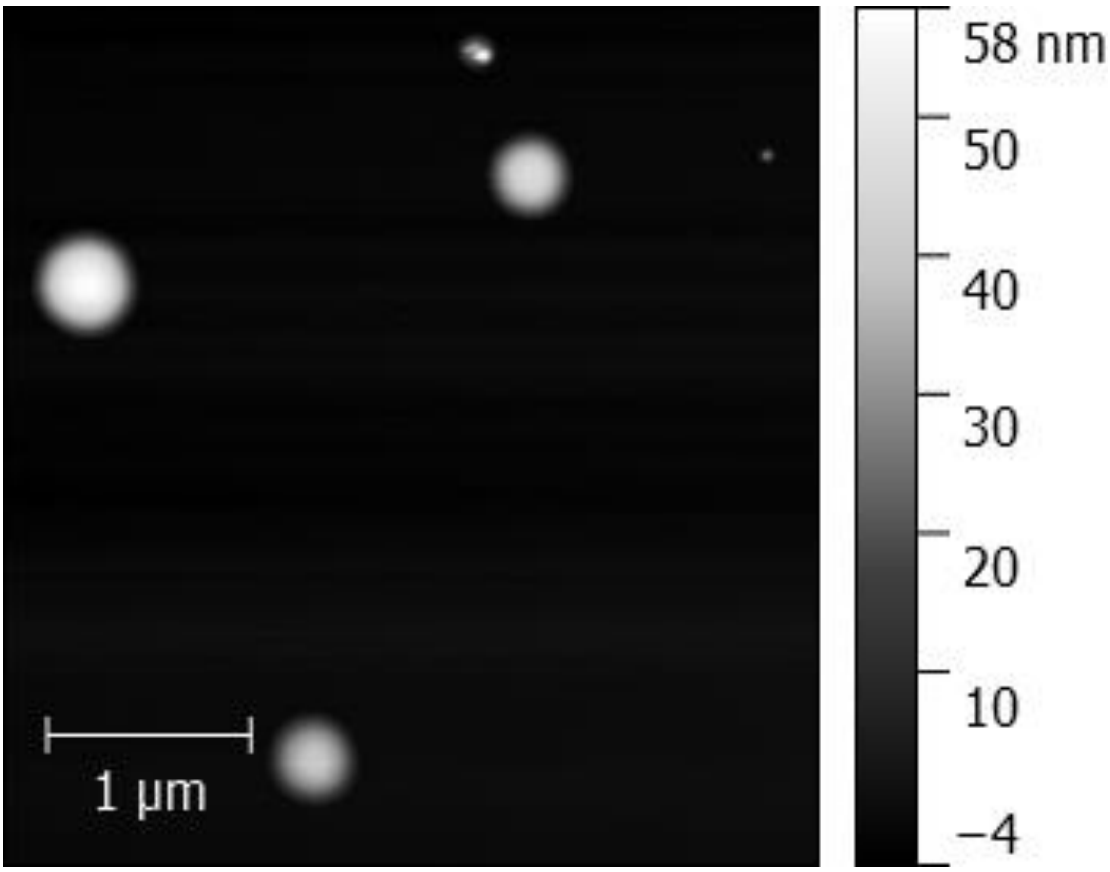

Figure 3.11. Atomic force microscopy tapping height image of (+) alpha tocopherol in the Tris vehicle. Samples were 3 mM dispersed in a 20% ethanol, 80% water, pH 7.4 vehicle

.

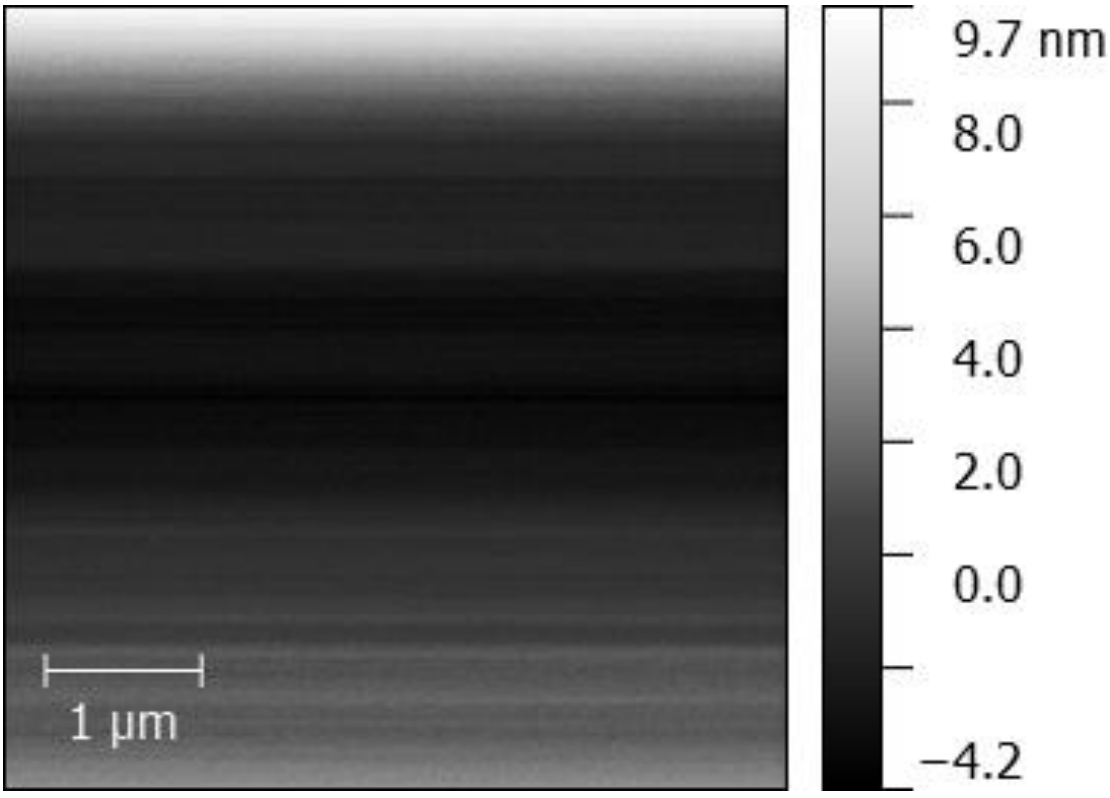

Figure 3.12. Atomic force microscopy tapping height image of the untreated mica.

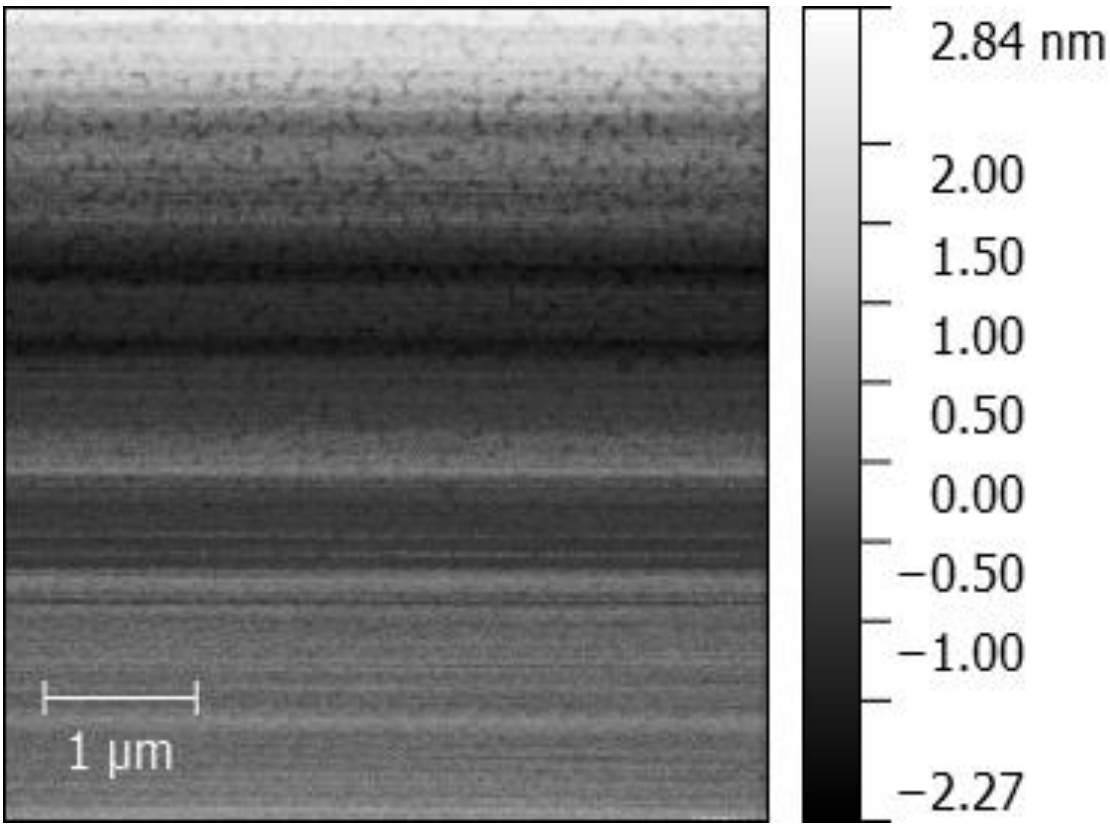

Figure 3.13. Atomic force microscopy tapping height image of the Tris (150mM) vehicle control. The samples were 20% ethanol, 80% water, pH 7.4 vehicle.

Interestingly the phase images showed that the (+) α-TP planar bilayer islands where viscoelastic and adhered/ were attracted to the silicon nitride cantilever probe as the oscillation angle was delayed by ~ 22.4 ° when in contact with the islands (Figure 3.14) relative to the mica/ Tris coated surface controls (Figure 3.17 and 3.18). The (+) α-TP thread-like cylinders were found to have some adhesive properties with the silicon nitride probe as the oscillating angle was delayed by up to ~ 19.2 ° but this was not consistent across the structure (Figure 3.15). The (+) α-T liposomes were not viscoelastic or adhesive relative to the mica and Tris surfaces as the oscillation angle delay was surprisingly reduced to ~ -22.9 ° when in contact with the liposomes suggesting the liposomes repulsed the silicon nitride probe (Figure 3.16).

i)

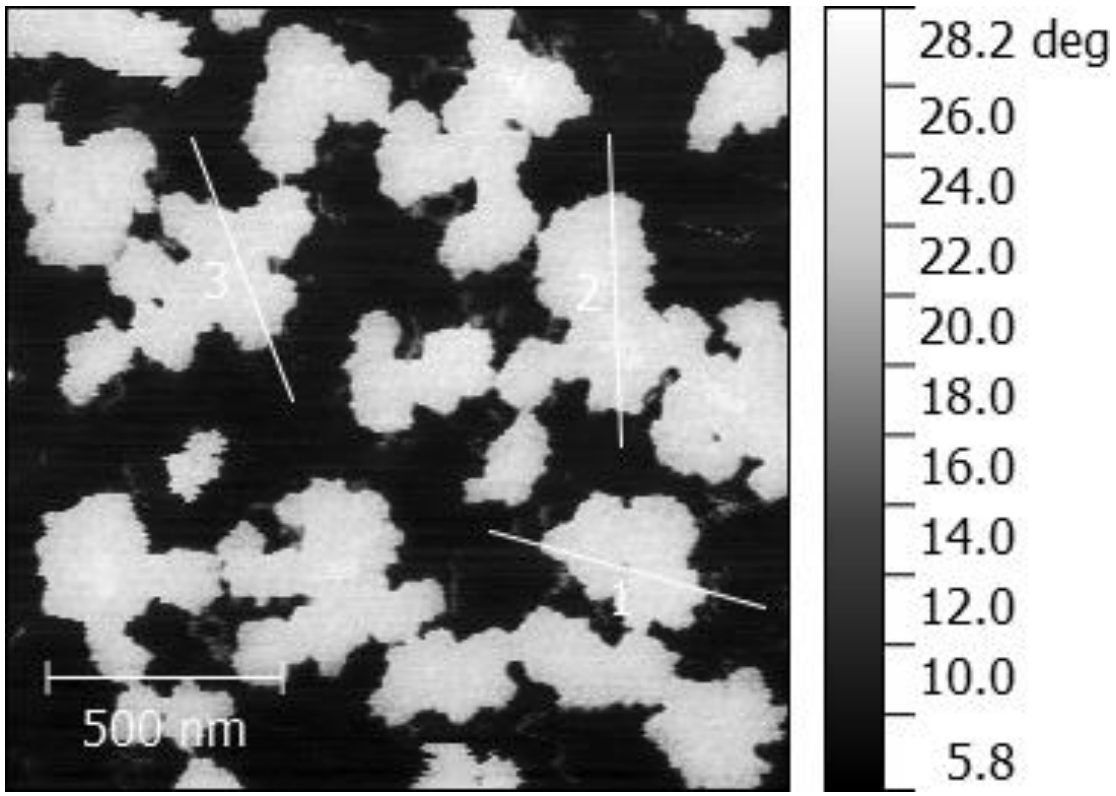

ii)

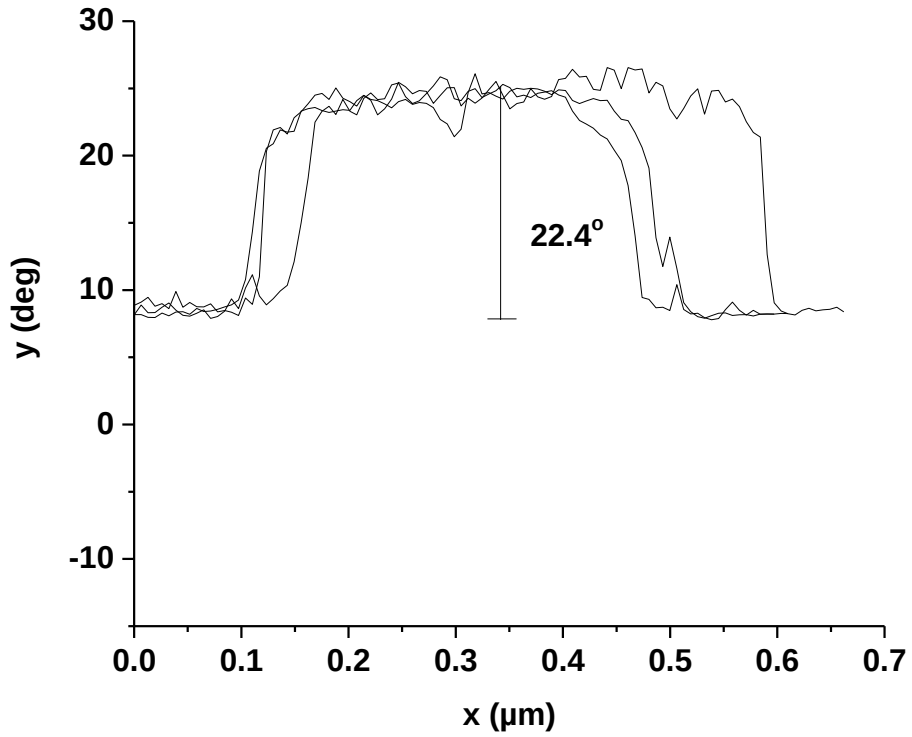

Figure 3.14. Atomic force microscopy tapping phase image (i), and cross-sectional profile (ii) of (+) alpha tocopheryl phosphate with Tris (150 mM). Samples were 3 mM/ 0.15% w/v dispersed in a 20% ethanol, 80% water, pH 7.4 vehicle.

i)

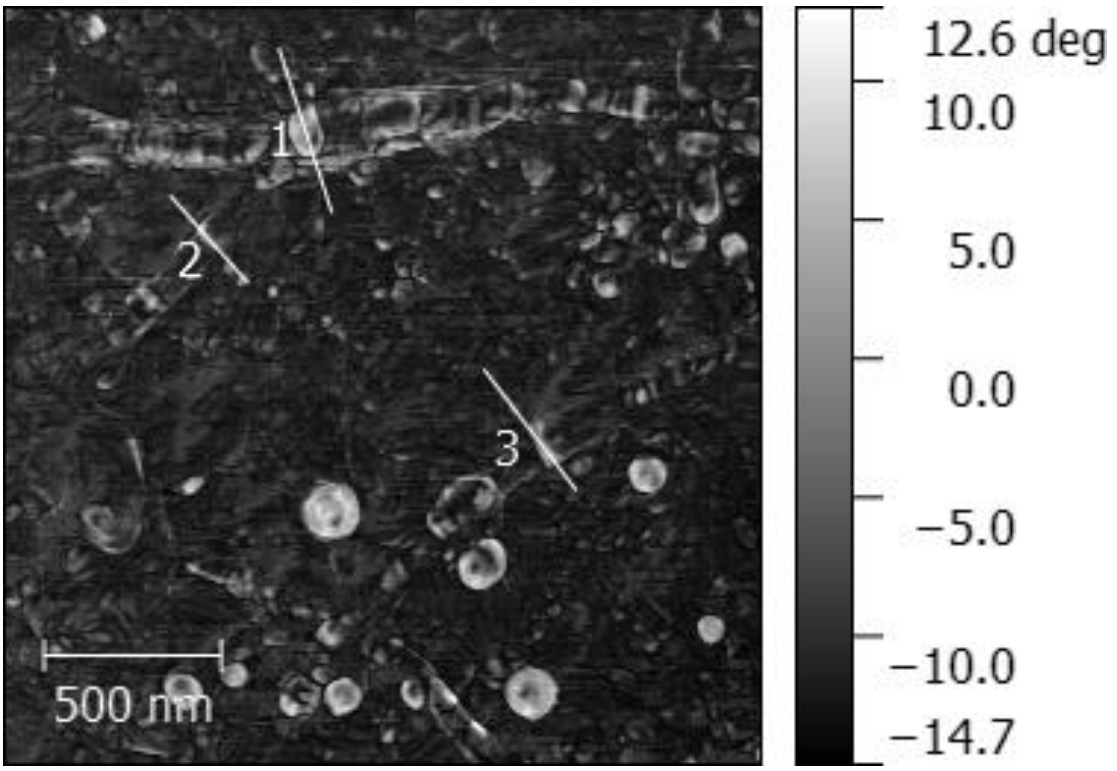

ii)

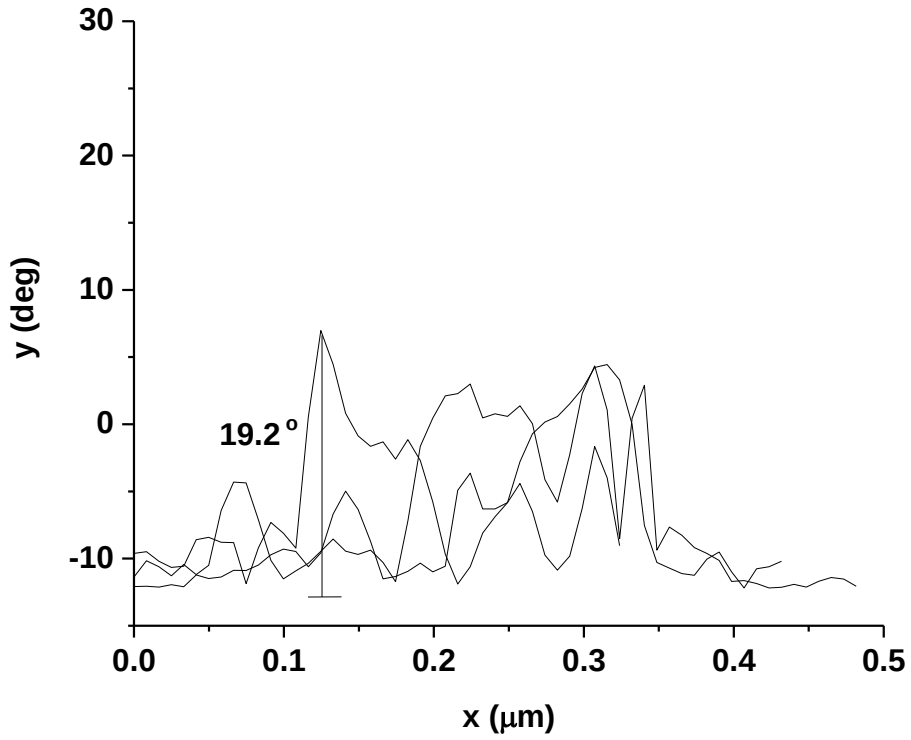

Figure 3.15. Atomic force microscopy tapping phase image (i), and cross-sectional profile (ii) of (+) alpha tocopheryl phosphate. Samples were 3 mM/ 0.15% w/v dispersed in a 20% ethanol, 80% water.

i)

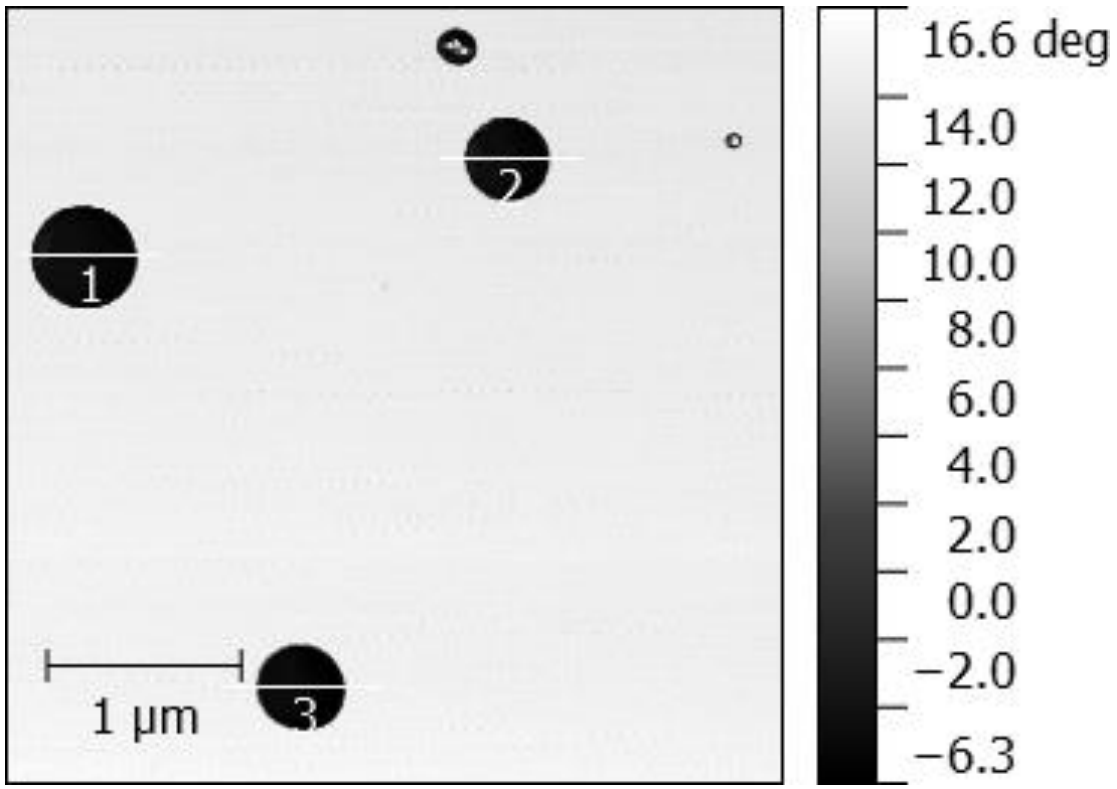

ii)

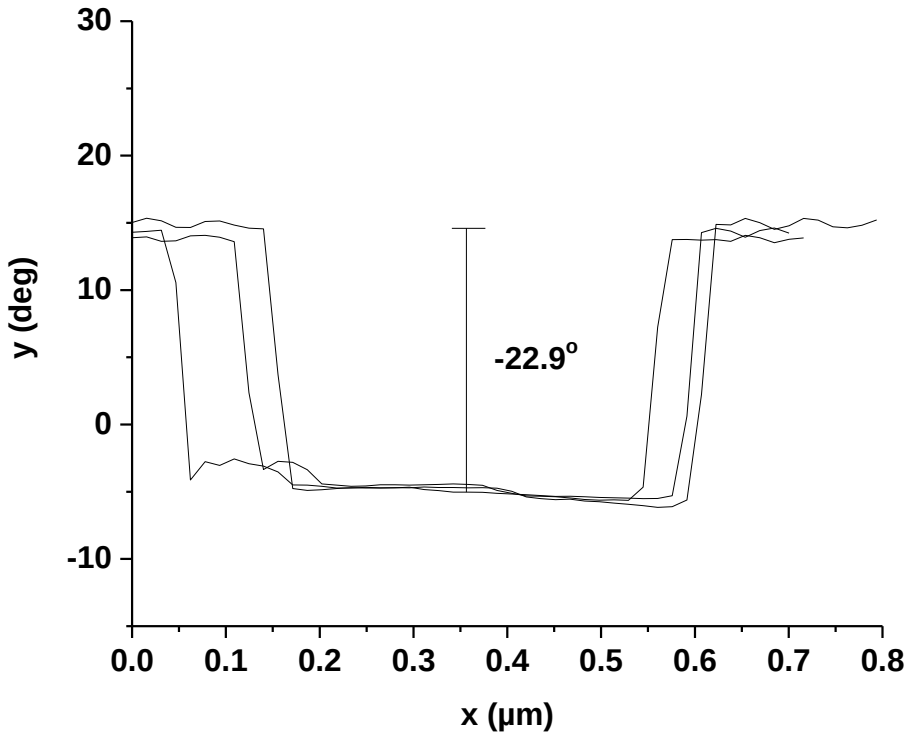

Figure 3.16. Atomic force microscopy tapping phase image (i), and cross-sectional profile (ii) of (+) alpha tocopherol with Tris (150 mM). Samples were 3 mM dispersed in a 20% ethanol, 80% water, pH

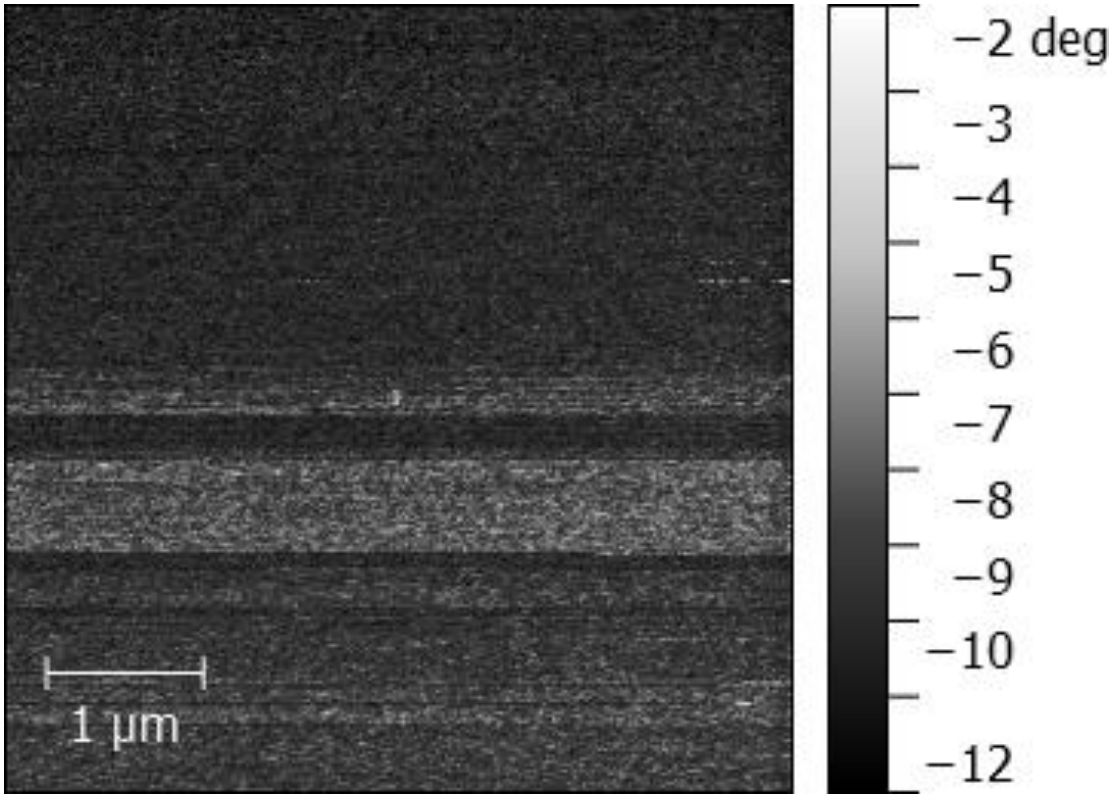

Figure 3.17. Atomic force microscopy tapping phase image of the untreated mica.

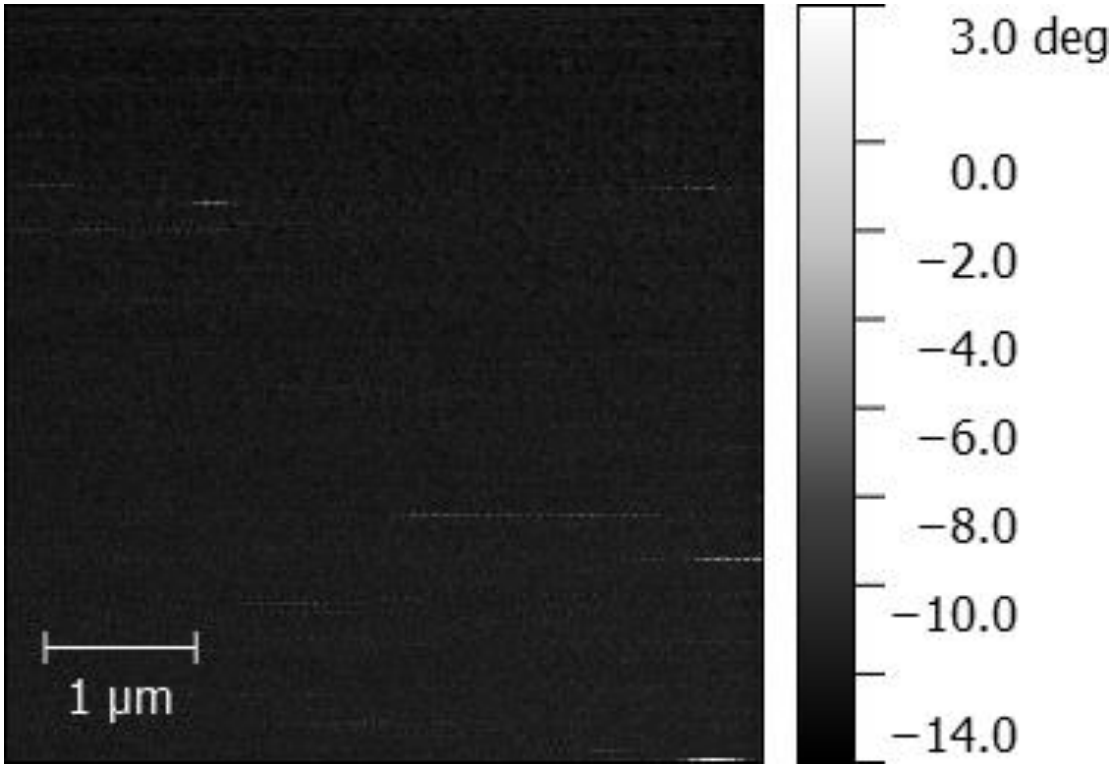

Figure 3.18. Atomic force microscopy tapping phase image of the Tris (150mM) vehicle control. The samples were 20% ethanol, 80% water, pH 7.4 vehicle.

3.5 Discussion

The *S. oralis* and *S. mutans* biofilm antimicrobial activity data showed that (+) α-TP was capable of retarding their growth time to inflection points and reducing their maximum bacterial population density in these studies. The maximum optical densities of the controls in these assays were comparable with previous work (Gan., 2010), which gave confidence that the test method was robust. The work carried out by Gan, 2010 found that zinc species increased the time to inflection points of *S. oralis* to ~ 4-9 hours depending on the formulation used and could reduce maximum population densities. It has been reported that histidine rich polypeptides are capable of increasing *S. mutans* lag phase by 4 h after a 1 hour pre-incubation (Mackay et al., 1984), in this study (+) α-TP increased *S. oralis* lag phase by ~3.5 h and *S. mutans* by 0.6 h after a 2 min incubation. In addition, other work assessing the growth retardation of another early stage tooth colonizer, *Streptococcus sanguinis*, a close relative of *S. oralis* (Zahner et al., 2011), was found to have a lag time of 8 hours when the 24 hour planktonic inoculum was treated with Listerine (1/2 dilution factor) for 15 seconds and was shown to have a dose dependent reduction in maximum population density (Fine et al., 1996). This shows that (+) α-TP had a mild antimicrobial efficacy as its effect on the *S. oralis* biofilms had ~ half the efficacy compared to a commercial product on planktonic with its potency against *S. mutans* being lower still. However, the (+) α-TP antimicrobial potency could perhaps be improved by changing the vehicle in order to provide weaker aggregates, providing more of the free drug. For example, the sensitivity of the (+) α-TP aggregates to electrolytes (in this case Tris) has been shown to transform the (+) α-TP nanostructure physical characteristics.

The (+) α-TP antimicrobial activity against the pioneering tooth colonising species *S. oralis* was shown in the growth retardation assays to be at least in part related the phosphorylation of

the compound because in comparison to (+) α-T, it had a far superior effect. Antimicrobial activity against pioneering tooth colonising species is important in the maintenance of oral health as later bacterial colonisers depend on these species in order to form plaque (March., 2000; Jakubovics & Palmer., 2013; Nobbs et al, 2009; Dorkhan et al., 2013).

The response of the bacteria to the (+) α-TP in the *S. oralis* biofilm assays when the neutralising rinse was employed was similar to CHX, a known substantive agent (Elworhy et al., 1996). This suggested that the (+) α-TP did have the capacity to bind to biofilms in order to increase the oral cavity resonance. The ionic strength of the vehicle used for α-TP samples reduced electrostatic polar head repulsion (Nagarajan., 2002), therefore (+) α-TP aggregates interacted with the Tris buffer to form a more lipophilic structure. The Tris buffer also had the added advantage that it had previously been shown to enhance bacteria surface permeability and was thought to increase the chances of observing a (+) α-TP antimicrobial effect (permeability changed by ion pairing with phospholipids as Tris is predominantly positively charged at physiological pH (pKa: 8.1)) (Hamouda & Baker (Jr)., 2000; Irvin et al., 1981; Ban et al., 2012) and therefore may have allowed the bacterial surface interactions to occur synergistically with the cell surface permeability increase effect of Tris.

CHX is known to primarily disrupt the cell membranes of bacteria by ion pairing to the negatively charged components on the membrane surface and hence altering the permeability of the cell (Koontongkaew & Jitpukdeebodintra., 1995). At low concentrations this results in low molecular weight substances, *e.g.* phosphates, leaking out of the cell and at high concentration CHX is bactericidal due to precipitation of cytoplasmic contents leading to cell death (Mohammadi & Abbott., 2009). In our planktonic studies we saw CHX being less potent against *S. oralis* than *S. mutans*. The increased susceptibility of *S. mutans* to CHX compared

to other streptococci species has been reported previously (Schaeken et al., 1994). (+) α-TP has been shown to have the opposite trend to CHX, this could be explained as *S. mutans* is known to be a more negatively charged species than *S. oralis*, with *S. mutans* (ATCC 25175) having a zeta potential of -75.52 ± 13.60 mV and *S. oralis* (ATCC 10557) having a zeta potential of -58.13 ± 11.22 mV (Saito et al., 1997) enhancing the cationic antimicrobial effect of CHX whilst seemingly inhibiting the antimicrobial effect of anionic (+) α-TP. In addition there have been shown to be hydrophobic differences in the bacterial surfaces of *S. oralis* and *S. mutans* with the former being much more hydrophobic (Saito et al., 1997) which could explain differences in antimicrobial activity.

CHX and CPC are both positively charged antimicrobial species that disrupt cell wall stability and cause cell lysis (McBain et al., 2003; Haps et al., 2008) and are considered antiseptics as they disrupt cell wall stability and cause cell lysis, negatively charged sodium lauryl sulphate micelles have been found to have bactericidal effects by solubilising cell membrane proteins again resulting in cell lysis (Wang et al., 2012; Mohamad., 2011). However, there is evidence from surfactant lipid preparations (SLP) that the aggregates can fuse with bacterial surfaces and become internalized whilst leaving the organism intact (Hamouda & Baker (Jr)., 2000) and hence had a bactericidal mechanism of action not caused by immediate cell wall/ membrane disruption; as (+) α-TP formed aggregates it is likely to have a similar mechanism especially in the presence of a cell membrane/ wall permeabiliser (Tris). In addition, (+) α-TP is endogenous in cells but appears to be highly restricted to only be present in ultralow concentrations and has been hypothesised as being a potent signalling molecule that targets enzymes including acid and alkaline phosphatases, adenosinetriphosphatase and diphosphopyridine nucleotidase to name just a few (Zingg et al, 2010) and or transcription factors (Gianelo et al., 2005). Moreover it has been suggested that (+) α-TP acts in a similar

way to thiamine di-phosphate in bacteria which directly binds and regulate mRNAs encoding enzymes involved in its biosynthesis controlling gene expression. Therefore if (+) α-TP was internalized at a high enough concentration it could become toxic.

In order to assess how the (+) α-TP nanostructures antimicrobial activity compared with established antimicrobials, the MBC was tested against the pioneering tooth coloniser *S. oralis* and the cariogenic bacterium *S. mutans*. The MBC of (+) α-TP against *S. oralis* being 1 μg/ mL was found to be lower than CHX which has been reported to have an MBC of 7.8 μg/ mL (Wang et al., 2012) suggesting a higher potency for the former. (+) α-TP also had a similar potency against this organism to cetylpyridinium chloride (7.8 μg/ mL) (McBain et al., 2004) and triclosan (5.2 μg/ mL) (Wang et al., 2012) which are two commonly used antimicrobial agents in the mouth. The MBC of (+) α-TP being more potent than CHX was interesting as the nanostructures were a little less potent compared to the CHX treatments in the growth retardation assays. The dispersal of the (+) α-TP planer bilayer islands in the broth (containing sugars, salts and other bacterial nutrients) used for the MBC experiments, most likely disrupted the aggregates providing more of the free drug, which could explain reversal in potency across the two experiments. However, the aggregation characteristics (+) α-TP when dispersed in the broth could not be monitored by the zetasizer as it was as it was only available as a yellow solution and so would have led to inaccurate readings and could not be measured by AFM as the images would include the crystallised sugars, salts *etc.* that were in the broth. A potential way forward would be dispersing the (+) α-TP planar bilayer islands in a clear solution that closely resembles that of the broth. Additionally, (+) α-TP was found to have a much lower potency against *S. mutans* (≥ 512 μg/ mL) than *S. oralis* (1 μg/ mL). CHX in comparison has been found to have a more potent antimicrobial activity against *S. mutans* of 1 μg/ mL (Hwang et al., 2000).

The data showed that (+) α-TP pre-treated HA discs were capable of halving multispecies biofilm formation after 18 h even after washing supported the notion that the effect of (+) α-TP would be substantive. The fact that (+) α-TP did not completely inhibit biofilm development was not considered to be a draw back as when developing new approaches to maintaining good oral health it is important to recognise that controlling the oral micro-organisms, rather than completely eradicating them, is the goal (March., 2000). When imaging close to the HA surface it was found that there was no bacterial infestation in the pellicle suggesting a sterile pellicle had formed. *S. oralis*, which has been shown to be susceptible to (+) α-TP's antimicrobial properties would likely have been among the first species of bacteria to come into contact with any adhered (+) α-TP on the tooth surfaces and so presumably did not attach possibly due to HA controlled release of (+) α-TP or an increase in HA surface hydrophobicity, however, this confocal experiment would need repeating with just *S. oralis* to prove this. A healthy pellicle can also improve oral health as it acts as a barrier to acid attack and prevents enamel demineralisation (Baek et al., 2009). (+) α-T pre-treated discs did reduce biofilm formation but this was not statistically different from the control HA disc.

The binding studies of (+) α-TP to HA suggested that the binding to teeth would also increase the oral cavity substantively of this molecule. It was surprising that the negatively charged aggregates interacted with HA to such a high degree as previous literature has shown poor adhesion of other negatively charged aggregates with HA with positively charged species having more adhesion (Nguyena et al, 2010) likely due to HA's overall negative surface charge around a neutral pH (Beachey, 1980). However, HA has been reported to interact with organic phosphates molecules such as phytate and phosphoserine (Ganesan., 2008). This is because HA is a amphoteric material made up of calcium phosphate [$Ca_{10}(PO_4)_6(OH)_2$] and therefore

has two types of binding sites, positively charged (Ca^{2+}) and negatively charged (PO_4^{2-}). It has been shown that enamel crystals have domains of positive and negative charge which allow positive and negative species to bind to it despite its overall negative charge (Wallwork et al., 2001). The (+) α-T did not bind to the HA and therefore the charged phosphate was responsible for the binding process. The chemical stability study in the previous Chapter indicated that chemical degradation did not influence the binding study's results.

In the previous Chapter it was seen that the introduction of the hydrophilic phosphate group into (+) α-T generated amphiphilic character, which reduced the nanostructures size, charge and derived count rate. Vitamin E derivatives such as α- tocopheryl polyethylene glycol succinate 1000 (α-TS) have been found to form spherical micelles with a critical micelle concentration of 20 μM (Sadoqi et al., 2009; Muthu et al, 2012). However, the (+) α-TP structures were thought to be cylindrical micellar or spherical liposomal because the packing parameter was calculated to be 0.50 and the aggregates were shown to be thread-like micellar by AFM. The (+) α-T was found to be spherical by AFM and so the introduction of the charged phosphate group increased polar head repulsion which transitioned the aggregates into thread-like structures. The reason why (+) α-TP aggregate structures were not spherical like that of α-TS was thought to a smaller head group whilst the transition into adhesive planar bilayer islands when formulated with a high ratio of salt (in this case Tris) was thought to be due to reduced head group repulsion (Nagarajan., 2002). This transition into planar bilayered structures may have also aided interactions with HA and bacteria as this would provide a greater surface area for the interactions to occur. The AFM phase images found that the whole of the (+) α-TP planar bilayer structures adhered uniformly to the silicon nitride probe (Si_3N_4), whilst the (+) α-TP cylinders had some adhesion but was not consistent across the structures. The (+) α-T spheres had no adhesion. Silicon nitride has similar physicochemical properties to

hydroxyapatite ($Ca_{10}(PO_4)_6(OH)_2$), in that both materials are overall charge neutral, both are hydrophilic and both have an overall net negative surface charge density (An & Friedman., 2000). Therefore the AFM data supported the HA adsorption results in that the (+) α-TP planar bilayer structures were substantive whilst the spherical (+) α-T structures were not. This affected the antimicrobial activity of the two species but the mechanism of action is unknown.

3.6 Conclusion

In this Chapter (+) α-TP has been shown to increase the growth time to inflection points and post-growth maximum population densities of *S. oralis* and *S. mutans* biofilms through cell surface interactions that were not displayed by (+) α-T. (+) α-TP was also found to adhere to HA and provide a substantive effect in inhibiting salivary biofilm growth over time that again was not displayed by (+) α-T. (+) α-TP self-assembled into adherent planar bilayer islands in aqueous Tris vehicles whilst (+) α-T generated non-adherent liposomes. Therefore these findings confirm that the chemically linked phosphate ester to (+) alpha tocopherol is critical for its substantive antimicrobial properties. The (+) α-TP potency was less than other agents that could be included in oral healthcare products, but as (+) α-TP showed the capacity to bind to hydroxyapatite it may prove more efficacious when used *in vivo*. In addition, the increase in potency in the MBC assay over CHX suggests that weakening the aggregate in biological fluids may improve potency. It is the effect of formulation counter ions which seems worthy of further study and so this will be investigated in Chapter 4.

CHAPTER FOUR

Influence of Electrolytes on Alpha Tocopheryl Phosphate's Antimicrobial Properties

4.1 Introduction

Bacteria often gain resistance to antimicrobial agents in biofilms as opposed to when they are observed in a planktonic state due to the incomplete penetration of the antimicrobial agents (Lewis., 2001). This biofilm resistance is a result of the bacteria producing extracellular polymeric substances (EPS), which often accounts for over 90% of the biofilm architecture and is responsible for biofilm cohesion (Flemming & Wingender., 2010). The EPS in oral biofilms is extensively negative charged which especially limits the penetration of cationic and anionic antimicrobials/ aggregates through the biofilms due to strong ionic interactions (electrostatic repulsion and attraction) at the EPS periphery (Shen et al., 2016). Neutral and zwitterionic phospholipid nanocarriers have been observed to penetrate biofilms and improve the drug delivery/ action of antimicrobials (Meers et al., 2008; Liu et al., 2016). In Chapter 2, the self-assembled anionic nanostructures of the phospholipid (+) α-TP were shown to have antimicrobial properties against *S. oralis* biofilms but the penetration depths were unknown. In addition, the large organic cation, Tris, was found to affect the shape and viscoelasticity of the anionic (+) α-TP nanostructures through ion-pairing giving the structure some zwitterionic character. Cationic Tris would also most likely interact with the negatively charged components in oral biofilms *i.e.* the EPS, dismantling the biofilms and neutralising there negative charge when applied in excess giving (+) α-TP access to potentially all the residing bacteria. Tris could therefore not only be influencing the (+) α-TP nanostructures physicochemical properties but also the physicochemical properties of the oral biofilms influencing the relationship between (+) α-TP interactions and biological activity on multiple levels. Therefore, the effect of Tris on the (+) α-TP nanostructures biofilm penetration required investigation to assess for (+) α-TP Tris synergisms.

Bacterial surfaces (cell wall and membranes) within oral biofilms also have net negative surface charges; therefore they have the ability to form ion pairs with positively charged species. Monovalent salt ion-pairing interactions have been shown to swell and modify the interactions between neighbouring membranes by reducing the electrostatic repulsion barrier and allowing coalescence (Petrache et al., 2006) and therefore could influence the interaction between bacterial membranes and the (+) α-TP planar bilayer islands. In addition, Tris has also been found to make the bacterial membranes more permeable (Vaara., 1992) because the positively charged species interacts with the phospholipid head groups causing the membranes to swell and as a consequence greater surface pressure membranes are more permeable due to their structure disruption. As a consequence this has been shown to improve the interaction of antibiotics with membranes and potentially improves diffusion uptake (Mecheri et al., 2004). However, it should be noted that the membrane is not solubilised when a positively charged species interacts with it unless the interacting species has detergent properties (Voss., 1967). Therefore, small positively charged organic non-surfactant molecules are not typically as antimicrobial alone but function to enhance the interactions of antimicrobial molecules with the bacterial membrane to increase antimicrobial potency, or perhaps, in some cases introduce molecular antimicrobial properties. Therefore, the effect of Tris on (+) α-TP nanostructure interactions with bacterial membranes should also be examined to understand the conditions required for achieving the maximum antimicrobial potency with the actual bacteria in addition to its biofilm penetration.

The aim of this study was to assess the importance of simple electrolytes to influence the interaction and antimicrobial activity of (+) α-TP nanostructures with gram-positive bacteria and salivary biofilms. The ions used to manipulate the properties of the (+) α-TP nanostructures were negatively charged phosphate and positively charged Tris (pH 7.4) and their effects on

artificial gram-positive bacteria membranes were assessed using a Langmuir trough. The nanostructure structures were probed using fluorescence, aggregate size analysis and zeta potential in the presence of the two ions. Confocal microscopy was used to investigate salivary biofilm penetration of the aggregates and aggregate antimicrobial action. The aggregates were also applied to *S. oralis* biofilms as they were shown to be susceptible to the antimicrobial action of (+) α-TP in Chapter 3 and so showed differences in antimicrobial activity under different ionic environments.

4.2 Materials

Tris (≥ 99%), (+) α-T (Type VI, ~ 40% purity), phosphorous oxychloride ($POCl_3$) (≥ 99%), tetrahydrofuran (THF) (anhydrous) (≥ 99.9%), trimethylamine (≥ 99%), trifluoroacetic acid (≥ 99%), cetylpyridinium chloride (CPC) (99.0-102%), brain heart infusion (BHI) broth and glycerol were purchased from Sigma Aldrich, UK. Absolute ethanol, propan-2-ol, hexane by fractions, disodium hydrogen phosphate, monosodium dihydrogen phosphate, blood agar (BA) plates containing blood agar base no. 2 with 5 % horse blood, 0.2 μM nylon syringe filters, hydrochloric acid and sodium hydroxide, were purchased from Fisher scientific Ltd, UK. De-ionised water was used from laboratory supply. Hydroxyapatite discs (5 mm diameter x 2 mm thick) were purchased from Himed inc, USA. Live/ dead ® BacLight™ bacterial viability kit, for microscopy, was purchased from Life Technologies, UK. *S. oralis* NCTC 7864T was purchased from LGC standards, USA. 1-palmitoyl-2-oleoyl-sn-3-glycerophospho-1-glycerol (POPG) and 1-palmitoyl-2-oleoyl-sn-3-glycerophosphocholin (POPC) were purchased from Avanti polar lipids, USA. Chromatographic paper, 10 mm x 100 m was purchased Whatman, Maidstone, UK. Plastic syringes (1 and 20 mL) were purchased from Terumo, Philippines. Syringe needles were purchased from Macrolance, Ireland. Disposable clear dynamic light

scattering cuvettes (macro, PMMA) and disposable folded capillary cells (DTS1070) were purchased from VWR, Germany. Clear sterile polyester adhesive films were purchased from Starlab, UK. Peptone Water (dehydrated) was purchased from BD Diagnostic Systems, USA. Human saliva was donated from volunteers that had fasted and had not used an oral hygiene product for a minimum of 8 hours. Basic media and Phosphate Buffered Saline (PBS) were prepared in house at Johnson &Johnson, Skillman, USA. 96 well Nunc® Plate, Nunc® Peg Lid and Nunc® White Plate (Cat. No 236105) were purchased from VWR, USA. BacTiter-Glo™ microbial cell viability assay was purchased from Promega, USA. ATP reagents (Celsis LuminATE™ and Celsis LuminEX™) were purchased from Celsis, USA.

4.3 Methods

4.3.1 (+) α-TP aggregate sample preparations

For Langmuir trough monolayer interaction experiments (+) α-TP (3 mM) samples were prepared by dissolving the appropriate amount in ethanol. Water was then added to initiate (+) α-TP thread-like micelle self-assembly, followed by the addition of aliquots of Tris or phosphate (0.5 M stock solutions). The pH was then adjusted to 7.4 and the samples were made to the mark with water to give final vehicle compositions of 20% ethanol (v/v), 80% water (v/v), 150 mM buffer concentration.

To compare the physicochemical properties of the different formulations the following process was developed; stock solutions of (+) α-TP (500 μM) was prepared by dissolving the appropriate amounts in ethanol. Water was then added to initiate (+) α-TP self-assembly,

followed by the addition of varied aliquots of Tris or phosphate (0.5 M stock solutions) to generate different ratios of α-TP: ion concertation and hence vary the amount of surface interaction of the nanostructures. The pH was then adjusted to 7.4 and the samples were made to the mark with water to give final vehicle compositions of 20% ethanol, 80% water with 100μM α-TP formulated with either Tris or phosphate ions at various concentrations.

For comparison of the different formulated aggregates on microbiology studies; α-TP stock solutions (4 mM) were prepared by dissolving the appropriate amounts in ethanol. Nanostructure development was then repeated as above with the exception that one ratio of α-TP: ion concentration was selected (800 μM: 150 mM (1:187.5) and the water and stock solutions were filter sterilised through a 0.2 μM nylon syringe filters. All samples were refrigerated and stored for a maximum of 8 days.

4.3.2 Bacterial membrane interactions

A Langmuir trough (Nima technology equipment, Coventry, UK) with a circular Teflon trough (5 cm^2, volume 20 ml) on a stir plate (Whatman stirrer, WC-303) was loaded with either a Tris or phosphate (10 mM, pH 7.4) and equilibrated until a stable surface pressure was obtained (drift in surface pressure, ≤ 0.2 mN/ m over 2 minutes using Nima TR516 software) (Figure 4.1). The phospholipids used to mimic a gram positive bacterial membrane were POPG and POPC as they have been previously used to form monolayers to mimic gram positive bacteria membranes (Chenga et al., 2011). The POPC: POPG (3:1 mg/ ml, dissolved in chloroform) (lipid ratio was optimised in preliminary experiments) lipids were added to the subphase until a 30 mN/ m pressure was reached in the Tris subphase (as this is the pressure of a bacterial membrane (Erbe et al., 2009)) or the maximum pressure achieved for the phosphate subphase.

The lipid monolayer was allowed to equilibrate over 30 minutes at room temperature. The α-TP samples (0.1 mL, 3 mM, in 20% ethanol, 80% water, 150 mM phosphate or Tris at pH 7.4) were injected into the subphase with pressure monitored over time at a constant surface area. Experiments were repeated in triplicate. Vehicle injections of 0.1 mL, 20% ethanol, 80% water (150 mM Tris, pH 7.4) were injected and pressure changes recorded as controls.

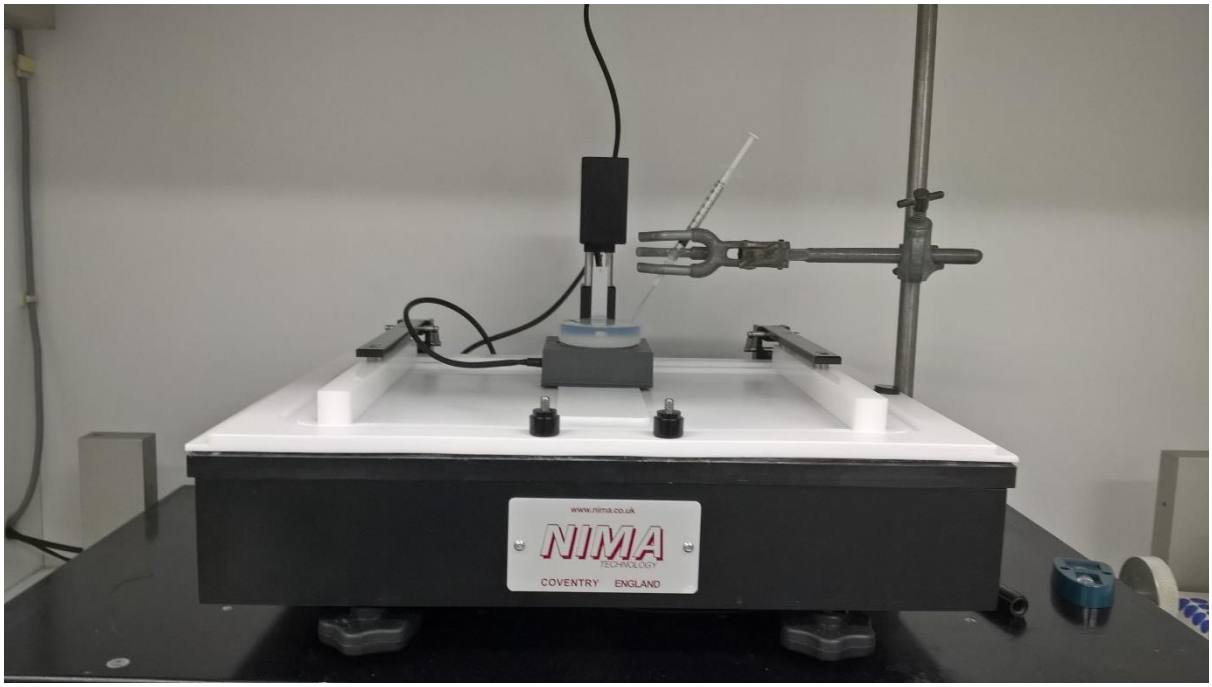

Figure 4.1. Photograph of the Langmuir trough set-up.

4.3.3 (+) α-TP aggregate characterisation

To examine the ion interactions with the aggregates fluorescence emission spectra of (+) α-TP (195 μM) aggregate solutions were recorded using a fluorescence spectrometer fitted with a Xenon pulse lamp (Varian Cary Eclipse Fluorescence Spectrometer, Agilent Technologies,

UK). A fluorescence cell (Helima fluorescence cell 10mm, Helima UK Ltd., UK) with a 10 mm path length was used. Excitation and emission slits were fixed at 5 nm. In all measurements, the excitation wavelength was set at 286 nm. The samples were scanned from 250 to 450 nm at a wavelength scan rate of 120 nm/ min with a PMT detector gain of 600 V. The experiments were performed at a temperature of 25 °C. Fluorescence emission intensity increases/ decreases at 310 nm were monitored and normalised as shown in equation 4.1. The normalised data points were then plotted against ion concentration (Tris or phosphate). Analysis of the spectra were conducted using OriginPro software (OriginPro version 2016, OriginLab Corporation, US) and the dose dependent analysis selected to assess trend patterns.

$$Fn(\%) = \frac{Fs - Fmin}{Fs - Fmax} X100 \qquad \text{[Equation 4.1.]}$$

Where Fn is the percentage normalised fluorescence, Fs is the sample fluorescence, Fmin is the minimum fluorescence and Fmax is the maximum fluorescence. The size of the aggregates (100 µM, n = 3) were analysed by photon correlation spectroscopy (Malvern Nanoseries Zetasizer, Malvern Instruments Ltd, UK). Detection of the light scattering signal was performed at 173 ° at 25 °C. The material refractive index was set at 1.59, the material absorbance at 0.01, the dispersant refractive index at 1.33 and the viscosity (cP) at 0.8872. Blank solutions (containing just solvent) were used as a control. The same instrument measured the zeta potentials using a dielectric constant of 78.5 and Smoluchowski (1.5) interpretation of the data with (+) α-T in Tris buffer (25mM) as a control. The chemical stability of the (+) α-TP was attained as described previously.

4.3.4 HPLC chemical stability study

The chemical stability of the (+) α-TP aggregates was as described in **2.3.9.**

4.3.5 *S. oralis* growth retardation

S. oralis was cultured, treated and growth monitored as described in **3.3.1**

4.3.6 UWMS biofilm formation inhibition

Pooled homogenized saliva (minimum 30 mL) was dispensed into clear 96 well Nunc® plates (175 µL/ well). Peg lids were placed in the plates containing saliva for 30 minutes, incubated at 35 ^{o}C aerobic to form the pellicle. Rows A and H, columns 1 and 12 (outer edges) of a second Nunc® 96 well plate were filled with 180 µl of water (to reduce the edge effect). Inoculum and media were prepared by mixing saliva and BM/ PBS (12mL PBS/ 100 mL BM) in a 1:1 ratio. This saliva BM/ PBS mixture were dispensed (120 µL) into each well except for rows A and H, columns 1 and 12 (outer edges). Samples were added by dispensing 60 µL of the treatment solution into each well (total volume in each well =180 µl, 1/ 3 sample dilution). A growth control consisting of 120 µl of saliva/ BM/ PBS mix + 60 µl of media was used. The wells were mixed 3 times using a multichannel pipettor. Each sample was plated in sextuplet (6 wells, 1 column). After the 30 minute pellicle formation, the peg lid was placed into the growth plate and incubated aerobically at 35^{o}C statically for 24 hours. The peg lid was transferred to a plate containing 200 µL/ well of a BactiterGlo (BactiterGlo bottle should be taken out of freezer and thawed out in warm water for 15 minutes)/ 0.1% Peptone water (dispersed in deionized water,

then filter sterilized) mix (1:1 ratio), and was left to sit statically for 5 minutes. Each of the well samples (10 µL) were aliquoted into the wells of a white Nunc® plate which was then placed into a suction filtration unit (Victor X, USA) and washed twice with PBS. The wells of the white Nunc® plate had there ATP content measured by luminescence detection (Berthold Luminometer, USA).

4.3.7 Biofilm penetration

One hydroxyapatite (HA) disc was added vertically to a micro centrifuge tube containing UWMS (one donor, 400 µL) and incubated at 37 °C for 18 h. After the 18 h of incubation in unsterilised UWMS the HA discs were removed, added to a fresh aliquot of sterilised heat treated (10 min, 80 °C) UWMS (200 µL) incubated at 37 °C for 24 h, removed, washed with saline (600 µL) and treated with Live/ dead ® BacLight^{TM} bacterial viability kits. Biofilms were observed with a confocal microscope (Leica TCS SP2, Leica microsystems, UK) with 488 and 568 nm excitation and 500-530 nm (green fluorescence representing up take of Syto 9 by live cells) and > 620 nm (Red fluorescence representing up take of propidium iodide by dead cells) emission filters using the 63x oil immersion objective. Images were taken near the centre of the HA discs both sides. There was no cross over between emission spectra and excitation intensities were ≤ 31%. The biofilm growth was considered normal if they grew 30 – 60 µM. Biofilm red / green ratios as a function of biofilm depth were measured using the z-stacking tool at 63x magnification taking an image every ~1 µm. The HA discs were then completely submerged in one of the three different α-TP aggregate test solutions (200 µL) in new micro centrifuge tubes for 2 minutes before being washed with saline (600 µL). HA discs were then re-exposed to live/ dead staining for 1 h and imaged again. Changes in the ratios of the red/ green staining as a function of biofilm depth demonstrated each of the three samples

biofilm kill penetration. These studies were repeated in triplicate for each test solution. CPC was used as a positive control. Each HA disc was imaged on both treated sides in two different areas near the centre of the discs. As a sterility control, sterile saliva was incubated with a sterile HA disc and showed no biofilm growth. In some cases discs were only imaged once, after biofilm test sample exposure, to ensure kill was caused by antimicrobial activity and not by the dual imaging and staining process.

4.3.8 Statistical analysis

All data were expressed as their mean ± standard deviation (SD). Statistical analysis of data was performed using Levine's homogeneity test and ensured all sample group data was of acceptable distribution ($P > 0.05$) before statistical significance between the sample groups was assessed by one way analysis of variance (ANOVA) tests with post-hoc Tukey analysis in Origin 2016. Statistically significant differences were assumed when $p \leq 0.05$.

4.4 Results

4.4.1 Bacterial membrane interactions

The Tris and phosphate subphases affected the phospholipid monolayer (gram-positive) maximum equilibration pressure and hence its lipid packing. The phospholipid monolayer was capable of reaching a maximum surface pressure of 38 ± 1.5 mN/ m when formed on a Tris subphase (at which point the addition of more POPG: POPC did not increase surface pressure further), but it was only capable of reaching a maximum surface pressure of 15.2 ± 8.5 mN/ m

when formed on a phosphate subphase (Figure 4.2). This demonstrated that the Tris was interacting with the monolayer, causing it to swell. When the (+)α-TP aggregates formulated with Tris where injected into the Tris subphase the monolayer equilibration pressure (set at 30 mN/ m to replicate the pressure of bacterial membranes) was found to increase by 2.7 ± 1.8 mN/ m (Figure 4.3). When (+) α-TP formulated with phosphate was injected into the phosphate subphase there was no increase in monolayer pressure showing no interaction of (+) α-TP with the monolayer. The injection of the vehicle alone was found to slightly reduce the monolayer pressure over time, presumably due to the monolayer solubilising effect of ethanol in the formulation.

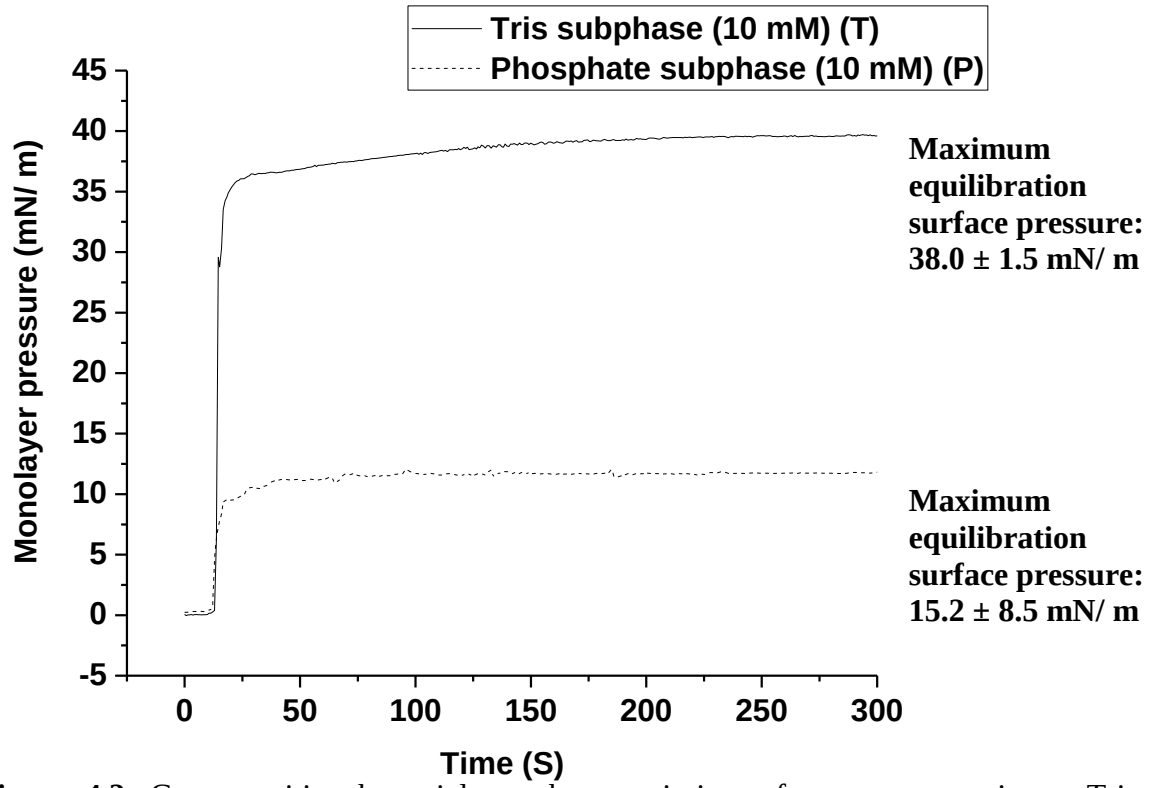

Figure 4.2. Gram positive bacterial membrane mimic surface pressure using a Tris or phosphate (10 mM) subphase. Representative pressure time graphs with annotated triplicate data.

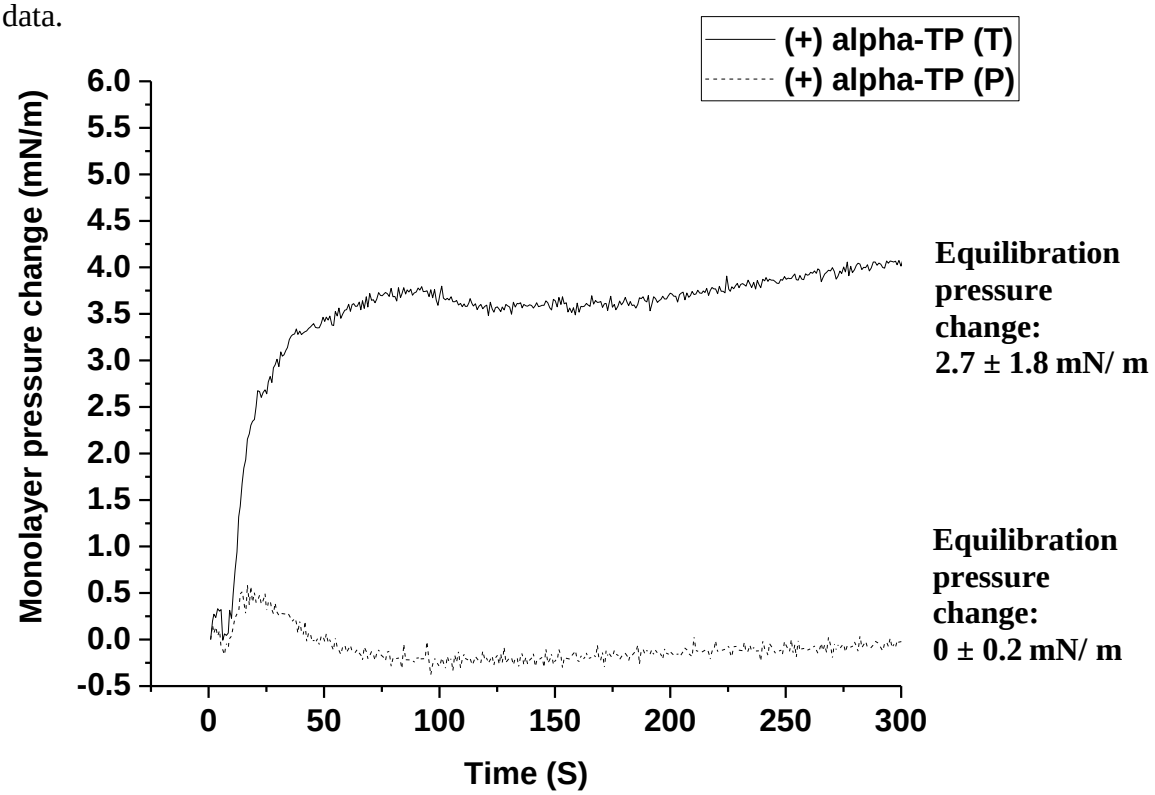

Figure 4.3. Surface pressure change when (+) alpha tocopheryl phosphate aggregates were injected into the Tris (30 mN/ m) supplying a gram positive bacterial membrane mimic or phosphate subphase (maximum mN/ m). Representative pressure time graphs with annotated triplicate data.

4.4.2 (+) α-TP aggregate characterisation

When (+) α-TP was dispersed in increasing concentrations of Tris the fluorescence emission intensity was found to increase (Figure 4.4). The converse was true when (+) α-TP was dispersed in a phosphate buffer solution (Figure 4.5), *i.e*., the fluorescence emission intensity was found to decrease. The (+) α-TP fluorescence signals are related to the ionic behaviour of Tris and phosphate with the aggregates and the data suggested all species interacted with the aggregates.

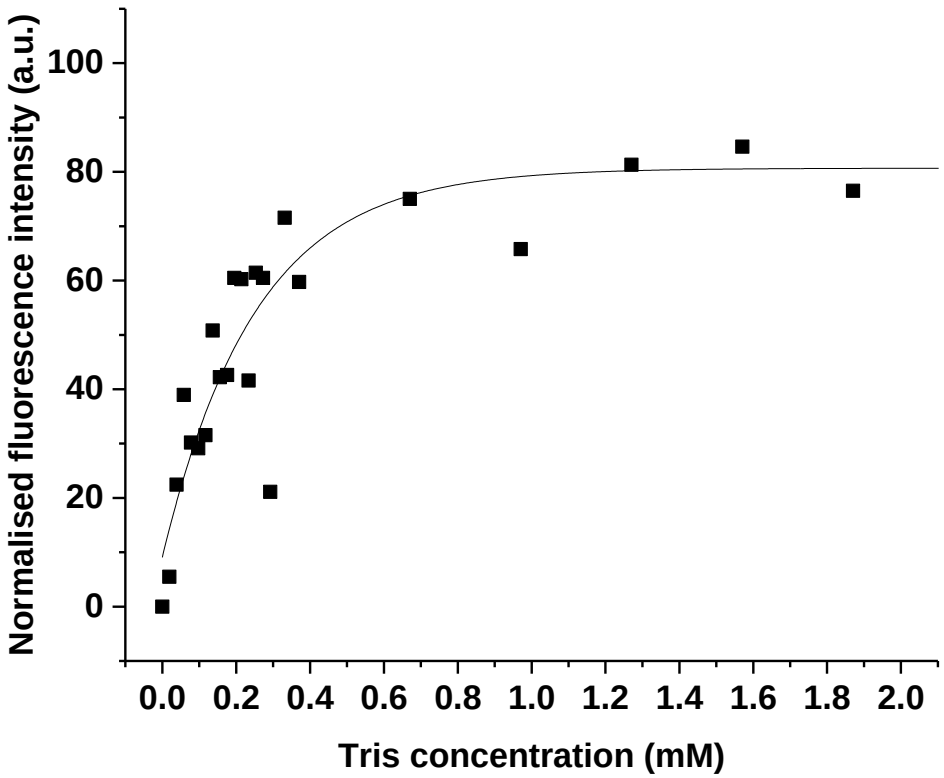

Figure 4.4. (+) α-tocopheryl phosphate aggregates (195μM) (20 h) fluorescence emission intensity changes as a function of varying phosphate concentration at 25 °C. Samples were dispersed in a 20% ethanol, 80% water at pH 7.4. N = 1 results.

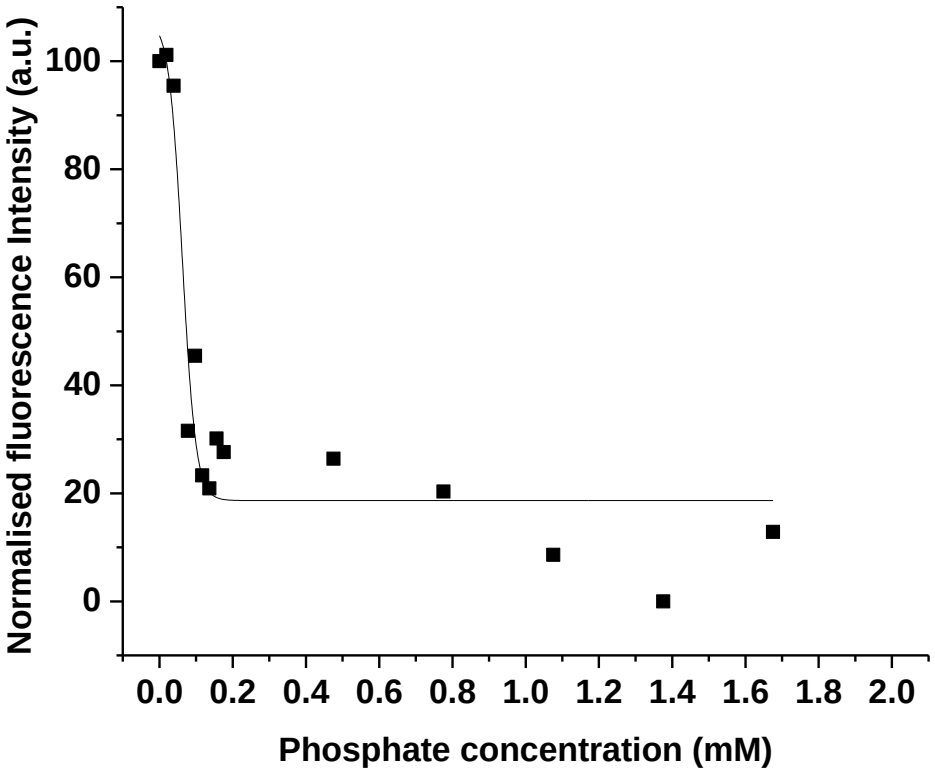

Figure 4.5. (+) α-tocopheryl phosphate aggregates (195μM) (20 h) fluorescence emission intensity changes as a function of varying phosphate concentration at 25 °C. Samples were dispersed in a 20% ethanol, 80% water at pH 7.4. N = 1 results.

There appeared to be no relationship between aggregate size and phosphate concentration (Figure 4.6), but increasing concentrations of Tris reduced (+) α-TP aggregate size, perhaps caused by head group conformation changes. (+) α-TP aggregates formulated with Tris were found to consistently have a less negative zeta potential values than when formulated with phosphate ($p < 0.05$) (Figure 4.7). As phosphate gave a dose dependent increase in negative surface aggregate charge it was assumed that the negative phosphate groups were associating with the aggregates through hydrogen bonding because this would allow the phosphate to interact with the aggregates in a manner that would not shield its charge. At the (+) α-TP: ion ratio used in the subsequent biological assessments (1:187.5), there was no statistical difference in nanostructure size across the two ion test systems ($p > 0.05$) and therefore any

microbiological activity differences would be due to aggregate charge variations and bacterial membrane permeability differences.

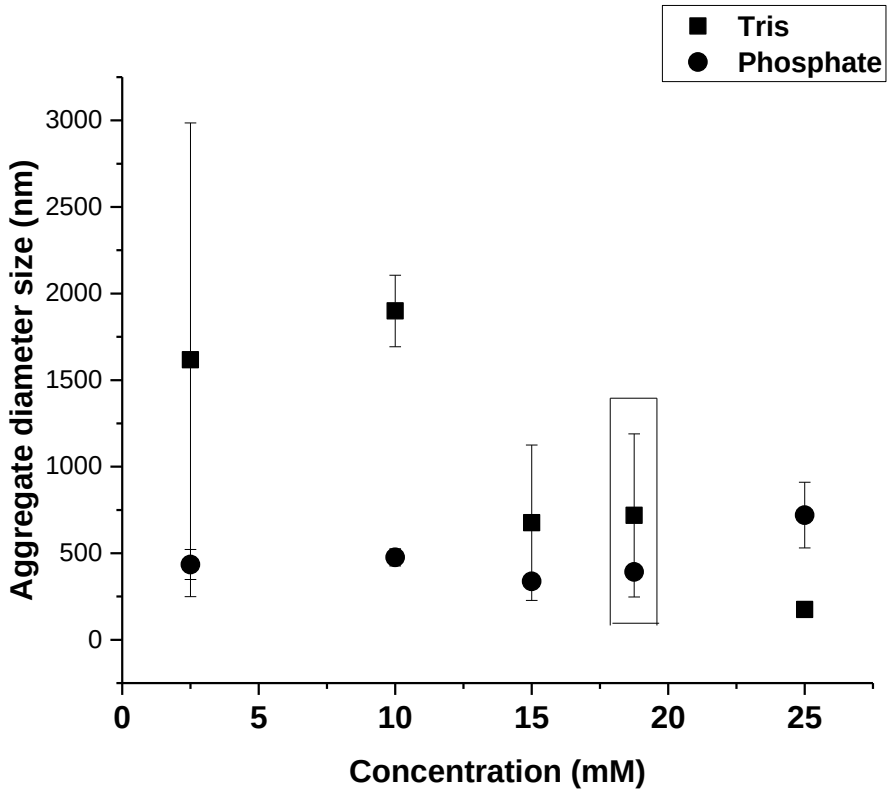

Figure 4.6. Comparison of (+) α-tocopheryl phosphate (0.1mM) (18 h) aggregate size when formulated with increasing concentrations of Tris or phosphate at pH 7.4 in 20% ethanol 80% water vehicles. The aggregate sizes for the selected ratio of (+) α-tocopheryl phosphate to ion concentration (1: 187.5) for microbiology treatment solutions are highlighted. n=3 results.

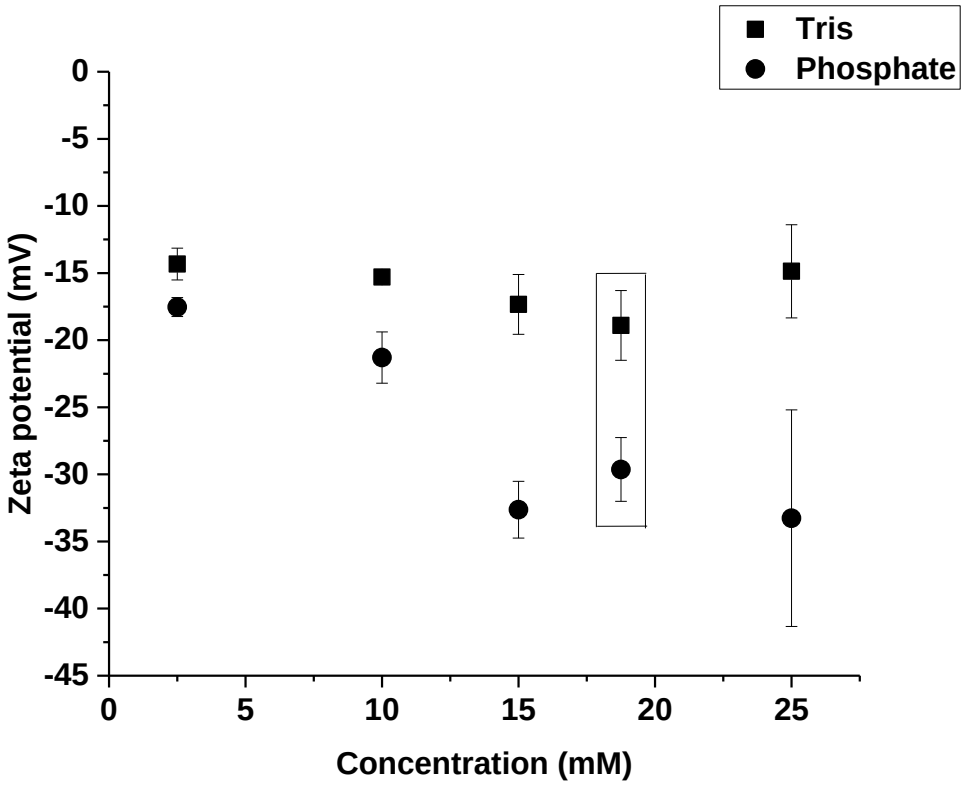

Figure 4.7. Comparison of (+) α-tocopheryl phosphate (0.1mM) (18 h) zeta potential when formulated with increasing concentrations of Tris or phosphate at pH 7.4 in 20% ethanol 80% water vehicles. The aggregate zeta potentials for the selected ratio of (+) α-tocopheryl phosphate to ion concentration (1: 187.5) for microbiology treatment solutions are highlighted. n=3 results.

4.4.3 (+) α-TP chemical stability comparison of formulations

The HPLC chemical stability study found that the different ions effected the (+) α-TP aggregate stabilities; in the Tris formulation the chemical degradation rate was 1.47 ± 0.31 µg/ mL/ week whereas (+) α-TP dispersed with phosphate ions was found to be more stable at 0.48 ± 0.27 µg/ mL/ week (Table 4.1). All samples were still commercially viable because there chemical degradation was below 10% of a 0.05% w/v (500 µg/ mL) solution over 12 weeks at 40°C (as seen in Chapter 2).

(+) α-TP (20 µg/ mL) pH 7.4 vehicle	T = 4 weeks (µg/ mL)	Degradation rate (µg/ mL/ week)	Degradation over 12 weeks at 37°C (µg/ mL)	Percentage of degradation of 0.05% w/v (500µg/mL) (%)
Phosphate (25 mM)	18.08 ± 1.1	0.48 ± 0.27	5.8 ± 3.24	1.2 ± 0.6
no buffer	15.18 ± 2.3	1.21 ± 0.57	14.50 ± 6.84	2.9 ± 1.4
Tris (25 mM)	14.17 ± 1.23	1.47 ± 0.31	17.64 ± 3.72	3.5 ± 0.74

Table 4.1: Chemical degradation rates of (+) alpha tocopheryl phosphate nanostructures dispersed in 20% ethanol, 80% water at pH 7.4 stored at 37℃ over 4 weeks when in formulation with different ions.

4.4.4 *S. oralis* biofilm growth inhibition

The (+) α-TP nanostructures formulated with Tris (-18.9 ± 2.6 mV, 718 ± 471 nm) displayed a 3.34 ± 0.52 h bacterial growth inflection point, which was statistically different from the Tris vehicle (1.69 ± 0.17 h, p = 0.0001) (Figure 4.8 A). (+) α-TP nanostructures formulated with phosphate (-29.6 ± 2.4 mV, 392 ± 6 nm) were found to give a bacterial infection time of 2.01 ± 0.30 h, which was not statistically different from the phosphate vehicle (1.81 ± 0.15, p > 0.05). Interestingly all α-TP species regardless of the formulation reduced the post-growth maximum population density of *S. oralis* (p = 0.02 with controls) (Figure 4.8 B). This difference in lag time and maximum population density profiles with formulation showed Tris allowed instant antimicrobial effect on *S. oralis* as the lag time was increased where as in the phosphate formulation the antimicrobial response appeared to be delayed as only the maximum population density was affected suggesting less interaction and perhaps a slower uptake. This was in agreement with Langmuir experimental data.

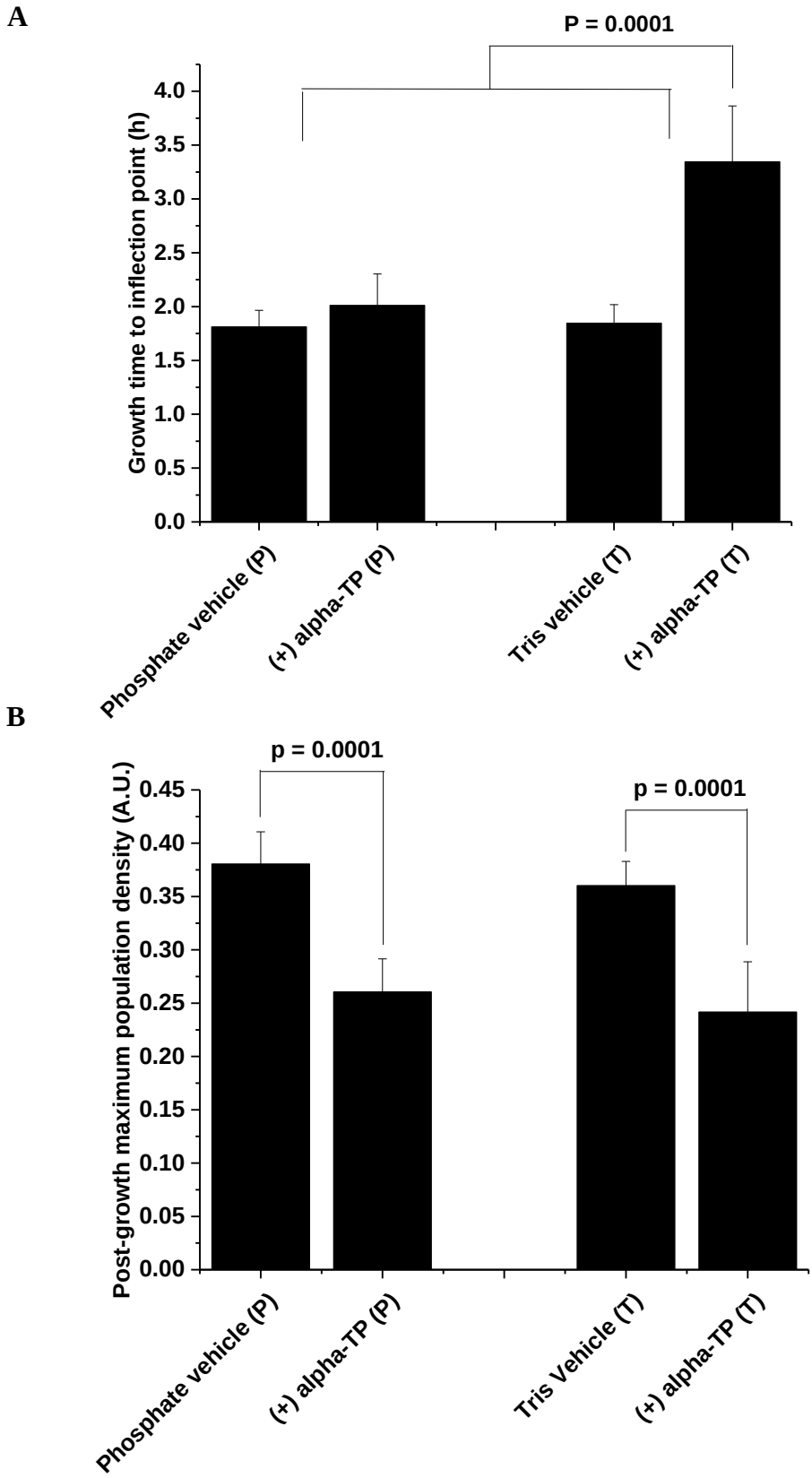

Figure 4.8. Growth time to inflection points (A) and post-growth maximum population densities (B) of *Streptococcus oralis* when treated with (+) alpha tocopheryl phosphate nanostructures formulated with phosphate or Tris. All treatments were dispersed in 20% ethanol, 80% water vehicle at pH 7.4. n=3 results.

4.4.5 UWMS biofilm formation inhibition

The salivary oral biofilms were found to develop to 5.95 ± 0.10 and 6.01 ± 0.14 relative light units (RLU, luminescence) when incubated in the presence of the media and water controls. The Tris and phosphate controls reduced biofilm attachment but the (+) α-TP nanostructures formulated with Tris (-18.9 ± 2.6 mV, 718 ± 471 nm) were found to inhibit the development of the oral salivary biofilms to 4.9 ± 0.25 RLU compared to the 5.55 ± 0.10 Tris vehicle control. The (+) α-TP phosphate formulations (-29.6 ± 2.4 mV, 392 ± 6 nm) were found not to inhibit the biofilms developments any more than the phosphate vehicle (Figure 4.9). The surfactant sodium lauryl sulphate (SLS) limited biofilm development to 4.53 ± 0.57 RLU which was none statistically different from the (+) α-TP Tris sample.

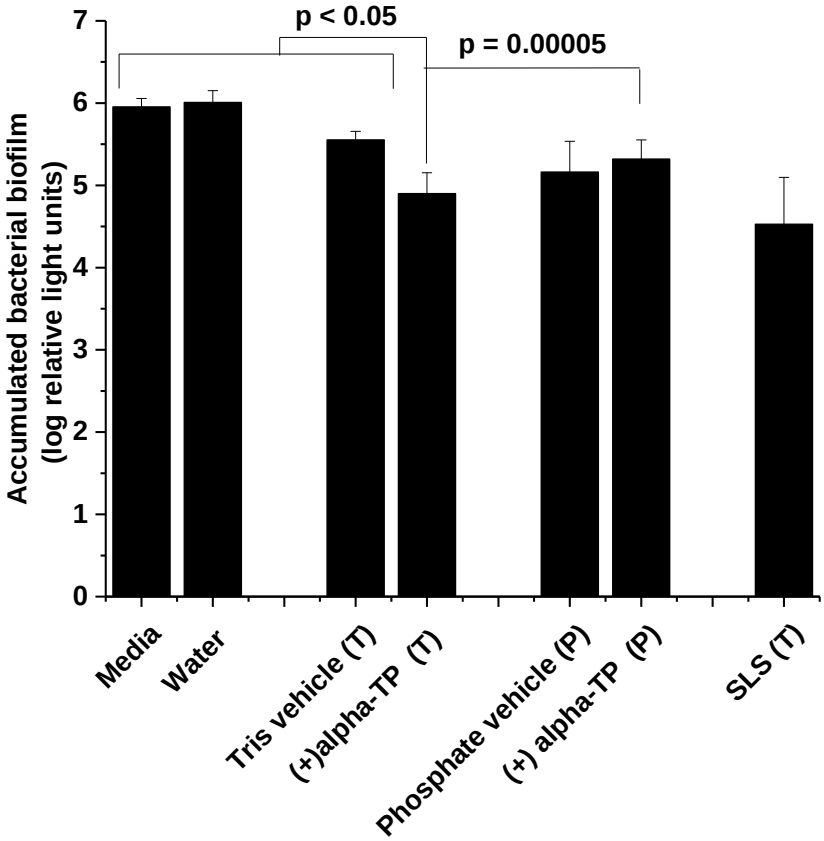

Figure 4.9. Salivary biofilm attachment to hydroxyapatite when the saliva was inoculated with (+) alpha tocopheryl phosphate nanostructures formulated with phosphate or Tris. All treatments were dispersed in 20% ethanol, 80% water vehicle at pH 7.4. n=3 results. Sodium lauryl sulphate (SLS) was a positive control. Media and water samples were negative controls.

4.4.6 UWMS biofilm kill penetration

The biofilm kill penetration depths were considered to be at point where the pre and post (+) α-TP application live/ dead staining ratio profiles overlapped (Figure 4.10)

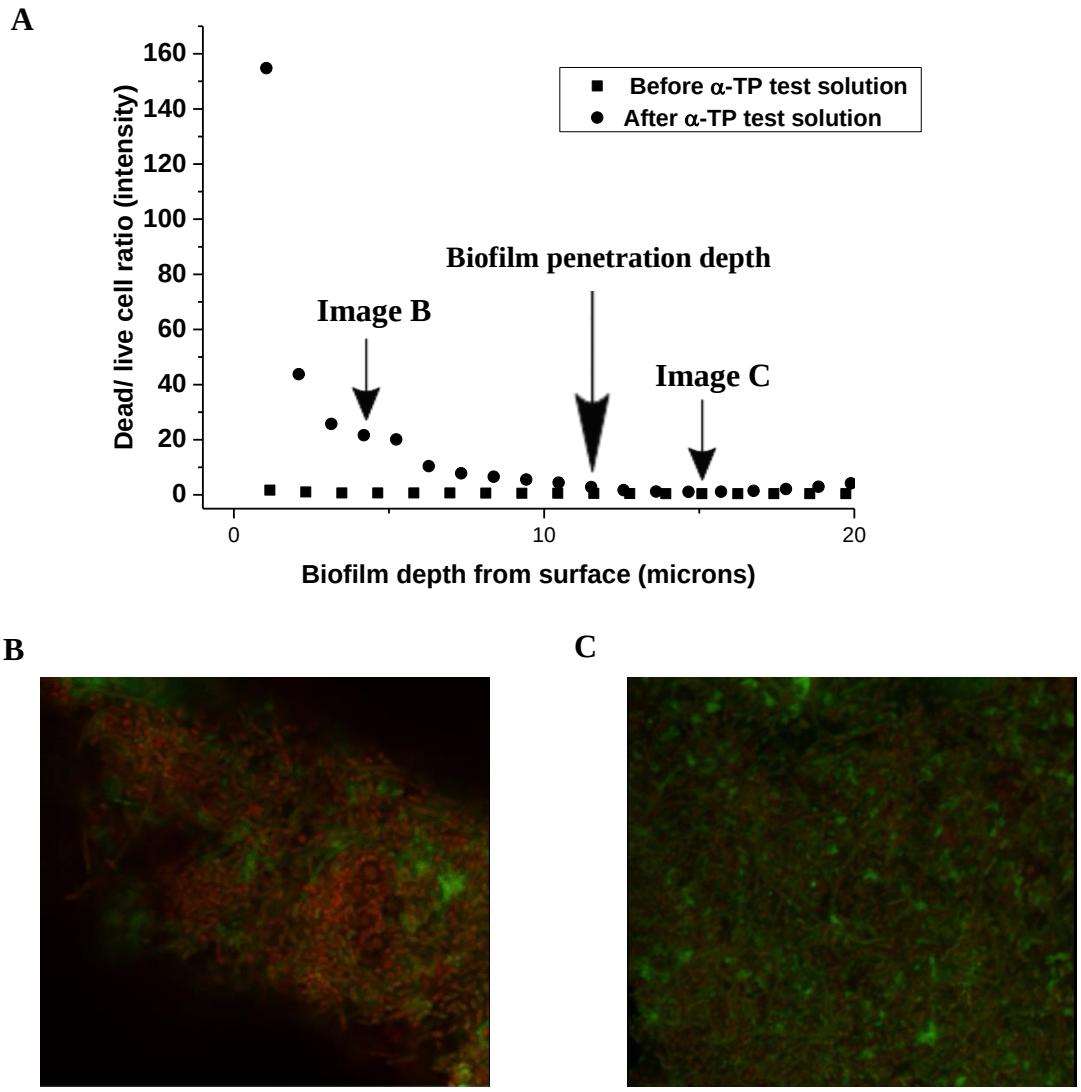

Figure 4.10. Unsterilized whole mouth saliva biofilm kill penetration depth of (+) alpha tocopheryl phosphate (0.8 mM, 0.04% w/v) nanostructures formulated with Tris (150 mM) monitored using a live/ dead viability assay via confocal microscopy (A), also showing an image at 4.2 microns showing a primarily dead biofilm layer (B) and an image at 15 microns showing a primarily live biofilm (C). Treatments were dispersed in 20% ethanol, 80% water vehicle at pH 7.4.

The (+) α-TP nanostructures formulated with Tris (-18.9 ± 2.6 mV, 718 ± 471 nm) where capable of penetrating the oral salivary biofilms and kill the bacteria to depths of 12.4 ± 3.6 μM, whilst the CPC positive control demonstrated bacterial kill to a depth of 16.1 ± 4.3 μM. The Tris vehicle was found not to have any kill efficacy on the salivary biofilms. The (+) α-TP dissolved in phosphate buffer (-29.6 ± 2.4 mV, 392 ± 6 nm) was not capable of killing bacteria in the biofilms (Figure 4.11).

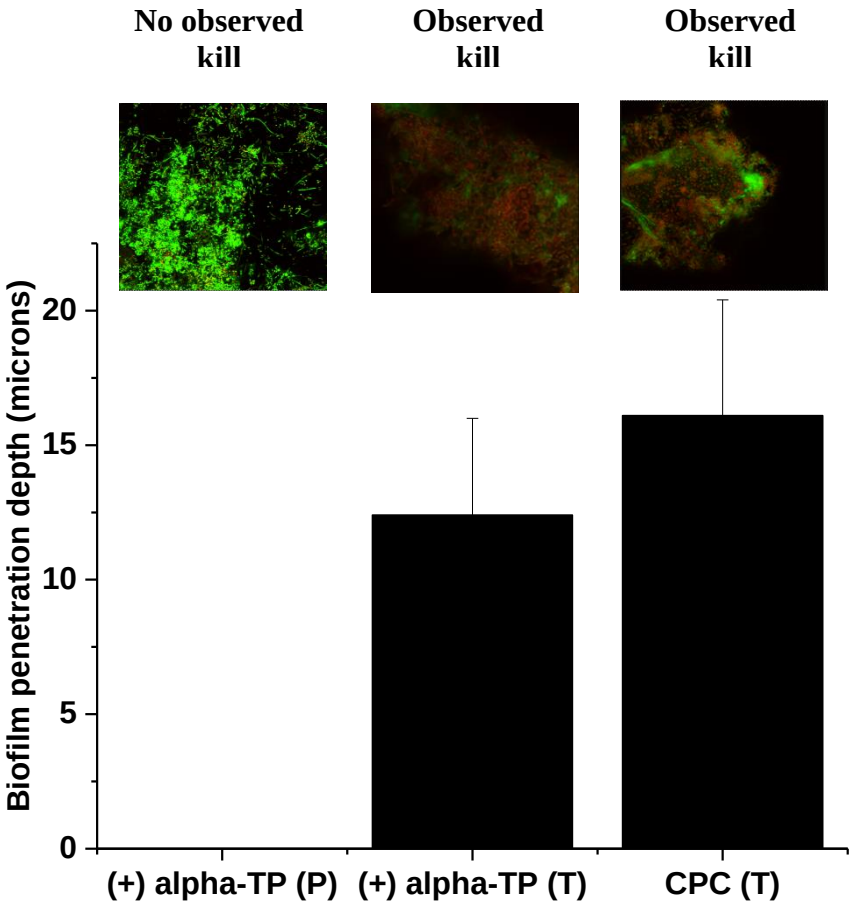

Figure 4.11. Unsterilized whole mouth saliva biofilm kill penetration depths of (+) alpha tocopheryl phosphate nanostructures (0.8 mM) when formulated with phosphate (150 mM) and Tris (150 mM). Live/ dead stain confocal microscopy images at 4.2 micron depths. Cetyl pyridinium chloride (0.8 mM) with Tris was a positive control. All treatments were dispersed in 20% ethanol, 80% water vehicle at pH 7.4. n=3 results.

4.5 Discussion

The set up to mimic gram-positive bacterial membranes were affected differently by the presence of the Tris and phosphate ions; the amount of phospholipids that can be applied onto a subphase before the surface pressure plateaus has been previously found to be influenced by the ions dissolved in the subphase and hence these phospholipid - ion interactions effect the monolayer architecture on which antimicrobial species come into contact with (Chou & Chang., 2000; Nowotarska et al., 2014). POPC is a zwitterion molecule, whilst POPG is anionic and hence the POPC: POPG (3:1) monolayer would have had a net negative charge. When this mixture of phospholipids was applied on the Tris subphase (25 mM), until the surface pressure plateaued, the maximum equilibrium surface pressure that could be achieved was higher compared to when this phospholipid mixture was applied onto the phosphate subphase (25 mM). The ability of Tris dispersed in the subphase to increase the phospholipids maximum monolayer equilibrium surface pressure was due to the effect of the organic Tris cations interacting with the anionic POPG head groups through ion pairing, resulting in a change in the monolayer self-assembly process which enabled a higher maximum surface pressure to be reached. At low concentrations the phospholipids form islands before reaching a concentration where they become a monolayer; it would appear that Tris allowed this self-assembly process to accommodate more of the phospholipid molecules because of ion pairing destabilising and swelling the phospholipid supramolecular structures, creating 'gaps' in the monolayer to be filled by additional phospholipids ascertaining higher surface pressure.

When the equilibration pressure of the monolayer on Tris was set to 30 mN/ m (that of bacteria) this meant there was ~8 mN/m capacity (gaps) for (+) α-TP molecules to exploit. When the (+) α-TP nanostructures were injected into the Tris subphase they instantly interacted with the 30

mN/ m monolayer but did not interact with the monolayers formed on the phosphate subphase. These observed interactions between anionic phospholipid species can be explained two fold, firstly by reducing the electrostatic repulsion, enabling the two species to interact and secondly due to the swelling phenomenon a potentially improved insertion into the membrane. There is evidence in the literature that when large organic monovalent cations, like Tris, interact with bacterial membranes they become more permeable but the mechanism of action for this permeability is not stated (Hamouda & Baker., 2000; Irvin et al., 1981; Ban et al., 2012; Asbell & Eagon., 1966; Vaara., 1992; Lambert., 2002; Angus Life Sciences., 2016). This work suggests the permeability mechanism is due to the ion pairing which enables the initial interaction due to reduced polar head electrostatic repulsion and causes the membranes to become disrupted and swell, creating a more porous membrane, increasing the uptake and potency of antimicrobials *i.e.* like that of the antibiotic tetracycline (Mecheri et al., 2004). However, proof of improved uptake *via* improved diffusion needs to be proved but the Tris ion pairing mechanism has been proven in the literature to be responsible for its permeabilising effect as it varied with pH; at pH 9 (predominantly neutral) the membrane of *Pseudomonas aeruginosa* has been shown to only have a 4.1 fold membrane permeability increase but at pH 7.4 (predominantly cationic) it was 133 fold more permeable (pKa of Tris, 8.1) (Hancock & Wong., 1984). In addition, the work carried out in this study used 150 mM Tris concentrations at pH 7.4 and applied to bacteria with Nano sized antimicrobial aggregates. Interestingly high concentrations of Tris (≥200 mM) have been observed to cause enhanced membrane permeable to supramolecular species *i.e.* the enzyme lysozyme, and therefore the interaction between the sensitized bacterial membrane mimics and the (+) α-TP nanostructures in the Langmuir experiments and subsequent antimicrobial effect is supported by the literature (Hancock & Wong., 1984). Therefore when a high concentration of cationic Tris is applied onto anionic gram-positive bacteria, *i.e. S. oralis*, it is likely that the membrane would increase in pressure

by swelling due to the ion-pairing interactions allowing for enhanced antimicrobial interaction to occur. The POPC: POPG monolayer pressure increase of 2.7 mN/ m when the (+) α-TP planar bilayers were injected into the subphase was considered show that the structures were becoming inserted into the monolayer and not rupturing it. This is because 19 residue polypeptide chains that insert into membranes have been found to increase the pressure of POPG: POPC monolayers by ~ 3 mN/ m (Posada et al., 2014).

In Chapter 3 (+) α-TP was found to form cylindrical micelles in water and planar bilayer islands when dispersed in Tris. This and the fluorescence studies in this Chapter confirmed the data from the Langmuir experiments that the addition of the different electrolytes affect the architecture of self-assembled phospholipids, but on these occasions the changes were observed in the pure (+) α-TP aggregates as opposed to the POPC: POPG monolayers. The Tris ions were found to increase fluorescent emission intensity whilst phosphate decreased it. Changes in supramolecular species fluorescent emissions commonly correspond with structural conformational changes (Langner et al., 2000) which may have contributed to activity, however, unlike in Chapter 3 the shape of the (+) α-TP nanostructure dispersed in phosphate buffer could not be observed through AFM due to the presence of large phosphate precipitates when drying the phosphate containing samples. To overcome this Transition electron microscopy (TEM) could be employed as this does not require dry samples. In addition increases in fluorescence intensity when salts are added have been linked to decreases in aggregate electrostatic surface potential due to a decreased value of the dielectric constant in the phospholipid polar head group region related in turn to decreased water organisation within the aggregate interface. Tris ion pairing with the aggregates appeared to reduce water organisation whilst phosphate interactions appeared to increase it though increasing the aggregates negative charge but needs to be proved. These different physiochemical properties

of the aggregates also unsurprisingly effected chemical stability but were all still within the threshhold of commercially viable.

The size of (+) α-TP aggregates when formulated with Tris or phosphate was similar, but the former was found to be capable of permeating the multispecies salivary biofilms to kill bacteria, increasing *S. oralis* biofilm growth time to inflection point and inhibiting biofilm development whilst the latter was not, which suggested in this case the nanostructures surface properties were more important than size in determining antimicrobial effects. The (+) α-TP dispersed in a phosphate buffer increased the aggregates negative charge and this reduced the interaction with the anionic bacterial monolayers due to greater electrostatic repulsion (Cherepanov et al., 2003). Therefore the antimicrobial mechanism of action for (+) α-TP appeared not to be like that of SLS (cell wall lysis) as it would be expected to increase in potency with more negatively charged aggregates (Wang et al., 2012) by associating with the positively charged environments in the monolayer (choline groups) but did not. This electrostatic repulsion appeared to be responsible for (+) α-TP phosphate formulations having a complete loss of UWMS biofilm growth inhibition, bacterial kill efficacy in the UWMS biofilms and a reduction in *S. oralis* biofilm growth inhibition. However, the (+) α-TP nanostructures formulated with phosphate were found to have an antimicrobial effect later in the *S. oralis* biofilm growth profile by limiting the maximum population and this suggested the (+) α-TP in phosphate buffer interacted with the *S. oralis* bacteria in some way, but to a lesser extent when in the presence of Tris, which has been previously reported (Schwab et al., 1999). These antimicrobial characteristics were also observed in the UWMS biofilm formation inhibition assays. In addition, the (+) α-TP tris formulations were again observed to produce a mild antimicrobial effect (as seen in in Chapter 3), by reducing biofilm formation by 0.65 log units, a log reduction of 3 is observed for potent antimicrobials *i.e.* a 99.9% reduction.

It should also be mentioned that if (+) α-TP antimicrobial mechanism was *via* targeting and inhibiting enzymes containing phosphate binding sites that the formulations with phosphate could have inhibited its action if the inhibited enzymes were in the cell membrane. However, (+) α-TP has been found to be within mammalian cells with intracellular biological properties and hence it is likely its antimicrobial mechanism of action occurs intracellularly and not on the cell surfaces but this needs to be confirmed. In addition, the presence of excess phosphate ions may also inhibit (+) α-TP's HA substantivity, seen in Chapter 3, as there would be less calcium binding sites.

It was also observed that the presence of Tris allowed the (+) α-TP nanostructures to penetrate salivary biofilms and kill the residing bacteria. The negatively charged EPS (bulk volume of oral biofilms) has been shown to inhibit the diffusion of positively charged oral antimicrobial agents *i.e.* CHX though electrostatic interactions (Shen et al., 2016) and would presumably hinder the diffusion of negatively charged antimicrobials through electrostatic repulsion. Therefore the flooding of multispecies oral biofilms with cationic Tris would not only have the benefit of sensitizing bacterial membranes to antimicrobials but would have also presumably had a neutralising effect on the EPS, changing the biofilm architecture in a way that would allow charged antimicrobials the ability to penetrate the biofilms more effectively to reach and kill bacteria. However, the sample group for saliva donation in the biofilm penetration studies would need to be larger in order to confirm (+) α-TP's antimicrobial potency on different biofilms and establish this methods robustness.

4.6 Conclusion

The combination of (+) α-TP nanostructures with the Tris facilitated interactions of (+) α-TP with the bacterial membranes, which inhibited *S. oralis* growth, inhibited biofilm development, facilitated biofilm penetration and killed the residing bacteria. The combination of the (+) α-TP aggregates with phosphate reduced aggregate zeta potential and presented the aggregate with membrane/ biofilms architectures which inhibited active membrane interactions, inhibited biofilm penetration and reduced (+) α-TP antimicrobial activity and hence would affect its ability to prevent plaque build-up and oral disease. Therefore different species of electrolytes do influence the interaction and antimicrobial activity of (+) α-TP with gram-positive bacteria and salivary biofilms. However, the oral soft tissue toxicity of (+) α-TP should be assessed for commercial viability, its aggregation properties probed further in an attempt to improve its biological activity further and assess if (+) α-TP could have additional therapeutic oral properties in addition to being a natural antimicrobial agent. Therefore the effect on α-TP aggregation characteristics, soft tissue toxicity and biological activity upon gum uptake will be assessed on its ability to treat periodontitis in Chapter 5.

CHAPTER FIVE

Engineering of Swellable (+) Alpha Tocopheryl Phosphate Nanostructures for use as Monocyte Control Agents to Treat Gingival Disease

5.1 Introduction

Both (+) α-T and (+) α-TP have anti-inflammatory properties (Cummings & Mattill., 1931; Libinaki et al., 2010), both self-assemble into nanostructures in aqueous environments and both could potentially treat gingival disease *i.e.* oral psoriasis, gingivitis and periodontal disease but their architecture will effect activity. The ability of nanostructures to swell can facilitate targeted delivery of agents (Paula & Koo., 2016; Singh & Singh., 2013; Socransky & Haffajee., 2005; Loesche & Grossman., 2001). Nanocarriers *i.e.* liposome, polymeric micelles, dendrimers and nanoparticles have been designed to target inflammatory diseases responding to a change in the micro environment into which they are administered for example pH, oxygen and temperature (Shaji & Lal., 2013). In the mouth nanocarriers can penetrate oral biofilms, but once within oral tissues it is desirable for the nanocarriers to swell to release the active. This type of delivery profile lends itself to self-assembled nanostructures made of an active but this type of system has not been for developed oral health drug delivery.

In Chapter 3, (+) α-T and (+) α-TP showed that they self-assembled into liposomes and planar bilayer islands. The non-water soluble (+) α-T, formed tight non-ionic liposomes, which were not sensitive to the presence of Tris and so probably have limited swellability properties. (+) α-TP is more water soluble, it formed anionic cylindrical micelles in water that transitioned into anionic planar bilayer island fragments in Tris buffered water and in Chapter 4 was structurally different when dispersed in phosphate buffered water. Therefore, its structure is sensitive to electrolyte environment change, which gives it potential to swell, and remove the individual molecular actives from the supramolecular structures in order to obtain higher concentrations intracellularly to inhibit cytokine responses more compared to α-T (Epstein-Barasha et al., 2010; Libinaki et al., 2010; Zingg et al., 2010).

Thus far, attempts at formulating oral health agents in order to achieve a substantive action have focused on bio-retention polymer systems (Pan., 2006; Ishikado et al., 2010). For example the non-substantive oral hygiene anti-inflammatory agent Triclosan (cyclo-oxygenase inhibition) has been formulated with the copolymers of methoxyethylene and maleic acid to extend its residency time and hence biological activity (Eley., 1999). In Chapter 3 the (+) α-TP nanostructures themselves were observed to adsorb to both biofilms and teeth and hence this show good potential to have a sustained effect on maintaining good periodontal health, but the action of the agent must release from the planar bilayer islands to antagonise the cell surface receptors and/ or pass into the mammalian cells because for gingival health the inhibition of chemokines (*i.e.* MCP-1), which can be generated in human gingival fibroblast (HGF-1) cells, is of primary importance (Urnowey et al., 2006). These chemokines are responsible for cell migration of white blood cells (*i.e.* monocytes) in response to oral infection/ injury, and if the recruited cells differentiate into macrophages and accumulate they can lead to gingival tissue destruction and tooth loss (Miyauchi et al., 1998; Park et al., 2014; Silva et al., 2014; Kim & Amar., 2006).

Therefore it would also be beneficial to deliver an agent with selective moderate toxicity towards macrophage cells to reduce their destruction and MCP-1 production as this could be effective in preventing gingival disease progression (Bettany & Wolowacz., 1998; Hanazawa et al., 1993). Anionic liposomes are known to preferentially target macrophages but their toxicity on the cell membrane is dependent on the aggregates physicochemical properties *i.e.* large liposomes are more toxic, and so swollen (+) α-TP structures would be expected to have enhanced selective macrophage toxicity *via* cell lysis (Kelly et al., 2011).

The aim of this Chapter was to assess how the architecture of the (+) α-TP planar bilayer islands in simple Tris environments (150 mM) would change when dispersed in complex solute systems (*i.e.* cell culture media which contains: 103-110 mM sodium chloride, 25 mM glucose and 18 mM sodium bicarbonate *ect.*) that resemble the complex systems in gum tissue in order to improve drug delivery and treat gingival disease. The nanostructure swelling properties of (+) α-T, (+) α-TP and (±) α-TP (8 isomer racemic mixture) were monitored to assess which vitamin E chemical parameters affected the swelling characteristics for drug delivery and subsequent gingival activity. Two cell lines HGF-1 and THP-1 were selected for cell viability and MCP-1, IL-6 and IL-8 expression studies (Melnyk & Morrison-Beedy., 2012). mRNA transcript expression assays were performed using q-PCR on HGF-1 cells for mechanistic understanding of MCP-1, IL-8 and IL-6 protein regulation by the three different vitamin E test agents. The inflammatory stimulus applied to the cells was heat killed bacteria from human saliva in an attempt to mimic the inflammatory environment found *in vivo* (Segura et al., 1999; Madianos et al., 2005).

5.2 Materials

(+) α-T (type (VI, ~ 40%), (±) α-TP (≥ 97%), chlorhexidine digluconate (CHX) (20% w/v aqueous solution), cetylpyridinium chloride monohydrate (CPC) (99.0-102%), Hanks balanced salt solution (HBSS) (Cat No H6648), 2-mercaptoethanol (99%), Dulbecco's phosphate buffered saline (PBS) (cat No D8537), trypan blue (0.4%), phorbol 12-myristate 13-acetate (PMA) (≥ 99%, film), trypsin-EDTA (0.25%) and TRI-Reagent® (Ambion) were purchased from sigma Aldrich, UK. Isopropanol, dimethyl sulfoxide (DMSO), hydrochloric acid, sodium hydroxide, heat-inactivated fetal bovine serum (FBS), penicillin G-streptomycin, MagMax™-

96 for Microarrays Kit (Ambion, AM1839), High-Capacity RNA-to-cDNA™ Kit (Applied Biosystems) and TaqMan universal PCR master mix (Applied Biosystems) were purchased from Fisher Scientific Ltd, UK. De-ionised water was used from laboratory supply. Dulbecco's modified Eagle's medium (DMEM) (ATCC 30-2002) cell culture medium and HGF-1 (ATCC CRL-2014) cells were purchased from the American type culture collection (ATCC) (USA). Roswell park memorial institute (RPMI) -1640 Medium (ATCC 30-2001) and the immortalised human peripheral blood monocyte cell line THP-1 (ATCC TIB-202) was sourced from LGC standards (UK). A colorimetric one step cell viability assay using a novel tetrazolium compound [3-(4,5-dimethylthiazol-2-yl)-5-(3-carboxymethoxyphenyl)-2-(4-sulfophenyl)-2H-tetrazolium, inner salt; MTS] and an electron coupling reagent (phenazine methosulfate; PMS) was purchased from Promega, USA. This has been previously used to assess toxicity of zinc oxide nanoparticles (Dechsakulthorn et al., 2007). Commercial enzyme-linked immunosorbent assays (ELISA's) including human MCP-1/ CCL2, human IL-8 and human IL-6 max deluxe sets were purchased from Biolegend, USA. Tissue culture flasks (25 and 75 cm^2 with ventilated caps) and 96-well plates where supplied by VWR (Germany).

5.3 Methods

5.3.1 Characterisation of (+) α-T, (+) α-TP, (±) α-TP aggregates in cell culture medium

The volume median diameters of (+) α-T, (±) α-TP and (+) α-TP were measured using a laser diffraction technique (Mastersizer X, version 2.15, Malvern Instruments, UK). The vitamin E

derivatives were formulated by dissolving the appropriate amount in ethanol, diluting with water, then Tris (0.5 M) with pH adjustment to 7.4 using sodium hydroxide or hydrochloric acid (2M) before being made to the mark with water to generate 20% ethanol, 80% water vehicles with 150 mM Tris, 3 mM sample concentrations. Samples were aliquoted and dispersed into 12 ml of stirring (max RPM) cell culture medium (either DMEM or RPMI without phenol red, FBS, or pen strep) liquid volume dispersing unit of the Malvern Mastersizer until the connected circulating cell reached an obscuration of 10% to 30% using a 180 µm size range lense. The volume median diameters were recorded as an average of three measurements and swelling monitored every 3 minutes for 15 minutes after dispersion of the formulation in the relevant cell culture media. Mathematical model was fitted to the data.

5.3.2 Gingival fibroblast and peripheral blood monocyte cell culture

HGF-1 cells were cultured in DMEM which included 10% FBS, and 1% of penicillin G-streptomycin (complete media A). The immortalised human peripheral blood monocyte cell line THP-1 was cultured in RPMI-1640 medium which included 10% FBS, 1% of penicillin G-streptomycin and 50 µM 2-mercaptoethanol (antioxidant) (complete media B). Both cell lines were initially cultured in 25 cm^2 tissue culture flasks and on subsequent subcultures 75 cm^2 flasks. Both cell lines were incubated at 37°C in a 5% CO_2, humidified atmosphere until HGF-1 cells reached confluence or until THP-1 monocytes reached $1x10^6$ cell/ mL. HGF-1 cells were adherent and so where subcultured using trypsin-EDTA (0.25%) (5 mL). The trypsin was then inactivated by adding complete media A (5 mL). The cells were harvested by centrifugation (500g for 5 min), resuspended in complete media A and reseeded at 50% of the initial confluent cell density. THP-1 monocytes where non-adherent and where subcultured

every 2-3 days by centrifugation (125 g for 5 min) and resuspended to achieve a seeding density of 2 x 10^5 cells/ mL complete media B. THP-1 cells were not allowed to exceed 1 x 10^6 cell/ mL during their flask culturing. HGF-1 and THP-1 cells used for experiments were between passages 3-8. There is not an ideal limit to cell passages and each cell line varies but value of 18 and 25 have been described as 'low' passage counts (ATCC., 2010).

5.3.3 Inflammatory stimuli preparation

The human saliva (0.1 mL per well, e.g. 10 wells was 1 mL) (1 donor) was collected and stored at 4°C. Saliva was inverted to form a homogenous solution and was added to falcon tubes (15 mL). The saliva was centrifuged (170 g, 10 min, Thermo Microlite RF temperature controlled microcentrifuge, Thermo Fisher Scientific, UK) and supernatant was removed and added to micro centrifuge tubes (1 mL/ tube). The supernatants were centrifuged (12,868 g, 10 min, Eppendorf 5810R temperature controlled centrifuge, Eppendorf UK Ltd, UK) to form bacterial pellets. Supernatants were discarded. Bacterial pellets were re-suspended in cell culture media (1 mL) (DMEM or RPMI-1640). Re-suspended bacteria were heat killed using a heating block (Grant, QBA1 series), UK) at 80 °C for 10 min followed by vortexing (Whirlimixer, Fisherbrand, UK). Samples were combined under sterile conditions and vortexed. The combined heat killed bacteria solution (200 μL) was added to one well in a 96 well plate and assessed by UV absorbance at 620 nm (iEMS Incubator/Shaker, Thermo Scientific, UK). The heat killed bacteria solution was diluted to 0.18 OD_{620} with cell culture medium under sterile conditions followed by a 1/100 dilution of the solution in cell culture medium. This was the inflammatory stimuli.

5.3.4 Determination of the HGF-1 and THP-1 cell line viability

The effects of (+)/ (±) α-TP, (+) α-T and heat killed human saliva bacteria, individually and in combination, were tested on HGF-1 and THP-1 cells. CHX and CPC were also tested on THP-1 macrophages as controls. To perform these assessments HGF-1 cells (passages 3-8) were seeded (1 x10^4 cells/ well) (Bedran et al., 2014) in 96 well microplates (100 µL/ well) and were incubated for 24 h at 37°C in a 5% CO_2 atmosphere to allow cell adhesion. The culture medium was then aspirated, and the cells were treated for 4 h with (+) α-TP (0.05, 0.5, 5, 50, 500, 5000 µM), (+) α-T (500, 5000 µM) or (±) α-TP (500 µM) (100 µL/ well) after which the test samples were aspirated, and the cells washed with HBSS (200 µL/ well). Either complete media or heat killed human bacteria from human saliva in complete media (1/100 dilution) were applied (100 µL/ well) and incubated for an additional 15 h at 37°C in a 5% CO_2 atmosphere to determine the cell viability of the vitamin derivatives alone and in with subsequent incubation with inflammation stimuli. The THP-1 monocytes were seeded (1 x10^4 cells/ well) with PMA (5 ng/ mL) (PMA films were diluted in DMSO to 5 mM stock solution then diluted to 200 ng/ mL aliquots and stored at -20: the 5 ng/ mL PMA solutions were prepared by thawing the 200 ng/ mL stocks and dispersing in RPMI cell culture media as appropriate) to allow monocyte differentiation and subsequent cell adhesion in 96 well microplates and were incubated for 48 h at 37°C in a 5% CO_2 atmosphere (Park et al., 2007). The culture medium was then aspirated, washed with HBSS and cultured in serum free media for 3 h before the cells were treated for 2 h (the time was reduced from 4 h to reduce the time the cells were starved from FBS) (Makon-Sébastien et al., 2014) with (+) α-TP (0.05, 0.5, 5, 50, 500, 5000 µM), (±) α-TP (500 µM), (+) α-T (500, 5000 µM), CHX (50, 100, 150, 500, 5000 µM) or CPC (0.05, 0.5, 5, 50, 500 µM)(100 µL/ well) after which the test samples were aspirated, and the cells washed with HBSS (200 µL/ well). Either complete media or heat killed

human bacteria from human saliva in complete media (1/100 dilution) were applied (100 µL/ well) and incubated for an additional 15 h at 37°C in a 5% CO_2 atmosphere. The 15 h supernatants were removed and used for ELISA assays and fresh complete media (100 µL) was added to the wells the colorimetric MTS cell viability assay (20 µL) was then added to each of the wells. Plates were then incubated at 37°C in a 5% CO_2 atmosphere for 4 h after which time absorbance's at 490 nm (iEMS Incubator/Shaker, Thermo Scientific, UK) were measured with reference subtractions at 650 nm. Untreated control cells were assigned a value of 100% viability (negative control), cell treated with 1% triton X (dispersed in cell culture media) were assigned a value of 0% viability (positive control). All the other conditions were compared to the controls using equation 5.1.: were As is the sample absorbance, Anc is the negative control absorbance and Apc is the positive control absorbance. Results are expressed as means ± standard deviations of triplicate assays from three different experiments. Lethal dose 50% (LD_{50}) values were calculated using the dose response model in origin 2016.

$$Cell\ viability\ (\%) = \frac{As-Apc}{Anc-Apc} X100 \qquad \text{[Equation 5.1.]}$$

5.3.5 Determination of cytokine secretion using ELISA assays

ELISA's were used to quantify MCP-1, IL-8 and IL-6 concentrations in the cell-free supernatants as follows. 1X capture antibody was diluted in coating buffer, added 100 µL/ well and was incubated for 18 h at 4 ˚C. Reagents were brought to room temperature and washed 4 times with wash buffer (300 µL/ well) and dried by firmly tapping on absorbent paper. To block non-specific binding and reduce background, 200 µL/ well of 1X Assay Diluent A was

added. Plates were sealed and incubated at RT for 1 hour. While plates were being blocked, the appropriate sample dilutions and standards were prepared. The cell-free supernatant samples were diluted 1/4 with 1X assay diluent A for MCP-1 and IL-8 quantification experiments and 1/40 for IL-6 quantification experiments in order for the concentrations of chemokines in the supernatants to be within the range of the generated calibration curve. These dilutions where found to be optimal in preliminary experiments. Top standards (1000 pg/ mL for IL-8 and 500 ng/ mL for IL-6 and MCP-1) were prepared from stock solutions in 1X Assay Diluent A (1000 µL). Six twofold serial dilutions of the top standards were performed with 1X Assay Diluent A in separate tubes. 1X Assay Diluent A served as the zero standard (0 pg/mL). The 1 h incubated plates were then washed 4 times with wash buffer before adding 100 µL/ well of standards or samples to the appropriate wells. Plates were sealed and incubated at RT for 2 hours. Plates were then washed 4 times with wash buffer before adding 100 µL of diluted detection antibody solution to each well. Plates were sealed and incubated at RT for 1 hour. Plates were washed 4 times with wash buffer before adding 100 µL of diluted Avidin-HRP solution to each well. Plates were sealed and incubated at RT for 30 minutes. Plates were washed 5 times with wash buffer before adding 100 µL of freshly mixed TMB substrate solution and incubated in the dark for 15 minutes. Positive wells turned blue in colour. The reaction was stopped by adding 100 µL of 2N sulphuric acid. Positive wells turned from blue to yellow. At the end of the experiment the absorbance's at 450 nm (iEMS Incubator/Shaker, Thermo Scientific, UK) were recorded using a microplate reader with the wavelength correction set at 570 nm for background subtraction.

5.3.6 mRNA expression assay

The HGF-1 cells were cultured and treated using the same method as the cell viability assay with the exception that after the 15 h incubation with the inflammatory stimuli supernatants were removed, the cells washed with PBS (100 µL/ well) and then harvested with TRI-Reagent® (100 µL/ well). Cell treatments groups were in quintuplet and were combined in micro centrifuge tubes at this stage (500 µL, 50,000 cells) (N = 3).

Total RNA was extracted using MagMax™-96 for Microarrays Kit following the Spin procedure. In summary, cells were homogenised in TRI- Reagent® for 5 minutes at room temperature. The homogenate was mixed 1–bromo–3–chloropropane (BCP) (50 µL) and centrifuged (12,000 g at 4°C for 10 minutes, Eppendorf 5810R temperature controlled centrifuge, Eppendorf UK Ltd, UK). The aqueous phase was collected and mixed with 100% isopropanol (50 µL). RNA was bound to RNA Binding Beads. The Beads were washed twice, total RNA was then eluted using Elution buffer. RNA was quantified using the NanoDrop (Thermo Scientific, UK). RNA integrity was analysed using the Bioanalyzer (Agilent, UK).

50 ng of total RNA per sample was converted to cDNA using High-Capacity RNA-to-cDNA™ Kit. Expressions of MCP-1, IL-6 and IL-8 were analysed using probes from the Universal Probe Library (UPL, Roche). Actin beta (ACTB), Selenocysteine lyase (SCLY) and tRNA-yW synthesizing protein 1 homolog (TYW1) were used as reference genes (for primer sequence and probe selection, see Tables 5.1 and 5.2). Assays were designed following instructions from the Universal Probe Library Assay Design Centre (Online). Quantitative PCR (qPCR) was performed using TaqMan Universal PCR Master Mix, following manufacturer's protocol. Each 10 µL reaction contained 0.2 µM forward primer and reverse primer and 0.1 µM UPL probe.

cDNA was diluted 10-fold, and 4 µL of diluted cDNA was used per reaction. qPCR was performed on Applied Biosystems 7900HT Real-Time PCR System under the following cycling conditions: 50°C for 2 minutes, 95°C for 10 minutes, followed by 40 cycles of 95 °C for 15 seconds and 60 °C for 1 minute. Data was collected at the end of each cycle and graphically expressed as the change in DNA threshold cycle (ΔCT) when (+) α-TP was incubated with the HGF-1 cells prior to the heat killed bacteria incubation over the ΔCT of the media treated cells prior to the heat killed bacteria incubation to provide a gene fold change ratio by were numbers greater than 1 showed a mRNA inhibition.

Gene name	*F primer*	*R primer*	*UPL probe*
MCP1	agtctctgccgcccttct	gtgactggggcattgattg	40
IL6	gatgagtacaaaagtcctgatcca	ctgcagccactggttctgt	40
IL8	gagcactccataaggcacaaa	atggttccttccggtggt	72

Table 5.1. Forward (F) and reverse (R) primer sequence and Universal Probe Library (UPL) probes for genes of interest.

Gene name	*F primer*	*R primer*	*UPL probe*
ACTB	agagctacgagctgcctgac	cgtggatgccacaggact	9
SCLY	gctgcgggaaacacaact	gctgaatacgggctgctg	1
TYW1	agccttggcagtcaagca	gcagtaggtaacgcccttca	1

Table 5.2. Forward (F) and reverse (R) primer sequence and Universal Probe Library (UPL) probes for reference genes.

5.3.7 Data analysis

All error values/ bars were expressed as their mean ± standard deviation (SD). Statistical analysis of data was performed using Levine's homogeneity test before statistical significance

between the sample groups was assessed by one way analysis of variance (ANOVA) tests with post-hoc Tukey analysis in Origin 2016 (Silverdale scientific ltd, UK). Statistically significant differences were assumed when $p \leq 0.05$.

5.4 Results

5.4.1 Aggregate characterisation in cell culture media

(+) α-TP was found to swell from nano sized bilayer planer fragments to micron sized structures when aliquoted into both DMEM and RPMI cell culture media. (+) α-TP was shown to swell at a faster rate when dispersed into the RPMI media as at the first time point (T = 0) the aggregates were 16.4 ± 1.0 µm whilst those in DMEM were 0.65 ± 0.04 µm (Figure 5.1 A). Although the aggregates in the RPMI media always had a mean volume diameter larger than those in DMEM there was not statistical significance after 3 minutes ($P > 0.05$) or 15 minutes (24.0 ± 4.9 µm and 28.52 ± 6.46 µm). The (+) α-T nano sized liposomes also swelled but to a lesser extent than the (+) α-TP. However, this was not observed in either DMEM or RPMI over the 15 minute time period (generated sizes of 3.7 ± 0.7 µm and 3.8 ± 0.6 µm at the 15 minute time point) as the swelling had already occurred at the '0' time point. The (±) α-TP aggregates (liposomes, 104 nm ± 1.3 nm, -38.7 ± 7.0 mV – obtained by personal communication) were found to swell faster as they were already micron size at time '0'and swelled to a greater extent compared to the (+) isomer in DMEM with a size of 19.7 ± 2.6 µm at 15 minutes (Figure 5.1 B) (not statistically different ($P > 0.05$) to (+) α-TP); The (±) α-TP isomer reduced in size over the 15 minute in both cell culture media which suggested the liposome was breaking down after it initial swelling.

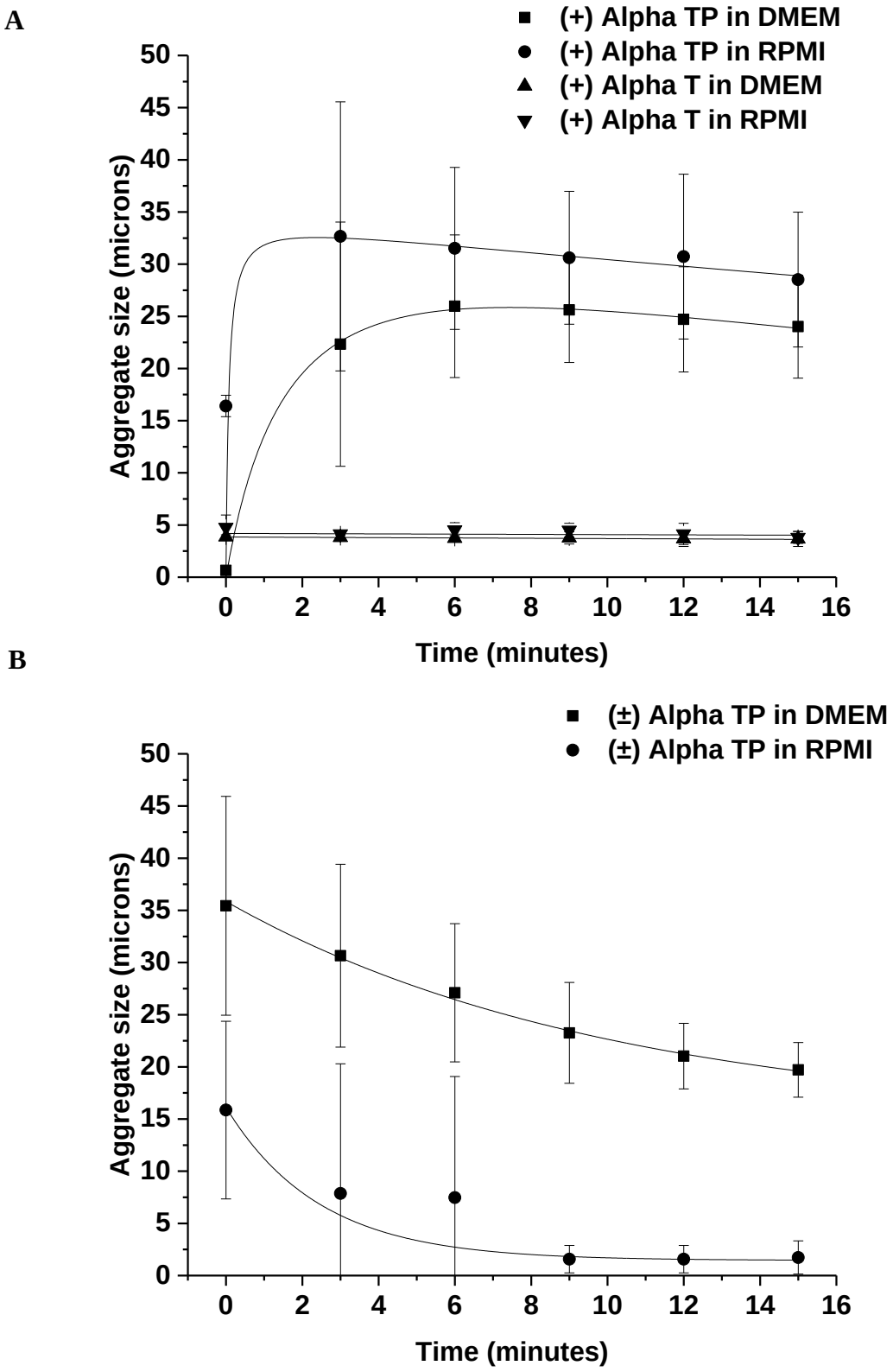

Figure 5.1. The swelling of stereo-pure alpha tocopheryl phosphate ((+) Alpha TP) (3 mM) (A), (+) alpha tocopherol ((+) Alpha T) (3 mM) (A) and racemic alpha tocopheryl phosphate ((±) Alpha TP) (B) in 20% ethanol, 80% water, 150 mM Tris at pH 7.4 when added into either Dulbecco's Modified Eagle's Medium (DMEM) or Roswell Park Memorial Institute (RPMI) 1640 medium. Data represented mean ± standard deviation (n = 3).

5.4.2 HGF-1 cellular response to the aggregates

(+) α-TP was well tolerated by HGF-1 until 5000 µM (0.25% w/v) where the cell viability was 75.5 ± 7.9% (Figure 5.2). The (+) α-TP LD_{50} in HGF-1 cells could not be calculated because at the maximum solubility of (+) α-TP in DMEM 50% of cell death was not achieved. Both the (±) and the (+) α-TP isomer (500 µM) were found to have the same effects on cell viability ($P > 0.05$) which suggested the stereochemistry was not a factor in toxicity. At 5 mM (+) α-T was shown not to be toxic, against HGF-1 cells (96.7 ± 6.1%) showing that the addition of the phosphate group had a significant effect on the cell viability.

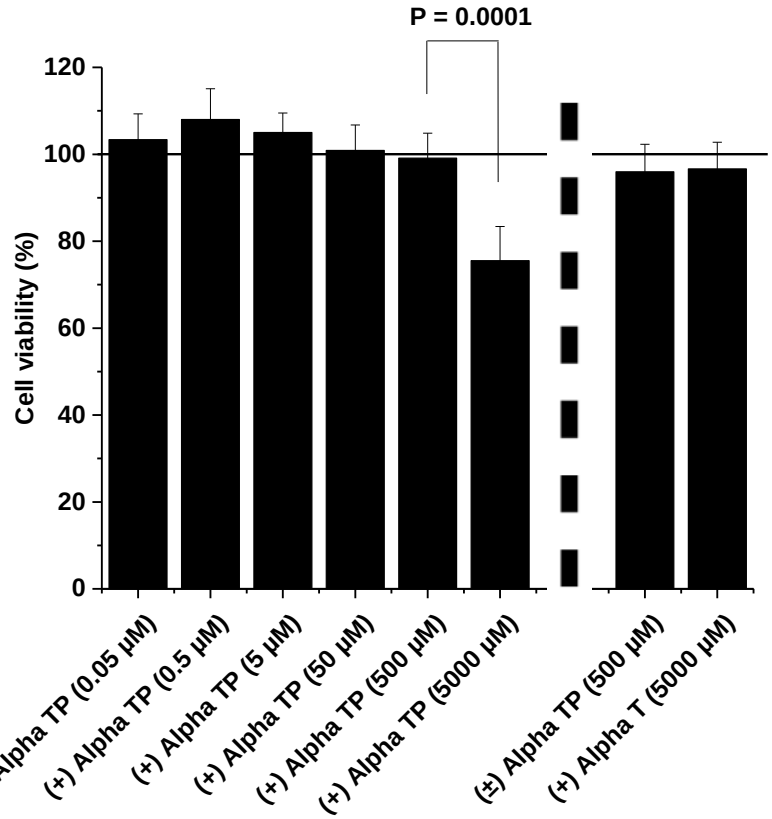

Figure 5.2. Cell viability of human gingival fibroblast cells (HGF-1) when treated with various (+) alpha tocopheryl phosphate (alpha TP) concentrations, (±) alpha TP (500 µM) or alpha tocopheryl (alpha T) (5000 µM), diluted in Dulbecco's modified eagle's cell culture medium (without FBS) at 37 °C for 4 hours. Data represented mean ± standard deviation (n = 3).

The inflammatory model developed using heat killed bacteria from human saliva was shown to be effective in upregulating MCP-1 from HGF-1 cells, the cells only treated with media throughout the experiment generated 21.6 ± 15.6 pg/ mL MCP-1, whilst those incubated with heat killed bacteria generated 673.5 ± 133 pg/ mL (Figure 5.3). Preliminary experiments showed there was no detectable amounts of MCP-1 in the heat killed bacteria itself showing that MCP-1 in the supernatant was generated from the HGF-1 cells. The reproducibility of this assay was considered acceptable as the relative standard deviation of the positive control was below 20% (DeSilva et al., 2003). As 500 μM concentrations of the test solutions where not toxic against HGF-1 cells, this concentration was used in the MCP-1 quantification to prevent MCP-1 release due to HGF-1 cell death. Pre-treatment with α-T (500 μM) was found not to inhibit MCP-1 production when the pre-treated HGF-1 cells where subsequently exposed to heat killed bacteria (619 ± 63 pg/ mL, $P > 0.05$). HGF-1 cells pre-treated with the (±) α-TP (500 μM) isomer were found not to statistically reduce MCP-1 generation compared to the non-pre-treated positive control (568 ± 107 pg/ mL, $P > 0.05$). However, (+) α-TP (500μM) was found to inhibit MCP-1 production (463.9 ± 68.9 pg/ mL) compared to the non-pre-treated positive control ($P = 0.007$), (+) α-T ($P = 0.005$) and (±) α-TP ($P = 0.04$). The inflammatory stimuli used was also found to produce IL-8 (8601 ± 600 pg/ mL) and IL-6 (18310 ± 896 pg/ mL). However, none of the vitamin E derivatives were found to have an inhibitory effect on IL-8 and IL-6 production (Figure 5.4) and so the (+) α-TP (500 μM) was MCP-1 specific in its inhibitory function.

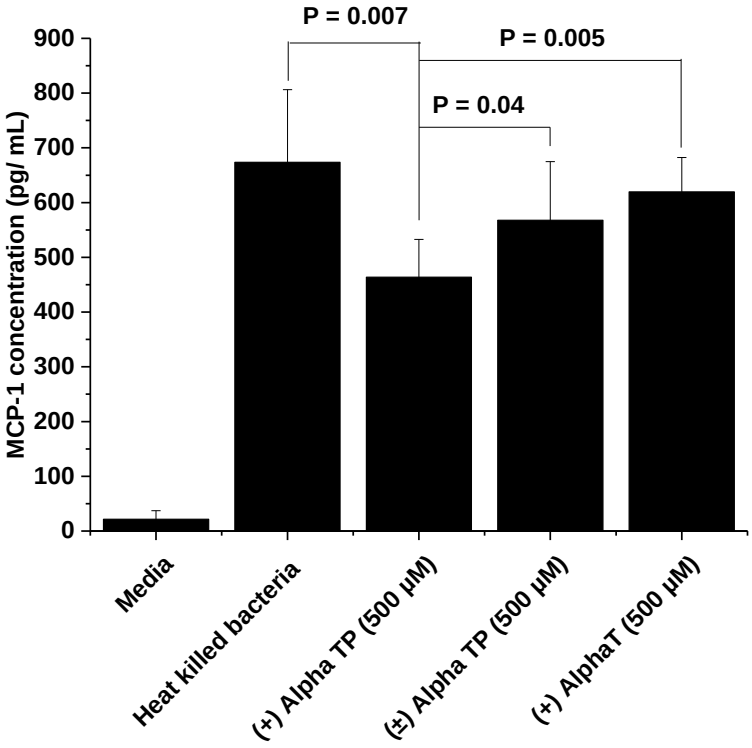

Figure 5.3. Quantity of monocyte chemoattractant protein-1 (MCP-1) secreted from human gingival fibroblast cells when pre-incubated with (+) alpha tocopheryl phosphate (alpha TP), (±) alpha TP or (+) alpha tocopherol (alpha T) samples for 4 h followed by 15 hours exposure to inflammatory stimuli.

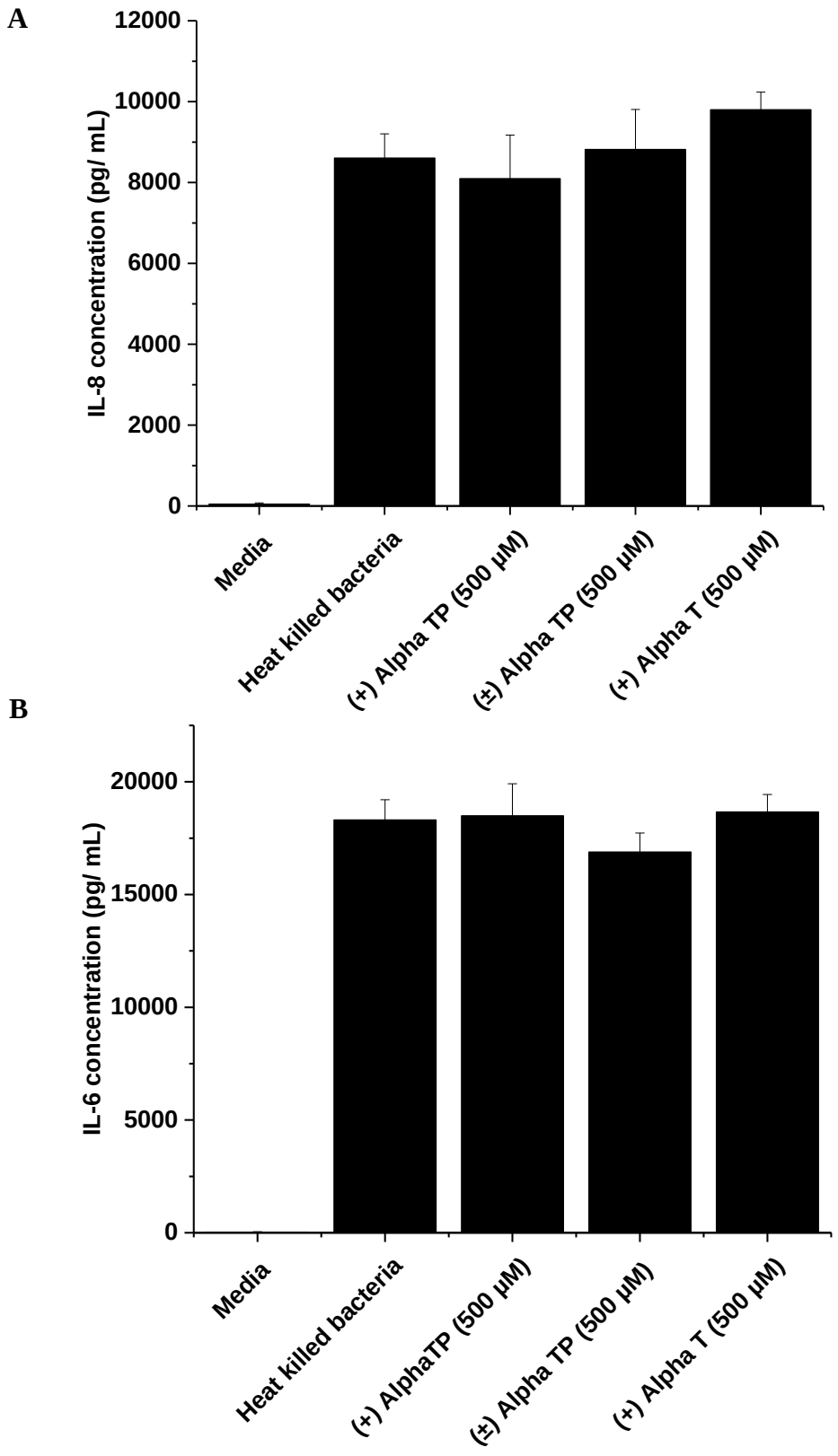

Figure 5.4. Quantity of interlukin-8 (IL-8) (A) and interlukin-6 (IL-6) (B) secreted from human gingival fibroblast cells when pre-incubated with (+) alpha tocopheryl phosphate (alpha TP), (±) alpha TP or (+) alpha tocopherol (alpha T) samples for 4 h followed by 15 hours exposure to inflammatory stimuli.

The selective inhibition of MCP-1 protein generation in HGF-1 cells by (+) α-TP was found not to be caused by a selective inhibition of MCP-1 mRNA transcription mechanism (Figure 5.5). This was because the pre-treatment of the HGF-1 cells with (+) α-TP before inflammatory stimulation did not statistically significantly reduce the transcription of MCP-1, IL-6 or IL-8 after data processing with the reference genes and comparison to the stimulated cells not pre-treated with (+) α-TP ($P > 0.05$).

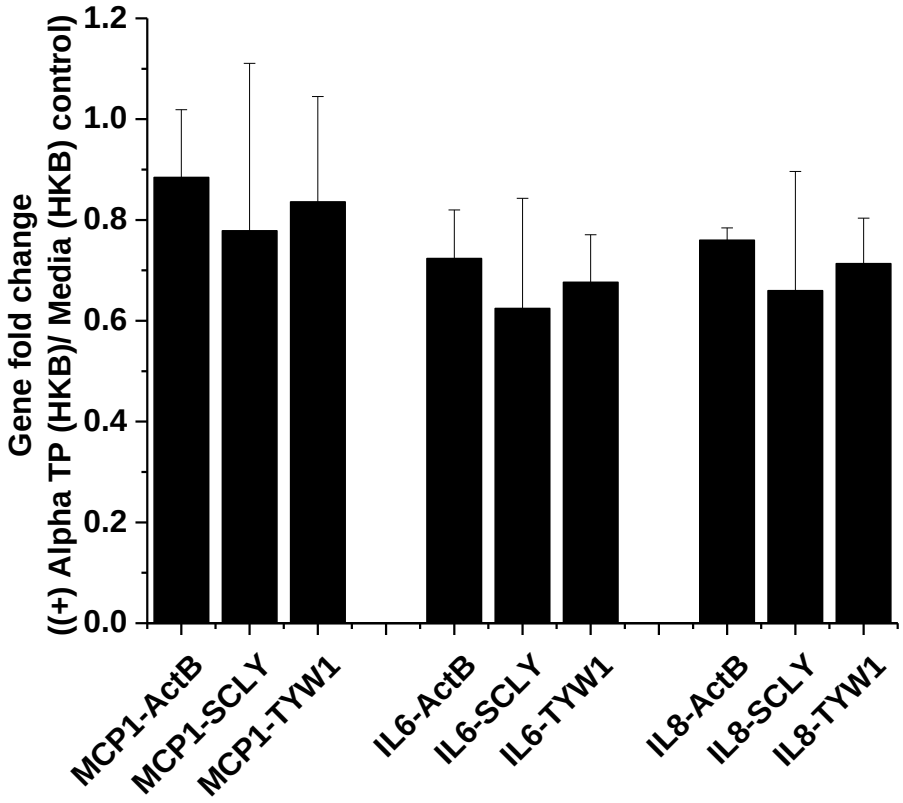

Figure 5.5. (+) Alpha tocopheryl phosphates ability to inhibit the mRNA transcription of MCP-1, IL-6 and IL-8 genes in HGF-1 cells when applied before stimulation with heat killed bacteria (HKB). Plotted with ActB, SCLY and TYW1 reference gene subtractions and the gene fold change (gene expression, ratio of mRNA (ΔCT)) as a function of that of the HKB stimulated cells not pre-treated.

5.4.3 THP-1 macrophage cellular response to the aggregates

(+) α-TP was less well tolerated by the differentiated THP-1 monocytes (macrophages) compared to the HGF-1 cells (Figure 5.6). The (+) α-TP LD_{50} against the macrophages was calculated to be 304 μM (20.0 ± 4.4% cell viability at 500 μM). Again (+) α-T (5 mM) was found to be well tolerated by the THP-1 macrophages at high concentrations (120.3 ± 33.6 %) but the (±) α-TP isomer was found to have a similar toxic effect to the (+) isomer (7.7 ± 4.6 % at 500 μM).

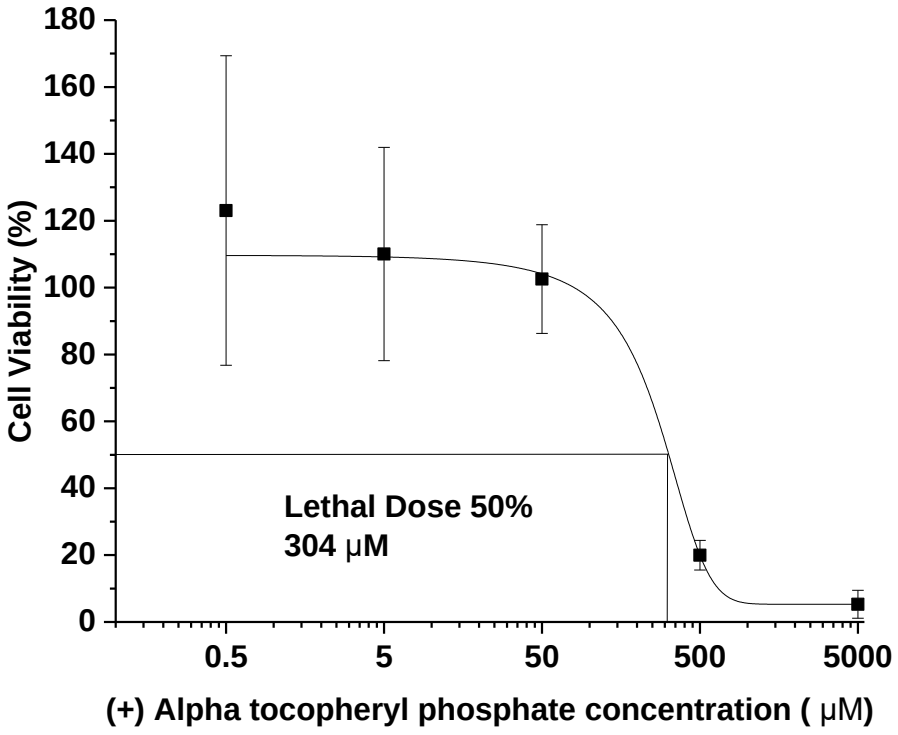

Figure 5.6. Lethal dose 50 of (+) alpha tocopheryl phosphate on THP-1 macrophages when diluted in Roswell Park Memorial Institute (RPMI) 1640 medium (without FBS) and incubated at 37 °C for 2 hours. Data represented mean ± standard deviation (n = 3).

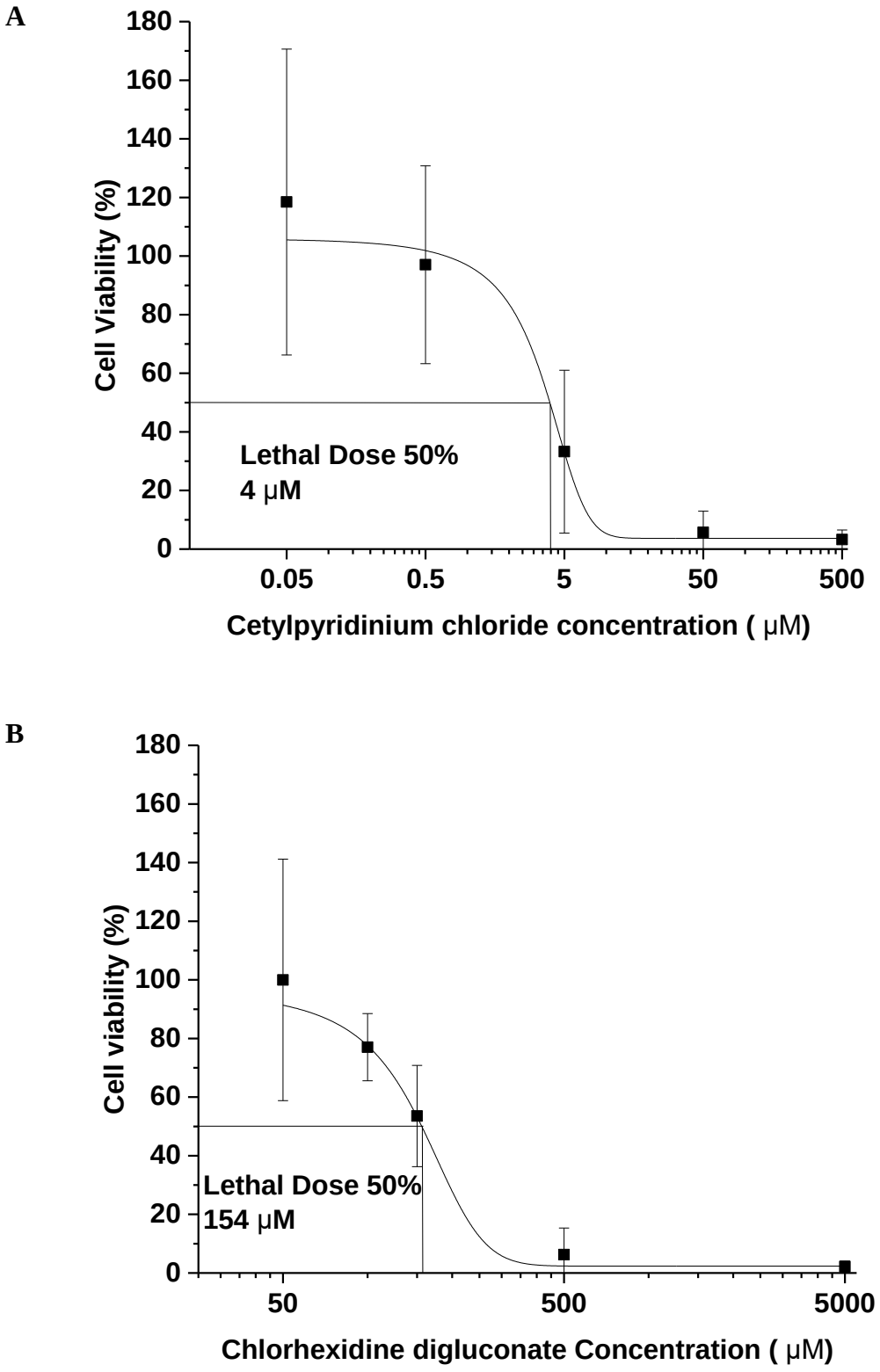

Figure 5.7. Lethal dose 50's of chlorhexidine (A) and cetylpyridinium chloride (B) on THP-1 macrophages when diluted in Roswell Park Memorial Institute (RPMI) 1640 medium (without FBS) and incubated at 37 °C for 2 hours. Data represented mean ± standard deviation (n = 3).

The inflammation model using the THP-1 macrophages showed a good upregulation of MCP-1 even though the concentration produced was much lower than that produced by HGF-1 cells (Figure 5.8). The media negative control was found to produce 6.0 ± 2.9 pg/ mL of MCP-1 whilst the macrophages treated with heat killed bacteria generated 57.3 ± 18.1 pg/ mL MCP-1 (Figure 5.8). (+) α-T was found not to inhibit MCP-1 generated from the THP-1 macrophages, 55.3 ± 31.7 pg/ mL was produced in the presence of the test agent. The (±) and (+) α-TP (500 μM) were both shown to inhibit the generation of MCP-1 from THP-1 macrophages (16.1 ± 5.1 pg/ mL for (±) isomer and 6.5 ± 3.2 pg/ mL for (+) isomer, $p = 0.003$) ((+) isomer, $p > 0.05$ with media control).

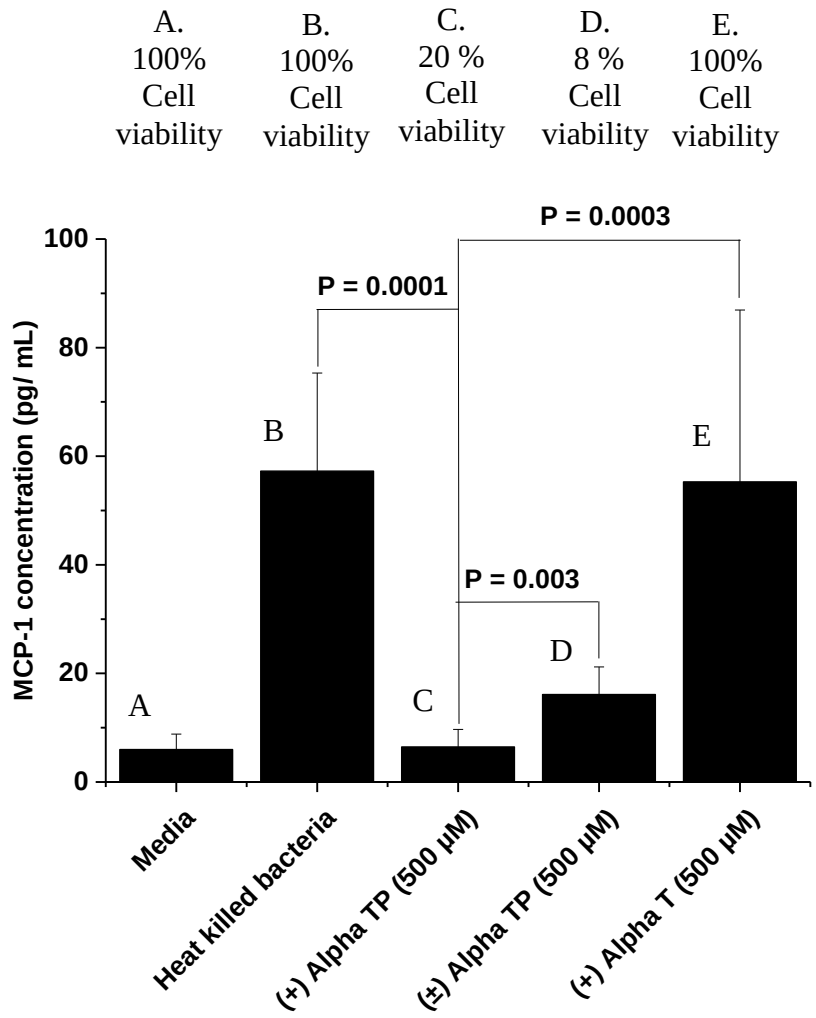

Figure 5.8. Comparison of monocyte chemoattractant protein (MCP-1) secretion from THP-1 macrophages when pre-incubated with (+) alpha tocopheryl phosphate (alpha TP), (±) alpha TP or alpha tocopherol (alpha T). Data represented mean ± standard deviation (n = 3).

5.5 Discussion

In Chapter 3, it was shown that the (+) α-TP forms thread-like micelles in water which transition into nano sized planar bilayer islands in the presence of Tris. However, when suspended in cell culture medium these nanostructures swelled to form micron sized aggregates; this was triggered due to the interactions with the cell culture electrolytes *i.e.* the sodium chloride and glucose in the complex electrolyte system. The swelling of the (+) α-TP in cell culture media was a consequence of the change in electrolyte composition which

influences the assembly of the aggregate structures. The swelling process in this self-assembled system was attributed to a transition from planar bilayer islands to multi-lamella liposomes. These changes in aggregate characteristics were thought to be potentially beneficial for (+) α-TP's biological activity because it acts intracellularly and swelling would destabilise the extracellular system and release more free molecules to provide a more effective cellular bioactivity (Gao et al., 2010). The (+) α-TP aggregates are not taken up into the cells rather the free α-TP is sequestered by the organic anionic transporter proteins (Negis et al., 2007).

It is unknown if the aggregates swelled and if so to what extent in the previous biofilm studies but they have been shown to have penetrated and killed the residing bacteria shown by the confocal microscopy. It is likely the Tris was present at high concentrations throughout the biofilms due to ion pairing with the EPS, dismantling the biofilms, whereas the Tris would be less likely to enter the gingiva in such high concentration but this needs to be proved. In any case the (+) α-TP nanostructure architecture would most likely be different between the biofilm and gingival penetration and hence would have different destabilising properties. In addition, the swelling mechanism may not be required for (+) α-TP uptake into bacterial cells as the Langmuir data showed the molecules inserted into the membranes and hence may be up taken through membrane diffusion in bacteria rather than uptake by organic anionic transporter proteins as in mammalian cells. (+) α-T swelled less than the (+) α-TP aggregates which could explain why (+) α-T had a lower biological activity compared to (+) α-TP. The (±) α-TP aggregates were also destabilised in both the cell culture media but in a different manner to the (+) isomer, they were destabilised more and hence showed that the chemical structure of (+) α-TP was specific to its action.

(+) α-TP was well tolerated by HGF-1 cells and it reduced MCP-1 production upon exposure to an inflammatory stimuli. As (+) α-TP has previously been shown to have anti-inflammatory properties (Libinaki et al., 2010) and in Chapter 3 it adhered to teeth, it was anticipated that this molecule could help to prevent gingival destruction in the mouth by being present during the introduction of an inflammatory stimuli and control the recruitment of monocytes and accumulation of macrophages. α-TP has been reported to influence enzymes such as acid and alkaline phosphatases, adenosinetriphosphatase and diphosphopyridine nucleotidase, it has signal transduction properties in regulating cytokine synthesis and can effect gene expression by directly binding and regulating mRNA encoding enzymes involved in their biosynthesis (Zingg et al., 2010; Zingg et al., 2012). In this work (+) α-TP has been found to inhibit MCP-1 upregulation, adding another biological function to this molecules activity. In addition the phosphate group was essential its activity as the (+) α-T analogue was not active. Interestingly the (±) α-TP racemic mixture was also not effective in supressing MCP-1 inhibition from HGF-1 but (+) α-TP was. Stereochemistry is known to have a major impact on the effectiveness of anti-inflammatory agents, for example it is known that Ibuprofen is most active in its S configuration (Wolf., 2007). α-TP has three chiral centres which result in 8 possible stereoisomers of which only the RRR configuration is natural. Each of these stereoisomers could have a different potency for inhibiting MCP-1, and racemic mixture (8 stereoisomers) may have diluted the overall activity such that it did not have statistically significant activity compared to the controls. The MCP-1 production pathway begins with the microbial recognition by cells *via* receptor activation; the cell then starts the process of producing the protein by transcribing the mRNA, releasing it from the nucleus and is then transcribed using tRNA and ribosomes, generating the protein (Madianos et al., 2005). Therefore if (+) α-TP was inhibiting MCP-1 production by acting as an antagonist on the microbial recognition receptors

the MCP-1 mRNA would not be generated but in this study it was and hence (+) α-TP does not appear to be a microbial recognition receptor antagonist.

When other cytokines in the HGF-1 cell free supernatants were tested *i.e.* IL-6 and IL-8, there was found to be no inhibition by (+) α-TP. This was surprising as previous literature found α-TP to inhibit these cytokines in atherosclerosis (Libinaki et al., 2010). The specificity of the (+) α-TP species to inhibit only MCP-1 was similar to the molecule Bindarit which has previously been shown to selectively inhibit MCP-1 through the inhibition of mRNA for MCP-1 (Sironi et al., 1999). There are chemical similarities between the molecules of Bindarit and (+) α-TP in that they both display fused rings and both display amphiphilic properties. However, (+) α-TP was found not to inhibit mRNA transcript expression, therefore (+) α-TP had a post mRNA transcription inhibitory activity on a downstream mechanism, perhaps inhibiting the mRNA translocation, translation into protein or signalling regulation at the protein level (for any of the enzymes employed in the protein synthesis post mRNA transcription) (Eskan et al., 2008).

The selective (+) α-TP toxicity against THP-1 macrophages was considered to be a desirable trait for a molecule that aims to treat gingival disease as it can control the excessive macrophage burden during an immune response in a similar way to tetracycline derivatives (Bettany & Wolowacz., 1998). However, it is not desirable to kill all macrophages as they perform a beneficial role of engulfing microbes and preventing the spread of systemic infection. (+) α-TP was found to be less toxic than two commercially used antimicrobial agents CHX and CPC and so it was thought capable of regulating macrophage accumulation without complete depletion. In addition MCP-1 generation was completely inhibited from THP-1 macrophages

treated with (+) α-TP (500 μM) and this would hopefully reduce the further recruitment of monocytes (Hanazawa et al., 1993). (+) α-T displayed no toxicity or MCP-1 inhibition towards THP-1 macrophages. The (±) α-TP racemic mixture had the similar effects on THP-1 macrophages as the stereo-pure α-TP isomer in terms of cell toxicity and MCP-1 inhibition suggesting that it may be an interaction with the macrophage cell membrane leading to lysis that kills the macrophages (Zingg et al., 2010). An instant cell lysis mechanism was presumably the reason why the THP-1 macrophages did not generate MCP-1 as this would not give the cells time to generate the MCP-1 inflammatory proteins before cell death. However, the effect of killing the macrophages on the overall periodontal inflammatory response need to be explored.

5.6 Conclusion

The (+) α-TP nanostructures became swollen and transitioned into macrostructures when dispersed in cell culture media. The phosphate moiety was found to enhance the swelling process. The swollen (+) α-TP structures were found to selectively inhibited MCP-1 (not IL8 or IL-6) generation in inflamed HGF-1 cells more so than both (+) α-T and (±) α-TP through a non-toxic post mRNA mechanism. The phosphate moiety in the swollen α-TP structures was also essential for introducing moderate toxicity to macrophages which inhibited their MCP-1 generation. Therefore in addition to (+) α-TP's moderate antimicrobial and anti-biofilm properties it is now thought to be a good candidate for professional applications in treating gingival disease *i.e.* oral psoriasis and periodontal disease through controlling the monocyte burden and hence prevent gingival destruction due to its swellable properties making it a novel multi-purpose agent for oral health applications. In addition, a lot of the oral care products to

date have focussed on antimicrobial agents to reduce the bacterial burden in the mouth to reduce the risk of gingival inflammation occurring, although there are some wound healing mouth rinses. A selection of these mouth rinse products have been applied to HGF-1 cells for 30 seconds and had cell viability monitored. It was found that a number of the commercial products had high toxicity towards these fibroblast cells which is undesirable (Bowen et al., 2015) whereas (+) α-TP was well tolerated by HGF-1.

CHAPTER SIX

General Discussion

The use of novel therapeutic compounds in denitrifies and mouthwash products to prevent oral disease is a growing area of research because of its economic value (Mintel., 2013). In addition, the fact that oral disease is now also being linked with serious systemic illnesses is increasing its importance (Kamera et al., 2008; Meurman et al., 2004; Abbayya et al., 2015; Ionel et al., 2016). As a consequence there have been a vast range of oral health compounds that target different components/ processes in the mouth; *i.e.* though controlling the bacterial burden by antimicrobial mechanisms (cell lysis/ enzyme inhibition), prevention of bacterial attachment, biofilm disruption, preventing the demineralisation of enamel, controlling biofilm pH and treating inflammation, reported in the literature (Wilson., 1996; Gallob et al., 2015; Huang et al., 2016; Serafini et al., 2012). However, oral health remains a significant problem and this suggests the ideal therapeutic solution has not yet been discovered (World Health Organisation., 2012).

Nanomaterials can be employed to improve the administration of therapeutic compounds through enhanced substantivity and/ or penetration and hence they are now being explored for dental applications (Narang & Narang., 2015; Ozak & Ozkan., 2013), but as yet they are not used clinically. In this work I explored the opportunity of using an amphiphilic natural biologically active molecule (+) α-TP as a novel nanomedicine to improve oral health.

(+) α-TP was employed because it is a natural anti-inflammatory agent with physicochemical properties that made it highly likely to self-assemble into nanosized aggregates when dispersed in aqueous environments (Ogru et al., 2003). The aim of the thesis was to assess if (+) α-TP formed nanostructures that had antimicrobial activity *via* membrane lysis, could bind to HA and have gingival anti-inflammatory properties related to its biophysical characteristics.

As a starting point, (+) α-TP was synthesised from (+) α-T in Chapter 2 because it was neither commercially available nor easy to extract from natural sources. It was also the naturally occurring stereoisomer that had the most biologically active form. Importantly (+) α-TP from this synthesis was still classified as natural due to the natural origin of the starting material (Moddresi., 2010). A method was developed from Nishio et al (2011), which generated the stereo-pure isomer in a 27% yield with ≥ 99% purity. Phosphorus, carbon, proton NMR, FTIR, mass spectrometry, HPLC and elemental analysis all confirmed the pure structure was successfully made. This synthesis procedure adds to the two published α-T phosphorylation reactions, but gives a more detailed description of the method and more extensive product characterisation ((Nishio et al., 2011; Gianello et al., 2005). In future work an attempt to scale up this reaction and make it commercially viable could be perused. This could be attempted by removing the immiscible solvent (+) α-TP extraction steps and directly purifying the 24 h water/ THF reaction mixture using column chromatography. This would reduce solvent usage making the reaction more 'green', reduce experiment time and it could improve the synthesis yield.

The CD data which was employed primarily to confirm the stereochemistry of the (+) α-TP product suggested the molecules were aggregating. The cotton effect signals seen in the spectra are a characteristic of supramolecular interactions (Cassim & Yang., 1967). Both the (+) α-T and (+) α-TP molecules were found to aggregate (light scattering), but the phosphorylation altered the aggregate architecture with the (+) α-T molecules self-assembling into 563 ± 1 nm, -10.5 ± 0.2 mV nanostructures and the (+) α-TP molecules self-assembling into 175 ± 21 nm, -14.9 ± 3.5 mV nanostructures showing the charged phosphate group was at the surface of the nanostructures. This analytical data was imperative to understand how the phosphorylation event altered the vitamins physical chemistry and how the agent would present itself to

bacterial biofilms, bacterial membranes, HA surfaces and soft oral tissue upon administration. The CAC of the (+) α-TP molecules was 5.5 ± 0.2 μM (18 h after preparation) and once the aggregates formed they did not change in diameter size or PDI upon concentration increased (up to 1.5 mM) or over time (8 days) showing the aggregates were physically stable (Wanga et al., 2012). However, the high PDI values (above 2) suggested the nano-assembly process generated a varierty of sizes. The (+) α-TP CAC was slightly lower than the vitamin E derivative (+) α-TS, which has previously been found to have a critical micelle concentration of 20 μM (Sadoqi et al., 2009; Muthu et al., 2012). This showed the (+) α-TP nanostructures had a superior physical stability compared to (+) α-TS when dispersed in the Tris vehicle.

The HPLC chemical stability method for (+) α-T and (+) α-TP was considered 'fit for purpose' based on the methods LOD, LOQ, precision and linearity. This assay provided a quick and reliable method for determining the chemical degradation of (+) α-T and (+) α-TP over time as well as subsequent analytical studies to determine the adsorption of the (+) α-TP nanostructures to HA. The (+) α-TP degradation rate was 1.2 μg/ mL/ week confirming that chemical degradation did not influence the biological results and that it was a commercially viable molecule. This was because it was within the industrial chemical degradation tolerance (10% degradation of a 0.05% w/v (500 μg/ mL) solution over 12 weeks at 40°C) and samples were only stored refrigerated for a maximums of 8 days. Interestingly (+) α-TP was much more chemically stable than (+) α-T, suggesting (+) α-TP was less susceptible to oxidation due to its inability to form a hydroxyl radical (Sabliov et al., 2009). Therefore the (+) α-TP was presumably hydrolysed back to (+) α-T for the established vitamin E degradation pathway to proceed.

Chapter 3 showed that the addition of a phosphate group not only improved the chemical stability of the molecules but it also generated antimicrobial nanostructures that inhibited the biofilm growth time to inflection point and maximum population density of the gram-positive bacteria *S. oralis* in a more potent manner compared to the (+) α-T nanostructures. This was considered to be beneficial to maintain good oral health as *S. oralis* is a highly proficient pioneering coloniser species. *S. oralis* provides a surface for the later bacterial colonisers to adhere to and is considered a major factor in the initialization of biofilm development (Dorkhan et al., 2013; Fujiwara et al., 2000). The controls used in this assay gave similar results to other bacterial growth curve data, which gave confidence this was a robust method and that (+) α-TP was a mildly active antimicrobial material (Gan., 2010; Mackay et al., 1984; Zahner et al., 2011; Fine et al., 1996).

The anti-biofilm activity of (+) α-TP was shown to be linked to the nanostructures having a substantive effect on the *S. oralis* biofilms. When a charge neutralising solution was used instead of saline to rinse off the (+) α-TP from the biofilms, both the inhibition of growth time to inflection points and the inhibition of the maximum population densities were reduced. The known substantive agent CHX (Elworhy et al., 1996; Koontongkaew & Jitpukdeebodintra., 1995) was found to have the same trend as (+) α-TP, but was more potent. This showed that the negatively charged phosphate group was allowing an interaction with the bacterial cell wall, tethering it in a similar way to the positive charge of CHX. It was surprising that the negatively charged (+) α-TP was interacting with the negatively charged cells walls of *S. oralis* so successfully as the physicochemical properties of the aggregate and the membrane were expected to repel. It was therefore suspected that the positively charged Tris molecules in the administration vehicle were influencing the (+) α-TP activity by interacting with all the negatively charged bacterial cell walls.

The (+) α-TP antimicrobial activity was found to influenced by the species of bacteria it was applied to; it was much less potent against the cariogenic bacterium *S. mutans* (Nobbs et al., 2009), unlike CHX, which displayed increased potency against this strain. This could be explained as *S. mutans* is known to have different cell wall architecture to *S. oralis*; it is more negatively charged and is more hydrophilic (Saito et al., 1997). This made it more prone to interacting with the cationic antimicrobial CHX whilst seemingly evading the antimicrobial effect of anionic (+) α-TP.

The MBC of (+) α-TP against *S. oralis* was found to be 1 µg/ mL which was more potent than CHX (Wang et al., 2012). This reversal in potency trend was considered to be a result of the (+) α-TP planar bilayer islands swelling and becoming disrupted when dispersed in BHI in a similar way to when the nanostructures were dispersed in cell culture media in Chapter 5. However, in future work, the MBC test should be performed on a wide range of other oral bacterial strains to fully understand its antimicrobial potential.

Chapter 3 found that the addition to the phosphate group also provided the vitamin with substantive anti-biofilm properties as it also facilitated the molecules ability to adsorb to HA. The mechanism of adsorption was considered to be the binding of the (+) α-TP phosphate group to the positively charged Ca^{2+} binding sites, a property observed with other organic phosphate species (Ganesan., 2008). This then reduced the extent of attachment of bacteria to the HA surface and inhibited salivary biofilm formation, but did not eradicate it. This was considered beneficial as controlling the oral micro-organisms, rather than completely eradicating them, is the goal (March., 2000). The (+) α-TP nanostructures antimicrobial interactions with *S. oralis* were likely a factor in delaying the salivary plaque maturation which could inhibit the attachment of the later pathogenic colonizing bacteria, which cause gum disease. Future work

should include assessing which micro-organisms were prevented from attaching to the HA/ pellicle surface, *i.e., S. oralis, S. mitis, S. gordonii ect* in order to better understand the mechanism of action in the prevention of plaque development/ maturation *i.e.* whether it was due to a change is HA physicochemical properties *(*hydrophobicity change) or an antimicrobial mechanism (controlled release of the (+) α-TP bilayer fragments).

The AFM images in Chapter 3 suggested that the differences in (+) α-T and (+) α-TP nanostructure shape contributed to the increased antimicrobial activity of (+) α-TP (Figure 6.1). The addition of the phosphate group reduced the aggregate size, increased negative charge, transitioned the shape from spherical liposomes and introduced viscoelastic properties. The phosphate group also made the vitamin E molecule sensitive to the presence of electrolytes (also seen in Chapter 5) as Tris transitioned the (+) α-TP from thread-like micelles to planar bilayer islands, increasing surface area and viscoelasticity whereas the architecture of the (+) α-T liposomes was unaffected by the presence of Tris. These shape transitions are observed when ionic surfactant like molecules are formulated with a high ratio of salt (in this case Tris) due to reduced head group repulsion (Nagarajan., 2002). The ability to manipulate and engineer the (+) α-TP nanostructures by carefully selecting electrolytes and/ or changing vehicle hydrophobicity could be used to optimise the compounds antimicrobial properties and should be investigated in future work *i.e.* application of the (+) α-TP macrostructures formed in cell culture media to biofilms, or formulation with ethanol and propylene glycol.

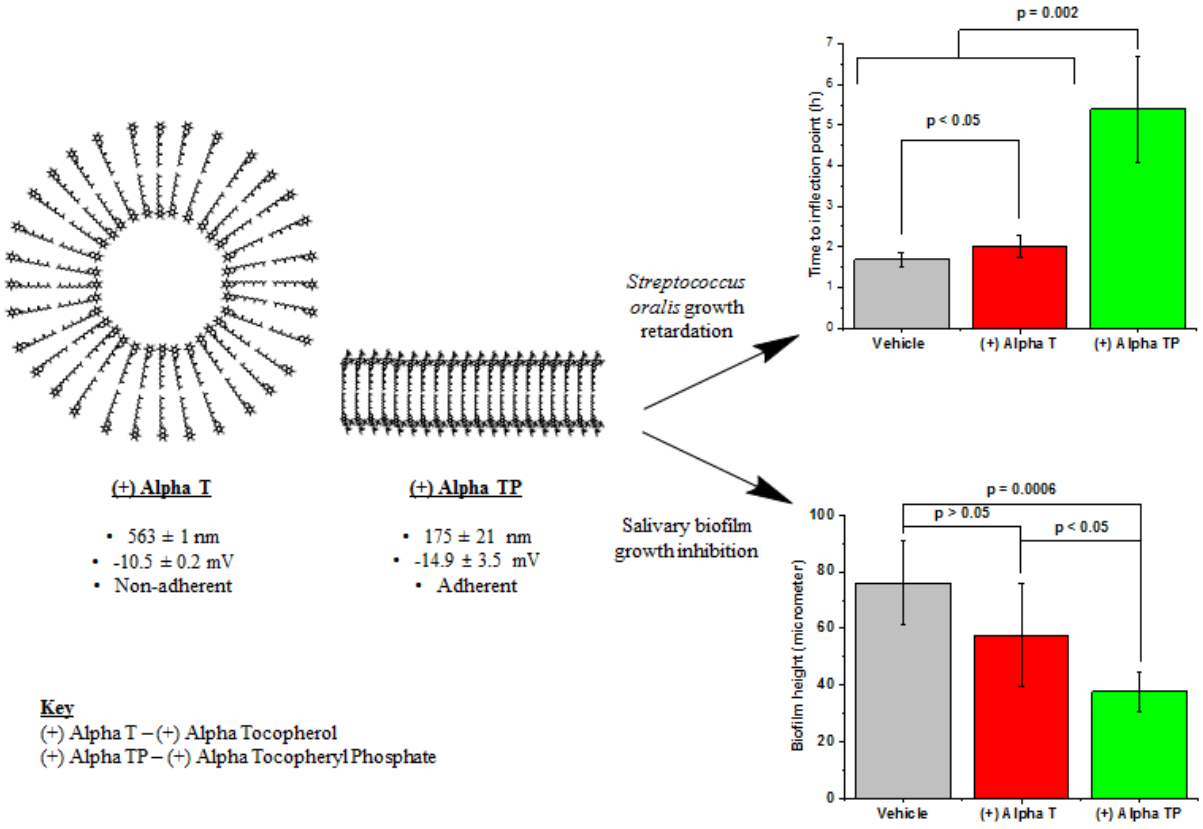

Figure 6.1. Correlation of (+) alpha tocopherol and (+) alpha tocopheryl phosphates nanostructure biophysical properties with their activity against *S. oralis* biofilm growth time to inflection points and salivary biofilm growth inhibition.

Chapter 3 also showed that the (+) α-TP substantive antimicrobial activity was related to the aggregates biophysical properties but the exact mechanism of action was not known. Therefore, in Chapter 4 the mechanism of action was investigated by monitoring the (+) α-TP membrane interactions. CHX and CPC are both positively charged antimicrobial species that disrupt cell wall stability and cause cell lysis (McBain et al., 2003; Haps et al., 2008). Negatively charged sodium lauryl sulphate micelles have been found to have bactericidal effects by solubilising cell membrane proteins again resulting in cell lysis (Wang et al., 2012; Mohamad., 2011). It was thought that (+) α-TP could also induce cell lysis. However, its membrane interactions

suggested otherwise. (+) α-TP is endogenous in cells and it appears in ultralow concentrations. It is a potent signalling molecule that targets enzymes including acid and alkaline phosphatases, adenosinetriphosphatase and diphosphopyridine nucleotidase to name just a few (Zingg et al, 2010) and or transcription factors (Gianelo et al., 2005). Moreover it has been suggested that (+) α-TP acts in a similar way to thiamine di-phosphate in bacteria which directly binds and regulate mRNAs encoding enzymes involved in its biosynthesis controlling gene expression. Therefore, (+) α-TP was thought to be acting *via* enzyme inhibition rather than cell lysis. Future work should involve selecting a number of enzymes that are known to play a part in the *S. oralis* metabolism and observe if (+) α-TP inhibits any of their activities to confirm its antimicrobial mechanism of action.

The antimicrobial properties of the (+) α-TP nanostructures were tested by altering the co-formulated counter ions. The (+) α-TP aggregates were influenced by phosphate and Tris in different manners according to the fluorescence emission spectra's. Nanostructure size, charge and chemical stability were all affected differently by co-formulation with either phosphate or Tris electrolyte species and this influenced the antimicrobial activity. The electrolyte selected was also found to have a huge effect on the packing of gram-positive bacterial membranes as the limiting equilibration pressure of the monolayer when formed on the Tris subphase was more than twice that of the pressure achieved on the phosphate subphase. This showed the Tris was ion-pairing with the phosphate head groups of the artificial bacterial membrane, becoming inserted into the surface of the monolayer, increasing pressure which could make the monolayer more permeable (Hamouda & Baker., 2000; Irvin et al., 1981; Ban et al., 2012; Asbell & Eagon., 1966; Vaara., 1992; Lambert., 2002). This was found to be vital for (+) α-TP's antimicrobial activity as only the monolayer formed on the Tris subphase allowed an instant interaction of the (+) α-TP planar bilayer islands. The monolayer pressure increase of

2.7 mN/ m when the (+) α-TP planar bilayers were injected into the subphase was considered to show that the structures were becoming inserted into the monolayer and not rupturing it as this is the monolayer pressure increase when polypeptides insert into monolayers (Posada et al., 2014).

In addition, the more negatively charged (+) α-TP aggregates formulated with phosphate did not interact with the monolayer, inhibit *S. oralis* growth time to inflection point or kill salivary bacteria were as the (+) α-TP planar bilayer islands did. This suggested that Tris was enabling the uptake of the (+) α-TP molecules and was inhibiting an intracellular process in a similar way to how Tris has been observed to increase the antibiotic properties of tetracycline (Mecheri et al., 2004) and antimicrobial supramolecular structures (Hancock & Wong., 1984). The internalisation of (+) α-TP molecules should in future be assessed by synthesising (+) α-TP using P^{31} and tracking its signal.

Unfortunately an AFM image of the (+) α-TP nanostructure in the phosphate buffer could not be obtained due to the way the phosphate buffer precipitated upon drying and so future work should include using transmission electron microscopy to observe the shape of these aggregates. Also, antimicrobial and AFM images of the (±) α-TP isomer should be investigated to understand if there are differences in antimicrobial isomer activity and if so whether they are related to physical and/ or chemical differences.

The positively charged Tris molecules were found to affect the architecture of the oral biofilms in a manner that allowed the (+) α-TP bilayer planer islands to penetrate the salivary biofilms, interact with and kill the residing bacteria (Figure 6.2). The bulk of biofilms are known to consist of negatively charged EPS, which has been shown to inhibit the diffusion of positively

charged oral antimicrobial agents *i.e.* CHX though electrostatic attraction (Shen et al., 2016) and presumably hindered the diffusion of negatively charged (+) α-TP nanostructures through electrostatic repulsion when the (+) α-TP was formulated in the phosphate vehicles.

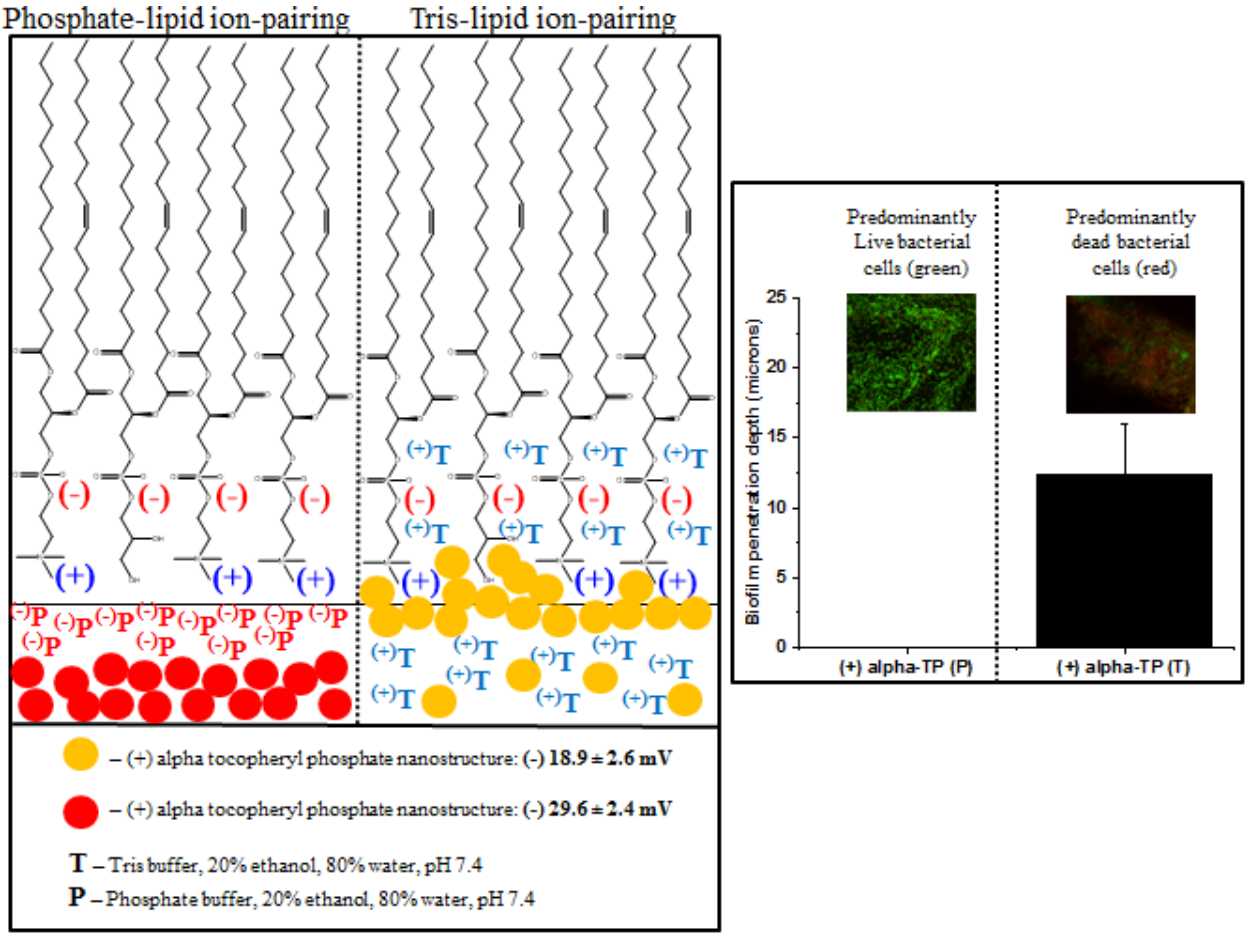

Figure 6.2. Interaction of (+) alpha tocopheryl phosphate nanostructures with an artificial gram-positive bacterial monolayer, salivary biofilm penetration and salivary bacterial kill when formulated with phosphate or Tris ions.

Another important area of oral health that has been explored in this thesis (Chapter 5) was the ability of (+) α-TP to target macrophages in the gingival tissue to maximise its anti-inflammatory properties (Nishio et al 2011; Munteanu et al., 2004; Kato et al., 2011; Libinaki et al., 2010). Chapters 3 and 4 showed that the variation in electrolyte presence effected nanostructure architecture and biological activity. When the (+) α-TP planar bilayer islands

were dispersed in DMEM and RPMI which simulated the environment of gum tissue they were found to rapidly swell from nanostructures to microstructures. The swelling was found to be a result of the phosphate group's sensitivity to electrolytes as the (+) α-T swelled less than the (+) α-TP aggregates. Interestingly the stereochemistry of α-TP also had an effect on the swelling process as the (±) α-TP aggregates were also destabilised but in a different manner to the (+) isomer, a characteristic that could have contributed to the observed biological activity differences. In future work the swelling process should be observed by environmental scanning electron microscopy and the effect of temperature change assessed *i.e.* 37 °C.These changes in aggregate architecture were thought to be beneficial for (+) α-TP's biological activity because it acts intracellularly and swelling would disrupt the system allowing the organic anionic transporter proteins to sequester more free α-TP providing a more effective cellular bioactivity (Gao et al., 2010; Negis et al., 2007) (Figure 6.3). In addition, it could help phagocytosis by macrophages.

Upon understanding the physical changes to the (+) α-TP nanostructures its gingival biological activity was assessed. The micron sized structures were found to be well tolerated by the HGF-1 cells, which are the major composition of gingival tissue. This was beneficial as the small selection of wound healing mouth rinse commercial products available have shown to be highly toxic against HGF-1 cells when applied for 30 seconds (Bowen et al., 2015). For future work it would be beneficial undertake these experiments in house for a more reliable comparison of the data as well as comparing them to the toxicity of CHX and CPC which are expected to have a higher toxicity to (+) α-TP due to their cationic interactions with membranes.

The phosphate group and the stereochemistry of (+) α-TP was found to have important biological activity as this microstructure was found to selectively inhibit the generation of

MCP-1 whilst (+) α-T did not and (±) α-TP had reduced activity. The sensitive relationship between structure and activity are commonly observed in cell signalling molecules (Wolf., 2007). However, the specificity of (+) α-TP to inhibit MCP-1 and not IL-8 or IL-6 was thought to due to the mRNA inhibition of MCP1-1 like that of the drug Bindarit (Sironi et al., 1999), but our studies found that the production of MCP-1 mRNA was not inhibited. Therefore the (+) α-TP post mRNA transcription inhibitory activity should be tested on downstream mechanisms in future work. (Eskan et al., 2008). In addition, the lack of activity against IL-6 and IL-8 was surprising as previous literature found α-TP to inhibit these cytokines in atherosclerosis (Libinaki et al., 2010). This may be due the (+) α-TP molecule having specific activity between mammalian cell types in a similar way to the differences in antimicrobial properties seen between the different species of bacteria. In addition the inflammatory stimuli (concentration, type and application time), the (+) α-TP effect on other cell lines (*i.e.* gingival epithelium cells) and other secreted cytokine species could be investigated to gain more understanding of the (+) α-TP anti-inflammatory properties for oral applications.

The stereochemistry of α-TP was found not to affect the moderate toxicity towards THP-1 macrophages (lesser than CHX and CPC), only the amphiphilic properties were required (phosphate group). The literature has already shown that phospholipids can lyse macrophages (Zingg et al., 2010). This toxicity profile was considered to be a desirable trait for a molecule that aims to treat periodontal disease as it can control the macrophage burden during chronic immune response (Bettany & Wolowacz., 1998). In a similar way to the biofilm burden it is not desirable to kill all macrophages in gum disease as they are beneficial in engulfing microbes and preventing the spread of infection into the systemic system; the aim was just to control the recruitment and accumulation which was achieved. The (+) α-TP toxicity to the macrophages was thought to be instant as they did not generate any MCP-1; dying macrophages can still

produce MCP-1 (Hanazawa et al., 1993), and so the α-TP MCP-1 inhibition was not likely to be enzymatic based but rather cell lysing. An LDH time response assay should be developed to explore the rate of toxicity in future work.

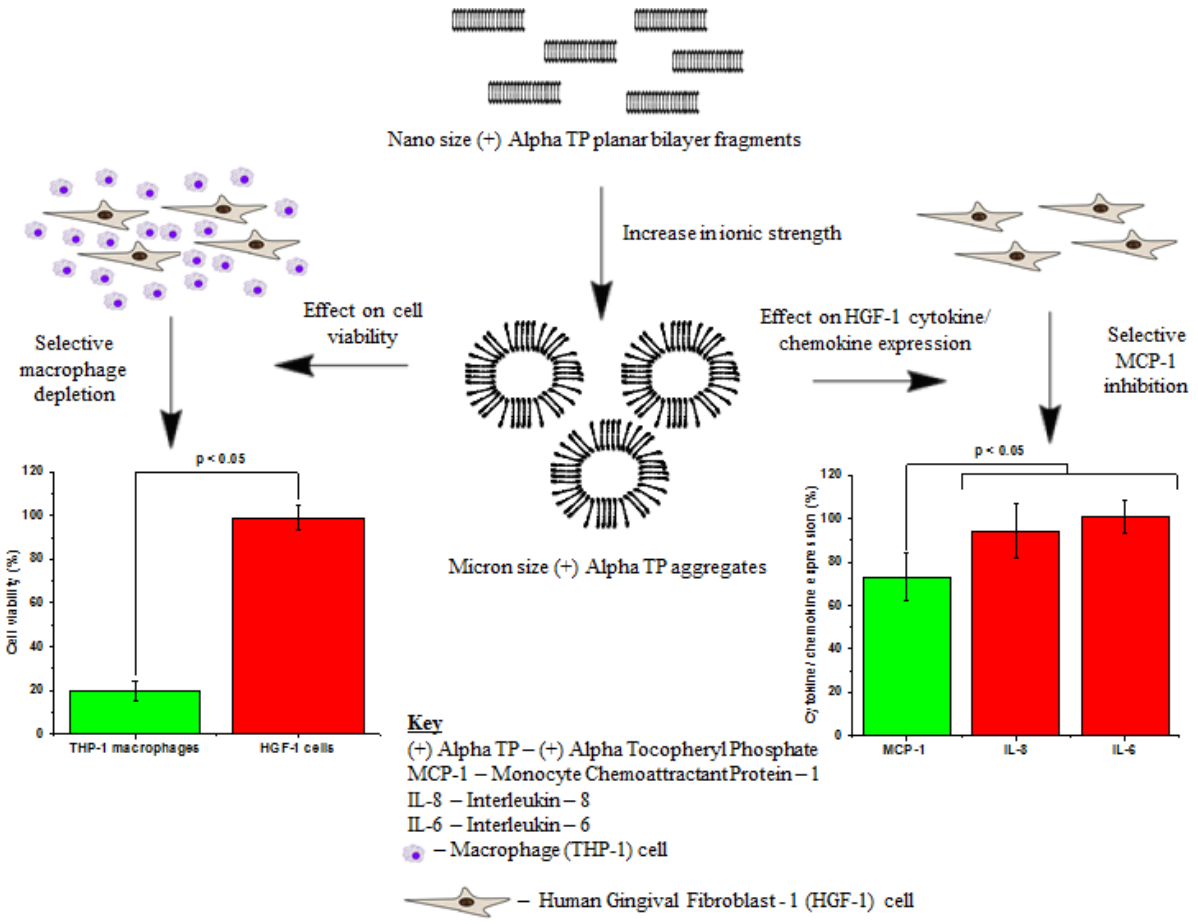

Figure 6.3. Swellability of (+) α-TP nanostructures upon gum uptake, their toxicity against human gingival fibroblast (HGF-1) cells/ THP-1 macrophages and their biological activity against inhibiting pro-inflammatory protein secretion from HGF-1 cells.

Overall, the data gathered in this thesis has shown that the vitamin E derivative (+) α-TP can be used as a multi-functional nanomedicine for topical oral health applications and should be tested in a commercial mouthwash product. This work has demonstrated that (+) α-TP nanostructure architectures are sensitive to their environment and can be used to manipulate

their anti-biofilm and gum disease treatment activity. This work provides a platform to explore this self-assembling biologically active molecule *in vivo* and hence its clinical therapeutic potential. For example, it may have activity against other gram-positive bacteria *i.e.* MRSA and gram-negative bacteria *i.e. E.coli*. Its actual specific antimicrobial mechanism of action still needs to be ascertained, upon doing so a library of bacterial strains that it would likely to effective against could be assembled and its activity tested to assess if it could be used in other body sites other than the mouth. Furthermore, it's inhibition of MCP-1 could be tested as a treatment for psoriasis (oral and skin) as these conditions are immune-mediated chronic inflammatory diseases linked to high expressions of the chemokine MCP-1 which leads to poor skin and oral health (Zablotna et al., 2016; Fatahzadeh & Schwartz., 2016). Additionally, (+) α-TP could be used synergistically as a nanocarrier encapsulating other therapeutic agents and have targeted controlled release in the mouth, this would increase the multifunctional capability of this agent.

References

Abbayya, K., Puthanakar, N. Y., Naduwinmani, S., and Chidambar, Y. S. (2015). Association between periodontitis and alzheimer's disease. *N Am J Med Sci*. **7(6)**: 241-246.

Åberg, C. H., Kelk, P., and Johansson, A. (2015). Aggregatibacter actinomycetemcomitans: Virulence of its leukotoxin and association with aggressive periodontitis. *Virulence*. **6(3)**: 188-195.

Addy, M., and Morann, J. M. (2000). Evaluation of oral hygiene products: science is true; don't be misled by the facts. *Periodontology*. **15**: 40-51.

Addy, M., Richards, J., and Williams, G. (1980). Effects of a zinc citrate mouthwash on dental plaque and salivary bacteria. *J Clin Periodontol*. **7**: 309-315.

Ahrari, F., Eslami, N., Rajabi, O., Ghazvini, K., and Barati, S. (2015). The antimicrobial sensitivity of streptococcus mutans and streptococcus sangius to colloidal solutions of different nanoparticles applied as mouthwashes. *Dent Res J (Isfahan)*. **12(1)**: 44–49.

Ai, D., Huang, R., Wen, J., Li, C., Zhu, J., and Xia, L. C. (2017). Integrated metagenomic data analysis demonstrates that a loss of diversity in oral microbiota is associated with periodontitis. *BMC Genomics*. **18(Suppl 1)**: 1041.

An, Y. H., and Friedman, R. J. (2000). Handbook of bacterial adhesion: Principles, Methods, and Applications. Humana press inc, Springer science + business media New York.
Andrews, J. M. (2001). Determination of minimum inhibitory concentrations. *J. Antimicrob. Chemother*. **48 (suppl 1)**: 5-16.

Angus® Life Sciences. (2016). *''Tris amino®''*. Available online at: https://webcache.googleusercontent.com/search?q=cache:Z8nuSYDb_MkJ:https://www.angus.com/literature/downloaddoc%3FfileName%3DANGUS_LifeSciences_TRISAMINO_TDS.pdf%26contentType%3DTechnical%2520Data%2520Sheet%26parentFolder%3DLiterature+&cd=3&hl=en&ct=clnk&gl=uk (Accessed 12/August/2016).

Ara, T., Kurata, K., Hirai, K., Uematsu, T., Imamura, Y., Furusawa, K., Kurihara, S., and Wang, P. L. (2009). Human gingival fibroblasts are critical in sustaining inflammation in periodontal disease. *J Periodontal Res*. **44**: 21-27.

Asbell, M. A., and Eagon, R. G. (1966). Role of multivalent cations in the organization, structure, and assembly of the cell wall of Pseudomonas aeruginosa. *J Bacteriol*. **92(2)**: 380-387.

ATCC. (2010). ''Passage number effects in cell lines''. Available online at: https://www.atcc.org/~/media/PDFs/Technical%20Bulletins/tb07.ashx (Accessed 12/February/2017).

Avila, M., Ojcius, D. M., and Yilmaz, Ö. (2009). The Oral Microbiota: Living with a Permanent Guest. *DNA Cell Biol*. **28(8)**: 405–411.

Baek, J. H., Krasieva, T., Tang, S., Ahn, Y., Kim, C. S., Vu, D., Chen, Z., and Wilder-Smith, P. (2009). Optical approach to the salivary pellicle. *J. Biomed. Opt*. **14**(4): 044001.

Baker, J. K. and Myers, C. W. (1991). One dimensional and two dimensional 1H- and 13C-nuclear magnetic resonance (NMR) analysis of vitamin E raw materials or analytical reference standards. *Pharm Res*. **8**: 763-770.

Balagopal, S., and Arjunkumar, R. (2013). Chlorhexidine: The Gold Standard Antiplaque Agent. *J. Pharm. Sci. & Res*. **5(12)**: 270 – 274.

Ban, S. H., Kim, J. E., Pandit, S., and Jeon, J. G. (2012). Influences of dryopteris crassirhizoma extract on the viability, growth and virulence properties of Streptococcus mutans. *Molecules*. **17**: 9231-9244.

Barrett-Bee, K., Newboult, L., and Edwards, S. (1994). The membrane destabilising action of the antibacterial agent chlorhexidine. *FEMS Microbiol Lett*. **119**: 249-253.

Beachey, E. H. (1980). Receptors and recognition, Series B volume 6, Bacterial Adherence, published by Chapman and Hall Ltd.

Bedran, T, B. L., Mayer, M. P. A., Spolidorio, D. P., Grenier, D. (2014). Synergistic anti-inflammatory activity of the antimicrobial peptides human beta-defensin-3 (hBD-3) and cathelicidin (LL-37) in a three-dimensional co-culture model of gingival epithelial cells and fibroblasts. *PLoS ONE*. **9(9)**: e106766.

Beiswanger, B. B., Doyle, P. M., Jackson, R. D., Mallatt, M. E., Mau, Ms., Bollmer, B. W., Crisanti, M. M., Guay, C. B., Lanzalaco, A. C., Lukacovic, M. F., et al. The clinical effect of dentifrices containing stabilized stannous fluoride on plaque formation and gingivitis--a six-month study with ad libitum brushing. *J Clin Dent*. **6 Spec No**: 46-53.

Berezow, A. B., and Darveau, R. P. (2011). Microbial Shift and Periodontitis. *Periodontol 2000*. **55(1)**: 36–47.

Bettany, J. T., and Wolowacz, R. G. (1998). Tetracycline derivatives induce apoptosis selectively in cultured monocytes and macrophages but not in Mesenchymal Cells. *Adv Dent Res*. **12:** 136-143.

Blout, E. R., and Stryer, L. (1959). Anomalous optical rotator Y dispersion of dye: polypeptide complexes. *Proc. N. A. S*. **45**: 1591 – 1593.

Boskey, A. L. (2007). Mineralization of bones and teeth. *Elements*. **3**: 387-393.

Bowen, J., Cole, C., and McGlennen, R. (2015). Comparison of antimicrobial and wound healing agents on oral fibroblast viability and in-vivo bacterial load. *Dentistry*. **5:** 6**.**

Bowen, W.H. (2013). The Stephan curve revisited. *Odontology*. **101**: 2-8.

Brading, M. G., and Marsh, P. D. (2003). The oral environment: the challenge for antimicrobials in oral care products. *Int Dent J*. **53**: 353-362.

Brielius-Flohe, R., and Traber, M. G. (1999). Vitamin E: function and metabolism. *FASEB J.* **13**: 1145-1155.

Caretto, S., Nisi, R., Paradiso, A., and De Gara, L. (2010). Tocopherol production in plant cell cultures. *Mol. Nutr. Food Res*. **54**: 726–730.

Cassim, J. Y., and Yang, J. T. (1967). Effect of molecular aggregation on circular dichroism and optical rotatory dispersion of helical poly-L-glutamic acid in solution. *Biochem. Biophys. Res. Commun*. **26**(1): 58-64.

Catuogno, C., Jones, M. N. (2003). The antibacterial properties of solid supported liposomes on Streptococcus oralis biofilms. *Int. J. Pharm*. **257**(1–2): 125–140.

Cekici, A., Kantarci, A., Hasturk, H., and van Dyke, T. E. (2014). Inflammatory and immune pathways in the pathogenesis of periodontal disease. *Periodontol 2000*. **64(1)**: 57–80.

Chandki, R., Banthia, P., and Banthia, R. (2011). Biofilms: A microbial home. *J Indian Soc Periodontol*. **15(2)**: 111–114.

Chenga, J. T. J., Haleb, J. D., Elliott, M., Hancock, R. E. W., and Strausa, S. K. (2011). The importance of bacterial membrane composition in the structure and function of aurein 2.2 and selected variants. *BBA. Biomembranes.* **1808(3)**: 622–633.

Cherepanov, D. A., Feniouk, B. A., Junge, W., and Mulkidjanian, A.Y. (2003). Low dielectric permittivity of water at the membrane interface: Effect on the energy coupling mechanism in biological membranes. *Biophys J*. **85(2)**: 1307–1316.

Chevalier, Y., and Chachaty, C. (1984). NMR investigation of the micellar properties of monoalkylphoshpates. *Colloid Polym. Sci*. **262**: 489-496.

Chou, T. H., and Chang, C. H. (2000). Thermodynamic characteristics of mixed DPPC/DHDP monolayers on water and phosphate buffer subphases. *Langmuir 2000*. **16**: 3385-3390.

Cohen, P. S., Krogfelt, K. A., Laux, D. C., Utley, M. (2000). Phospholipids having antimicrobial activity with or without the presence of antimicrobials. Patent application number US6165997 A.

Correia, R. F., Viseu, M. I., Prazeres, T. J. V., and Martinho, J. M. G. (2012). Spontaneous vesicles, disks, threadlike and spherical micelles found in the solubilization of DMPC liposomes by the detergent DTAC. *J Colloid Interface Sci*. **379**(1): 56-63.

Cummings, M. J., and Mattill, H. A. (1931). The auto-oxidation of fats with reference to their destructive effect on vitamin E. *J. Nutr*. **3**: 421–432.

Cummins, D. (1991). Zinc citrate/ triclosan: a new anti-plaque system for the control of plaque and the prevention of gingivitis: short-term clinical and mode of action studies. *J Clin Periodontol*. **18**: 455-461.

Dalgaard, P., and Koutsoumanis, K. (2001). Comparison of maximum specific growth rates and lag times estimated from absorbance and viable count data by different mathematical models. *J Microbiol Methods*. **43**: 183 – 196.

Dechsakulthorn, F., Hayes, A., Bakand, S., Joeng, L., and Winder, C. (2007). In vitro cytotoxicity assessment of selected nanoparticles using human skin fibroblasts. *Proc. 6th World Congress on Alternatives & Animal Use in the Life Sciences*. **AATEX 14, Special Issue**: 397- 400.

DeSilva, B., Smith, W., Weiner, R., Kelley, M., Smolec, J., Lee, B., Khan, M., Tacey, R,, Hill, H., and Celniker, A. (2003). Recommendations the bioanalytical method validation of ligand-binding assays to support pharmacokinetic assessments of macromolecules. *Pharm. Res*. **20(11)**: 1885 – 1900.

Devulapalle, K. S., and Mooser, G. (1994). Subsite specificity of the active site of glucosyltransferases from Streptococcus sobrinus. *J. Biol. Chem*. **269**: 11967-11971.

Di Caprio, R., Lembo, S., Di Costanzo, L., Balato, A., and Monfrecola, G. (2015). Anti-inflammatory properties of low and high doxycycline doses: an in vitro study. *Mediators Inflamm*. **2015**: Article ID 329418.

Dorkhan, M., Svensäter, G., and Davies, J. R. (2013). Salivary pellicles on titanium and their effect on metabolic activity in Streptococcus oralis. *BMC Oral Health*. **13**: 32.

Drulis-Kawa, Z., and Dorotkiewicz-Jach, A. (2010). Liposomes as delivery systems for antibiotics. *Int. J. Pharm*. **387**: 187–198.

Dziedzic, A., Wojtyczka, R. D., and Kubina, R. (2015). Inhibition of oral streptococci growth induced by the complementary action of berberine chloride and antibacterial compounds. *Molecules*. **20**: 13705-13724.

Eley, B. M. (1999). Periodontology: Antibacterial agents in the control of supragingival plaque — a review. *Br. Dent. J*. **186**: 286 – 296.

Eley, B. M., and Cox, S. W. (1992). Cathepsin B/L-, elastase-, tryptase-, trypsin- and dipeptidyl peptidase IV like activities in gingival crevicular fluid: A comparison of levels before and after periodontal surgery in chronic periodontitis patients. *J Periodont*. **63(5)**: 412-417.

Elworhy, A., Greenman, J., Doherty, F. M., Newcombe, R. G., and Addy, M. (1996). The substantivity of a number of oral hygiene products determined by the duration of effects on salivary bacteria. *J Periodontol*. **67**: 572-6.

Epstein-Barasha, H., Gutmana, D., Markovskya, E., Mishan-Eisenberga, G., Koroukhova, N., Szebenib, J., Golomba, G. (2010). Physicochemical parameters affecting liposomal bisphosphonates bioactivity for restenosis therapy: Internalization, cell inhibition, activation of cytokines and complement, and mechanism of cell death. *J. Controlled Rel*. **146(2):** 182–195.

Erbe, A., Kerth, A., Dathe, M., and Blume, A. (2009). Interactions of KLA amphipathic model peptides with lipid monolayers. *ChemBioChem*. **10(18)**: 2884–2892.

Erriu, M., Pili, F. M. G., Tuveri, E., Pigliacampo, D., Scano, A., Montaldo, C., Piras, V., Denotti, G., Pilloni, A., Garau, V., and Orrù, G. (2013). Oil essential mouthwashes antibacterial activity against aggregatibacter actinomycetemcomitans: A comparison between antibiofilm and antiplanktonic Effects. *International Journal of Dentistry*. Article ID 164267.

Eskan, M. A., Rose, B. G., Benakanakere, M. R., Zeng, Q., Fujioka. D, Martin, M. H., Lee, M. J., and Kinane, D. F. (2008). TLR4 and S1P receptors cooperate to enhance inflammatory cytokine production in human gingival epithelial cells. *Eur. J. Immunol*. **38:** 1138–1147.

Fatahzadeh, M., and Schwartz, R. A. (2016). Oral Psoriasis: An overlooked enigma. *Dermatology*. **232**: 319–325.

Fatima, T., Rahim, Z. B. H. A., Lin, C. W., and Qamar, Z. (2016). Zinc: A precious trace element for oral health care? *J Pak Med Assoc*. **66(8)**: 1019-1023.

Featherstone, J. D. B. (1999). Prevention and reversal of dental caries: role of low level fluoride. *Community Dent Oral Epidemiol*. **27(1)**: 31–40.

Ferreira Zandoná, A., Santiago, E., Eckert, G. J., Katz, B. P., Pereira de Oliveira, S., Capin, O. R., Mau, M., and Zero, D. T. (2012). The natural history of dental caries lesions. *J Dent Res*. **91(9)**: 841–846.

Ferretti, G. A., Brown, A. T., Raybould, T. P., Lillich, T. T. (1990). Oral antimicrobial agents-chlorhexidine. *NCI Monogr*. **(9)**: 51-5.

Filoche, S., Wong, L., and Sissons, C. H. (2010). Oral biofilms: Emerging concepts in microbial ecology. *J Dent Res*. **89(1)**:8-18.

Fine, D. H., Furgang, D., Lieb, R., Korik, I., Vincent, J. W., and Barnett, M. L. (1996). Effects of sublethal exposure to an antiseptic mouthrinse on representative plaque bacteria. *J Clin Periodontol*. **23**(5): 444–451.

Fitzgerald, J. E., and Kreutzer, D. L. (1995). Localization of interleukin-8 in human gingival tissues. *Oral Microbiol Immunol*. **10(5)**: 297-303.

Flemming, H-C., and Wingender, J. (2010). The biofilm matrix. *Nature Rev. Microbiol*. **8**: 623-633.

Flotra, L., Gjermo, P., Rolla, G. and Waerhaug, J. (1971). Side effects of chlorhexidine mouth washes. *Eur. J. Oral Sci*. **79 (2)**: 119-125.

Fujiwara, T., Hoshino, T., Ooshima, T., Sobue, S. and Hamada, S. (2000). Purification, characterization and molecular analysis of the gene encoding glucosyltransferase from Streptococcus oralis. *Infect Immun.* **68**: 2475–2483.

Gallob, J. T., Lynch, M., Charles, C., Ricci-Nittel, D., Mordas, C., Gambogi, R., Revankar, R., Mutti, B., Labella, R. (2015). A randomized trial of ethyl lauroyl arginate-containing mouthrinse in the control of gingivitis. *J Clin Periodontol*. **42(8)**: 740–747.

Gan, S. Y. (2010). PhD thesis, King's College London. Antimicrobial activity of zinc chelator complexes.

Ganesan, k. (2008). Ph.D. thesis. University of Duisburg-Essen, Germany. Functionalization of calcium phosphate nanoparticles with organic phosphates.

Gao, W., Chan, J., and Farokhzad, O. C. (2010). pH-responsive nanoparticles for drug delivery. *Mol Pharm*. **7(6)**: 1913–1920.

GCI magazine. (2012). *''Bites Back in Oral Care''*. Available at: http://www.gcimagazine.com/marketstrends/segments/oralcare/138401434.html (Accessed 10 March 2017).

Gianelo, R., Libinaki, R., Azzi, A., Gavin, P. D., Negis, Y., Zingg, J. M., Holt, P., Keah, H. H., Griffey, A., Smallridge, A., West, S. M., and Ogru, E. (2005). Alpha-tocopheryl phosphate: a novel, natural form of vitamin E. *Free Radic. Biol. Med*. **39**: 970-976.

Gitlin, J. M., and Loftin, C. D. (2009). Cyclooxygenase-2 inhibition increases lipopolysaccharide-induced atherosclerosis in mice. *Cardio Res*. **81(2)**: 400-407.

Gliszczyńska-Świgło, A., Sikorska, E., Khmelinskii, I., and Sikorski, M. (2007). Tocopherol content in edible plant oils. *Pol. J. Food Nutr. Sci*. **57**: 157-161.

Goldberg, M., Kulkarni, A. B., Young, M., and Boskey, A. (2011). Dentin: Structure, composition and mineralization: The role of dentin ECM in dentin formation and mineralization. *Front Biosci (Elite Ed)*. **1(3)**: 711–735.

Golub, L. M., Lee, H. M., Stoner, J. A., Sorsa, T., Reinhardt, R. A., Wolff, M. S., Ryan, M. E., Nummikoski, P. V., and Payne, J. B. (2009). Subantimicrobial-dose doxycycline modulates gingival crevicular fluid biomarkers of periodontitis in postmenopausal osteopenic women. *J Periodontol*. **79(8)**: 1409–1418.

Gonçalves, P. F., Sallum, E. A., Sallum, A. W., Casati, M. Z., de Toledo, S., Nociti, F. H. Jr. (2004). Dental cementum reviewed: development, structure, composition, regeneration and potential functions. *Braz J Oral Sci*. **4(12)**: 651-658.

Hamouda, T., and Baker (Jr), J. R. (2000) Antimicrobial mechanism of action of surfactant lipid preparations in enteric Gram-negative bacilli. *J. Appl. Microbiol*. **89(3)**: 397–403.

Hanazawa, S., Kawata, Y., Takeshita, A., Kumada, H., Okithu, M., Tanaka,. S, Yamamoto, Y., Masuda, T., Umemoto, T., and Kitano, S. (1993). Expression of monocyte chemoattractant protein 1 (MCP-1) in adult periodontal disease: increased monocyte chemotactic activity in crevicular fluids and induction of MCP-1 expression in gingival tissues. *Infect Immun*. **61(12)**: 5219-24.

Hancock, R. E. W., and Wong, P. G. W. (1984). Compounds which increase the permeability of the Pseudomonas aeruginosa outer membrane. *Antimicrob. Agents Chemother*. **26(1)**: 48-52.

Handfield, M., Baker, H. V., and Lamont, R. J. (2008). Beyond good and evil in the oral cavity: Insights into host-microbe relationships dfrom transcriptional profiling of gingival cells. *J Dent Res*. **87(3)**: 203–223.

Haps, S., Slot, D. E., Berchier, C. E., and Van der Weijden, G. A. (2008). The effect of cetylpyridinium chloride-containing mouth rinses as adjuncts to toothbrushing on plaque and parameters of gingival inflammation: a systematic review. *Int J Dent Hygiene*. **6**: 290–303.

Harrap, G. J.. Saxton, C. A., and Best, J. S. (1983). Inhibition of plaque growth by zinc salts. *J. Periodont. Res*. **18**: 634-642.

Hasan, A., and Palmer, R. M. (2014). A clinical guide to periodontology: Pathology of periodontal disease. *Br. Dent. J*.**216**: 457 – 461.

Hienz, S.A., Paliwal, S., and Ivanovski, S. (2015). Mechanisms of bone resorption in periodontitis. *J Immunol Res*. **2015**: Article ID 615486.

How, K. Y., Song, K. P., and Chan, K. G. (2016). Porphyromonas gingivalis: An overview of periodontopathic pathogen below the gum line. *Front Microbiol*. **7**: 53.

Huang, R., Li, M., and Gregory, R. L. (2011). Bacterial interactions in dental biofilm. *Virulence*. **2(5)**: 435–444.

Huang, X., Schulte, R. M., Burne, R. A., and Nascimento, M. M. (2016). Characterization of the arginolytic microflora provides insights into pH homeostasis in human oral biofilms. *Caries Res*. **49(2)**: 165–176.

Hwang, J. K., Shim, J. S., and Pyun, Y. R. (2000). Antibacterial activity of xanthorrhizol from Curcuma xanthorrhiza against oral pathogens. *Fitoterapia*. **71**(3): 321–323.

Ionel, A., Lucaciu, O., Bondor, C., Moga, M., Ilea, A., Feurdean, C., Buhăţel, D., Hurubeanu, L., and Câmpian, R. S. (2016). Assessment of the relationship between periodontal disease and cardiovascular disorders: a questionnaire-based study. *Clujul Med*. **89(4)**: 534-541.

Irvin, R. T., Macalister, T. J., and Costerton, J. W. (1981). Tris(hydroxymethyl)aminomethane buffer modification of Escherichia coli outer membrane permeability. *J. Bacteriol*. **145(3)**: 1397-1403.

Ishikado, A., Uesaki, S., Suido, H., Nomura, Y., Sumikawa, K., Maeda, M., Miyauchi, M., Takata, T., Makino, T. (2010). Human trial of liposomal lactoferrin supplementation for periodontal disease. *Biol Pharm Bull*. **33(10):** 1758-62.

Islam, B., Khan, S. N., Khan, A. U. (2007). Dental caries: From infection to prevention. *Med Sci Monit*. **13(11)**: RA196-203.

Jakubovics, N. S., and Palmer, R. J. (2013). Jr. Oral microbial ecology: Current research and new perspectives. Caster academics press. 134-139.

Kamera, A. R., Craiga, R. G., Dasanayake, A. P., Brys, M., Glodzik-Sobanska, L., de Leon, M. J. (2008). Inflammation and Alzheimer's disease: Possible role of periodontal diseases. *Alzheimers Dement*. **4(4)**: 242–250.

Kaplan, J. B. (2010). Biofilm dispersal: Mechanisms, clinical implications, and potential therapeutic uses. *J Dent Res*. **89(3)**: 205–218.

Kato, E., Sasaki, Y., and Takahashi, N. (2011). Sodium dl-α-tocopheryl-6-O- phosphate inhibits PGE2 production in keratinocytes induced by UVB, IL-1β and peroxidants. *Bioorg Med Chem*. **19(21)**: 6348-6355.

Kelly, C., Jefferies, C., and Cryan, S. A. (2011). Targeted liposomal drug delivery to monocytes and macrophages. *J drug deliv*. **2011:** 727241.

Kim, J., and Amar, S. (2006). Periodontal disease and systemic conditions: a bidirectional relationship. *Odontology*. **94(1)**: 10–21.

Kolenbrander, P. E., Palmer, R. J. Jr., Periasamy, S., and Jakubovics, N. S. (2010). Oral multispecies biofilm development and the key role of cell–cell distance. *Nature Rev. Microbiol*. **8**: 471-480.

Koontongkaew, S., and Jitpukdeebodintra, S. (1995). Interaction of chlorhexidine with cytoplasmic membranes of Streptococcus mutans GS-5. *Caries res*. **29**(5): 413-417.

Kreth, J., Merritt, J., and Qi, F. (2009). Bacterial and host interactions of oral streptococci. *DNA Cell Biol*. **28(8)**: 397–403.

Lagdive, S. S., Lagdive, S. B., Mani, A., Anarthe, R., Pendyala, G., Pawar, B., and Marawar, P. P. (2013). Correlation of mast cells in periodontal diseases. *J Indian Soc Periodontol*. **17(1)**: 63–67.

Lambert, P. A. (2002). Cellular impermeability and uptake of biocides and antibiotics in Gram-positive bacteria and mycobacteria. *J. Appl. Microbiol*. **92(s1)**: 46S–54S.

Langner, M., Pruchnik, H., and Kubica, K. (2000). The effect of the lipid bilayer state on fluorescence intensity of fluorescein-PE in a saturated lipid bilayer. *Z. Naturforsch*. **55c**: 418-424.

Laugisch, O., Schacht, M., Guentsch, A., Kantyka, T., Sroka, A, Stennicke, H. R., Pfister, W., Sculean, A., Potempa, J., and Eick, S. (2012). Periodontal pathogens affect the level of protease inhibitors in gingival crevicular fluid. *Mol Oral Microbiol*. **27(1)**: 45–56.

Lewis, K. (2001). Riddle of biofilm resistance. *Antimicrob Agents Chemother*. **45**(4): 999-1007.

Li, X., Wang, J., Joiner, A., and Chang, J. (2014). The remineralisation of enamel: a review of the literature. *J Dent*. **42(Supplement 1)**: S12–S20.

Libinaki, R., Ogru, E., Gianello, R., Bolton, L., and Geytenbeek, S. (2005). Evaluation of the safety of mixedtocopheryl phosphates (MTP)-A formulation of alpha-tocopheryl phosphate plus alpha-di-tocopherylphosphate. *Food Chem. Toxicol*. **44(7)**: 916–932.

Libinaki, R., Tesanovic, S., Heal, A., Nikolovski, B., Vinh, A., Widdop, R. E., Gaspari, T. A., Devaraj, S., and Ogru, E. (2010). Effect of tocopheryl phosphate on key biomarkers of inflammation: Implication in the reduction of atherosclerosis progression in a hypercholesterolaemic rabbit model. *Clin Exp Pharmacol Physiol*. **37(5-6)**: 587-592.

Lienau, A., Glaser, T., Krucker, M., Zeeb, D., Ley, F., Curro, F., and Albert, K. (2002). Qualitative and quantitative analysis of tocopherols in toothpastes and gingival tissue employing HPLC NMR and HPLC MS coupling. *Anal Chem*. **74**: 5192-5198.

Liu Y., Busscher H. J., Zhao B., Li Y., Zhang Z., van der Mei H. C., Ren Y., and Shi L. (2016). Surface-adaptive, antimicrobially loaded, micellar nanocarriers with enhanced penetration and killing efficiency in Staphylococcal biofilms. *ACS Nano*. **10**(4): 4779-89.

Loe, H. (2000). Oral hygiene in the prevention of caries and periodontal disease. *Int Dent J*. **50**: 129-139.

Loesche, W. J., and Grossman, N. S. (2001). Periodontal disease as a specific, albeit chronic, infection: diagnosis and treatment. *Clin Microbiol*. **14**: 727–752.

Lynch, R. J. M. (2011). Zinc in the mouth, its interactions with dental enamel and possible effects on caries; a review of the literature. *Int Dent J*. **61(Suppl. 3)**: 46–54.

Mackay, B. J., Denepitiya, L., Iacono, V. J., Krost, S. B., and Pollark, J. J. (1984). Growth-inhibitory and bactericidal effects of human parotid salivary histidine-rich polypeptides on Streptococcus mutans. *Infect. Immun*. **4**(3): 695-701.

Madianos, P. N., Bobetsis, Y. A., and Kinane, D. F. (2005). Generation of inflammatory stimuli: how bacteria set up inflammatory responses in the gingiva. *J Clin Periodontol*. **32 (Suppl. 6)**: 57–71.

Makon-Sébastien, N., Francis, F., Eric, S., Henri, V. P., François, L. J., Laurent, P., Yves, B., and Serge, C. (2014). Lycopene modulates THP1 and caco2 cells inflammatory state through transcriptional and nontranscriptional processes. *Mediators Inflamm*. **Article ID 507272.**

March, P. D. (2000). Role of the oral microflora in health. *Microb. Ecol. Health Dis*. **12**: 130–137.

Marcotte, H., and Lavoie, M. C. (1998). Oral microbial ecology and the role of salivary immunoglobulin A. *Microbiol Mol Biol Rev*. **62(1)**: 71–109.

Marketing magazine. (2011). *''Sector insight: Oral healthcare''*. Available at: http://www.marketingmagazine.co.uk/article/1068895/sector-insight-oral-healthcare (Accessed 10 March 2017).

Marsh, P. D. (1994). Microbial ecology of dental plaque and its significance in health and disease. *Adv Dent Res*. **8(2)**: 263-271.

Marsh, P. D. (2000). Role of the oral microflora in health. *Microb. Ecol. Health Dis.* **12**: 130–137.

Marsh, P. D., and Bradshaw, D. J. (1995). Dental plaque as a biofilm. *J Ind Microbiol* **15**: 169-175.

Marsh, P. D., and Bradshaw, D. J. (1997). Physiological approaches to the control of oral biofilms. *Adv Dent Res*. **11(1)**: 176-185.

Marsh, P. D., and Martin, M. (1992). Oral microbiology (3rd edition): Chapter 7 – periodontal diseases. Published by Chapman & Hall.

Marsh, P. D., Lewis, M., Williams, D., Martin, M. V. (2009). Oral microbiology, 5th ed, published by Churchill Livingstone.

Matsui, R. and Cvitkovitch D. (2010). Acid tolerance mechanisms utilized by Streptococcus mutans. *Future Microbiol*. **5**(3): 403–417.

Mazza, J. E., Newman, M. G., and Sims, T. N. (1981). Clinical and antimicrobial effect of stannous fluoride on periodontitis. *J Clin Periodontol*. **8**: 203-212.

McBain, A. J., Bartolo, R. G., Catrenich, C. E., Charbonneau, D., Ledder, R. G., and Gilbert, P. (2003). Effects of a chlorhexidine gluconate-containing mouthwash on the vitality and antimicrobial susceptibility of in vitro oral bacterial ecosystems. *Appl Environ Microbiol*. **69**: 4770-4776.

McBain, A. J., Ledder, R. G., Sreenivasan, P., and Gilbert, P. (2004). Selection for high-level resistance by chronic triclosan exposure is not universal. *J. Antimicrob. Chemother*. **53**: 772–777.

Mcdonnell, G., and Russle, A. D. (1999). Antiseptics and disinfectants: activity, action, and resistance. *Clin. Microbiol. Rev*. **12(1)**: 147-179.

Mecheri, B., Gambinossia, F., Nocentinib, M., Puggellia, M., and Caminati, G. (2004). Modulation of tetracycline–phospholipid interactions by tuning of pH at the water–air interface. *Biophys. Chem*. **111(1)**: 15–26.

Meers, P., Neville, M., Malinin, V., Scotto, A. W., Sardaryan, G., Kurumunda, R., Mackinson, C., James, G., Fisher, S., and Perkins, W. R. (2008). Biofilm penetration, triggered release and in vivo activity of inhaled liposomal amikacin in chronic Pseudomonas aeruginosa lung infections. *J. Antimicrob. Chemother*. **61**: 859-868.

Mellberg, J. R. (1992). Hard-tissue substrates for evaluation of cariogenic and anti-cariogenic activity in situ. *J Dent Res*. **71**: 913-919.

Melnyk, B. M., and Morrison-Beedy, D. (2012). Intervention research designing, conducting, analysing and funding a practical guide for success, in press. Springer publishing company.

Meurman, J. H., Sanz, M., and Janket. S-J. (2004). Oral health, atherosclerosis, and cardiovascular disease. *CROBM*. **15(6)**: 403-413.

Mintel. (2013). *''Oral healthcare-UK-June 2013''*. Available at: http://store.mintel.com/oral-healthcare-uk-june-2013 (Accessed 10 March 2017).

Mirbagheri, S. A., Nezami, B. G., Assa, S., and Hajimahmoodi, M. (2008). Rectal administration of d-alpha tocopherol for active ulcerative colitis: a preliminary report. *World J Gastroenterol*. **14**(39): 5990-5995.

Miyauchi, M., Takata, T., Ito, H., Ogawa, I., Kudo, Y., Takekoshi, T., and Nikai, H. (1998). Distribution of macrophage lineage cells in rat gingival tissue after topical application of lipopolysaccharide: an immunohistochemical study using monoclonal antibodies: OX6, ED1 and ED2. *J Periodontal Res*. **33(6)**: 345-51.

Moddresi, M. (2010). Ph.D. thesis. London College of Fashion, University of the Arts London, London, UK. The use of nanotechnology in enhancing the efficacy of cosmetic actives of natural origin.

Mohamad, M. M. (2011). Bsc thesis, University of Manchester, In vitro investigations into the antimicrobial and microecological effects of selected anti-plaque agents.

Mohammadi, Z., and Abbott, P. V. (2009). The properties and applications of chlorhexidine in endodontics. *Int Endod J*. **42**(4): 288-302.

Mout, R., Moyano, D. F., Rana, S., and Rotello V. M. (2012). Surface functionalization of nanoparticles for nanomedicine. *Chem Soc Rev*. **41(7)**: 2539–2544.

Mukhim, T., Dey, J., Das, S., Ismail, K. (2010). Aggregation and adsorption behavior of cetylpyridinium chloride in aqueous sodium salicylate and sodium benzoate solutions. *J Colloid Interface Sci*; **350(2)**: 511-5.

Munteanu, A., Zingg, J. M., Ogru, E., Libinaki, R., Gianello, R., West, S., Negis, Y., Azzi, A. (2004). Modulation of cell proliferation and gene expression by α-tocopheryl phosphates: relevance to atherosclerosis and inflammation. *Biochem Biophys Res Commun*. **318**: 311-316.

Muthu, M. S., Kulkarni, S., Liu, Y., and Feng, S. S. (2012). Development of docetaxel-loaded vitamin E TPGS micelles: formulation optimization, effects on brain cancer cells and biodistribution in rats. *Nanomedicine*. **7**(3): 353-64.

Nagarajan, R. (2002). Molecular packing parameter and surfactant self-assembly: The neglected role of the surfactant tail. *Langmuir*. **18**: 31-38.

Nair, S. C., and Anoop, K. R. (2012). Intraperiodontal pocket: An ideal route for local antimicrobial drug delivery. *J Adv Pharm Technol Res*; **3(1)**: 9–15.

Narang, R. S., and Narang, J. K. (2015). Nanomedicines for dental applications-scope and future perspective. *Int J Pharm Investig*. **5(3)**: 121–123.

Negis, Y., Meydani, M., Zingg, J. M. and Azzi, A. (2007). Molecular mechanism of alpha-tocopheryl-phosphate transport across the cell membrane. *Biochem Biophys Res Commun*. **359(2)**: 348-53.

Negis, Y., Zingg, J. M., Ogru, E., Gianello, R., Libinaki, R., and Azzi, A. (2005). On the existence of cellular tocopheryl phosphate, its synthesis, degradation and cellular roles: A hypothesis. *IUBMB Life*. 57: 23-25.

Negis. Y., Meydani, M., Zingg, J. M., Azzi, A. (2007). Molecular mechanism of alpha-tocopheryl-phosphate transport across the cell membrane. *Biochem Biophys Res Commun*. **359**: 348-353.

Neu, H.C., and Gootz, T. D. (1996). Medical Microbiology. 4th edition. Chapter 11.

Nguyen, S., and Hiorth, M. (2015). Advanced drug delivery systems for local treatment of the oral cavity. *Ther. Deliv*. **6(5)**: 595–608.

Nguyena, S., Solheima, L., Byea, R., Rykkeb, M., Hiortha, M., and Smistada, G. (2010). The influence of liposomal formulation factors on the interactions between liposomes and hydroxyapatite. *Colloids Surf., B*. **76**(1): 354–361.

Nibali, L., Fedele, S., and Donos, N. (2013). The role of interleukin 6 in oral disease. *Dimens Dent Hyg*. **11(1)**: 28, 30, 32–34.

Nishio, K., Ishida, N., Saito, Y., Ogawa-Akazawa, Y., Shichiri, M., Yoshida, Y., Hagihara, Y., Noguchi, N., Chirico, J., Atkinson, J. and Niki, E. **(**2011). α-tocopheryl phosphate: uptake, hydrolysis, and antioxidant action in cultured cells and mouse. *Free Radic. Biol. Med*. **50**(12): 1794-1800.

Nizam, N., Discioglu, F., Saygun, I., Bal, V., Avcu, F., Ozkan C. K., and Serder, M. A. (2014). The effect of α-tocopherol and selenium on human gingival fibroblasts and periodontal ligament fibroblasts in vitro. *J Periodontal*. **85(4)**: 636-44.

Nobbs, A H., Lamont, R. J., and Jenkinson, H. F. (2009). Streptococcus adherence and colonization. *Microbiol Mol Biol Rev*. **73**:407–450.

Nowotarska, S. W., Nowotarski, K. J., Friedman, M., and Situ, C. (2014). Effect of structure on the interactions between five natural antimicrobial compounds and phospholipids of bacterial cell membrane on model monolayers. *Molecules*. **19**: 7497-7515.

Nzai, J. M., and Proctor, A. (1998). Determination of phospholipids in vegetable oil by fourier transform infrared spectroscopy. *JAOCS*. **75**(10): 1281 –1289.

Obando, D., Widmer, F., Wright, L. C., Sorrell, T. C., Jolliffe, K. A. (2007). Synthesis, antifungal and antimicrobial activity of alkylphospholipids. *Bioorg Med Chem*. **15**(15): 5158-65.

Ogru, E., Gianello, R., Libinaki, R., Smallridge, A., Bak, R., Geytenbeek, S., Kannar, D. and West, S. (2003). Vitamin E Phosphate: An endogenous form of vitamin E. Free radicals and oxidative stress: chemistry, biochemistry and pathophysiological implications. Meeting of the Society for Free Radical Research Ioannina, Greece, June 26-29: 127-132.

Ozak, S.T., and Ozkan, P. (2013). Nanotechnology and dentistry. *Eur J Dent*. **7(1)**: 145–151.
Page, R. (1991). The role of inflammatory mediators in the pathogeneisis of periodontal disease. *J Periodont Res*. **26**: 230 – 242.

Pan, P. C. (2006). Patent; WO2006123234 A1. Oral care compositions having improved substantivity.

Pan, P. H., Finnegan, M. B., Sturdivant, L., Barnett, M. L. (1999). Comparative antimicrobial activity of an essential oil and an amine fluoride/stannous fluoride mouthrinse in vitro. *J Clin Periodontol*. **26**: 474-6.

Pankey, G. A., and Sabath, L. D. (2004). Clinical relevance of bacteriostatic versus bactericidal mechanisms of action in the treatment of gram-positive bacterial infections. *Clin Infect Dis*. **38(6)**: 864-870.

Park, E. K., Jung, H. S., Yang, H. I., Yoo, M. C., Kim, C., and Kim, K. S. (2007). Optimized THP-1 differentiation is required for the detection of responses to weak stimuli. *Inflamm Res*. **56:** 45-50.

Park, E., Na, H. S., Kim, S. M., Wallet, S., Cha, S., Chung, J. (2014). Xylitol, an anticaries agent, exhibits potent inhibition of inflammatory responses in human THP-1 derived macrophages infected with Porphromonas gingivalis. *J periodontal*. **85(6):** 212-223.

Paula, A. J., and Koo, H. (2016). Nanosized building blocks for customizing novel antibiofilm approaches. *J. Dent. Res*. Critical Reviews in Oral Biology & Medicine: 1-9.

Person, R. V., Monde, K., Humpf, H. U., Berova, N., and Nakanishi, K. (1995). A new approach in exciton-coupled circular dichroism (ECCD) insertion of an auxiliary stereogenic center. *Chirality*. **7**: 128-135.

Petrache, H. I., Tristram-Nagle, S., Harries, D., Kučerka, N., Nagle, J. F., and Parsegian V. A. (2006). Swelling of phospholipids by monovalent salt. *J Lipid Res*. **47(2)**: 302–309.

Phaechamud, T., and Setthajindalert, O. (2017). Cholesterol in situ forming gel loaded with doxycycline hyclate for intra-periodontal pocket delivery. *Eur. J. Pharm. Sci*. **99**: 258-265.

Pihlstrom, B. L., Michalowicz, B. S., and Johnson, N. W. (2005). Periodontal diseases. *The Lancet*. **366(9499)**: 1809–1820.

Pitten, F. A. and Kramer, A. (2001). Efficacy of cetylpyridinium chloride used as oropharyngeal antiseptic. *Arzneimittelforschung*, **51(7)**: 588-95.

Posada, I. M. D., Busto, J. V., Goñi, F. M., and Alonso, A. (2014). Membrane binding and insertion of the predicted transmembrane domain of human scramblase 1. *BBA. Biomembranes*. **1838(1) Part B**: 388–397.

Pupe, C. G., Villardi, M., Rodrigues, C. R., Rocha, H. V. A., Maia, L. C., de Sousa, V. P., and Cabral, L. M. (2011). Preparation and evaluation of antimicrobial activity of nanosystems for the control of oral pathogens streptococcus mutans and candida albicans. *Int J Nanomedicine*. **6**: 2581–2590.

Qin, J., Chai, G., Brewer, J. M., Lovelace, L. L., and Lebioda L. (2006). Fluoride inhibition of enolase: crystal structure and thermodynamics. *Biochemistry*. **45(3)**: 793-800.

Rao, D., Arvanitidou, E., Du-Thumm, L., and Rickard, A. H. (2011). Efficacy of an alcohol-free CPC-containing mouthwash against oral multispecies biofilms. *J Clin Dent*. **22**: 187-94.

Ravoo, B. J., and Engberts, J. B. F. N. (1994). Single-tail phosphates containing branched alkyl chains. Synthesis and aggregation in water of a novel class of vesicle-forming surfactants. *Langmuir*. **10**: 1735-1740.

Renz, A., Ide, M., Newton, T., Robinson, P., and Smith, D. (2007). The Cochrane Collaboration., published by the Cochrane library, Issue 2.

Sabliov, C. M. Fronczek, C., Astete, C. E, KhachaturyanL, M., Khachatryan, L., and Leonardi, C. (2009). Effects of temperature and UV light on degradation of α-tocopherol in free and dissolved form. *J Am Oil Chem Soc*. **86**: 895.

Sadoqi, M., Lau-Cam, C. A., and Wu, S. H. (2009). Investigation of the micellar properties of the tocopheryl polyethylene glycol succinate surfactants TPGS 400 and TPGS 1000 by steady state fluorometry. *J Colloid Interface Sci*. **333**(2): 585-589.

Saglie, R., Newman, M. G., Carranza Jr, F. A., and Pattison, G. L. (1982). Bacterial invasion of gingiva in advanced periodontitis in humans. *J Periodontol*. **53(4)**: 217-222.

Saito, T., Takatsuka, T., Kato, I. T., Ishihara, K., and Okuda, K. (1997). Adherance of oral streptococci to an immobilised antimicrobial agent. *Archs oral Bid*. **42**(8): 539-545.

Schaeken, M. J. M., van der Hoeven, J. S., and van der kieboom, C. W. A. (1994). Effects of chlorhexidine varnish on streptococci in dental plaque from occlusal fissures. *Caries res*. **28**: 262-266.

Schulze-Siebert, U., Homeyer, J., soll, G., Schultz, P. K., Stumpf, J. B., Mudd, W. D. (2000) Vitamin E from natural origin. *Seventh International Symposium on Plant Lipids*, University of California: Davies CA, Plenum Press, New York.

Schwab, U., Gilligan, P., Jaynes, J., and Henke, D. (1999). In vitro activities of designed antimicrobial peptides against multidrug-resistant cystic fibrosis pathogens. *Antimicrob. Agents Chemother*. **43(6)**: 1435-1440.

Segre, G., and Hammarström, S. (1985). Aspects of the mechanisms of action of benzydamine. *Int J Tissue React*. **7(3)**: 187-93.

Segura, M., Stankova, J., and Gottschalk, M. (1999). Heat-killed Streptococcus suis capsular type 2 strains stimulate tumor necrosis factor alpha and interleukin-6 production by murine macrophages. *Infect Immun*. **67(9)**: 4646–4654.

Seow, Y. X., Yeo, C. R., Chung, H. L., and Yuk, H. G. (2014). Plant essential oils as active antimicrobial agents. *Crit Rev Food Sci Nutr*. **54(5)**: 625-44.

Serafini, G., Trevisan, S., Saponati, G. and Bandettini, B. (2012). Therapeutic efficacy and tolerability of the topical treatment of inflammatory conditions of the oral cavity with a mouthwash containing diclofenac epolamine a randomized, investigator-blind, parallel-group, controlled, phase III study. *Clin Drug Investig*. **32(1)**: 41-49.

Shaji, J., and Lal, M. (2013). Nanocarriers for targeting inflammation. *Asian J Pharm Clin Res*, **6** (**Suppl. 3)**: 3-12.

Sharma, S., Lavender, S., Woo, J., Guo, L., Shi, W., Kilpatrick-Liverman, L., Gimzewski, J. K. (2014). Nanoscale characterization of effect of l-arginine on streptococcus mutans biofilm adhesion by atomic force microscopy. *Microbiology*. **160**: 1466–1473.

Sheen, S., and Addy, M. (2003). An in vitro evaluation of the availability of cetylpyridinium chloride and chlorhexidine in some commercially available mouthrinse products. *Br. Dent. J*. **194**: 207 – 210.

Shen, Y., Zhao, J., Fuente-Núñez, C., Wang, Z., Hancock, R. E. W., Roberts, C. R., Ma, J., Li, J., Haapasalo, M., and Wang, Q. (2016). Experimental and theoretical investigation of multispecies oral biofilm resistance to chlorhexidine treatment. *Sci. Rep*. **6**: 27537.

Silhavy, T. J., Kahne, D. and Walker, S. (2010). The bacterial cell envelope. *Cold Spring Harb Perspect Biol 2*. a000414.

Silva, N., Abusleme, L., Bravo, D., Dutzan, N., Garcia-Sesnich, J., Vernal, R., Hernandez, M., and Gamonal, J. (2015). Host response mechanisms in periodontal diseases. *J Appl Oral Sci*. **23(3)**: 329–355.

Silva, S. D., Rosa, N. F., Ferreira, A. E., Boas, L. V., and Bronze, M. R. (2009). Rapid determination of α-tocopherol in vegetable oils by fourier transform infrared spectroscopy. *Food Anal. Methods.* **2**: 120–127.

Singh, A., Wyant, T., Anaya-Bergman, C., Aduse-Opoku, J., Brunner, J., Laine, M. L., Curtis, M. A., and Lewis, J. P. (2011). The capsule of porphyromonas gingivalis leads to a reduction in the host inflammatory response, evasion of phagocytosis, and increase in virulence. *Infect Immun*. **79(11)**: 4533-4542.
Singh, B., and Singh, R. (2013). Gingivitis – A silent disease. *IOSR-JDMS.* **6(5)**: 30-33.

Sironi, M., Guglielmotti, A., Polentarutti, N., Fioretti, F., Milanese, C., Romano, M., Vigini, C., Coletta, I., Sozzani, S., Bernasconi, S., Vecchi, A., Pinza, M., and Mantovani, A. (1999).

A small synthetic molecule capable of preferentially inhibiting the production of the CC chemokine monocyte chemotactic protein-1. Eur Cytokine Netw. **10(3):** 437-42.

Socransky, S. S., and Haffajee, A. D. (2005). Periodontal microbial ecology. *Periodontol 2000*. **38**: 135–187.

Sreenivasan, P. K., and Gaffar, A. (2008). Antibacterials as anti-inflammatory agents: Dual action agents for oral health. *Antonie Van Leeuwenhoek*. **93(3)**: 227-39.

Stoker, H. S. (2012). General, Organic, and Biological Chemistry, 6th ed, published by Cengage Learning US.

Sutariya, V. B., and Pathak, Y. (2015). Biointeractions of Nanomaterials. Published by CRC press.

Tada, A., Nakayama-Imaohji, H., Yamasaki, H., Hasibul, K., Yoneda, S., Uchida, K., Nariya, H., Suzuki, M., Miyake, M., and Kuwahara, T. (2016). Cleansing effect of acidic l-arginine on human oral biofilm. *BMC Oral Health*. **16**: 40.

Tahan, G., Aytac, E., Aytekin, H., Gunduz, F., Dogusoy, G., Aydin, S., Tahan, V., and Uzun, H. (2011). Vitamin E has a dual effect of anti-inflammatory and antioxidant activities in acetic acid-induced ulcerative colitis in rats. *Can J Surg*. **54(5)**: 333–338.

Tanford, C. (1972). Micelle shape and size. *J. Phys. Chem. A*. **76**(21): 3020 -3024.

Tanomaru, J. M. G., Nascimento, A. P., Watanabe, E., Matoba-Júnior, F., Tanomaru-Filho, M., and Ito, I. Y. (2008). Antibacterial activity of four mouthrinses containing triclosan against salivary Staphylococcus aureus. *Braz J Microbiol*. **39**(3): 569–572.

Tao, L., and Tanzer, J. M. (2002). Novel sucrose-dependent adhesion co-factors in Streptococcus mutans. *JDR*. **81(7)**: 505-510.

Thiele, J. J., Hsieh, S. N., and Ekanayake-Mudiyanslege, S. (2005). Vitamin E: critical review of its current use in cosmetic and clinical dermatology. *Dermatol. Surg*. **31**: 805-813.

Touger-Decker, R., and van Loveren, C. (2003). Sugars and dental caries. *Am J Clin Nutr*. **78(4)**: 881S-892S.

Tribble, G. D., and Lamont, R. J. (2010). Bacterial invasion of epithelial cells and spreading in periodontal tissue. *Periodontol 2000*. **52(1)**: 68–83.

Universal Probe Library Assay Design Centre. (Online). Available online at: https://lifescience.roche.com/en_gb/brands/universal-probe-library.html (accessed 5/Jan/2017).

Urnowey, S., Ansai, T., Bitko, V., Nakayama, K., Takehara, T., and Barik, S. (2006). Temporal activation of anti- and pro-apoptotic factors in human gingival fibroblasts infected with the periodontal pathogen, Porphyromonas gingivalis: potential role of bacterial proteases in host signalling. *BMC Microbiol*. **6:** 26.

Vaara, M. (1992). Agents that increase the permeability of the outer membrane. *Microbiol Rev*. **56(3)**: 395-411.

Viscio, D., Gaffar, A., Fakhry-Smith, S., and Xu, T. (2000). Present and future technologies of tooth whitening. *Compend Contin Educ Dent Suppl*. **28**: S36-43; quiz S49.

Voss, J. G. (1967). Effects of organic cations on the gram-negative cell wall and their bactericidal activity with ethylenediaminetetra-acetate and surface active agents. *J. gen. Microbiol*. **48**: 391-400.

Wa, F K., and Gebicki, J. M. (1983). Oxidation of α-tocopherol in micelles and liposomes by the hydroxyl, perhydroxyl, and superoxide free radicals. *Arch. Biochem. Biophys.* **226**(1): 242-251.

Waaler, M. B. C. (2014). Thesis, university of Oslo, Norway. The effect of brushing, acid etching and fluoride dentifrice on the surface of human enamel.

Wallwork, M. L., Kirkham, J., Zhang, J., Smith, D. A., Brookes, S. J., Shore, R. C., Wood, S. R., Ryu, O., and Robinson, C. (2001). Binding of matrix proteins to developing enamel crystals: An atomic force microscopy study. *Langmuir*. **17**: 2508-2513.

Wang, B. Y., Hong, J., Ciancio, S. G., Zhao, T., and Doyle, M. P. (2012). A novel formulation effective in killing oral biofilm bacteria. *J Int Acad Periodontol*. **14**(3): 56-61.

Wang, X., Liu, L., Ramström, O., and Yan, M. (2009). Engineering nanomaterial surfaces for biomedical applications. *Exp Biol Med (Maywood)*. **234(10):** 1128–1139.

Wanga, J., Suna, J., Chena, Q., Gaoa, Y., Lia, L., Lia, H., Lenga, D., Wanga, Y., Suna, Y., Jingb, Y., Wanga, S., Hea, Z. (2012). Star-shape copolymer of lysine-linked di-tocopherol polyethylene glycol 2000 succinate for doxorubicin delivery with reversal of multidrug resistance. *Biomaterials*. **33**(28): 6877–6888.

White, R. R., Hays, G. L., and Janer, L. R. (1997). Residual antimicrobial activity after canal irrigation with chlorhexidine. *J Endod*. **23**: 229-31.

Wijeyeweera, R. L., and Kleibergn, I. (1989). Arginolytic and ureolytic activities of pure cultures of human oral bacteria and their effects on the pH response of salivary sediment and dental plaque in vitro. *Archs oral Bid*. **34(I)**: 43-53.

Wilson, M. (1996). Susceptibility of oral bacterial biofilms to antimicrobial agents. *J. Med Microbiol*. **44**: 79-87.

Witt, J., Bsoul, S., He, T., Gibb, R., Dunavent J., and Hamilton, A. (2006). The effect of toothbrushing regimens on the plaque inhibitory properties of an experimental cetylpyridinium chloride mouthrinse. *J Clin Periodontol*. **33(10)**: 737-742.

Wolf, C. (2007). Dynamic stereochemistry of chiral compounds principles and applications, in press. RSC publishing.

Wolff, L. F., Pihlstrom B. L., Bakdash. M. B., Aeppli, D. M., and Bandt, C. L. (1989). Effect of toothbrushing with 0.4% stannous fluoride and 0.22% sodium fluoride gel on gingivitis for 18 months. *J Am Dent Assoc*. **119**: 283-289.

World Health Organisation. (2012). *''Oral health – Fact sheet N^{o} 318''*. Available at: http://www.who.int/mediacentre/factsheets/fs318/en/ (Accessed 10 March 2017).

Wu, H., Su, K., Guan, X., Sublette, M. E., and Stark, R. E. **(**2010). Assessing the size, stability and utility of isotropically tumbling bicelle systems for structural biology. *Biochim Biophys Acta*. **1798**(3): 482-488.

Xie, Y., He, Y., Irwin, P. L., Jin, T., and Shi, X. (2011). Antibacterial activity and mechanism of action of zinc oxide nanoparticles against Campylobacter jejuni. *Appl Environ Microbio*. **77(7)**: 2325–233.

Yazdankhah, S. P., Scheie A. A., Hoiby, E. A., Lunestad, B., Heir, E., Fotland, T. O., Naterstad, k., and Kruse, H. 2006. Triclosan and Antimicrobial Resistance in Bacteria: An Overview. *Microb Drug Resist*. **12(2)**: 83-90.

Zablotna, M., Sobjanek, M., Purzycka-Bohdan, D., Szczerkowska-Dobosz, A., Nedoszytko, B., and Nowicki, R. (2016). The -2518 A/G MCP-1 and -403 G/A RANTES promoter gene polymorphisms are associated with psoriasis vulgaris. *Clin. Exp. Dermatol*. **41(8)**: 878–883.

Zahner, D., Gandhi, A. R., Yi, H., Stephens, D. S. (2011). Mitis group streptococci express variable pilus islet 2 pili. *PLoS ONE*. **6**(9): e25124.

Zhao, Y., Lee, M., Cheung, C., Ju, J., Chen, Y., Liu, B., Hu, L., and Yang, C. S. (2011). Analysis of multiple metabolites of tocopherols and tocotrienols in mice and humans. *J Agric Food Chem*. **58**(8): 4844–4852.

Zingg, J. M., Meydani, M., and Azzi, A. (2010). α-Tocopheryl phosphate – An active lipid mediator? *Mol. Nutr. Food Res*. **54**: 679–692.

Zingg, J. M., Meydani, M., and Azzi, A. **(**2012). α-tocopheryl phosphate – an activated form of vitamin E important for angiogenesis and vasculogenesis? *Biofactors*. **38(1)**: 24-33.